Effectiveness Demonstration of Fugitive Dust Control Methods for Public Unpaved Roads and Unpaved Shoulders on Paved Roads

Final Report

DRI Document No. 685-5200.1F1

December 31, 1996

PREPARED BY:

Dr. John G. Watson
Dr. Judith C. Chow
Dr. John A. Gillies
Dr. Hans Moosmüller
Dr. C. Fred Rogers
Mr. David DuBois
Mr. Jerry Derby

Desert Research Institute
P.O. Box 60220
Reno, Nevada 89506

PREPARED FOR:

California Regional Particulate Air Quality Study (CRPAQS)
c/o Technical Support Division
California Air Resources Board
2020 L Street
Sacramento, California 95814

UNDER SPONSORSHIP BY:

CRPAQS

San Joaquin Valley Unified Air Pollution Control District (SJVUAPCD)
1999 Tuolumne Street, Suite #200
Fresno, California 93721

Western States Petroleum Association (WSPA)
505 North Brand Boulevard, Suite 1400
Glendale, California 91203

DISCLAIMER

This report was prepared by researchers at the Desert Research Institute (DRI) and does not necessarily reflect the policies or views of the California Regional Particulate Air Quality Study, the San Joaquin Valley Unified Air Pollution Control District, or the Western States Petroleum Association. The mention of trade names and commercial products does not constitute an endorsement for those products.

The San Joaquin Valley Unified Air Pollution Control District includes the following disclaimer:

> Testing and analysis of the non-hazardous crude oil containing materials was done under a separate contract for $40,000 with the Western States Petroleum Association and is in addition to the study conducted under contract with the San Joaquin Valley Unified Air Pollution Control District for $404,405.
>
> The San Joaquin Valley Unified Air Pollution Control District does not at any time endorse commercial products. Nothing contained in this report is or should be construed as an actual or implied endorsement of any product or material referenced herein. On-site use (within the oil field) of non-hazardous crude oil containing materials is not currently restricted, except by regulations against creating an odor nuisance. Off-site application of non-hazardous crude oil containing materials is restricted to materials that are commercially processed in a facility that has a current District issued Permit to Operate.

ACKNOWLEDGMENTS

Mr. Rodney Langston of the San Joaquin Valley Unified Air Pollution Control District, and Mr. Steve Arita of the Western States Petroleum Association, are acknowledged for their oversight and advice. The dust suppressants were applied by the following vendors: Ophir Oil Company, Newcastle, CA ("EMC Squared"); Midwest Industrial Supply, Canton, OH ("Soil Sement"); Reed and Graham, Inc., Sacramento, CA ("Coherex PM"); Environmental Products and Application Company, Lake Elsinore, CA ("Enduraseal"); Chem Shield Inc., Sparks, NV ("Hydroshield"); and J and M Land Restoration, Inc., Bakersfield, CA ("DSS-40"). The "Non-Hazardous Crude Oil-Containing Materials" suppressant was provided under the auspices of the Western States Petroleum Association. The kind cooperation of the following landowners was crucial in conducting the Fields Road measurements: Mrs. Wolstenholme, Mr. and Mrs. Roy Richards, Mr. and Mrs. Tim Erickson, and Mr. and Mrs. Trey Jones. Mr. John Graves, the Merced County Road Superintendent, and the Merced County Department of Public Works provided excellent cooperation and assistance throughout the study. Mr. Mike Wade and the staff of the Merced

County Farm Bureau responded to our inquiries, providing assistance in contacting the appropriate landowners. We would also like to extend our appreciation to Mr. Joe Neumann and Mr. Chuck Berkowitz for their efforts in the field, to Ms. Barbara Hinsvark and Ms. Brenda Cristani for their able assistance in the DRI laboratory, and to Mr. Norman Mankim at the editor's desk.

TABLE OF CONTENTS

TABLE OF CONTENTS (continued)

TABLE OF CONTENTS (continued)

LIST OF TABLES

LIST OF TABLES (continued)

LIST OF TABLES (continued)

LIST OF FIGURES

LIST OF FIGURES (continued)

LIST OF FIGURES (continued)

EXECUTIVE SUMMARY

Experimental Approach

Experiments were conducted from July 1995 to August 1996 in order to determine the efficiencies of different suppressant materials on unpaved public roads and unpaved shoulders along paved roads. The objectives of these experiments were:

- To review published studies of dust emission rates and dust suppression, and based on this experience, choose the field measurement and data analysis approaches most promising for the quantification of PM_{10} emission rates and suppressant effectiveness.

- To apply those approaches in order to determine which unpaved road stabilizing substances and practices have a high potential to reduce PM_{10} emissions from public unpaved roads and unpaved shoulders of paved public roads.

- To demonstrate the amount by which contributions to ambient PM_{10} concentrations are reduced by applying these methods and to establish the long-term efficiencies of the suppressant applications.

- To determine the practicality and costs of applying these control measures to reduce fugitive dust emissions in the San Joaquin Valley.

For unpaved roads, the PM_{10} sampling plan involved upwind and downwind measurements that eliminated the most objectionable assumptions associated with previous studies. PM_{10} emission rates were estimated by a profile method including of two overhead samplers to allow a more full characterization of dust plumes. Net PM_{10} emissions from suppressant test sections were obtained by subtracting the upwind-source profile from the downwind source profile, and by combining the resulting PM_{10} mass concentrations with meteorological data. Concurrently, a program of detailed soil surface measurements tracked the mechanical properties of the treated surfaces. The PM_{10} emissions were combined with detailed records of vehicle traffic in order to provide: 1) the emission rates as PM_{10} mass produced per vehicle-kilometer traveled for each of the suppressant test sections; 2) the efficiencies of the different suppressants in reducing PM_{10} emissions.

For the unpaved shoulder study, a different approach was required because the dust plumes were much more localized and short-lived. In addition to upwind and downwind PM_{10} sampling, fast-response observations from light scattering and turbulence sensors were used to characterize the dust events. The full complement of surface measurements was also performed in order to characterize the mechanical properties of the shoulder surfaces. This broad approach gave: 1) two measures of PM_{10} emissions, one which summed all emissions over several hours, and one which responded to and measured each dust plume created by one vehicle; 2) a three-dimensional measurement of the turbulence caused by each passing vehicle, because this air motion initiates the dust plumes; and 3) the mechanical behavior of the suppressant. measurements

For both the unpaved road and unpaved shoulder test sites, the PM_{10} emission rates, surface properties, and suppressant efficiencies were measured over a period of about one year, so that the effects of weather and aging could be evaluated.

In an initial survey, more than 60 specific suppressant products were identified. These fell into categories of: 1) salts; 2) asphalt or petroleum emulsions; 3) emulsions of other materials; 4) polymers; 5) surfactants; 6) bitumens; 7) adhesives; 8) solid materials; fibers and mulches; 9) hydroseed vegetation; and 10) miscellaneous products.

Four suppressant products were applied to one-third mile test sections of Fields Road, near Merced, California: 1) "Non-Hazardous Crude-Oil-Containing Materials"; 2) "EMC Squared", a biocatalyst product; 3) "Soil Sement" polymer emulsion mixture; and 4) "Coherex PM" petroleum emulsion and polymer mixture. Three suppressants were applied to one-half mile test sections of unpaved shoulders along Bellevue Road, a suburban thoroughfare near Merced: 1) "Enduraseal" organic emulsion; 2) "Hydroshield" endosperm hydrate; and 3) "DSS-40" acrylic co-polymer.

Conclusions were drawn with respect to: 1) efficiency and durability of each suppressant; 2) fugitive dust emission rates; and 3) zones of influence of fugitive dust emissions.

Suppressant Efficiency

Suppressant efficiency is defined as the percent reduction in emissions achieved on the suppresant-treated test section, as compared to a nearby untreated test section.

- "Soil Sement" and "Non-Hazardous Crude-Oil-Containing Materials" were effective suppressants, even after vehicular use including about 100 vehicle passes per day during the intensive study periods, and the effects of an unusually wet winter. The efficiencies of "Soil Sement" and "Non-Hazardous Crude-Oil-Containing Materials" exceeded 80%, on average, during the final measurement period, 12 months after application.

- "Coherex PM's" average efficiency was 73% after three months, and 49% after 12 months.

- "EMC Squared's" average efficiency was 33% immediately after application; after 3 and 12 months' aging, it seemed completely ineffective.

- The major properties that define low-emitting, well-suppressed surfaces are: 1) surface silt loading; and 2) the strength and flexibility of suppressant material as a surface layer or cover.

- Silt loading is the best indicator of suppressant efficiency. Loading of less than 20 grams of loose silt per square meter of surface area (g/m^2) are associated with

efficiencies that exceed 90%. Silt loadings that exceed 200 g/m^2 are no different from untreated sections in terms of efficiency.

- None of the shoulder suppressants was effective for any appreciable period. The suppressants applied to Bellevue Road shoulder test sections broke down quickly under the effects of ordinary vehicle traffic such as daily mail deliveries to residences, and random shoulder traffic such as temporary passenger car pullovers. It appeared that these activities caused major deterioration in suppressant efficiencies even without winter weather.

Emission Rates

Emission rates are defined as the total mass of PM_{10} particulate matter emitted by one vehicle traveling one mile (or kilometer) on the unpaved road, or along the road bordered by the unpaved shoulders. The rate is measured for a certain vehicle speed or range of speeds.

- Emission rates estimated from the untreated and suppressant-treated unpaved road sections ranged from zero to 2.9 pounds of PM_{10} per vehicle-mile-traveled (VMT) (zero to 800 grams per vehicle-kilometer-traveled [VKT]) for a vehicle speed of 25 mph (40 km/h) and from zero to 5.0 pounds of PM_{10} per VMT (1.4 kilograms per VKT) for a vehicle speed of 35 mph (55 km/h).

- Unpaved road emission rates from this study are similar to, but as variable as, those found in other studies. A study conducted on unpaved agricultural roads by the University of California at Davis found emission factors ranging from about 0.1 to about 5 pounds of PM_{10} per VMT at 25 mph. The U.S. EPA "AP-42" Empirical Dust Emission Model underpredicts by as much as a factor of three when it is applied to the unpaved road conditions pertinent to this study.

- Silt loading, rather than silt content, in the emission rate equation improves the emission rate estimate.

- PM_{10} emission rates from unpaved shoulders are estimated to be 0.03 ± 0.015 pounds per VMT (8 ± 4 grams per VKT) for large vehicles (trucks, semis, vehicles with trailers) traveling from 50 to 60 mph.

- It is doubtful that fugitive dust emission rates from roads and shoulders can ever be estimated by better than a factor of two or three. There will always be large uncertainties in these estimates owing to: 1) problems of natural variability, such as varying wind directions and speeds; and 2) problems involved in using a limited number of samplers to accurately sample turbulent, particle-laden plumes.

Zone of Influence

The "Zone of Influence" is defined in two ways. First, it is the distance from a source at which PM_{10} concentrations have fallen off to 10% of their values close to the source. Second, it is also be defined from the receptor's perspective, as the distance at which the source's emissions result in a measured 1 $\mu g/m^3$ increment above the ambient background. The findings concerning the zone of influence of the unpaved road PM_{10} emissions are as follows:

- PM_{10} concentrations decrease exponentially with distance downwind.
- PM_{10} concentrations decrease by 90% from near-road concentrations within 50 meters (165 feet) downwind of the road.
- Extrapolating to 1 $\mu g/m^3$ shows downwind distances of about 150 meters. This is the effective zone of influence for detecting emissions from a single source. Ambient concentrations usually result from the superimposed contributions of many individual sources.

1.0 INTRODUCTION

This report documents the methods and results of a control method demonstration project for fugitive dust emissions from unpaved public roads and unpaved shoulders alongside paved public roads in California's San Joaquin Valley. This study, carried out between July 1995 through August 1996, is a component of the California Regional Particulate Air Quality Study (CRPAQS), a multi-year effort to understand the causes of suspended particle concentrations that exceed national and state air quality standards in central California.

1.1 Background and Motivation

Fugitive dust in the San Joaquin Valley consists of geological material that is injected into the atmosphere by natural wind and by anthropogenic sources such as paved and unpaved roads, construction and demolition of buildings and roads, storage piles, wind erosion, and agricultural activities (Ahuja *et al.*, 1989; Houck *et al.*, 1989, 1990). The main chemical constituents of these particles are oxides of silicon, aluminum, and iron, and some calcium compounds. Most of the suspended dust deposits within a short distance of its origin, yet a portion of it can be transported long distances by wind (Chow and Watson, 1992). These suspended particles have been shown to constitute more than 50% of PM_{10} (particles with aerodynamic diameters less than 10 micrometers, Federal Register, 1987a) in many urban and nonurban areas of the San Joaquin Valley and elsewhere (Watson *et al.*, 1989a; Chow *et al.*, 1992, 1993, 1994a, 1994b, 1996a, 1996b).

Since the promulgation of PM_{10} standards in 1987, more than 75 "moderate" nonattainment areas (Federal Register, 1991; 1994) and 5 "serious" nonattainment areas (Federal Register, 1993) have been designated by the U.S. Environmental Protection Agency (EPA). The San Joaquin Valley Unified Air Quality Control District is one of these serious areas, and under the 1990 Clean Air Act and its amendments (U.S. Government Printing Office, 1991), it must develop and submit State Implementation Plans (SIPs) specifying the technologies and activities that will be applied to reduce the emissions causing excessive PM_{10} concentrations (Federal Register, 1987b). It is especially unlikely that the PM_{10} standards can be attained in the western U.S. unless significant reductions in fugitive dust emissions are achieved. The U.S. EPA requires estimates of fugitive dust contributions to PM_{10} and identification of control measures in most PM_{10} SIPs (U.S. EPA, 1987).

The U.S. EPA recently proposed new air quality standards for suspended particles (Federal Register, 1996):

- Twenty-four-hour average $PM_{2.5}$ not to exceed 50 $\mu g/m^3$ for a three-year average of annual 98th percentiles at any population-oriented monitoring site in a spatial averaging zone.

- Three-year average $PM_{2.5}$ not to exceed 15 $\mu g/m^3$ for three annual spatial average concentrations from population-oriented monitoring sites in a spatial averaging zone.

- Twenty-four-hour average PM_{10} not to exceed 150 $\mu g/m^3$ for a three-year average of annual 98th percentiles at any population-oriented monitoring site in a spatial averaging zone.

- Three-year average PM_{10} not to exceed 50 $\mu g/m^3$ for three annual average concentrations at any population-oriented monitoring site in a spatial averaging zone.

The $PM_{2.5}$ NAAQS are new. While the PM_{10} NAAQS retain the same values as the prior NAAQS (U.S. EPA, 1987a), their form and areas of application are new. The new forms for these standards are intended to provide more robust measures for the PM indicator. Fugitive dust is a significant, though not the major, contributor to $PM_{2.5}$ concentrations in the SJV.

Emission rates for fugitive dust are difficult to measure or model. The largest emitting categories include dust from unpaved roads, paved roads, construction and demolition, and wind erosion of open soil. There are many subcategories within these major categories, such as paved roads with unpaved shoulders, sanded roads, publicly maintained unpaved roads, nonmaintained "desert shortcuts", and agricultural unpaved roads. Less ubiquitous activities, such as golf course turf replacement, feedlot and dairy operations, equestrian events, off-road vehicle competitions, parking lot sweeping, and industrial transfer and storage operations may be large contributors at certain times and places.

Although qualitative descriptions of fugitive dust emissions are easy to understand, translating these descriptions into quantitative estimates of emission rates, locations, temporal variability, and contributions to PM_{10} measured at receptors has been a scientific and engineering challenge. While existing emissions inventories may have some validity when annually averaged over the entire U.S., they become much less precise when used to estimate contributions to a single receptor or on a single day which registers a high PM_{10} reading. The current methods of quantifying fugitive dust PM_{10} emissions need improvement.

1.1.1 PM_{10} Emissions From Unpaved Roads and Shoulders

As shown by Chow *et al.* (1992), the major contributing source types to ambient PM_{10} measurements in the San Joaquin Valley (SJV) are not ducted primary emissions, but instead, widely distributed area emitters including fugitive dust, primary engine exhaust, residential and agricultural burning, and gaseous precursors of secondary aerosol. Fugitive dust is the largest contributor to excessive PM_{10} concentrations during the spring, summer, and fall at urban and agricultural sites. Vehicle movements associated with agricultural tilling and harvesting, with transport of agricultural products along unpaved roads, and along

paved roads with unpaved shoulders, are believed to cause large contributions to the fugitive dust components in PM_{10}.

Of the estimated 3.4×10^5 kg/day (3.79×10^2 tons/day) of PM_{10} fugitive dust emitted within the SJV, 1.0×10^5 kg/day (1.1×10^2 tons/day) derives from unpaved road emissions and 0.5×10^5 kg/day (0.53×10^2 tons/day) from paved roads (California Air Resources Board, 1991). Much of the paved road emissions are suspected to be from dust carried out of unpaved roads and subsequently deposited on the paved roads. A second source of dust emissions is from unpaved shoulders along the sides of paved roads. The data base describing the actual lengths of unpaved roads and unpaved shoulders that provide sources for PM_{10} emissions in the counties within the SJV is limited. However, unpaved road lengths are estimated to be 98 km in Kings County, 129 km in Fresno County, and 930 km in Merced County. Speed limits are not often posted on these roads and most of them are minimally patrolled.

Unpaved roads generally consist of a graded and compacted road bed that is usually created from the parent material present at the site. Well-constructed unpaved roads are usually finished by topping with a hard surface material such as gravel or crushed rock, but this is not always the case. Characteristics of the road surface such as road bed load capacity (Rosbury and Zimmer, 1983), silt content (mass of particles < 74 μm in geometric diameter) (Cowherd *et al.*, 1990), and hardness of the surface material have all been considered as variables that affect emission rates.

The forces created by the rolling wheels of vehicles remove fine particles from the road bed and also pulverize aggregates lying on the surface. The dust is suspended by the turbulent vehicle wakes and ejected into the air by the shearing force of the tires (Nicholson *et al.*, 1989). Dust emission rates have been found to depend on the fine particle content of the road (Cowherd *et al.*, 1990), soil moisture content, and vehicle speed (Nicholson *et al.*, 1989). The U.S. EPA (1988) also reported that the emission rate of fine particles was exponentially related to vehicle weight and number of wheels.

Dust suspension from unpaved roads is also affected by natural wind forces. Mud and dust are tracked from unpaved surfaces to paved roads, where particles are suspended by the larger traffic volumes. Unpaved shoulders share similar characteristics with unpaved roads. However, emissions from these surfaces are usually associated with entrainment caused by aerodynamic forces associated with the turbulent wakes of high-speed, high-profile vehicles such as semi-tractor trailers.

The effectiveness of control methods for reducing dust emissions from unpaved roads and shoulders has not been well-measured or documented. The U.S. EPA (1988) examined several fugitive dust control method demonstration projects and found that many of them were poorly designed and yielded inconclusive results. Even when projects were well designed, the benefits of the control application for air quality were often undetectable because the control methods being applied had not been understood or correctly implemented. Evaluating these studies is difficult because the mechanics of particle suspension from road surfaces is poorly understood.

1.2 Study Objectives

The objectives of this fugitive dust control effectiveness demonstration study are as follows:

- Evaluate published studies of dust emission rates and dust suppression and select field measurement and data analysis methods that best quantify PM_{10} emission rates and suppressant effectiveness.

- Determine which unpaved road stabilizing substances and practices have a high potential to reduce PM_{10} emissions from public unpaved roads and unpaved shoulders of paved public roads.

1.3 Overview of Demonstration Study Report

Section 2 reviews current knowledge about airborne dust, including the road or land surface variables that affect dust emissions and the surface properties that might be changed by applying suppressants. Published dust emission and suppression studies are critically reviewed. Section 3 presents an extensive, categorized list of commercially-available dust suppressant compounds. The suppressant options and the criteria for inclusion in this experiment are summarized.

Section 4 presents the criteria developed for public unpaved road test sites, and the candidate sites that were examined in the process of making a final decision. The characteristics of the chosen test site are summarized. The field measurement setup is described, and the field and laboratory measurement procedures are documented. Section 5 presents similar information for the unpaved shoulder test sites, documenting the site characteristics, the measurement setup, and the measurement procedures. The measurement requirements of the unpaved shoulder tests were significantly different from those for the unpaved road tests.

Section 6 presents the results and findings for the unpaved road experiments. The measured ambient PM_{10} background concentrations and the PM_{10} concentrations resulting from controlled traffic are tabulated. PM_{10} emissions rate formulae are derived and applied to the data acquired from three experiments conducted between July 1995 and July 1996. Comparison of the suppressant-treated sections' emission rates to an untreated section allows a PM_{10} suppression efficiency to be estimated for each suppressant. Road surface property measurements track changes in critical physical properties. These include silt loadings, silt contents, moisture contents, and surface strengths as the surfaces age and experience both winter and summer weather. These measures are analyzed to determine which ones best correspond to the observed changes in PM_{10} emissions as suppressants degrade throughout the year.

Section 7 presents the results and findings for the unpaved shoulder experiments. The measurement and analytical approach was necessarily different from the unpaved road case,

because the dust plumes were much more localized and short-lived. A full complement of surface measurements was also performed on shoulders to characterize their mechanical properties. The data are analyzed in order to estimate emission rates and suppressant efficiencies.

Section 8 compares the emission rates estimated in this Demonstration Study to the values calculated for the same conditions by the US EPA empirical dust emission model, AP-42. The "Zone of Influence" of the PM_{10} emissions measured downwind from the unpaved road is defined and quantified. Physical specifications for efficient suppressant products are also presented. The study summary and recommendations are presented in Section 9.

2.0 CONCEPTUAL MODEL OF DUST EMISSION AND SUPPRESSION

Dust particles composed of mineral fragments and some variable amounts of organic matter are lifted from soil surfaces and suspended in the atmosphere by wind and vehicle-induced forces. The soil surface properties that appear most influential in this process are: 1) particle size distributions; and 2) the presence or absence of materials which cause particles to adhere to each other. For example, the application of a light water spray on an unpaved road will briefly alleviate dust emissions caused by light vehicle traffic.

Ambient wind suspends small particles by a combination of aerodynamic lift and pressure forces. Some larger particles "saltate", causing the disruption of additional surface material when they again impact the surface. Vehicle-related factors include weight and speed, and the detailed nature of the physical interaction between the vehicle and the road. Usually, rubber-tired vehicles are involved, but emissions increase when the vehicle is equipped with tracks or other devices that disrupt the surface to a greater depth. The aerodynamic turbulence generated by the vehicle: 1) lifts particles from the surface; and 2) injects particles into the ambient flow. The turbulent forces are a function of vehicle configuration and speed.

Suspended dust distributions include particles ranging in size from less than one micrometer (μm) to greater than 50 μm (Chow *et al.*, 1994). The highest mass concentrations are measured closest to sources, because dilution and gravitational fallout act continually to reduce downwind concentrations. Some suspended particles are resuspended after settling onto paved roads downwind; this also occurs when unpaved shoulder material deposits onto the adjacent pavement, and when vehicles track soil onto paved roads.

This section addresses this conceptual model by reviewing previous studies, and gives their findings concerning: 1) soil properties that affect dust emissions; 2) physical interactions of vehicles with unpaved surfaces; 3) enhancements of emissions by wind and turbulence; and 4) suppressant products and their mechanisms for dust suppression. Previous dust emission rate studies are critically reviewed and their emission rate estimates are summarized.

2.1 Soil Properties

The key soil surface properties affecting dust emissions are: 1) surface loadings of suspendable material; 2) size distributions of the surface particulate matter; 3) moisture; 4) surface roughness. Many of these factors provide explicit or implicit inputs to the U.S. EPA's AP-42 empirical dust emission model.

2.1.1 Surface Loading

Most soil surfaces are limited reservoirs; the suspendable dust is depleted after a short time period. Theoretical considerations of the time dependence of resuspension by wind suggest that it may be represented as a negative exponential function (Anspaugh *et al.*, 1975;

Linsley, 1978). An inverse relationship between suspension and time has also been proposed (Reeks *et al.*, 1985; Garland, 1979). In an empirical wind tunnel study of resuspension processes, Nicholson (1993) found that the decay rate of particle emissions from surfaces followed an inverse time relationship. However, the decay rate could be more complicated in the natural environment due to the large range of surface and environmental conditions.

On exposed land, deflation of fine particles often results in the exposure of larger non-erodible sediments that shield the suspendable particles from the wind. The larger non-erodible elements also absorb momentum, thereby decreasing the wind's ability to erode the surface (Marshall, 1971; Raupach, 1992). When surfaces are continually disturbed by very intense winds, by vehicular movement, or by other human activities, they may become unlimited reservoirs that emit dust whenever winds exceed threshold suspension velocities. There are few (less than 500 for the entire U.S.) reported data on the surface loadings of silt (less than 74 μm geometric diameter) and published data on surface loadings of PM_{10} for surfaces included in fugitive dust emission inventories.

2.1.2 Particle Size Distribution

The current air quality standard applies to particles that are less than 10 μm in aerodynamic diameter (PM_{10}). The "aerodynamic diameter" is defined as the diameter of a sphere of unit density (1.0 g/cm^3). Therefore, for soil particles, the aerodynamic diameter corresponds to actual, geometric diameters less than 7 μm because the density of soil particles is about 2.65 g/cm^3, and the aerodynamic diameter varies inversely with the square root of the density (Hinds, 1986). The concern with PM_{10} is health-related, because it represents the upper limit of aerodynamic size class that may enter the respiratory system. The particle size distribution is an important variable for determining dust emission and transport.

Figure 2-1 shows residence times based on gravitational settling velocities for various aerodynamic diameters homogeneously distributed through a 100-meter mixed layer. The "stilled chamber" model assumes that there is no vertical mixing for remaining particles following suspension, while the "stirred chamber" model assumes there is instantaneous mixing throughout the layer (Davies, 1966). The real situation probably lies somewhere between these extremes. More than half of the particles with diameters less than 2.5 μm may remain suspended for more than a week, while those between 2.5 and 10 μm may remain suspended from about six hours to four days. Most particles larger than 20 μm settle out in less than two hours.

The larger particles are also much heavier than the smaller particles and have a lower probability of being mixed to 100 m heights in the first place. Every particle attains an equilibrium between these forces at its terminal settling velocity. The settling velocity increases as the square of the particle diameter or when the particle density increases. For very small particles (less than 10 μm diameter), vertical air movements caused by turbulence can counteract the gravitational settling velocity and such particles can remain suspended for long time periods. Deposition for particles larger than ~20 μm diameter is dominated by

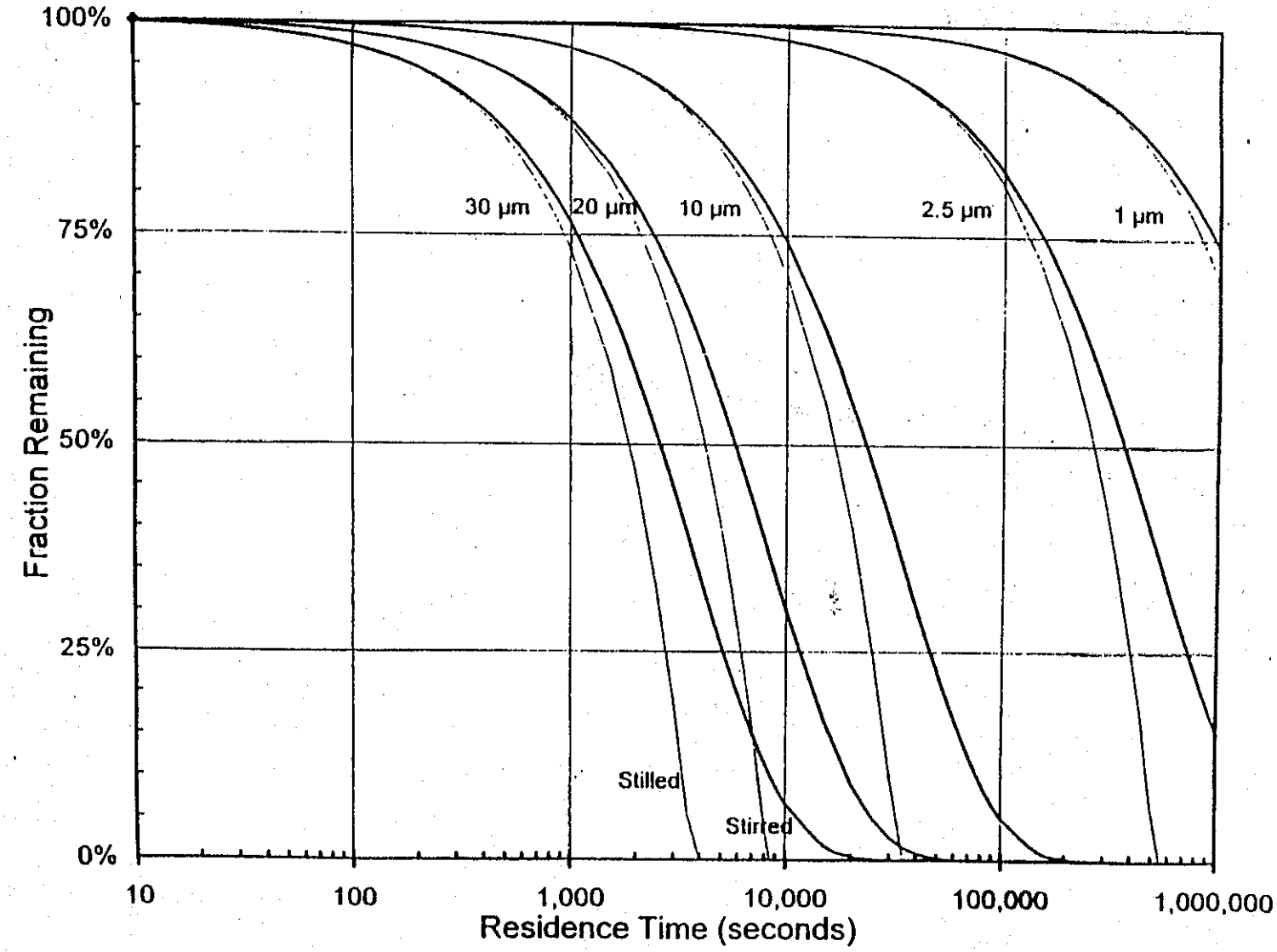

Figure 2-1 Aging times for homogeneously distributed particles of different aerodynamic diameters in a 100 m deep mixed layer. Gravitational settling is assumed for both still and stirred chamber models (Hinds, 1982).

gravity. Transport distance depends on the initial elevation of a particle above ground level, the horizontal wind velocity component in the direction of interest at the particle elevation, and the gravitational settling velocity.

Little is known about the PM_{10} size fraction in surface dust deposits, despite its adverse health potential, long residence time, and high potential for vertical mixing. The most comprehensive information on particle sizes in geological material is contained in soil surveys compiled by the Federal and State Soil Conservation Services. The particle size distribution information in the soil survey data sheets represents the distribution of a wholly-disaggregated sample and describes the mineral grain size composition. These surveys provide boundaries for different soil types on 7.5-minute maps corresponding to U.S. Geological Survey (USGS) maps. The codes are associated with data in a printed summary that accompanies the maps for each survey area. Table 2-1 shows textural characteristics of soils in the northern area of Merced County in California's San Joaquin Valley, from the U.S. Department of Agriculture (USDA) soil survey (USDA, 1962).

Particle sizes are indicated by qualitative descriptions of the amount of sand (50 to 2,000 μm geometric diameter), silt (2 to 50 μm geometric diameter), and clay (less than 2 μm geometric diameter) (USDA, 1960). The soil survey definition for silt differs from that used in fugitive dust emission factors (less than 75 μm geometric diameter) and even from the sieve fractions reported in the soil survey, which are less than 4,760, less than 2,000, less than 420, and less than 74 μm in geometric diameter. The soil survey's less-than-74-μm sieve fraction is considered equivalent to a less-than-75-μm fraction for practical purposes. These particle size fractions in the soil surveys are estimated by the individuals conducting the survey based on the visual similarity of the observed soils to a subset of soil samples which are submitted to particle size analyses in a laboratory.

The particle sizing procedure (American Society for Testing and Materials, 1990a; 1990b) most commonly followed for soil surveys creates a soil/water suspension in which soil aggregates are broken into their component parts prior to sieving. The material designated as sand is washed through a series of sieves to determine the particle size distribution.

The distribution of the finer particles (silts and clays) is determined by methods based on the calculated fall velocities of the different sized particles through a column of water with a chemical dispersant. While the particle size distribution of the disaggregated sediment is useful for agricultural, construction, and other land uses, it is not especially useful for estimating air pollution emissions, because it does not estimate the size of the dust aggregates which are entrained and suspended by surface winds.

Gillette *et al.* (1980) applied two methods to determine the particle and aggregate sizes in soil that might be entrained by winds. The first method ("gentle sieve") consists of drying the soil sample and sieving it gently on a 1 mm sieve with about twenty circular gyrations parallel to the plane of the sieve. A similar methodology was described by Cowherd *et al.* (1990) for estimating the modal aggregate size of sediment samples removed

Table 2-1
Soil Types and their Textural Characteristics
in the Merced County Study Area

Soil Name	Layer Depth (m)	% Sand	% Silt	% Clay
Montpellier coarse sandy loam	0-0.20	66	24	10
Redding gravelly loam	0-0.08	47	36	17
	0.08-0.20	46	35	19
Whitney fine sandy loam	0-0.13	23	51	26
	0.13-0.35	21	49	30
Snelling sandy loam	0-0.10	73	22	5
	0.10-0.40	75	16	9

from unpaved roads. Cowherd *et al.* (1990) adapted their methodology from a rotary sieving procedure described by Chepil (1952) which is considered to be the standard technique for determining the aggregate size distribution of soils. Gillette *et al.* (1980) related the modal aggregate size of loose surface sediment to the threshold friction velocity (u_*, meters per second) which is a measure of the force required to entrain the surface sediment by the wind and is related to the wind speed.

The second method ("hard sieve") consists of up to one-half hour of vigorous shaking (usually using a shaking machine). The gentle sieve method is assumed, without quantitative validation, to be a more suitable approach for determining the potential suspension properties of a soil because it attempts to sample the sediment with its *in situ* characteristics intact. Silt fractions and amounts determined by the hard sieve method probably provide a reasonable indicator of small particles from roads where vehicle tires abrade the surface. Gillette *et al.*'s (1980) threshold suspension velocity measurements apply to soil characteristics obtained by the gentle sieve method.

Table 2-2 shows soil properties determined by the gentle and hard sieve methods for five samples taken from a stony, sandy loam soil (Badland Verdico, USDA, 1980) in Reno, Nevada. The samples of Badland Verdico soils were retained in airtight plastic bags prior to testing to minimize contamination and evaporation of moisture. Table 2-2 includes qualitative observations regarding visible resuspension of the surfaces by wind (simulated by blowing air over the land surface). The moist soil and the desert crust did not visibly suspend, while the remaining disturbed and dry soils suspended easily with moderate blowing.

Table 2-2 shows a high reproducibility of the silt measurements among the construction soil samples. The silt fraction (less than 75 μm geometric diameter) increased by a factor of ten when aggregates were broken up by vigorous sieving. Even with the hard sieve, the suspendable fraction was less than one-tenth the values from the soil survey particle size distributions. Table 2-2 also shows that the majority of the silt fraction consists of particles larger than 38 μm geometric diameter, as a negligible fraction of material passed through the final sieve even with vigorous shaking.

Cowherd *et al.* (1988) recommend that dry sieving to determine silt content using a shaker must be done in discrete time intervals and the change in mass of the bottom pan be closely monitored. When the change in the mass of sediment collected in the pan is less than 3% between two successive shaking periods, Cowherd *et al.* (1990) consider this to be an indication that all the natural silt has passed through the 74 μm sieve; additional mass results from the grinding of larger aggregates by the shaking method. Newer sieves allow bulk sizing to a fraction below 25 μm geometric diameter (corresponding to approximately 40 μm aerodynamic diameter), but other methods must be applied to obtain smaller size fractions.

Figure 2-1 shows examples of size distributions in dust from paved and unpaved roads, agricultural soil, sand and gravel, and alkaline lake bed sediments that were measured in a laboratory resuspension chamber (Chow *et al.*, 1994). The less-than-38-μm sieve

Table 2-2
Sampled Soil Characteristics in Reno, NV

Soil Type	Characteristics	Moisture (%)	Gentle Sieve % <75 μm (% <38 μm)	Hard Sieve % <75 μm (% <38 μm)
Residential Construction Site	Dry vehicle track in graded area between housing foundations. Dust is visually suspended by moderate blowing at the surface.	3.56	0.28 (0.0)	3.46 (0.43)
Residential Construction Site	Wet vehicle track in graded area between housing foundations. Dust was not suspended with vigorous blowing.	17.97	0.19 (0.0)	2.91 (0.81)
Piles of Fill Dirt	Construction pile. Dust is visibly suspended by moderate blowing.	6.45	0.27 (0.02)	2.37 (0.46)
Unbroken Desert Pavement with Sagebrush Cover	Desert crust. Undisturbed area typical of what was present prior to construction. Only top 1 cm sampled. Dust is not suspended by vigorous blowing.	3.23	0.044 (0.0)	5.38 (0.46)
Broken Desert Pavement	Soil underneath desert crust. Dust is visibly suspended by moderate blowing.	10.1	0.07 (0.0)	4.27 (0.29)

fraction was suspended in this chamber and sampled through $PM_{1.0}$, $PM_{2.5}$, PM_{10}, and TSP inlets. TSP corresponds approximately to a PM_{30} size fraction. Fractions in Figure 2-1 are normalized to the TSP mass concentration in the resuspended dust. The $PM_{1.0}$ abundance (6.9%) in the alkaline lake bed dust is twice its abundance in paved and unpaved road dust. Approximately 10% of TSP is in the $PM_{2.5}$ fraction and approximately 50% of TSP is in the PM_{10} fraction. The PM_{10}/TSP distribution is consistent with previous comparisons between PM_{10} and TSP samples in ambient air (Watson *et al.*, 1983; Watson and Chow, 1993). Sand/gravel dust is the exception, where 65% of the mass consists of particles larger than the PM_{10} fraction. The $PM_{2.5}$ fraction of TSP in alkaline lakebeds and sand/gravel is approximately 30% to 40% higher than the other soil types. These finer gradations in particle size are available only for a limited number of soil types.

The size distribution of dust particles affects the suspension process. A flat bed of particles with diameters less than 20 μm is very difficult to suspend by wind. Bagnold (1937) showed that fine Portland cement could not be entrained by wind friction velocities in excess of 1.00 m/s. In this situation, there is no large cross section for wind to act on. In addition, adhesive forces such as van der Waals, electrostatic, and surface tension of adsorbed liquid films (Hinds, 1986) increase the force required to entrain the particles. These adhesive forces increase with relative humidity and surface roughness, but decrease with increasing particle size (Corn and Stein, 1965).

Suspension of fine particles is also mitigated by the presence of larger non-erodible particles if they are present in sufficient quantities. Particles that exceed 840 μm in size are considered too large to be entrained by normal wind velocities (Chepil, 1942) and can act to shelter smaller particles in their lee. Gillette and Stockton (1989) sprinkled glass spheres with diameters ranging from 2,400 to 11,200 μm onto a bed of glass spheres with sizes from 107 to 575 μm and found major reductions in the horizontal flux of the smaller particles. However, Logie (1982) found that erosion of a sand surface was enhanced when low concentrations of larger non-erodible roughness elements were present on the surface. She suggested that the increased erosion was due to acceleration of the wind flow around the isolated elements which scoured the loose sand. Bagnold (1941) estimated that 800 μm particles are the most susceptible to suspension by wind, even though their large masses cause them to settle to the surface very rapidly.

Past studies (e.g., Rosbury and Zimmer, 1983) indicate that unpaved roads with certain types of road aggregates are more efficient emitters of dust than roads with higher silt contents. This suggests that measurement of the percent of aggregates and primary mineral grains in the size range of sand (50 μm - 2,000 μm) and gravel (2,000 μm - 8 cm) (U.S. Department of Agriculture, 1960) are important and directly related to the emissions of fine particles resuspended by the tires of moving vehicles. The percent of large aggregates on the road surface has not been previously reported in publications assessing dust emissions from unpaved roads.

According to Rosbury and Zimmer (1983) in their study of haul roads, the correlation between dust emissions and silt content was not as simple as was reported by Cowherd *et al.*

(1988). Rosbury and Zimmer (1983) observed that there were increased emissions of dust from surfaces with less silt content, but higher gravel content. This observation was also reported by Flocchini *et al.* (1994). The gravel appears to provide, in conjunction with its activation into movement by tires, a high energy source that actively abrades the surface creating a source of fine particles. In addition, the bouncing gravel particles may entrain dust into their aerodynamic wakes, drawing it away from the surface and into the air stream. Such a mechanism has been suggested as a means of entraining dust particles and ejecting them into the air stream in wind erosion processes.

2.1.3 Moisture

Water adheres to individual soil particles, thus increasing their mass, adding surface tension forces, and mitigating suspension and transport. Cohesion of the wetted particles often persists after the water has evaporated due to the formation of aggregates and surface crusts. The threshold shear velocity of soils increases significantly when soil surface moisture is increased by less than 1% from its dry state (Chepil, 1956; Belly, 1964; Bisal and Hsieh, 1966; Svasek and Terwindt, 1974). For example, the wet vehicle track sample reported in Table 2-2 contained ~18% moisture and did not show visible dust suspension in the presence of wind.

The dust-suppressing effectiveness of moisture on unpaved roads is well-documented (Cowherd *et al.* 1990). Nicholson *et al.* (1989) found that the moisture content of the road surface and the presence of strong winds influenced the amount of dust suspended by vehicles. Higher moisture content reduced dust suspension while higher winds tended to enhance dust emissions caused by passing vehicles. Rosbury and Zimmer (1983) found that moisture content affects the ejection of particles by vehicles, as well as the strength of the road bed and hence its ability to deform under vehicle loading. The addition of water as a suppressant, which produced surface moisture contents greater than 2%, achieved greater than 86% reduction in emission rates of PM_{10} compared to the control surface which had an average moisture content of approximately 0.56% (Flocchini *et al.*, 1994).

The road surface-moisture content is also important in enhancing the strength characteristics of surface crusts and the stability of aggregates (Bradford and Grossman, 1982; Lehrsch and Jolley, 1992).

Kinsey and Cowherd (1992) show how watering might reduce emissions at a construction site. Significant dust control benefits are derived initially by doubling the area that is watered; however, benefits are reduced as more water is applied to the site. Ultimately, control efficiency is limited because grading operations are continually exposing dry earth and burying the moistened topsoil. Figure 2-2 shows the effects of moisture content on downwind TSP concentrations measured near an active construction site, including heavy equipment moving at a rate of one vehicle pass per minute. As illustrated in Figure 2-2, downwind (50 m from emissions point) concentrations differ by a factor of five for the range of silt contents and moisture contents shown.

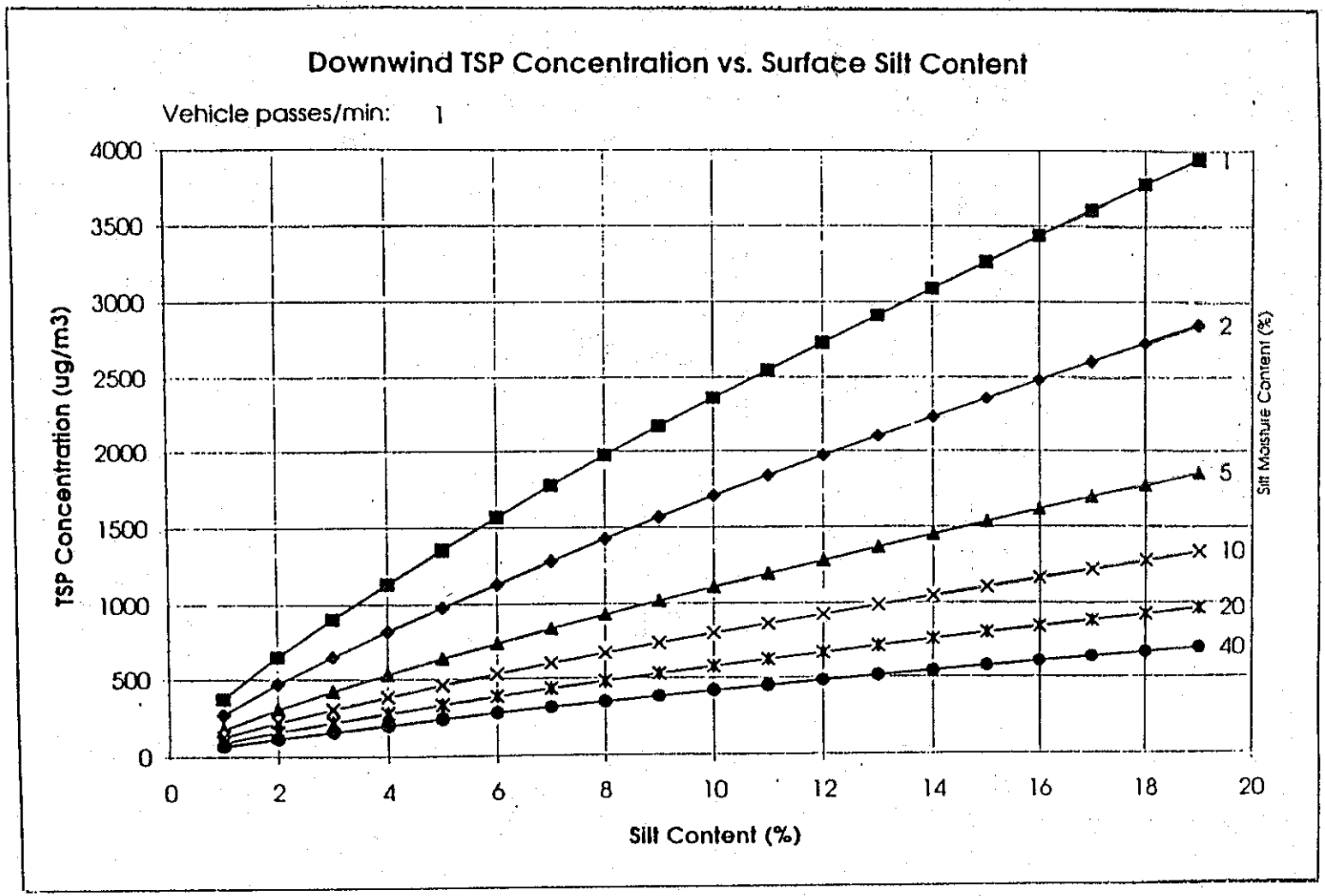

Figure 2-2 TSP emissions versus silt content for different moisture levels (Kinsey and Englehart, 1984). Applies to concentrations 50 m downwind of the emission point for TSP.

Moisture also causes dust to adhere to vehicle surfaces so that it can be carried out of unpaved roads, parking lots, and staging areas. Carryout also occurs when trucks exit heavily-watered construction sites. This dust is deposited on paved (or unpaved) roadway surfaces as it dries, where it is available for suspension far from its point of origin. Fugitive dust emissions from paved roads are often higher after rainstorms in areas where unpaved accesses are abundant, even though the rain may have flushed existing dust from many of the paved streets.

While the moisture capacities of different geological materials are well documented in the soil surveys, the actual moisture content at a given time or place is not recorded. Thornthwaite (1931) proposed the ratio of precipitation to evaporation as an indicator of the availability of moisture for soils. Thornthwaite's major concern was the agricultural potential of land in different areas. The precipitation-evaporation effectiveness index (P-E index) is ten times the sum of the monthly precipitation to evaporation ratios. Using precipitation, evaporation, and temperature data taken prior to 1921 at 21 U.S. monitoring sites, Thornthwaite (1931) established the empirical relationship:

$$P - E \text{ index} = 115 \sum_{i=1}^{12} \left[\frac{P_i}{(T_i - 10)} \right]^{1.11} \qquad (2\text{-}1)$$

where:

I = 1 to 12 for each month of a year

P_i = the inches of precipitation recorded during month

T_i = the average monthly temperature in degrees Fahrenheit

Thornthwaite (1931) used this relationship to classify all North America as wet (P-E index > 128), humid (64 < P-E index < 128), sub-humid (32 < P-E index < 64), semi-arid (16 < P-E index < 32), or arid (P-E index < 16). Much of the Western U.S. is in the arid and semi-arid categories. The P-E index has been used to estimate the moisture content of different soils, as an input to calculate emission factors for different surface types.

Moisture, measured as the average number of days on which precipitation exceeded 0.254 mm during a year, will also effect the availability of dust for transport. These data are recorded in National Weather Service Local Climatological Summaries. The Climatic Atlas of the United States shows approximately 60 days of measurable (greater than 0.254 mm) precipitation in the vicinity of Reno, NV, approximately 30 days of measurable precipitation in the vicinity of Las Vegas, NV, less than 20 days of measurable precipitation in California's Imperial Valley, and 40 to 60 days of measurable precipitation in most of the San Francisco Bay area, the San Joaquin Valley, and Southern California (U.S. Department of Commerce, 1968). The moisture content of soils will vary throughout the year depending on the frequency and intensity of precipitation events, irrigation, and relative humidity and temperature of the surrounding air. Large amounts of rain falling during one month of a year

will not be as effective in stabilizing dust as the same amount of rain interspersed at intervals throughout the year.

The measurement of soil moisture content with gravimetric techniques is simple and well-verified. If performed correctly with an adequate number of samples, this technique is precise, accurate, and has accepted as a calibration standard (Weems, 1991; Ley, 1994).

2.1.4 Surface Roughness

The roughness of the surface over which the wind blows effects the magnitude of the drag force exerted by the wind on the surface. The aerodynamic roughness length (z_0) is the apparent distance above the surface at which the average wind velocity approaches zero and is considered to be a measure of the drag force on the surface (Raupach *et al.*, 1991). According to Wieringa (1993), z_0 is a height-independent description of surface roughness influence on flow dynamics near the surface. In reality, the wind velocity does not become zero at this predicted height. At this height above the surface, the wind velocity no longer follows a logarithmic velocity profile as the surface is approached. The aerodynamic roughness length is related to the actual surface roughness and according to Greeley and Iversen (1985) can be approximated for surfaces with a uniform distribution of particles from the relationship:

$$z_0 = D/30 \tag{2-2}$$

where D is the average particle diameter. For surfaces with a more widely dispersed cover of uniform grains that are spaced a center to center distance of approximately twice the diameter, z_0 values can be higher than are predicted using Equation 2-2. In this situation Greeley and Iversen (1985) suggest the relationship is better approximated by the relationship:

$$z_0 = D/8 \tag{2-3}$$

However, the relationship between the surface roughness and the magnitude of the aerodynamic roughness length is not well understood for complex natural surfaces (Gillies, 1994). Accurate estimation of the aerodynamic roughness requires physical measurements in the actual experimental setting.

2.2 Interaction of Vehicles

Dust on paved roads, unpaved roads, parking lots, and construction sites is suspended by natural winds and vehicular movement. Vehicular traffic in these areas adds to suspension because tire contact creates a shearing force with the road that lifts particles into the air (Nicholson *et al.*, 1989). Unpaved roads and other soil surfaces act as almost unlimited reservoirs of dust loading when vehicles travel over them. These surfaces are always being disturbed, and wind erosion seldom has an opportunity to deflate the fine surface sediment and increase the surface roughness sufficiently to attenuate particle

suspension. The grinding of particles by tires against the road surface shifts the size distribution toward smaller particles, especially those in the PM_{10} fraction.

In an early study that recognized the importance of road surfaces as a source for atmospheric dust, Roberts *et al.* (1975) examined the cost and benefits of road dust control in Seattle's Industrial Valley. Emission rates for dust particles from unpaved road surfaces were determined using cascade impactor samplers (Pilat *et al.*, 1970). In this study the samplers were mounted on trailers towed behind a vehicle. Roberts *et al.* (1975) found that the quantity of dust generated by vehicles increases exponentially with wind speed. For vehicles traveling at 32 km/h on their test gravel roads, Roberts *et al.* (1975) found that 27 percent of the suspended dust plume was composed of particles less than 10 μm and approximately 3.5 percent were below 2 μm.

Pinnick *et al.* (1985) found the distribution of particle sizes within a vehicle-created dust plume was bimodal, with a coarse mode of approximately 50 μm and a fine mode of 2.5 μm. Patterson and Gillette (1977) reported a similar distribution for naturally-generated dust plumes; however, there were proportionately fewer large particles in the natural plume dust in comparison to the vehicular case. The bimodal distribution was attributed to grinding processes caused by tires for the vehicle dust (Pinnick *et al.*, 1985) and to a sandblasting process for wind-generated dust (Patterson and Gillette, 1977). According to Nicholson *et al.* (1989), the size of the particles and the amount of dust resuspended by vehicles are dependent on the velocity of the vehicle. Nicholson *et al.* (1989) found that larger particles were more readily suspended than smaller ones, and speeds of between 24 and 32 km/h were required to suspend particles 4.2-9.5 μm in diameter.

Nicholson and Branson (1990) found that a minimum velocity of 22 km/h is necessary to suspend dust from a paved road surface. The velocities required to entrain particles on unpaved roads are probably significantly less than for paved roads. An important process occurring on unpaved roads is the activation of larger particle sizes by the tires. These particles are effective in mobilizing dust particles upon impact with the surface, similar to saltating particles in a natural erosion system (Gillette, 1977; Gomes *et al.*, 1990). These bouncing particles impact on the surface and eject a range of particle sizes into the air stream, and may also shed micron- or sub-micron-sized secondary particles on impact with the surface or another object (Rosinski *et al.*, 1976; Gillette, 1977). The physics of saltation for sand-sized particles in natural erosion systems is reasonably well understood (Anderson *et al.*, 1990). However, the ejection of dust-sized particles by the saltation process is still poorly understood (John *et al.*, 1991).

2.3 Effects of Wind and Turbulence

Moving vehicles create turbulent wakes that behave much like natural winds to lift and suspend particles. Mollinger *et al.* (1993) found that the shapes of vehicles may have a large impact on the amount of resuspension. They examined the shape variable by mounting a cylinder, an elliptical cylinder, and a rectangular solid on a pendulum that swung back and forth over dust-covered test areas. After twenty passes by the cylinder and elliptical cylinder,

65% and 45% of the dust remained in the test area, respectively. After twenty passes by the rectangular solid traveling at the same velocity, less than 20% of the dust remained. Vehicle shape appears to affect the turbulent structure of the wake shed by the vehicle, creating conditions which favor or reduce the entrainment of dust (Mollinger *et al.*, 1993), suggesting that it is possible to reduce suspension from road surfaces by altering the shape of vehicles.

Theoretical considerations support these observations. The strength of the wake turbulence seems to be a function of vehicle shape and speed. For a large, rectangular shaped vehicle, such as a tractor-trailer, much stronger wakes will be shed due to the flow separation at the trailing edge of the vehicle. This is similar to the Mollinger *et al.* (1993) experiment involving the rectangular solid. The flow separation/wake generation process is enhanced by the 90-degree corner at the trailing edge of the vehicle. Tapered forms with streamlined trailing edges suppress flow separation. Flow separation zones generate vortices which may stream continually behind the vehicle; or they may "shed", i.e., propagate away from the vehicle and its immediate wake structure. Whether the vortices stream behind the vehicle or are shed with a regular periodicity will be a function of the vehicle shape, size, and speed. These highly turbulent air masses still move in the direction of the traveling vehicle until they lose energy and are dissipated into the ambient wind. The shapes of modern passenger cars are designed to have low coefficients of drag and hence lower degrees of flow separation.

These initially fast moving vortices have potentially very high shear forces in them that can cause entrainment of particles. From boundary layer theory, the surface shear stress can be approximated by the Reynolds stress in a fluid:

$$\tau = \rho\overline{u'w'} \tag{2-4}$$

where:

ρ = fluid density (kg m^{-3})

u' = fluctuating horizontal wind speed (m s^{-1})

w' = fluctuating vertical wind speed (m s^{-1})

Extending this argument to the traveling vortices, the shear stress should scale as a function of the horizontal speed of the vortices, which will also be some function of vehicle speed, and the magnitude of the vertical velocity components.

These high-speed vortices are somewhat analogous to the "sweep events" observed in natural turbulent flow (Rao *et al.*, 1971). Flow visualization techniques, usually in liquid flows, indicate how turbulent vortices form and subsequently break down. During the cycle, an initial horseshoe-shaped vortex forms that moves outwards, then undergoes a partial breakdown into turbulence. As the vortex reaches some height above the boundary, there is a sweep and inrush of a vortex with a relatively high velocity towards the boundary, resulting in an increase in the shear stress. Almost simultaneously the "head" of the vortex bursts; that is, the motion within it becomes highly disordered. This cycle of bursting and sweeping

contributes prominently to the Reynolds stress making these events the main creators of small-scale turbulence near the bed (Allen, 1985). The sweep and inrush in the bursting cycle exerts a comparatively large boundary shear stress and is considered to be an important process in moving grains from the bed into the outer flow.

In aeolian sediment transport experiments in wind tunnels, the initiation of sediment movement has been reported to occur in semi-organized "flurries" of activity that are often followed by relatively quiescent periods. The flurries are attributed to the sweeps of flow associated with the burst and sweep sequence in boundary layers (Anderson *et al.*, 1990). Personal observation of natural wind erosion events will also show this same type of "patchy" distribution of sediment entrainment. For the controlled flow regimes over a flat plate, Williams (1986) presents strong circumstantial evidence linking both the nature and spatial pattern of initial grain movement to structural features of the flow, specifically to the velocity signature of burst-sweep events. Bratten *et al.* (1993) found characteristic velocity patterns associated with particle entrainment that they termed ejection-sweep events. These were very similar to organized fluid motions previously observed in laboratory flows and in the atmospheric boundary layer.

Best (1993) also notes that in systems with larger roughness elements, vorticity resulting from eddy shedding is a third component of turbulence that must be considered. This vorticity is not formed the same way as the horseshoe vortex structures that have been observed even in smooth boundary layer flows. The role of these secondary structures in the turbulence is not well understood in terms of their potential to entrain sediment. The wakes shed by vehicles may be more analogous to these turbulent structures than to those created during the burst-sweep cycle.

2.4 Empirical Dust Emission Models

The U.S. Environmental Protection Agency emission model AP-42 (U.S. EPA, 1988; Cowherd *et al.*, 1990) has been utilized as a predictor to estimate the emission of dust from unpaved roads, given as inputs either direct or surrogate measurements of the emission-controlling factors which have just been discussed. The form of the AP-42 equation for unpaved roads is:

$$e = 0.61\left(\frac{s}{12}\right)\left(\frac{S}{48}\right)\left(\frac{W}{2.7}\right)^{0.7}\left(\frac{w}{4}\right)^{0.5}\left(\frac{365-p}{365}\right) \qquad (2\text{-}5)$$

where e = PM_{10} emissions (kg/Vehicle Kilometer Traveled)
s = percent silt content of road bed
S= average vehicle speed (km/h)
W = average vehicle weight (Mg)
w = number of tires (dimensionless)
p = number of days with ≥ 0.254 mm of precipitation

In the AP-42 model percent silt content applies to the percentage of particles in the road material that is <75 μm. The estimate of silt content is derived from grain size analysis of bulk surface samples that are swept from the surface.

This empirical relationship has been used to predict emission rates in many geographically diverse areas. Although the AP-42 equation is based on oversimplified assumptions, it provides a useful, approximate means of attributing dust emissions to underlying physical factors. Several authors have advocated its use as a predictive tool (e.g., Cowherd *et al.*, 1988, 1990), although these applications have been criticized because of inadequacies in the AP-42 model and the data from which it was developed. Principally, there is great uncertainty in the relationship between the amounts of PM_{10} size particles present in the road sediment and the processes or surface conditions that control their resuspension either by entrainment in turbulent vehicle wakes or by the shearing action of tires.

Zimmer *et al.* (1992) note that of AP-42 is often applied outside of the ranges of variables from which it was derived, and the results are thereby suspect. They also question the relationship between surface silt loadings and PM_{10} emission previously found for paved roads (Cowherd *et al.*, 1990). Recent evaluations by Zimmer *et al.* (1992) of dust emissions from paved roads in Denver, Colorado found no discernible relationship between the percent silt loading and PM_{10} emissions.

Muleski and Stevens (1992) found that the AP-42 model did not perform better than a simple regression model that only accounted for vehicle velocity in relation to dust emissions from unpaved road surfaces in the Phoenix, Arizona area. These investigators note that more than 90% of the tests that constitute the AP-42 data base were conducted with vehicle speeds lower than 56 km/hr and more than 80% of the data were derived from industrial haul roads involving use by very heavy vehicles. Muleski and Stevens (1992) also found legal vehicle speeds on unpaved roads in Arizona ranged between 56 and 89 km/hr, which was outside the vehicle velocity range of the original AP-42 data base.

However, the AP-42 formalism continues to provide some insight in terms of its approximate, empirical accounting of the major factors that influence emissions from unpaved roads.

2.5 Suppressant Properties and Method of Control

Chemicals are often applied to dusty surfaces to reduce emissions. These chemicals bond with the earth material to produce either a sealing effect or provide a cementing agent that keeps the dust-sized particles locked in the material matrix or attached to the larger non-entrainable particles. Chemical applications to road surfaces within agriculturally productive areas must meet standards set by the U.S. Department of Agriculture's Food Products Act. In the San Joaquin Valley Unified Air Pollution Control District, suppressant products must also conform to Rule 4641, which restricts the use of certain asphalt products due to their potential for emission of volatile organic compounds (VOC) and potential for surface and

groundwater contamination. Wet suppression is often used on industrial haul roads and is accomplished by repeated irrigation with water trucks during periods when traffic is present. This is not a viable option for public roads that have irregular usage.

Cowherd *et al.* (1990) classify suppressant compounds as bitumens, salts, and adhesives. ("Bitumen" is a generic term for coal, petroleum or asphalt compounds.) A more detailed classification is as follows:

1. Salts: These are hygroscopic compounds such as magnesium chloride or calcium chloride. They adsorb water when the relative humidity exceeds about 50%. Water improves the adherence of the soil particles to each other. Salts are often depleted by precipitation and runoff owing to their high solubility.

2. Resin or petroleum emulsions: These are non-water-soluble organic carbon compounds that are "emulsified" or suspended in water. When these emulsions are sprayed onto soil, they stick the soil particles together, and eventually harden to form a solid mass. There are several emulsion products based on tree resin, petroleum, or asphalt compounds.

3. Polymers: These act as adhesives which may be more effective than ordinary resins because their molecular structure is a long chain which in theory may be able to stick to more particles, or bridge larger particle-to-particle gaps.

4. Surfactants: These reduce water surface tension, allowing available moisture to more effectively wet the particles and aggregates in the surface layer.

5. Bitumens: These include materials such as asphalt or road oil that effectively pave the surface.

6. Adhesives: These include lignin sulfonate, a syrupy wood product (paper mill by-product) which creates a sticky but water-soluble layer.

7. Solid Materials: These include a petroleum industry by-product, made by mixing recycled materials with earth materials.

Some materials require repeated application at weekly to monthly intervals to retain their suppressant properties. The precise interval depends on the surface preparation, amount applied, traffic volume, vehicle weight, and environmental factors such as precipitation and temperature. Most suppressant manufacturers recommend grading and wetting roads before applying their products. Many suppressants can then be dispensed as liquids from a truck equipped with a tank and spray bar. The spray is intended to inject the suppressant as deeply as possible into the road material. Solid materials are spread and then mixed into the road with a grader.

2.6 Fugitive Dust Control Demonstration Studies

Beggs (1985) evaluated several demonstration studies according to the U.S EPA (1981) workbook guidelines for evaluating effectiveness of dust suppressant technology and found many of the published studies lacking in completeness and rigor. These early dust suppressant studies were concerned with measuring TSP (total suspended particulate); size-segregated particulate measurements were a secondary priority.

ETC (1981) examined the changes in TSP using high-volume (hivol) samplers placed at different heights and locations within Erie County, NY, near three major industrial processing plants (Donner Hanna Coke Plant, Republic Steel Plant, and Hanna Furnace Plant). ETC (1981) tried to place samplers in predominately upwind and downwind positions with respect to the emissions sources to which suppressants were applied. Samples were collected during periods with and without precipitation to measure the effectiveness of natural suppression agents such as rain or snow. Tests were conducted over 8 hours intervals when the wind direction was nearly aligned with the sampler array. Suppression techniques were: 1) vacuum sweeping on paved roads; and 2) application of a petroleum-based oil product on unpaved roads. ETC reported 40-60 percent reductions in TSP from sweeping and vacuuming of paved roads and a 40-60 percent reduction in TSP with oiling of unpaved roads. Beggs (1985) questioned the reliability of the ETC (1981) conclusions. Only a small number of tests were carried out (3 to 7) over a short time period. In addition, the sampling network was probably influenced by source activities even at "upwind" sites.

The Clark County Health District (1981) in Las Vegas, NV, attempted to evaluate the cost-effectiveness of magnesium chloride and Coherex suppressants in a similar study. Beggs (1985) found design shortcomings similar to those of ETC (1981).

Kinsey and Jirik (1982) evaluated the effectiveness of water spraying to reduce fugitive dust emissions from construction activities in Minneapolis, MN, using a receptor-oriented approach. TSP and intermediate size particles were measured upwind and downwind of the construction activity with 15 μm size-selective high-volume samplers and a 5-stage cascade impactor. $PM_{2.5}$ and PM_{10} concentrations were interpolated from the resulting size distributions. Beggs (1985) found the sampling and analysis procedures followed by Kinsey and Jirik (1982) to be sufficient. They extensively measured meteorological variables such as wind speed and direction, temperature and relative humidity, and other independent variables such as vehicle speed and number of passes.

Beggs (1985) criticized the small number of samples acquired by Kinsey and Jirik (1982), which is a typical criticism of most demonstration studies. The number of areas studied and the number of samples taken is directly proportional to the resources available, and these are always limited. Beggs (1985) also notes that road work during the experiment confounded the comparisons between the untreated and treated surfaces. Kinsey and Jirik (1982) attempted to simulate conditions without surface changes via regression analyses. Other contributors to the ambient measurements were also discovered when data were analyzed, also confounding the differences between emissions from treated and untreated

surfaces. Kinsey and Jirik (1982) concluded that watering was the only viable control strategy for fugitive dust emissions from construction sites. Beggs (1985), however, did not believe that the other treatments were adequately evaluated by this experiment.

Seton *et al.* (1983) examined sweeping of paved roads to ameliorate dust emissions. They evaluated several potential test sites prior to the measurements and planned for a large number of samples. They selected two test areas with four sampling locations for collocated TSP, PM_{15}, and $PM_{2.5}$ samplers. Two sampling stations were within the first test area and one was within the second area. A fourth control site, used for measuring ambient loadings and as an indicator of regional trends, was established in a similar area but outside the influence of the sweeping operations. The street sweeping followed a rigorous schedule, and important variables such as atmospheric dust concentrations, meteorological conditions, and traffic flow were monitored on a 24-hour basis. Seton *et al.* (1983) showed no statistically significant differences in particulate loadings at any of the three sites and the differences in air quality were attributed to random variations in the generation of particulate matter rather than to the effect of the control. This study represents an effective research design that reached meaningful, statistically-significant conclusions based on sound analysis of a sufficient amount of data.

Several other studies to evaluate street cleaning as an active means of reducing dust emissions failed to reach a definitive conclusions owing to the difficulty of testing one independent variable while other influential independent variables are not controlled. Record and Bradway (1978) and Hewitt (1981) examined the effectiveness of vacuum street cleaning, but they did not examine changes in meteorological conditions and traffic patterns. These uncontrolled variables could account for the differences in the ambient concentrations used to infer emissions.

Cuscino *et al.* (1983a) evaluated the effectiveness of vacuum sweeping using particle size-resolved vertical profile measurements of atmospheric dust loading. They found wide variability in particle concentrations measured through time after a sweeping/vacuuming event, noting that this was most likely related to the meteorological variability rather than to emissions changes. This study illustrates the importance of measuring independent variables that potentially have a greater effect on the dust loading than the intended control measure.

Rosbury and Zimmer (1983) made a significant methodological advance in estimating suppressant efficiencies by testing five suppressants on unpaved haul roads (watering, hygroscopic salt, surfactant, adhesive and bitumen). They used the methodology referred to by Frankel (1993) as "exposure profiling". This technique involves tower monitoring of the ambient concentrations of suspended particles upwind of the source and of the dust plume directly downwind. A ten meter was equipped with TSP and $PM_{2.5}$ stacked filter unit (SFU) samplers (Cahill, 1979) mounted at 1, 2, 5 and 9 m elevations. Their emission calculations for exposure profiling are based on the concept of conservation of mass (Rosbury and Zimmer, 1983). Mathematically, the emission rate per length of road for a given test was expressed as:

$$E = \int_0^H \frac{M(h)}{a} dh \qquad (2\text{-}6)$$

where:

E = emission rate (mg/cm^2)

M = net particulate mass collected by profiler sampler (mg)

a = sampler intake area (cm^2)

h = vertical distance of sampler above ground level (cm)

H = vertical extent of the plume above ground level (cm)

Rosbury and Zimmer (1983) expressed the weight of particulate mass collected on the filters as "net exposures" (mg/cm^2) by dividing the mass (mg) by the sampler intake area (cm^2). The upwind and downwind particulate exposures were determined by particle size, from which the net exposure, attributable to the road at the sampling location, was calculated. The net exposure was calculated as the difference between total downwind and upwind exposures at each height. Rosbury and Zimmer (1983) estimated the vertical extent of the plume is by extrapolating the net exposure values from the measured profile to an intersection with the height axis using a linearly scaled axis. The intersection of the extrapolated line with the height axis was assumed as the plume height. The net exposure at the 1 m sample height was assumed constant to ground level. Above 1 m, the net exposure was assumed to be a continuous linear function between measurements at adjacent elevations.

Based on their emission calculations from treated and untreated roadway sections, Rosbury and Zimmer (1983) estimated emissions reduction efficiencies by:

$$C = (1 - Ec / Eu) \times 100 \qquad (2\text{-}7)$$

where:

C = control efficiency (%)

Ec = controlled emission rate (mg/cm^2)

Eu = uncontrolled emission rate (mg/cm^2)

Each of the test sites was monitored simultaneously so a specific control efficiency could be calculated for each test surface. There was considerable variability in dust emission rates for the treated and untreated surfaces. Much of this variation was attributed to the changing meteorological conditions (especially precipitation), the types of vehicles using the road, and the initial road conditions. With simultaneous measurements, all the variables except roadway surface treatment were the same for each section of road, providing a

measure of control in the experiment. The general results of their suppressant control efficiency comparisons for chemical applications are shown in Table 2-3.

Rosbury and Zimmer (1983) did not develop emission factors. To obtain emission factors that could be applied over a broad range of conditions, the variation in measured emission rates must be evaluated with respect to simultaneously monitored, independent variables that characterize all the relevant physical and chemical conditions at the surface. Much of the variability that was observed in their emission rates was attributable to these variables.

The emission rate estimates were compromised by the three assumptions concerning the concentration versus height relationship in the dust plume: 1) the intersection of the extrapolated line with the height axis was accepted as the representative height of the plume; 2) the net exposure calculated at the 1 m sampling height was assumed constant to ground level; and 3) the net exposure was assumed to be a continuous linear function between two consecutive data points. These assumptions are not well supported by work that has measured mass concentration with height in dust plumes.

Field observations by several investigators show that dust concentrations over eroding surfaces decrease as a power function of height with exponents ranging from -0.25 to -0.35 (Chepil and Woodruff, 1957; Shinn *et al.*, 1976; Gillette, 1977; Nickling, 1978). Goosens (1985) found a lower exponent value of -0.186 for a slowly-moving dust cloud raised by the passage of motor vehicles. Net exposure profiles that are constant with height overestimate emission rates because the vertical extent of the plume is overestimated by linear extrapolation. The assumption of constant concentration with height below 1 m is also unsupported. The Rosbury and Zimmer (1983) methodology represents a significant advance over previous approaches, and their control efficiencies provide reasonable relative measures of suppressant effectiveness. Their tests were taken soon after the suppressants were applied, however; the effects of long-term degradation were not evaluated owing to resource constraints.

Muleski and Cowherd (1987) employed a methodology similar to that of Rosbury and Zimmer (1983) to evaluate the effectiveness of chemical dust suppressants on private unpaved roads associated with the iron and steel industry. These investigators sampled particles in PM_{15}, PM_{10}, and $PM_{2.5}$ size fractions at heights up to 6 m above the surface. Control efficiencies were assessed up to 70 days after suppressant applications. They also measured silt fractions, moisture contents, and the amount of loose surface material (kg/m^2) at different intervals after suppressant application.

Muleski and Cowherd (1987) report emission rates for their unpaved road surfaces similar to those found by Rosbury and Zimmer (1983). Average control efficiencies of approximately 50% or more were found for the first 30 days after application. Additionally, they found that for comparisons of control efficiency between suppressants, there were virtually no differences between suppressant types after 30 days.

Table 2-3
Comparison of Control Efficiency Results for Chemicals from Rosbury and Zimmer (1983)

Control	Device	Particle Size Cut, μm	Height, m	Isokinetic Flow	Average Calculated Control Efficiency (in percent) Mine 2 Mix	Mine 2 Top	Mine 2 Time, weeks	Mine 3 Mix	Mine 3 Top	Mine 3 Time, weeks
Salt	Tower,	30	1-9	yes	44	58	1-4	10	21	2-3
	TSP SSI	15	1.5	no	52	56		7	10	
	Tower, FP	2.5	1-9	yes	43	41		24	8	
	Ram-1	3.0	1.0	no	44	46		6	0	
Surfactant[a]	Tower,	30	1-9	yes		33	1-5		19	1-2
	TSP SSI	15	1.5	no		19			25	
	Tower, FP	2.5	1-9	yes		25			33	
	Ram-1	3.0	1.0	no		46			28	
Adhesive	Tower,	30	1-9	yes	54	35	1-4	38		1-3
	TSP SSI	15	1.5	no	47	29		49		
	Tower, FP	2.5	1-9	yes	37	30		46		
	Ram-1	3.0	1.0	no	36	48		27		
Bitumen	Tower,	30	1-9	yes	20	24	1-4	44	56	
	TSP SSI	15	1.5	no	22	36		55	80	
	Tower, FP	2.5	1-9	yes	26	28		33	73	
	Ram-1	3.0	1.0	no	54	51		50		

[a] All topical applications.

Chow *et al.* (1990) conducted a street sweeping study specifically addressing the potential reduction of PM_{10} emissions from paved roads. Chow *et al.* (1990) used receptor models to determine the contributions from dust and from primary motor vehicle exhaust. They compared the ratio of primary geological contributions to motor vehicle contributions to PM_{10} between sweeping and non-sweeping periods. This comparison showed no significant differences in geological contributions between the different periods. The authors concluded that daily street sweeping with a regenerative air vacuum sweeper resulted in no detectable reductions in geological contributions to PM_{10} in the sweeping area. The street sweeper used in the study proved to be ineffective for reducing the PM_{10} emissions from the road surface.

Stevens (1991) used exposure profiling and a conservation of mass approach to calculate emission rates of PM_{10} and TSP from unpaved road surfaces in Arizona. The purpose of the study was to recommend a mathematical model for estimating emissions from unpaved road surfaces and examine the feasibility of using an ambient concentration standard to regulate public unpaved roads in Arizona. Although not a dust suppressant effectiveness study, Stevens (1991) provides emission rate estimates for three locations in Arizona along with some measures of surface characteristics, including silt and moisture content.

Grau (1993) evaluated methods for controlling dust emissions from surfaces that may emit dust during military operations, including unpaved roads. This study included a screening process; suppressant-treated soil specimens were prepared under controlled laboratory conditions to determine their performance when subjected to simulated field conditions. The screening tests included one minute blasts from 80 km/hr and 160 km/hr air jets at 20° from the horizontal, simulated rainfall, a repeat of the air impingement test, and simulated jet fuel spills followed by another air jet test. Forty-nine suppressants were screened; eleven were accepted and subjected to limited field tests. Suppressant effectiveness judgments were based on observers' subjective perceptions. The lack of quantitative data compromises this study and it cannot be placed in the context of previous work.

Mitra *et al.* (1993) proposed a tracer technique for estimating emission rates of PM_{10} from road surfaces. Mitra *et al.* (1993) believe that tracer species obviate the need for measuring vertical profiles and meteorological variables. A tracer substance is released along the roadway at the level of dust suspension. Emission rates are calculated from the tracer release rate and downwind measures of dust and tracer concentrations:

$$Q_P = Q_t \times \frac{C_p}{C_t} \tag{2-8}$$

where:

Q_p = PM_{10} emission rate (µg/m s)

Q_t = measured tracer release rate (µg/m s)

C_p = downwind PM_{10} concentration ($\mu g/m^3$)

C_t = downwind tracer concentration ($\mu g/m^3$)

A critical assumption in applying the tracer method is that the tracer and the dust disperse from the source in similar ways. A second assumption is that deposition of particles between the source and the downwind samplers is minimal because the tracer does not undergo deposition. The use of gaseous tracers for estimating PM_{10} is promising only if these assumptions are justified (Frankel, 1993). Their validity depends on the emission height and the meteorological conditions. For example, if the dust emission are close to the ground, significant deposition may occur within 100 m downwind from the source, especially under certain weather conditions. Significant reflection of the tracer from the ground could occur over the same distance while the dust would tend to remain on the surface. Mitra *et al.* (1993) recommend sulfur hexafluoride as a tracer gas.

In order for this method to be employed successfully, Frankel (1993) recommends that the dust source geometry and tracer source location must facilitate plume mixing, and that both dust and tracer sampling should be done at a number of locations and distances. Mitra *et al.* (1993) propose that the tracer data be utilized to optimize a roadway dispersion model so the model can be used with measured PM_{10} concentrations to back-calculate PM_{10} emission rates. If the model provides reasonably accurate predictions based on tracer data,

Flocchini *et al.* (1994) quantify fugitive dust emissions of PM_{10}-size particles from unpaved roads that are dominated by agriculture-related vehicular traffic in California's San Joaquin Valley for several suppressants. Watering, gravel cover, lignin sulfonate, magnesium chloride, oiling, and non-hazardous crude oil suppressants were compared. PM_{10} and size-segregated particle mass concentrations were measured with IMPROVE (Eldred *et al.*, 1988) and DRUM (Raabe *et al.*, 1988) samplers at upwind and downwind locations with respect to the control and treated test areas. The suspended sediment concentration gradients with height were measured in $PM_{2.5}$ and coarse (TSP minus $PM_{2.5}$) size ranges with SFUs (Flocchini *et al.*, 1981). In addition to the emission rates, Flocchini *et al.* (1994) measured surface characteristics associated with each of their test plots. Samples of loose surface material were collected for each test plot to determine the soil type, mass per unit area, moisture content, and percentage of fine silt (less than 75 μm particle diameter). Surface samples were also analyzed using laboratory resuspension chamber techniques to measure the relative potential for PM_{10} emissions from each surface.

Flocchini *et al.* (1994) isolated the unpaved road contributions by using upwind measurements as background. The upwind concentration measurements ($\mu g/m^3$) were subtracted from downwind measurements, leaving only the concentrations at the measurement location (10 m downwind, 3.3 m in height) resulting from vehicles traveling on the unpaved roads. Emission rates in mg/km were calculated from the equation:

$$X = \frac{VHC}{N} \times 3600 \frac{\text{sec}}{hr} \qquad (2\text{-}9)$$

where:

X = emission rate per vehicle (mg/km)

V = wind speed perpendicular to road (m/s)

H = box height (m)

C = PM_{10} aerosol concentration 10 m from middle of road ($\mu g/m^3$)

N = number of vehicles per hour

The emission estimates are based on the "sliding box" model (Feeney *et al.*, 1975; Barone *et al.*, 1981), which uses the airborne PM_{10} concentrations in an air volume over a sample period to quantify the emission rate. The "box" dimensions are based on an estimated length determined by the wind speed perpendicular to the road and the height is determined from the vertical profile of TSP measured from 3 to 9 m. The box height is determined by integrating aerosol concentrations with height between 3 and 9 m, then dividing by the maximum measured concentration, producing a value with the units of length. The horizontal mass flux per unit of road length and time is calculated by multiplying the PM_{10} concentration ($\mu g/m^3$) measured 10 m downwind from the road by windspeed (m/s) and box height (m). Dividing by the number of vehicles per hour results in the mass emission per vehicle distance traveled. The effectiveness of a suppressant is estimated by comparing the emission rates from an untreated site with the emission rates measured at the suppressant application sites, as expressed in Equation 2-7. The rankings of the unpaved road treatments for their effectiveness in reducing PM_{10} emissions are listed in Table 2-4.

Three of the suppressants were applied under controlled conditions by contractors (lignin, MgCl, and non-hazardous crude oil), but the road oil and gravel treatments were done at an earlier time with no indication of the time between application and the emission testing. The choice of three different locations for the suppressant tests increases the difficulty of comparison because textural differences in the road bed between the sites may differ. For this study, only 28 tests were carried out, with a maximum of three tests per treatment site.

The methodologies and critical points of these published dust control demonstration studies are summarized in Table 2-5. The accurate estimation of dust emissions from a line or area source requires upwind and downwind exposure profiling. Tracer approaches show some promise, but they require unproven assumptions concerning the similarity of gaseous tracer material and depositing particles. Most previous exposure profiling studies have used short suppressant test sections, limited sampling arrays, and short intervals after suppressant application.

Emission rates and suppressant effectiveness data derived from selected studies are summarized in Table 2-6. These estimates are uncertain because:

- Particle measurements close to the emitting source give point estimates of concentrations embedded within clouds and plumes of material that are highly variable in space and time.

- Particle measurements taken at any appreciable distance from the source are depleted when heavier particles fall out of the plume before it reaches the sampler, and because the plume is dispersed in the horizontal and vertical directions.

- Particle measurements taken near the surface may not accurately represent the concentrations of particles at higher levels in the plume (i.e., significant uncertainties are involved in assuming plume structure by extrapolating upwards).

Table 2-4
Rankings of the Unpaved Road Treatments for their Effectiveness in Reducing PM_{10} Emissions from Flocchini *et al.* (1994)

Effectiveness Rank	Treatment	PM_{10} Reduction Efficiency
1	Recycled Oil Mix	~ 99%
2	Lignin Sulfonate	99%
3	Magnesium Chloride	98%
4	Water	87% ± 6%
5	Oiled Road	59% ± 12%
6	Speed Reduction (25 to 10 mph)	58% ± 3%
7	Speed Reduction (25 to 15 mph)	42% ± 35%
**	Gravel	Emissions from the gravel test section appeared to exceed those of the untreated section.

Table 2-5
Summary of Previous Dust Demonstration Research

Study	Purpose	Methodology	Comments
Roberts *et al.* (1975)	Examine the cost and benefits of road dust control in Seattle's Industrial Valley.	Moving point source measurements.	Quantity of dust generated by vehicles increases exponentially with wind speed. Paving was the most cost effective method for reducing dust emissions.
Seton *et al.* (1983)	Examine the effectiveness of street vacuuming as a control measure.	A receptor-oriented approach.	No statistically-significant difference in particulate loadings at any of the three sites. An effective research design that reached meaningful conclusions based on sound analysis of the collected data.
Record and Bradway (1978)	Examine the effectiveness of street vacuuming as a control measure.	A receptor-oriented approach.	Failed to consider or report the effects related to the meteorological conditions and traffic patterns.
Hewitt (1981)	Examine the effectiveness of street vacuuming as a control measure.	A receptor-oriented approach.	Failed to consider or report the effects related to the meteorological conditions and traffic patterns.
Cuscino *et al.* (1983)	Examine the effectiveness of street vacuuming as a control measure.	Size resolved vertical profile measurements of atmospheric dust loading.	Found wide variability in the dust concentrations measured through time after sweeping/vacuuming. Independent variables have potentially greater effects on the dust loading than the intended control measure.
Chow *et al.* (1990)	Examine the effectiveness of street vacuuming as a control measure for PM_{10}.	Receptor models to determine the contributions from dust and from primary motor vehicle exhaust.	Daily street sweeping with a regenerative air vacuum sweeper resulted in no detectable reductions in geological contributions to PM_{10} in the sweeping area.

Table 2-5 (continued)
Summary of Previous Dust Demonstration Research

Study	Purpose	Methodology	Comments
ETC (1981)	Examine the changes in TSP emissions before and after suppression.	A receptor oriented methodological approach.	Only a small number of tests were carried out (3 to 7) and there was no rigorous application of statistical analysis.
Clark County Health District, Air Pollution Control Division, 1981	Evaluate the cost-effectiveness of two chemical suppressants.	A receptor oriented methodological approach.	Effectiveness of one suppressant over the other was not established because of poor experimental design.
Kinsey and Jirik (1982)	Evaluate the effectiveness of water spraying to reduce fugitive dust emissions from construction sites.	A receptor oriented methodological approach. Fine particles and PM_{10} were interpolated.	Insufficient sample sizes, lack of strict controls.
Dyck and Stukel, 1976	Describe dust emissions by vehicle transport over the "infinite line source".	Develop emission rate equation for vehicles traveling on unpaved roads.	Methodological approach for calculating emission rates could be used for comparison purposes in a strategy that deployed receptor measurements at one height downwind of the road.
Rosbury and Zimmer (1983)	Study effectiveness of five types of dust suppressants on unpaved haul roads (watering, hygroscopic salt, surfactant, adhesive and bitumen).	Exposure profiling, emission rates calculated with conservation of mass principles.	Determined control efficiencies, observed that variability in the variables were key to explaining the measured emission rates, and compared effectiveness of suppressants.

Table 2-5 (continued)
Summary of Previous Dust Demonstration Research

Study	Purpose	Methodology	Comments
Muleski and Cowherd (1987)	Evaluate the effectiveness of chemical dust suppressants on unpaved roads at industrial sites.	Exposure profiling, emission rates calculated with conservation of mass principles.	Determined temporal changes in effectiveness through 30-70 days of road use.
Stevens (1991)	Recommend a mathematical model for estimating emissions from unpaved roads in Arizona.	Exposure profiling, emission rates calculated with conservation of mass principles.	Emission rate estimates for three locations in Arizona along with some measures of surface characteristics including silt content and moisture content.
Grau (1993)	Evaluate methods for controlling dust emissions from surface that may emit dust during military operations.	Subjective assessment of plume intensity from emitting surfaces.	Used an extensive pre-screening process to determine best potential suppressants for field study. A qualitative study.
Flocchini *et al.* (1994)	Quantify fugitive dust emissions of PM_{10} size particles from unpaved roads by agriculture vehicle use.	The "sliding box " model. Upwind-downwind sampling.	Sampling strategy appears sound, however, the design and execution make it difficult to objectively discern the apparent effectiveness attributed to the suppressants.

Table 2-5 (continued)
Summary of Previous Dust Demonstration Research

Study	Purpose	Methodology	Comments
Mitra *et al.* (1993)	Develop a tracer technique for estimating emission rates of PM_{10} from road surfaces.	Knowledge of the tracer release rate and downwind concentration measures of dust and tracer results in dust emission rate calculation.	The assumptions of similar dispersion and no particulate deposition are questionable. The validity of the assumptions would be dependent on the emission height and the meteorological conditions.

Table 2-6
PM_{10} Emission Rates

Study	Treatment	Surface Characteristics: Silt Content (percent)	Silt Loading (g/m^2)	Moisture Content (percent)	Vehicle Speed (km/h)	Emission Rate (g/KVT)[a]
Stevens (1991)	none	11	110	0.2	45	630
	none	11	110	0.2	55	910
	none	11	110	0.2	35	430
	none	7	32	0.2	45	700
	none	7	32	0.2	55	1,340
	none	7	32	0.2	35	490
	none	4	11	0.2	35	730
	none	4	11	0.2	55	1,560
	none	4	11	0.2	45	1,780
Flocchini *et al.* (1995)	none	22	181	0.6	40	3,620
	none	21	174	0.5	24	1,190
	none	22	192	0.5	16	1,440
	lignin sulfonate	4	13	6.1	40	50
	lignin sulfonate	4	12	6.1	40	40
	none	21	184	0.7	40	3,610
	none	21	197	0.6	24	3,010
	none	22	223	0.5	16	1,610
	MgCl	4	14	2.4	40	320
	MgCl	4	15	2.2	40	340
	oil	11	62	0.8	40	120
	oil	11	62	0.8	40	150
	oil	11	67	0.4	40	180
	gravel	7	99	1.4	40	410
	gravel	10	180	1.3	40	480
	gravel	8	165	1.2	40	460
	none	14	168	0.6	40	440
	none	11	80	10.5	40	420
	none	13	109	13.0	40	670
	none	13	100	13.3	40	480

[a] Grams per vehicle-kilometer-traveled.

3.0 SUPPRESSANT OPTIONS AND SELECTION

Many individual products are available on the commercial market for dust suppression. Only a few of these could be evaluated in this study. This section lists the options available and describes the criteria for selecting the suppressants applied to an unpaved public road and an unpaved shoulder alongside a heavily traveled paved road.

3.1 Suppressant Options

The following types of suppressants are unsuitable for this demonstration study: 1) products that do not comply with SJVUAPCD Rule 4641, or any other applicable statutes regarding water quality or product toxicity; 2) water sprays, owing to their temporary nature; 3) vegetation, with the possible exception of already-existing vegetation on the unpaved shoulder test sites; and 4) products involving extraordinary logistical requirements, transportation costs, or application technologies.

Table 3-1 lists suppressant products determined by a survey and literature review at the initiation of this study. These products are categorized according to their composition and the suppressant mechanism they employ.

Cost information obtained during this study is summarized in Table 3-2. Where available, material, and application costs for both unpaved roads and shoulders are given. Suppressant material costs ranged from $0.09 to $1.22 per square yard. One mile by ten feet of lane equals 5,867 square yards. Costs per mile for each ten feet of lane width are ~$600 for a suppressant costing $0.10 per square yard, and ~$5,870 for a suppressant costing $1.00 per square yard.

The costs of surface preparation are usually included in the application costs cited in Table 3-2. These data indicate that application costs often exceed the costs of the suppressant materials, on a per-square-yard basis. The surface preparation and application costs vary widely from one product to another. They are difficult to specify concisely and on a common basis. Vendors typically want the unpaved surface prepared according to their specific specifications, making it difficult to compare costs for different products. One manufacturer may call for a combination of grading and scarifying, with applications repeated at certain intervals. Another manufacturer may want grading and rolling with different application intervals, etc. There are also cost differentials that depend on the proximity of the vendor to the application site, the total amount of roadway to be treated, and the supply of and demand for the suppressant material. Specific cost quotes need to be obtained prior to undertaking a roadway treatment.

For comparison to the cost figures cited in Table 3-2, Mr. John Graves, Merced County Road Superintendent, indicated that the cost of grading and watering Fields Road prior to this study totaled ~$1,000, or about 4 cents per square yard.

3.2 Selection Criteria and Procedure

Table 3-1 presents the vendors that were requested to respond to a proposal for suppressant application. Vendors were given the locations of the study sites and asked to scope coverage of test segments, either on Fields Road, or of unpaved shoulders on both sides of Bellevue Road in Merced County. Proposals were reviewed and suppressants were selected on the basis of: 1) obtaining a representative variety of modern products which meet toxicity and VOC criteria; 2) cost effectiveness; and 3) feasibility of logistics and application method.

Beyond normally scheduled grading provided by the Merced County Department of Public Works, surface preparation and suppressant application were the sole responsibility of the suppressant manufacturer. Test segments were assigned to each vendor, and suppressant application was supervised by the study field manager. Table 3-3 describes suppressants applied and their corresponding roadway segments. The unpaved road and shoulder suppressants were applied on July 13-18, 1995, except for "Non-Hazardous Crude-Oil-Containing Materials", which was applied on October 17-19, 1995.

Table 3-1
Suppressants and Vendors

Product Name and Active Ingredient	Vendor Information
A. SALTS	
Calcium Chloride	Lee Chemical, Inc. 21250 Box Springs Road Moreno Valley, CA 92387 Attn: Bud Bardsley (909) 369-5292
Calcium Chloride	Hill Brothers Chemical Company 1675 N. Main Street Orange, CA 92667 Attn: Alfred McCarthy (714) 998-8800
Magnesium Chloride	Western Spreading and Transportation, Inc. 641 Rock Springs Road Escondido, CA 92025 Attn: Nick Izzi (909) 784-7411
MgCl ("Dust-Off")	South Western Sealcoating, Inc. 23644 Adams Ave. Murietta, CA 92562 (909) 677-6228
MgCl ("Dust-Off")	California-Fresno Oil Company PO Box 527 Fresno, CA 93709 (209) 486-0220
MgCl	Jim Good Marketing P.O. Box 717 Shafter, CA 93263 Attn: Jim Good (805) 746-3783

Table 3-1 (continued)
Suppressants and Vendors

Product Name and Active Ingredient	Vendor Information
A. SALTS (continued)	
MgCl	Chemical Distributors, Inc. 201 Bryce Court Henderson, NV 89105 Attn: Carrie Burgess (702) 565-4904
MgCl	Soil Stabilization Products Co. P.O. Box 2779 Merced, CA 95344 Attn: Glen Gates or Marsh Pitman (800) 523-9992
MgCl	Dustpro, Inc. 2432 W. Peoria Ave. Suite #1160 Phoenix, AZ 85029 Attn: Greg Frey (602) 944-8411
"Brine"	Leslie Salt Co. 7200 Central Ave. Newark, CA 94560 (415) 790-8169
B. ASPHALT/PETROLEUM EMULSIONS	
Coherex (Petroleum resin emulsion)	WITCO, Golden Bear Division P.O. Box 456 Chandler, AZ 85244-0161 Attn: Roy McNeal (602) 963-2267
Retain (asphalt emulsion)	Diversey Corp Attn: Linda Coffee or Randy Bryan (818) 961-6305

Table 3-1 (continued)
Suppressants and Vendors

Product Name and Active Ingredient	Vendor Information
B. ASPHALT/PETROLEUM EMULSIONS (continued)	
Asphotac (asphalt emulsion)	Pragma, Inc. P.O. Box 1658 Sutter Creek, CA 95685 Attn: Ray Hunter (209) 267-5072
Dust Oil Emulsion (asphalt emulsion)	Morgan Emultech, Inc. 7200 Pit Road P.O. Box 1500 Redding, CA 96099 (916) 241-1364
Pennzsuppress D	Pennzoil Products Company 12070 Telegraph Road Suite #324 Santa Fe Springs, CA 90670 Attn: Brad Welshans (310) 906-4300
FlowPro 1505 (petroleum resin emulsion)	Betz Water Management Group Big Valley District Office 4201 Ardmore Way ,#7 Bakersfield, CA 93309 (805) 835-9194
C. OTHER EMULSIONS	
Road Oyl (tree resin emulsion)	Soil Stabilization Products Co. P.O. Box 2779 Merced, CA 95344 Attn: Glen Gates or Marsh Pitman (800) 523-9992

Table 3-1 (continued)
Suppressants and Vendors

Product Name and Active Ingredient	Vendor Information
C. OTHER EMULSIONS (continued)	
Pineseal (tall oil pitch, tall oil rosin, and lignin)	Western Emulsions Inc. Dust Control Division 22155 Big Timer Road Moreno Valley, CA 92557 Attn: Nicolas J. Izzi (909) 784-7411
Enduraseal 100 and 200 (organic, water-based emulsions)	Cascadia Technologies Ltd. 602-626 West Pander St. Vancouver, B.C., Canada V6B1V9 Attn: Glenn Coward (800) 665-2994 Environmental Products and Applications Co. 15017 Notnil Way Lake Elsinore, CA 92530 Attn: John Vermillion (909) 674-9174
Entac (organic emulsion)	Diversified Services, Inc. P.O. Box 337 Elizabethton, TN 37644 Attn: John McDonnell (615) 542-9100
D. LIGNIN SULFONATE	
Lignin Sulfonate	RBJ Transport, Inc 1735 N. Ashby Road Merced, CA Attn: Tim Prothro (209) 722-2731

Table 3-1 (continued)
Suppressants and Vendors

Product Name and Active Ingredient	Vendor Information
D. LIGNIN SULFONATE (continued)	
Lignin Sulfonate	Midwest Industrial Supply, Inc. P.O. Box 8431 Canton, OH 44711 Attn: Frank Elswick (805) 937-7157
Lignin Sulfonate ("Calbinder")	California-Fresno Oil Company PO Box 527 Fresno, CA 93709 (209) 486-0220
DUSTAC	Georgia Pacific Monrovia, CA (800) 955-5498
E. POLYMERS	
Coherex PM (petroleum emulsion with polymer)	WITCO, Golden Bear Division P.O. Box 456 Chandler, AZ 85244-0161 Attn: Roy McNeal (602) 963-2267 Reed and Graham, Inc. 8280 14th Ave. Sacramento, CA 95826 Attn: Steve Aguirre (916) 454-2560
Soil Sement (polymer emulsion)	Midwest Industrial Supply, Inc. P.O. Box 8431 Canton, OH 44711 Attn: Frank Elswick (805) 937-7157

Table 3-1 (continued)
Suppressants and Vendors

Product Name and Active Ingredient	Vendor Information
E. POLYMERS (continued)	
Soil Master WR (co-polymer with "Tripolycate")	Environmental Soil Systems Inc. 13234 Whistler Ave. Granada Hills, CA 91344 Attn: Rick Granard (800) 368-4115
DC-1000	Native Soil Technology, Inc. P.O. Box 502 Danville, CA 94526 Attn: Bob Crandall (510) 837-5362
DSS-40 (acrylic co-polymer)	S&S Seeds P.O. Box 1275 Carpenteria, CA 93013 Attn: Victor Schaff (805) 684-0436
DSS-40 (acrylic co-polymer)	Karleskint-Crum, Inc. PO Box 5358 San Luis Obispo, CA 93403 (805) 543-3304
DSS-40 (acrylic co-polymer)	J&M Land Restoration, Inc. 1640 James Rd. Bakersfield, CA 93308 (805) 872-7039
Eco-Polymer	Eco-Polymers, Inc. P.O. Box 4860 Cerritos, CA 90703-4860 Attn: Ron Reed (310) 407-3090

Table 3-1 (continued)
Suppressants and Vendors

Product Name and Active Ingredient	Vendor Information
E. POLYMERS (continued)	
Marloc (co-polymer)	Reclamare Company 20727 - 7th Avenue S. Seattle, WA 98198 Attn: Edward R. Johston (206) 824-2385
Soil Seal	Soil Seal Corporation 3015 Supply Avenue Los Angeles, CA 90040 (213) 727-0654
Terrafirma	AET Group 655 Lewelling Blvd., Suite 315 San Leandro, CA 94579 Attn: Regan Jones (209) 836-4884
ECO-110 and C-50	Dynaguard, Inc. 1034 N. Lemon Street Orange, CA 92667 Attn: Craig Hoad (714) 771-7411
Blend R40 Series (polymer emulsions)	Rohm and Haas Company Toxicology Department 727 Norristown Road P.O. Box 904 Spring House, PA 19477-0904 Attn: J.D. Hamilton (215) 641-7000
Polymers/Enzymes	Boston/ASTC 521 Westminster Ave. Newport Beach, CA 92663 (714) 646-1207

Table 3-1 (continued)
Suppressants and Vendors

Product Name and Active Ingredient	Vendor Information
F. FIBERS AND MULCHES	
Agri-Fiber	Precision Hydroseeding Company P.O. Box 12336 Palm Desert, CA 92255 Attn: Jim Sullivan (619) 360-2851
A/F 2000	American Fiber Company 10820 Beverly Blvd., Suite 322 Whittier, CA 90601 (310) 693-4072
Fiberwood (hydroseeding mulch)	Fiberwood 5854 88th Street Sacramento, CA 95828 Attn: Rob Rischback (800) 655-9754
Fibercraft (hydromulch cellolose fiber)	Dynamis, Inc. P.O. Box 397 Sanger, CA 93657 (209) 875-0800
Stabilizer (organic binder)	Stabilizer, Inc. 4832 East Indian School Phoenix, AZ 85018 Attn: Tim Myers (602) 952-8009
Dewatered Residual Wood Fiber	C.E.T.I. 15568 Slover Ave. Fontana, CA 92334 Attn: Steve McGuire (909) 428-6861

Table 3-1 (continued)
Suppressants and Vendors

Product Name and Active Ingredient	Vendor Information
F. FIBERS AND MULCHES (continued)	
Dewatered Residual Wood Fiber	Envirosorb 1815 Wright Ave. La Verne, CA 91750 Attn: Steve McGuire (909) 392-5878
Soil Guard (bonded fiber matrix)	S&S Seeds P.O. Box 1275 Carpenteria, CA 93013 Attn: Victor Schaff (805) 684-0436
Excel-Fibermulch II (Aspen wood mulch)	American Excelsior Company 8320 Canford Street Pico Rivera, CA 90660-3702 Attn: Larry Halweg (310) 949-2461
Cellulose Fiber (Ecology Controls "M-Binder")	Sanders Hydroseeding, Inc. 1708 South Santa Fe Santa Ana, CA 92705 (714) 973-TURF
Cellulose Fiber (Ecology Controls "M-Binder")	S&S Seeds P.O. Box 1275 Carpenteria, CA 93013 Attn: Victor Schaff (805) 684-0436
Hydrophilic colloid derived from seed husks ("Sentinel")	Albright Seed Company 487 Dawson Drive Bay 55 Camarillo, CA 93012 (805) 484-0551

Table 3-1 (continued)
Suppressants and Vendors

Product Name and Active Ingredient	Vendor Information
F. FIBERS AND MULCHES (continued)	
Ecotak-OP and Ecotak-SAT	Elloitt Landscaping 68-315 Durango Road Cathedral City, CA 92234 Attn: Mukul Joisher (619) 320-0176
G. UNCLASSIFIED	
AGRI-LOCK and DUST-LOCK (synthetic resin and organic compound)	SWIFT Adhesives 2400 Ellis Road Durham, NC 27703-5543 Attn: Wes McCoy (800) 213-4804
Calcium sulfate hemihydrate (plaster) and cellulose or wood fiber mixture ("Airtrol Plaster")	United States Gypsum Company Industrial Gypsum Division PO Box 803871 Chicago, IL 60680-3871
P.E.P. (liquid asphalt)	Environmental Products & Applications 15017 Notnil Way Lake Elsinore, CA 92530 Attn: John Vermillion (909) 674-9174
EnviroCycle (solid material: hydrocarbon-soil mix)	EnviroCycle, Inc. 21992 Hiway 33 McKittrick, CA 93251 Attn: John Webb, President (800) 324-4484
Dust Buster Systems (chemical suppressants and application equipment)	Martin Marietta Magnesia Specialties, Inc. 9308 Nickam Court Bakersfield, CA 93311 Attn: Robert Samson Jr. (805) 663-0625

Table 3-1 (continued)
Suppressants and Vendors

Product Name and Active Ingredient	Vendor Information
G. UNCLASSIFIED (continued)	
Dust Sorb 1118 (acrylic resin)	Aqua Chem Ltd. P.O. Box 1138 Bakersfield, CA 93389 (805) 323-8308
Biocatalyst ("EMC Squared")	Ophir Oil Company PO Box 898 Newcastle, CA 95658 (916) 885-0491
DC 300 (non-ionic surfactant)	Compaction Compounds, Inc. 101 First Street, Suite 402 Los Altos, CA 94022 Attn: Mary Anne Rosenthal (415) 948-5900
Organic Soil Stabilizer (soil additive)	Desert Rock Supply P.O. Box 924 La Quinta, CA 92253 Attn: Jim Marquardt (619) 360-1345
Lime mixture ("POZ-O-CAP")	Metamorphosis Hydroseeding, Inc. 1022A San Andreas Rd. La Selva, CA 95076 (800) 99-4SEED
Sandcastles Dust Control Mix	Sandcastle Hydroseeding 42529 8th St. East Lancaster, CA 93535 Attn: Betty McWilliams (805) 723-0515

Table 3-1 (continued)
Suppressants and Vendors

Product Name and Active Ingredient	Vendor Information
G. UNCLASSIFIED (continued)	
Endosperm product ("Hydroshield")	Chem Shield 1475 E. Greg Street Sparks, NV 89434 Attn: Richard L. Maile (702) 323-4540
Sodium Silicate	PQ Corporation ICD Sales Department 8401 Quartz Ave. South Gate, CA 90280-2589 (213) 560-4891
Raybinder	ITT Rayonier P.O. Box C-68967, Suite 900 Seattle, WA 98188 (800) 228-0604

Table 3-2
Dust Suppressant Material and Application Costs (1995)[a]

Suppressant Product	Composition	Material Cost per square yard	Application Cost Unpaved Roads, per square yard	Application Cost Unpaved Shoulders, per square yard
1.) "Dustguard"	Salt: MgCl	$0.23	$0.24	not available
2.) "Enduraseal"[b]	Tree Resin Emulsion	$1.22	$0.26	$0.26
3.) "Road Oyl"	Tree Resin Emulsion	$0.22	$0.51	$0.77
4.) "DSS-40"[b]	Acrylic Copolymer	$0.35	$0.09	$0.09
5.) "Soil Sement"[b]	Polymer Emulsion [c]	$0.29-0.47	$0.07-0.11	not available
	Polymer Emulsion [d]	$0.75	$0.18	not available
6.) "Coherex PM"[b]	Petroleum Emulsion with Polymer	$0.25 $0.30	$0.30	$0.26
7.) "EMC Squared"[b]	Biocatalyst Stabilizer	$0.27	$0.42	$0.52
8.) "Hydroshield"[b]	Sodium Endosperm Hydrate	$0.09	not available	not available

[a] Cost information from responses to DRI Request for Proposal 5202-01, May, 1995.
[b] Product used in this Demonstration Study.
[c] Topical application, used in this study.
[d] Scarified application.

Table 3-3
Suppressants Applied in Demonstration Study

Test Segment	Segment Length	Suppressant
Fields Road 1	541 m	"Non-Hazardous Crude-Oil-Containing Materials
Fields Road 2	541 m	"EMC Squared" Biocatalyst
Fields Road 3	541 m	"Soil Sement" Polymer Emulsion
Fields Road 4	541 m	"Coherex PM" Petroleum Emulsion with Polymer
Fields Road 5	541 m	Untreated
Bellevue Road Shoulders 1	746 m	"Enduraseal" Organic Emulsion
Bellevue Road Shoulders 2	606 m	Untreated
Bellevue Road Shoulders 3	782 m	"Hydroshield" Endosperm Hydrate
Bellevue Road Shoulders 4	750 m	"DSS-40" Acrylic Co-polymer

4.0 EXPERIMENTAL APPROACH FOR UNPAVED ROADS

This section describes the unpaved road study location, the locations of the monitoring sites on Fields Road, and the instrumentation used to measure ambient PM_{10} concentrations and the test surface characteristics.

4.1 Road Selection

Criteria applied in the search for appropriate unpaved public road test sites in California's San Joaquin Valley included length, direction, topography and traffic.

- **Length:** The test strip for each suppressant should be several hundred meters long, preferably 300 to 1000 m, to minimize downwind mixture of emissions from each strip. Dust trackout from one strip to the adjacent strip may cover the suppressant in the 10 to 50 m portion at each end of the strip. The road tested needs to be several kilometers long to test several suppressants at the same time.

- **Direction:** A significant component of the prevailing wind direction should be perpendicular to the roadway during sampling periods. The prevailing wind direction in the San Joaquin Valley is from north-northwest to south-southeast, along the Valley's axis. Most of the roads in the Valley run north to south, with the exception of the two major highways (I-5 and SR 99) that follow the Valley's axis. Lacking unpaved roads with south-southwest to north-northeast orientations, east-west roads were sought in preference over north-south roads.

- **Topography:** Upwind and downwind sampling requires unobstructed terrain on both sides of the road for a distance of 1 km or more. This assures that winds will be consistent across the entire set of test sections and allows for the convenient placement of downwind samplers. Flat terrain also ensures that each sampler obtains measurements in the same part of the plume from each test section and that particles to not deposit onto obstructions. Sites immediately adjacent to other sources were avoided to prevent confounding contributions from emissions other than those from the road.

- **Traffic:** Traffic volumes and types should be typical of those on unpaved public roads throughout the San Joaquin Valley. This is fairly light, with ~100 vehicle passes per day for most days of the year, with mostly light-duty vehicles. This is in contrast to agricultural roads that experience heavy traffic over short periods of time during harvests.

County road superintendents, commissioners, and maintenance supervisors sere consulted in Merced, Madera, Fresno, Kings, Tulare, and Kern Counties to identify and evaluate possibilities. Public unpaved roads meeting these criteria were not found in the western part of Kern County included in the SJVUAPCD, though several good candidates were identified in the Mohave Desert portion of the county. Possibilities in Madera and

Tulare Counties were limited. Several possible test sites were identified in Merced, Fresno, and Kings Counties. The Fields Road location in Merced County was selected for the experiment because it best complied with the test criteria cited above.

4.2 Experimental Setup

4.2.1 Fields Road

The selected unpaved road test site is Fields Road, located in Merced County. Major work on Fields Road last took place in 1984, and small amounts of rock and aggregate have been applied since then. The road is graded twice a year, once after the rainy season ends in March or April, and again during the summer to help reduce dust emissions. Principal users of Fields Road are local ranchers who live and work in the area and sportsmen who use a golf course located to the northeast. Fields Road soil types the are silty and sandy loams, mainly the Montpelier, Corning, Redding, Whitney, Rocklin, Yokohl, Ryer, and Pentz types (United States Department of Agriculture, 1962).

Figure 4-1 shows the locations of the unpaved road and shoulders test sites in Merced County. Figure 4-2 shows Fields Road, its surroundings, and the locations of five 0.5 km test segments. The landscape surrounding Fields Road is grazing land, completely covered by grasses. This vegetation generally eliminates other PM_{10} dust emissions in the immediate vicinity of Fields Road. Landowner permissions were sought and obtained prior to the deployment of the towers on which the PM_{10} samplers and meteorological equipment were mounted adjacent to the test sections

4.2.2 PM_{10} Sampling

Minivol portable PM_{10} samplers (AIRMETRICS, Springfield, OR) were used to measure suspended particles upwind and downwind of test sections. The Minivol uses a rechargeable battery pack to power a pump that draws ambient air through a single filter pack at a flow rate of 5 L/min. The aerosol size cutpoint is achieved by a single-stage impactor with a greased impaction plate; PM_{10} and $PM_{2.5}$ configurations are available.

The Minivol PM_{10} sampler is a relatively recent technological development. Early versions suffered some degradation of performance due to air leaks and problems with filter holders. The Minivol sampler configuration deployed in this study benefits from improvements implemented during several recent air quality studies. These improvements include:

- Daily inspection of impactor inlets, with cleaning and greasing when excessive particle deposits were observed.
- Filter processing procedures that included including filter selection (Teflon), acceptance testing, pre-weighing, loading and field handling, and the use of improved filter holders.

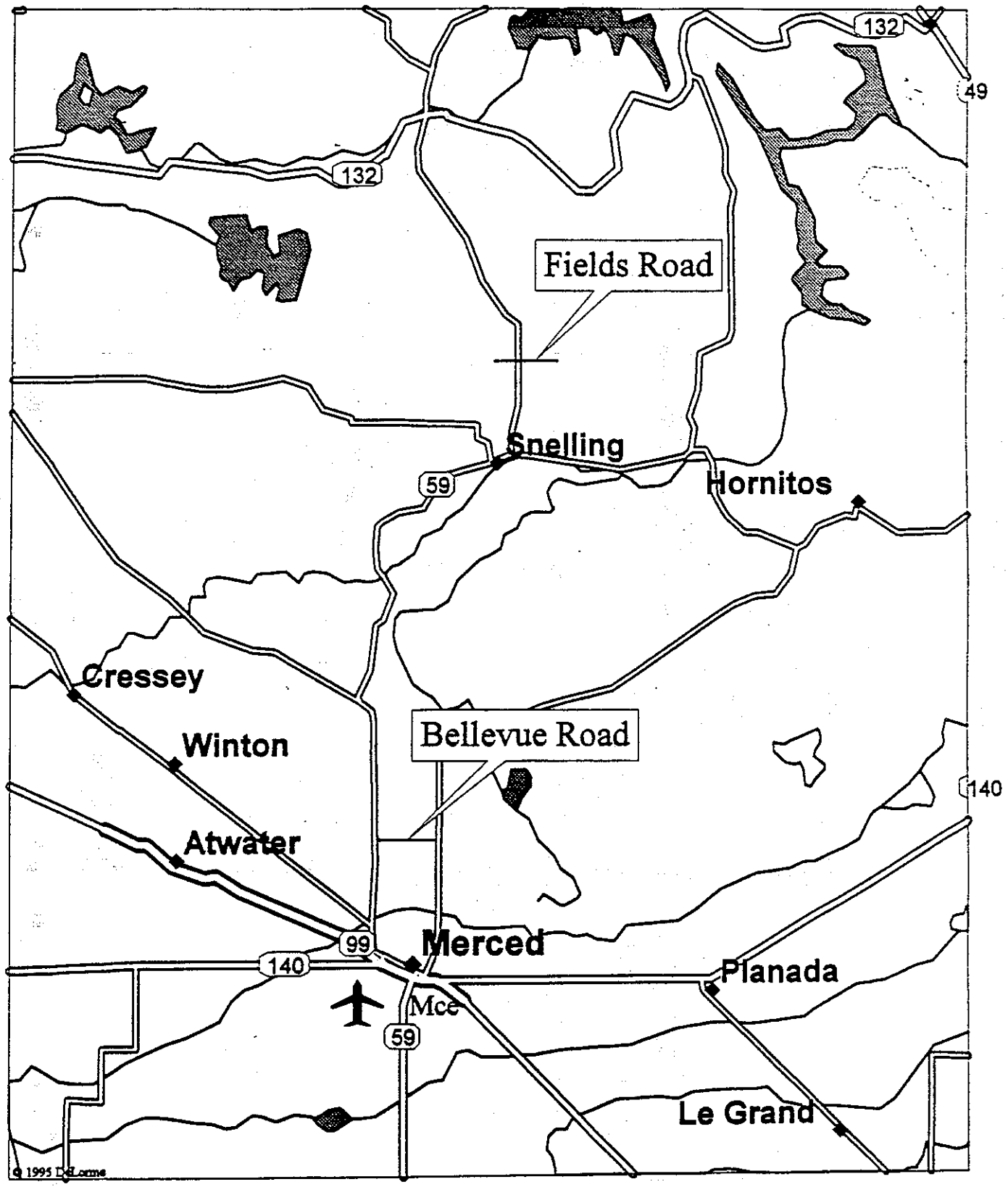

Figure 4-1 Merced County study sites.

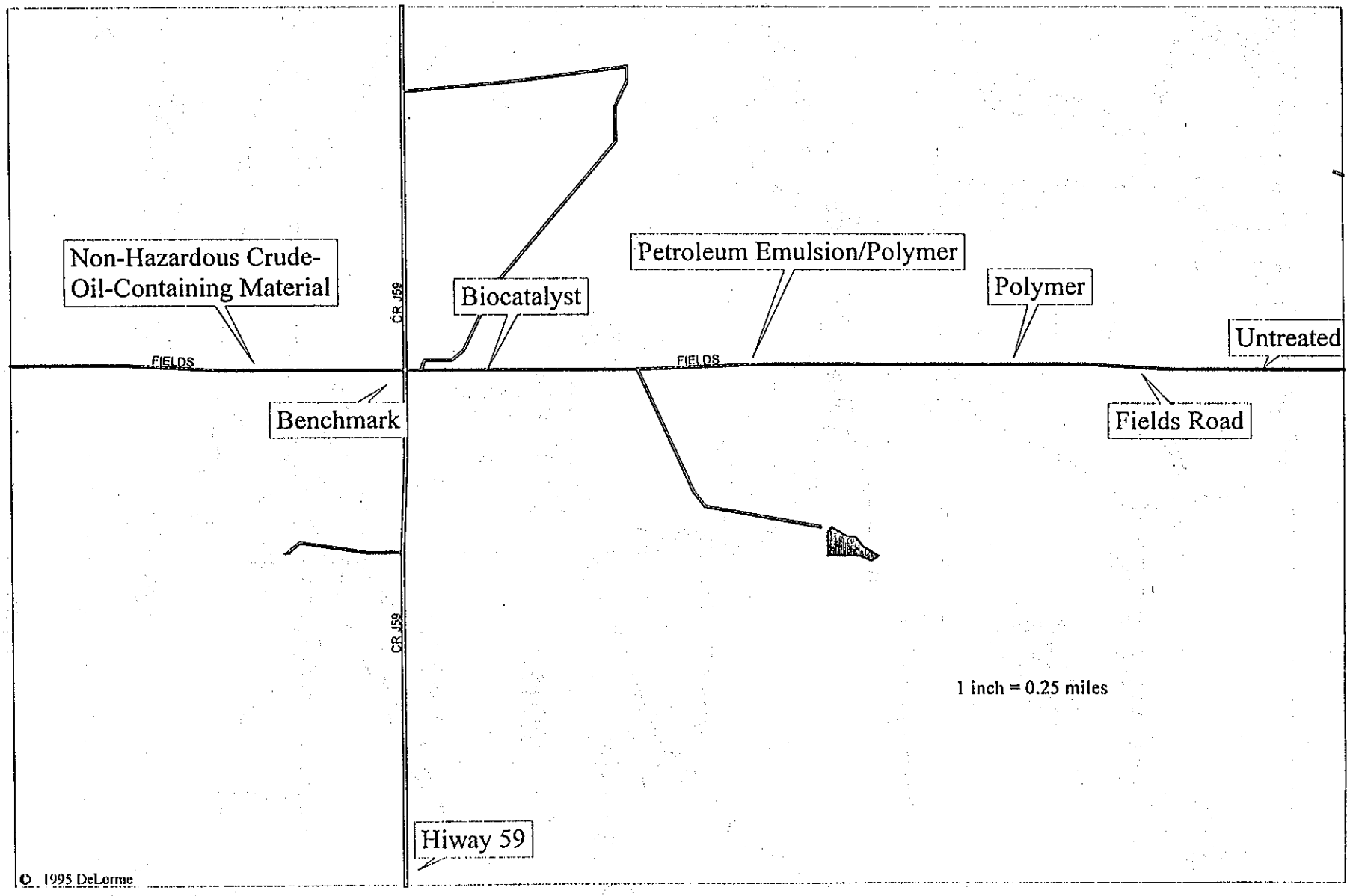

Figure 4-2 Fields Road study sites.

- Extensive performance testing of sampler components and programming prior to field deployment.

PM_{10} sampler data include uncertainties resulting from flow variations and mass determinations. Predictions of overall uncertainties based on these components usually underestimate the net uncertainty because not all component uncertainties are accurately assessed (Mathai *et al.*, 1990). A better indication of net uncertainty is obtained by collocating two or more identical samplers, and comparing their estimates of the mass concentrations of PM_{10} obtained during simultaneous runs. Chow and Watson (1997) present collocated portable sampler PM_{10} measurements with an estimated precision of 1.2 $\mu g/m^3$. This measure indicates that PM_{10} concentration differences exceeding about 1 $\mu g/m^3$ are not resolvable by portable samplers. High filter blank loadings and/or variability would add to this uncertainty level, but the blank levels in this study did not indicate any unusual loadings or variability.

The location of each sampler was marked noted by position and sampler ID number on the first day of the experiment. Subsequently on each sampling day and through each sampling period, the same sampler was placed at the same location. The only reason for replacement of a sampler at its designated position was either poor performance or complete malfunction. Each morning, ID-coded filter packs were loaded in the sampler. The internal flow rate was checked and adjusted if necessary, and the sampler was placed in its hanger bracket. The sampling date, start time, stop time, sampler ID, sampler position, flow rate, and elapsed time were recorded on field data sheets. At the end of each sampling interval, the flow rate was recorded to account for any drift, and the elapsed time was noted to provide an exact measure of the operating time. These field data were used to determine the volume of air for each sample to allow concentrations of PM_{10} concentrations to be calculated with known uncertainties.

4.2.3 Upwind Sampling

The Fields Road PM_{10} emission rates were estimated by a profile method enhanced by the placement of two overhead sampling positions to allow better characterization of the dust plume. The profile methodology offers the best approach to characterize the initial conditions of the background dust concentration profile as well as the immediate downwind profile. The sampling configuration is illustrated in Figure 4-3. Each test segment was equipped with an upwind and downwind sampler array located at or near its midpoint, in order to minimize the effects of suppressant material tracked in from adjoining test sections. The upwind samplers were deployed in order to measure PM_{10} transported into the section from upwind sources. Since Fields Road is distant from any sources, the incoming upwind particle distributions may be assumed to have reached equilibrium. This allows the application of existing dust transport models (e.g., Lancaster and Nickling, 1993) in order to describe the variations of concentrations and particle sizes as a function of elevation.

Three PM_{10} samplers were mounted on a 10 m tower located approximately 1 m upwind of the road surface. These samplers measured the upwind concentration profiles,

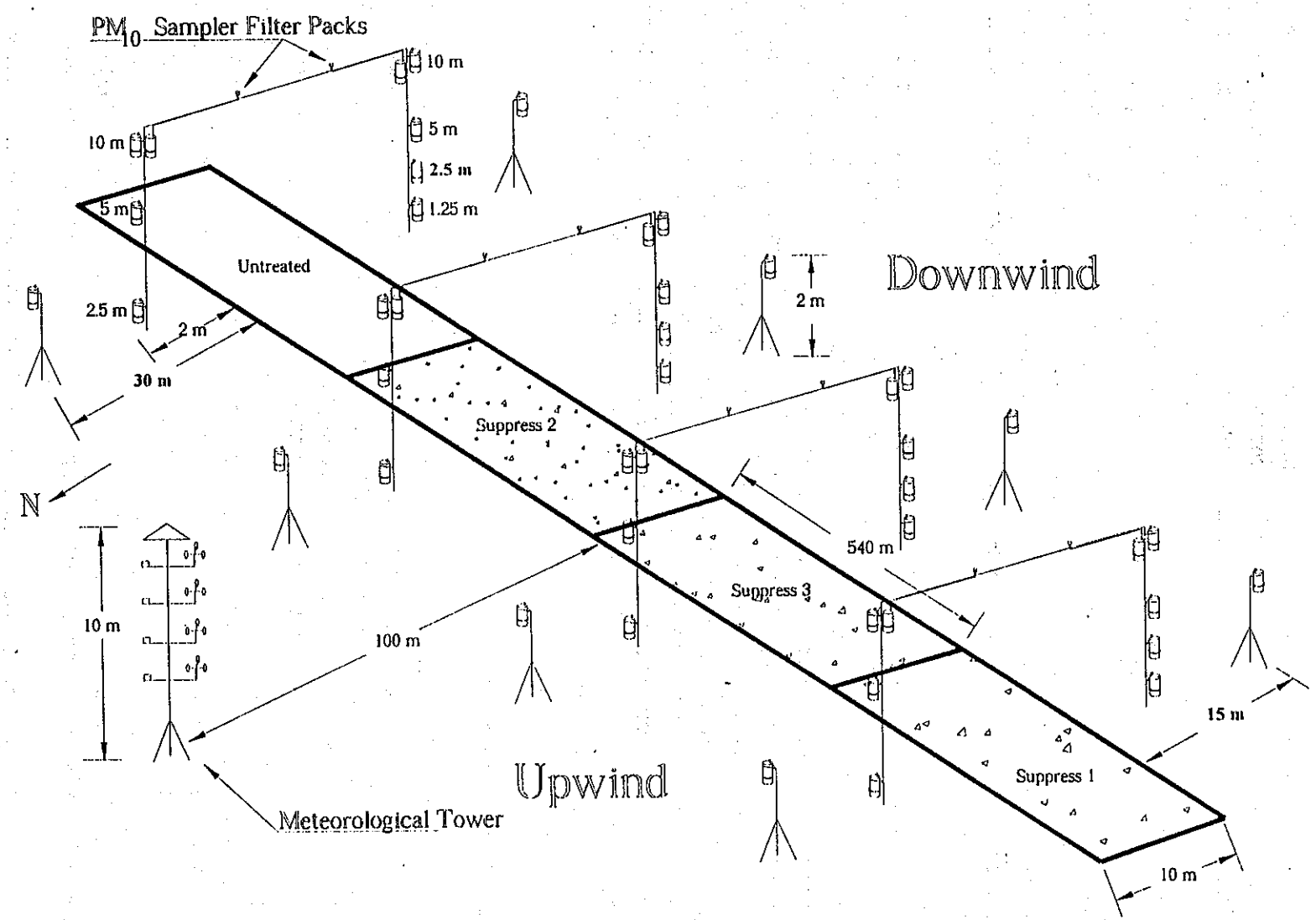

Figure 4-3 Unpaved road sampler array.

which are then compared to the theoretically estimated profiles. The upwind tower data may be redundant with the theoretical estimates, which were extrapolated from the farthest-upwind sampler and based on the equilibrium assumption. However, they eliminate complete reliance on the theory, which would amplify the overall uncertainty of the flux measurement in cases when upwind PM_{10} concentrations are significant compared with the downwind values. Comparison of the tower data with equilibrium estimates also helps to indicate whether or not emissions from the test road section are contaminating the upwind samplers during low wind speed conditions, indicating that the dust plume is spreading out on either side of the road. This arrangement also allowed sampling if the wind direction was opposite to the expected predominant wind direction (from the north instead of the south).

4.2.4 Overhead and Downwind Sampling

Downwind sampling presents a more difficult challenge than the upwind case, because for any manageable distance from the source, equilibrium of particulate properties as a function of height cannot be assumed. There is no basis for assuming that the top of the emitted plume is lower than 10 m for sampling locations close to the source because, depending on atmospheric stability and the detailed turbulent air velocity field created by the passage of a vehicle (especially a non-aerodynamic vehicle such as a tractor-trailer combination), PM_{10} particles may be lofted above the road to heights greater than 10 m. Using sampler data taken at lower levels and extrapolating to the "top" of the plume is inaccurate because there is no clear physical relationship upon which to base the extrapolation.

The sampler configuration illustrated in Figure 4-3 utilized portable PM_{10} samplers deployed over the top of the test section, on a ten-meter tower, and at the surface downwind, in order to obtain a more accurate estimation of the summed PM_{10} emissions. The available sampler inventory was deployed in a design intended to maximize the return of data from the most critical locations. The tower-mounted samplers were deployed with the same or improved spatial resolution compared to previous studies (Rosbury and Zimmer, 1983; Muleski and Cowherd, 1987). Additional overhead samplers were deployed to characterize plumes that had risen to heights greater than 10 m. The net PM_{10} flux from the test section is obtained by subtracting the upwind-source profile from the downwind source profile, and combining the resulting mass concentration data with the wind speed profile. This calculation is described in Section 6.

This PM_{10} measurement approach was applied in all three emission measurement intensives. However, extra PM_{10} samplers were added during the last (June 1996) intensive. This change was implemented because of the realization, during the first and second intensive measurements, that for southerly winds the emissions estimates would be lower because the north tower had one less sampler than the south tower. In this case the concentration measured at one point (2.5 meters) would be averaged over a greater vertical distance, thus lowering the estimated emission rate. For the final emissions measurement the sampler configuration on the north tower was made to be a mirror image of the south tower to make up for this deficiency: one additional sampler was placed on the north tower at a

height of 1.25 meters.

In order to better estimate the zone of influence of emissions, three additional downwind samplers at 2 meters height were added to the untreated test section during the last intensive. Four $PM_{2.5}$ samplers (1 upwind, 3 downwind) set at one sampling height (2 m) were also added during June 1996 to provide some indication of fine particle emissions from unpaved roads. These data are relevant to the proposed new fine particle standard.

4.2.5 Meteorological Instrumentation

A 9-meter tower was erected 100 meters north of Fields Road approximately halfway between the start and end of the four test sections located east of Highway J59. The tower was instrumented as follows: four cup anemometers at 1.25, 2.5, 5, and 9 meters to characterize the wind speed profile; two wind vanes at 1.25 and 9 meters to monitor wind direction; and one temperature and relative humidity sensor at 5 meters. These data were used mainly to estimate average wind speeds at each PM_{10} sampler location and the angle at which the wind approached the road, as required for the calculation of PM_{10} emission rates from the test surfaces. Average wind speeds were calculated based upon two-second readings averaged over fifteen minutes.

4.2.6 Sampling and Characterization of Surface Material

Measurable surface properties which both affect dust emissions and are expected to be affected by suppressant application were discussed in Section 2. These properties are:

1. suspendable dust (silt) loading;
2. particle size distributions;
3. moisture content; and
4. surface strength.

Samples were taken from each test section prior to suppressant application, during each intensive study after suppressant application, and at monthly follow-up visits. Determining the surface sediment characteristics that influence the potential dust emissions involves two collection techniques. Both sweeping and vacuum techniques are used to collect the loose surface sediments on the road for subsequent analysis of the total silt content. The two techniques are compared by analyzing the relationships of their respective silt composition estimates to the measured dust emission rates. For bulk surface samples, a small stiff-bristled brush and dust pan were used. The vacuum collection system was based on a commercial vacuum cleaner. The vacuum was modified by the addition of an axle and roller bearings to the collection head, raising it to 10 mm above the road. Raising the head above the surface standardized the collection method, and avoided scouring of the surface by the head itself and collection of larger pebbles.

The surface sampling strategy for collection of the loose surface material is adapted from the sampling procedure outlined in Cowherd *et al.* (1990). Sampling the loose surface material involves collecting the sediment at two sections within each test section. A sample of the sediment is removed by the vacuum and sweep method along a line approximately 0.3 m wide spanning the entire width of the road or both sides of the unpaved shoulders. If necessary, more areas are sampled to obtain sufficient masses of sediment for analysis. According to the sampling strategy of Cowherd *et al.* (1990), at least 6 kg of mass should be collected per 0.5 km of unpaved road. If the treated sections of unpaved road surface and unpaved shoulders are sufficiently sealed, with no appreciable amounts of loose surface sediment present, the sampling procedure follows the recommendations of Cowherd *et al.* (1990) for paved roads: sampling a strip 3 to 9 m wide provides sufficient sample sizes for analysis of the silt content.

The Proctor Penetrometer® was used for determining the penetration resistance of the test surfaces. The Penetrometer measures an unconfined compression strength for the unpaved road and shoulder surface. It applies a vertical force, perpendicular to the surface. It is designed to measure the penetration resistance of fine-grained soils and conforms to ASTM standards (for test D-1558). The unit consists of a special calibrated-spring dynamometer with a pressure-indicating scale on the stem of the handle. The pressure scale is calibrated to 45.5 kg by 0.45 kg subdivisions. The Proctor Penetrometer offers a much wide range of strength measurements because of its use of interchangeable penetration probes with different surface areas. It is similar to, but not an exact replication of, the modulus of rupture test used by Gillette *et al.* (1982) to assess the strength of desert soil crusts which they related to wind erosion susceptibility. Its strongest advantage is that it provides an *in situ* measure of strength.

The strength measurements are carried out based on a transect sampling arrangement with measurements of the surface strength characteristics taken 0.25 m apart across the width of the road and shoulder. This provides approximately 40 measurements per transect covering the:

1. shoulder region;
2. tire track regions;
3. center line area.

Finally, surface scrapings obtained with a small blade were collected for moisture content analysis.

4.2.7 Vehicle Type and Traffic Monitoring

The DRI test vehicle was a pickup truck weighing approximately 1500 kg, with four wheels. During a six-hour test run the vehicle was driven continually and logged approximately 50 kilometers of travel for each test section. Traffic monitoring was accomplished during the intensive monitoring periods by keeping a log of the number of

vehicle passes and kilometers traveled with the DRI test vehicle. These data were supplemented by the addition of traffic counters, which gave the total number of vehicle passes on the Fields Road test sections. These counts give the additional vehicle passes on the test sections, in addition to the intensive studies' controlled vehicle passes. The traffic counter also was left in place for extended periods of time to estimate daily traffic volumes for Fields Road during non-intensive monitoring periods.

The traffic counters are electromechanical devices triggered by pneumatic pulses generated when two wheels in succession pass over rubber tubing (K-Hill Model GMH, K-Hill Signal Co., Uhrichsville, OH). The count accumulates cumulatively until reset by an operator. The counter modules are housed in secure, locked aluminum boxes that were chained to power poles.

4.2.8 Measurement Coordinates

In order to establish precise coordinates for the data acquired in this study, all measurements at the Fields Road sites will be referenced to a single benchmark, the intersection of Fields Road and La Grange Highway (37° 33.931′ N, 120° 25.556′ W). Table 4-1 gives the coordinates for each PM_{10} sampler location. The coordinates include a height measurement above the surface, where the zero elevation level is defined as the road surface at the tower location in each test section.

4.3 Fields Road Measurement Schedule and Conditions

PM_{10} measurements were conducted during three intensive study periods between July 1995 and June 1996. Surface characterization measurements that were used to evaluate the state of the different treatments and to characterize aging of the surfaces were performed at the time of each emission test as well as during intervening periods. Table 4-2 lists the dates of the suppressant applications, emissions measurements, and also the site visits for surface characterization measurements.

The first set of emission measurements was on July 22, 1995, four to eight days after Fields Road was treated with the suppressants. This was due to the arrangements made with the manufacturers and contractors to accommodate both their schedules and additional preparatory work if it was required. During this period between application and emissions testing, the surfaces were allowed to dry and cure to ensure that the treatments had successfully bonded with the road material before being driven upon by vehicle traffic. A "road closed" sign was posted at the entrance to Fields Road to minimize local vehicle traffic during this time. Subsequent intensive measurement periods were carried out in October 1995 (October 17,18, 20-22), and in June 1996 (June 13-18) to observe changes in emissions as a function of time and changing surface conditions.

The weather conditions that prevailed through the three intensive measurement periods are summarized as follows. Hot and dry weather conditions preceded and lasted through the first intensive, July 22-27, 1995. Daytime temperatures during the measurement period (0800 - 1400) often exceeded 30 °C with average temperatures in the high twenties to lower thirties. The average wind speed measured at 10 m ranged between 3 and 6 m/s and

Table 4-1
Fields Road Unpaved Road Test Location PM_{10} Sampler Coordinates

Sampler Number	North Latitude Minutes	Height Above Surface Meters	Distance from North Sampler Meters
Untreated Section[a]			
1	33.947	2.00	0
2	33.931	1.25	30
3	33.931	2.50	30
4	33.931	5.00	30
5	33.931	9.00	30
6	33.931	9.00	33
7	33.925	9.00	37
8	33.925	9.00	40
9	33.925	5.00	40
10	33.925	2.50	40
11	33.925	1.25	40
12	33.922	2.00	55
13	33.919	2.00	70
14	33.916	2.00	85
Coherex PM Section[b]			
1	33.947	2.00	0
2	33.931	1.25	30
3	33.931	2.50	30
4	33.931	5.00	30
5	33.931	9.00	30
6	33.931	9.00	33
7	33.925	9.00	37
8	33.925	9.00	40
9	33.925	5.00	40
10	33.925	2.50	40
11	33.925	1.25	40
12	33.922	2.00	55
Soil Sement Section[c]			
1	33.947	2.00	0
2	33.931	1.25	30
3	33.931	2.50	30
4	33.931	5.00	30
5	33.931	9.00	30
6	33.931	9.00	33
7	33.925	9.00	37
8	33.925	9.00	40
9	33.925	5.00	40

Table 4-1 (continued)
Fields Road Unpaved Road Test Location PM_{10} Sampler Coordinates

Sampler Number	North Latitude Minutes	Height Above Surface Meters	Distance from North Sampler Meters
10	33.925	2.50	40
11	33.925	1.25	40
12	33.922	2.00	55
EMC[2] Section[d]			
1	33.947	2.00	0
2	33.931	1.25	30
3	33.931	2.50	30
4	33.931	5.00	30
5	33.931	9.00	30
6	33.931	9.00	33
7	33.925	9.00	37
8	33.925	9.00	40
9	33.925	5.00	40
10	33.925	2.50	40
11	33.925	1.25	40
12	33.922	2.00	55
Non-Hazardous Crude-Oil-Containing Materials[e]			
1	33.947	2.00	0
2	33.931	1.25	30
3	33.931	2.50	30
4	33.931	5.00	30
5	33.931	9.00	30
6	33.925	9.00	33
7	33.925	9.00	37
8	33.925	9.00	40
9	33.925	5.00	40
10	33.925	2.50	40
11	33.922	1.25	40
12	33.914	2.00	55

[a] North Latitude 37 Degrees plus minutes shown; West Longitude 120 Degrees, 24.389 Minutes for all sampler positions.
[b] North Latitude 37 Degrees plus minutes shown; West Longitude 120 Degrees, 24.722 Minutes for all sampler positions.
[c] North Latitude 37 Degrees plus minutes shown; West Longitude 120 Degrees, 25.056 Minutes for all sampler positions.
[d] North Latitude 37 Degrees plus minutes shown; West Longitude 120 Degrees, 25.389 Minutes for all sampler positions.
[e] North Latitude 37 Degrees plus minutes shown; West Longitude 120 Degrees, 25.729 Minutes for all sampler positions.

Table 4-2
Schedule of Suppressant Applications and Measurements on Fields Road

Suppressant Application or Measurement Event	Date
Application of "EMC Squared", "Soil Sement", and "Coherex PM" suppressants	July 13-18, 1995
First Intensive Study	July 22-27, 1995
Surface Characterization Measurements	July 21, 1995
Surface Characterization Measurements	September 22, 1995
Second Intensive Study	October 17-22, 1995
Application of "Non-Hazardous Crude-Oil-Containing Material" (NHCOCM) Suppressant	October 17-19, 1995
Surface Characterization Measurements	October 21, 1995
Surface Characterization Measurements	December 28, 1995
Surface Characterization Measurements	March 26, 1996
Third Intensive Study	June 13-18, 1996
Surface Characterization Measurements	June 15, 1996
Surface Characterization Measurements	July 15, 1996
Surface Characterization Measurements	August 23, 1996

came consistently from the northwest. During the second intensive period (October 17-22, 1995), conditions preceding the period were dry and remained dry through the sampling period. Temperatures were cooler than the first intensive, with averages between 16 to 22 °C for the 0800-1400 sampling period. Winds were light, but more variable during the October sampling interval. The final measurement period was postponed from an original start date of early May because of rain during the first week of that month. Rain also fell in Merced County on several days later in the month. After the last recorded precipitation event (May 21), three weeks' drying period were allowed before the final intensive period, June 6-18, 1996. The weather conditions during this intensive were warm and dry with average day time temperatures between 25 to 30 °C, under sunny skies, and moderate winds.

4.4 Laboratory Measurements

4.4.1 Filter Measurements

Over 900 ambient and blank filter samples were acquired in the three intensive measurement periods of this Demonstration Study. The 47-mm-diameter filters which were exposed in the "Minivol" portable PM_{10} sampler were prepared and processed according to DRI Standard Operating Procedures for Portable PM_{10} Survey Sampler Field Operations; Gravimetric Analysis Procedures; Field, Mass, and Chemical Data Processing and Data Validation for Aerosol and Gas Data. Laboratory operations pertaining to the determination of PM_{10} mass collected on filters begin with acceptance testing and initial weight determinations for all filters. Each accepted filter is assigned an ID code, which registers it both for subsequent data analyses, and for chain-of-custody requirements.

Filters are weighed on a Cahn C-31 electronic microbalance in a humidity and temperature-controlled clean working area. The microbalance is subject to rigorous quality control and quality assurance procedures. The mass determination resolution is 1 microgram for filters in this weight range. All filter initial weights are determined twice by two independent operators, in sets of ten. If any one filter initial reweight differs from the first determination by more than 10 micrograms, the entire set of ten filters is again weighed, until the criterion is met. The balance zero and 200 mg span are checked before and after every ten filter set; the span is established by a Class 1.1 calibration weight. If the result differs by more than 5 micrograms from the exact values, the balance is recalibrated and the filters are reweighed. The mass data are recorded manually and are simultaneously written to a computer file via a computer/microbalance interface.

The prepared filters are then loaded into filter holders that are configured for the portable samplers. Each holder is a sealed unit packaged to avoid filter contamination during shipping. Exposed filters are returned to the laboratory for post-exposure weighing, using the same holder and shipping system. Blank filters are subjected to identical preparation, filter holder loading, shipping, field handling, return shipping, and unloading procedures as the exposed filters, with the exception that ambient air is not drawn through the blanks by the portable samplers in the field. These are "dynamic blanks"; their mass accumulations measure all sources of contamination that affect the deliberately exposed filters.

The exposed filters are unloaded and inspected by a laboratory technician. All deviant conditions, such as damage, presence of insects or visible objects, or suspect appearance are noted and entered according to a flagging code on the permanent data record for the filter. The filters are then reweighed according to the same procedures applied for initial weights. The mass data are then examined and validated. The precision of the accumulated PM_{10} mass determination is about 6 to 9 micrograms per filter.

4.4.2 Surface Characterization Measurements

To complete the surface characterization measurements, samples of the loose material removed from the road were returned to DRI for subsequent analysis. A standard series of procedures were initiated upon the return of the samples to the lab. Each sample was assigned an identification code and the information logged concerning the date of collection, the site where it was collected, and the collection methodology (e.g., sweep or vacuum method of collecting the surface sample).

The bulk soil samples collected by both methods, sweep and vacuum, were weighed and the weight recorded. Samples greater than 2 kg were weighed using a triple beam balance. The sweep samples were then subdivided using a Soiltest CL-280 sample splitter to obtain samples in the recommended mass range for the silt content and aggregate size distribution analysis. Subsequent analysis of the sweep samples was carried out on a portion of the original sample. All weighing of the sieved soil fractions were done on an electronic balance accurate to 0.1 g.

The methodology for determining the grain size distribution is the ASTM standard for wet sieving (ASTM, 1990a) to determine the distribution of particle sizes in the gravel and sand range. Pipette analysis was used to determine the percentage of silt and clay (ASTM, 1990b). Detailed procedures for obtaining particle size distributions and surface silt content are given in Appendix B.

The size distributions of surface particles and aggregates were determined from subsamples of the surface material collected by the sweep and the vacuuming techniques. Each sample is split into three subsamples, and the following tests are performed:

1. Sieving and pipette analysis to determine the grain size distribution and assess the texture of the road base material (method of Folk, 1980);

2. Soft sieve analysis (method of Cowherd, *et al.*, 1990) to assess the aggregate distribution of each test section; and

3. Aggregate stability (method of Toogood, 1978).

The moisture content of the road surface was determined gravimetrically and expressed as a percent moisture content. The methodology for determining percent moisture content is based on standard ASTM methods.

The Cowherd *et al.* (1990) "soft sieve" technique is employed to characterize aggregate stability by monitoring changes in the aggregate size distribution through time. A relative measure of the stability of the aggregates on the surface is determined by the methodology of Toogood (1978). In this procedure approximately 5 g of air-dried samples of aggregates 1 to 2 mm in diameter are sieved vigorously on a 1 mm sieve for one minute. The sample is re-weighed and then sieved vigorously for an additional four minutes. The weight of sample remaining after five minutes, expressed as a percentage of the weight remaining after one minute, is used to indicate the stability of the dry aggregates (Toogood, 1978).

4.5 Data Base Structure and Features

The data base files for this study have the following attributes:

- They contain the ambient observables needed to assess PM_{10} flux from the unpaved road site;
- They are available in a well-documented, computerized form accessible by personal computers;
- Measurement methods, locations, and schedules are documented;
- Quality control and quality audits are documented;
- Precision and accuracy estimates are reported; and
- Validation flags are assigned.

The Dust Demonstration Study data are available on floppy diskettes for convenient distribution. Detailed file structures are presented in Appendix A and are referred to below as Tables A-1 through A-16. The file extension identifies the file type according to the following definitions:

- TXT = ASCII text file
- DOC = Microsoft Word 6 document
- XLS = Microsoft Excel 5 spreadsheet file
- DBF = Xbase (i.e., dBase, FoxPro) data base file
- FPT = FoxPro memo field file

The Xbase data base files (*.DBF) can be read directly into a variety of popular statistical, plotting, data base, and spreadsheet programs without having to use any specific conversion software.

Each file structure was established by defining the fields for data to be stored. One of five field types, character, date, numerical, logical, or memo, can be assigned to each observable. Sampling sites and particle size fractions are defined as "Character" fields, sampling dates are defined as "Date" fields, and measured data are defined as "Numeric" fields. "Logical" fields are used to represent a "yes" or "no" value applied to a variable, and "Memo" fields accommodate large blocks of textual information and can be used to document the data validation results.

Data contained in different Xbase files can be linked by indexing on and relating to common attributes in each file. Sampling site, sampling hour, sampling period, particle size, and sampling substrate IDs are, in general, the common fields among various data files which can be used to relate data in one file to the corresponding data in another file.

To assemble the final data files, information was merged from several data sets derived from field monitoring and laboratory analyses by relating information on the common fields cited above.

Documentation files include project, data description, and site description files. Data files include PM_{10} mass concentrations and the surface characterization and meteorological measurements.

Table 4-3 summarizes the validated data files that constitute the Dust Demonstration ambient PM_{10}, surface measurement, and meteorological data base. Tables A-1 through A-9 identify the number of records, file dates, missing value codes, and data precisions for the ambient data. The field sequence, field name, data type and format, and description of each field name are also documented. Documentation for the FoxPro field descriptions, naming conventions, and measurement units used in the ambient data bases is given in the file "DDFLDNAM.DBF" (Table A-2). Tables A-8 and A-9 are field and laboratory validation flags for the PM_{10} data.

Table 4-3
Summary of the SJV Dust Demonstration Study Data Bases

Category	Data Base File	Data Base Description	Number of Records	Reference Table Numbers
I. DATA BASE DOCUMENTATION				
	FRSITE.DBF	Site description, location, and data collected at Fields Road.	50	Table A-1
	BRSITE.DBF	Site description, location, and data collected at Bellevue Road.	4	Table A-2
	DDFLDNAM.DBF	Defines the FoxPro fields and measurement units used in the ambient and meteorological data bases.	55	Table A-3
II. $PM_{2.5}$ and PM_{10} MASS DATA				
PM_{10}	AMB_POR1.DBF	Contains ambient PM_{10} mass concentration data collected during the first intensive period at the Bellevue Road sites (July 15-20, 1995) and Fields Road sites (July 22-27, 1995).	348	Table A-4
$PM_{2.5}$ & PM_{10}	AMB_POR2.DBF	Contains ambient $PM_{2.5}$ and PM_{10} mass concentration data collected during the second intensive period at the Bellevue Road sites (October 14-16, 1995), and the Fields Road sites (October 17-22, 1995).	308	Table A-5
PM_{10}	AMB_POR3.DBF	Contains ambient PM_{10} mass concentration data collected during the third intensive period at the Bellevue Road sites (June 6-11, 1996), and the Fields Road sites (June 13-18, 1996).	586	Table A-6

Table 4-3 (continued)
Summary of the SJV Dust Demonstration Study Data Bases

Category	Data Base File	Data Base Description	Number of Records	Reference Table Numbers
III. METEOROLOGICAL AND NEPHELOMETER DATA				
Met.	FRMET.DBF	Contains 15-minute average meteorological data from the Fields Road tower, for all three Intensive Periods	2,738	Table A-7
Met.	BRMET3.DBF	Contains 15-minute average meteorological data collected at the Bellevue Road site during the third intensive period from June 6-11, 1996.	181	Table A-8
Neph.	BRCOLL3.DBF	Contains nephelometer data from the five co-located nephelometers at the Bellevue Road site during the third intensive period from June 6-11, 1996.	20,047	Table A-9
Met. & Neph.	BRNESON3.DBF	Contains nephelometer data and 2-second averages of sonic anemometer measurements taken at the five non-co-located nephelometers at the Bellevue Road site during the third intensive period from June 6-11, 1996.	74,706	Table A-10
Met.	BRSONIC3.DBF	Contains consecutive measurements with the sonic anemometer taken at the Bellevue Road site during the third intensive period from June 6-11, 1996.	456,746	Table A-11

Table 4-3 (continued)
Summary of the SJV Dust Demonstration Study Data Bases

Category	Data Base File	Data Base Description	Number of Records	Reference Table Numbers
IV. SURFACE CHARACTERIZATION DATA				
Strength	DDSTRNG.DBF	Contains surface strength measurements given at points along transects crossing Fields Road and Bellevue Road.	114	Table A-12
Surface	DDSURF.DBF	Contains surface characterization measurements collected along Fields Road and Bellevue Road.	57	Table A-13
Vac	DDVAC.DBF	Contains surface samples collected from Fields Road and Bellevue Road using the vacuum technique.	89	Table A-14
V. DATA VALIDATION FLAGS				
	AMBFLAG.DOC	Contains the field sampling data validation flags.	NA	Table A-15
	MASSFLAG.DOC	Contains the gravimetric analysis data validation flags.	NA	Table A-16

5.0 EXPERIMENTAL APPROACH FOR UNPAVED SHOULDERS

5.1 Site Selection

Due to its proximity to Fields Road, Bellevue Road in Merced County, between Highway 59 and G Street, was chosen for the unpaved shoulder test site. The selection criteria listed in Section 4 were applied. Bellevue Road is a well-used, paved suburban thoroughfare. The road runs east-west and has only a few meters of vertical relief along its 3-km length. On either side of the road the land use is predominantly agricultural. Agricultural activity on the north side is mainly pasture with a small orchard and some very small plots of tilled soil. The south side of Bellevue Road is planted in cotton extending west from G-street approximately 2 km towards Highway J-59. To the west of the cotton fields the land use is again primarily for livestock grazing. Although there were times when agricultural activity was noted on the cotton fields for the most part the wind blows from the north to north west which would minimize any contributions to the road side sampling. Only on a few occasions were emissions attributable to agricultural activities on the north side observed.

The majority of single family dwellings along Bellevue Road are located on the north side. However, all mail boxes are located on the south side and all garbage pick-up occurs on the north side. Both of these activities result in on-shoulder vehicle traffic. On-shoulder vehicle activity was also observed for various tractor and farm implement configurations.

The Bellevue Road/G Street intersection benchmark coordinates are as follows: 37° 21.710′ N, 120° 28.220′ W. The Bellevue Road test sites are shown in Figure 5-1. The boundary coordinates for the test sections are given in Table 5-1.

5.2 Experimental Setup

5.2.1 PM_{10} and Surface Measurements

Because the unpaved shoulder dust plumes occur on a much shorter time scale than the deliberate traffic patterns on the unpaved road, the full PM_{10} sampler array was not deployed on Bellevue Road. Instead, the measurement strategy was designed with more emphasis on fast-response observations from light scattering and turbulence sensors.

Unpaved shoulder PM_{10} sampling utilized the portable PM_{10} sampler described in Section 4. During the first intensive, two samplers per section were used, one on the north shoulder (usually the upwind side) and one on the south shoulder (usually downwind). For the second and third intensives, a second sampler was added 20 m downwind from the first south-shoulder unit. This provided additional downwind "zone of influence" data. For the third (June 1996) intensive an extra pair of samplers was deployed in positions far upwind and downwind (75 m) of Bellevue Road. This was done to more clearly delineate the upwind background concentration of PM_{10} and the zone of influence of emissions in the downwind direction. All samplers were mounted on tripods at 2 m above the surface.

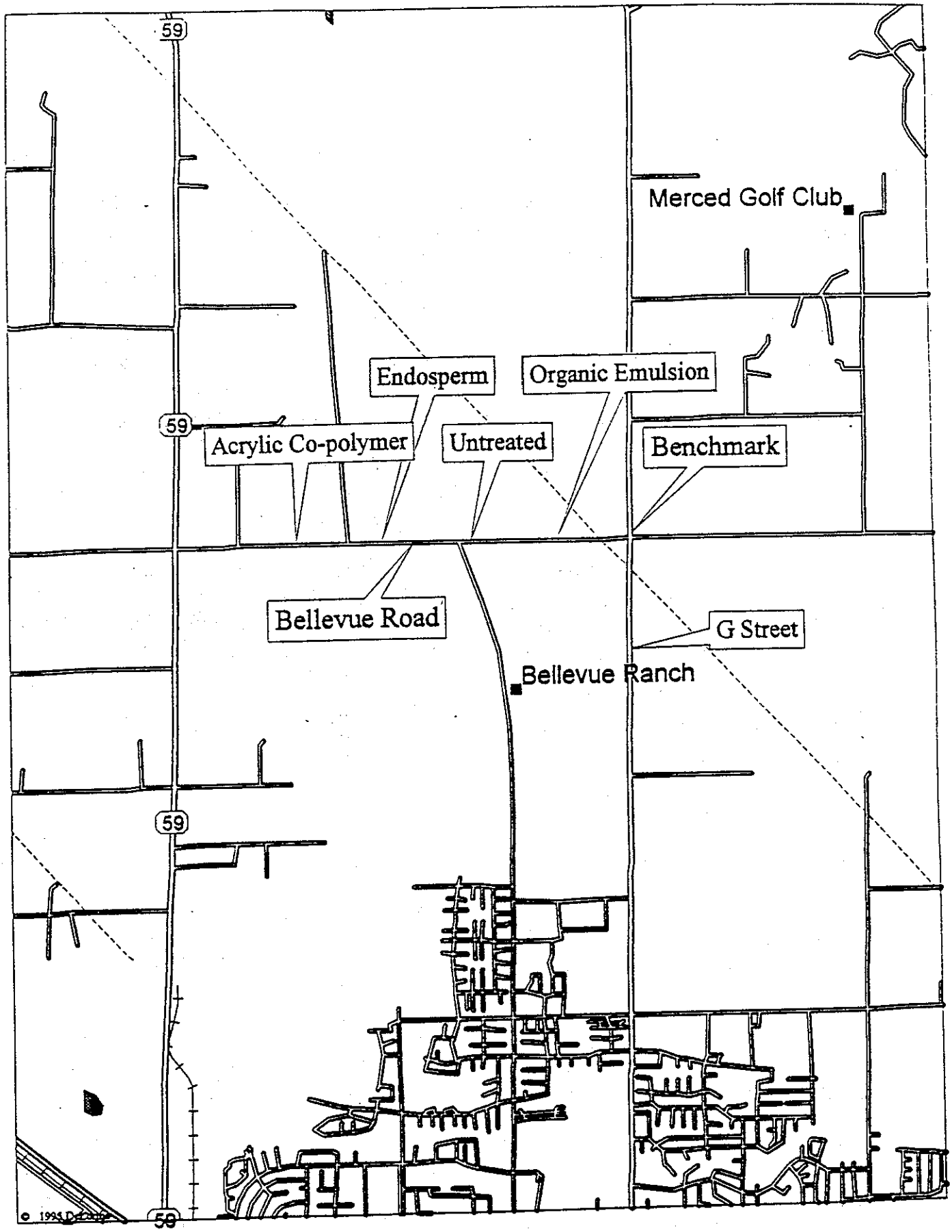

Figure 5-1 Bellevue Road study sites.

Table 5-1
Bellevue Road Test Section Boundaries[a]

Suppressant	East Boundary [b,c]	West Boundary [b]
Enduraseal	120 28.220'	120 28.680'
Untreated	120 28.680'	120 29.054'
HydroShield	120 29.054'	120 29.537'
DSS-40	120 29.537'	120 30.000'

[a] North Latitude constant at 37 degrees, 21.710 minutes
[b] West Longitudes expressed in degrees, minutes, seconds
[c] Enduraseal Section starts at intersection of Bellevue Road and G Street, 120 28.220'

The full complement of surface characterizations, as described in Section 4, was also performed according to the schedule shown in Table 5-2.

5.2.2 Light Scattering Measurements

Light is scattered by the dust particles in the plumes created at the unpaved shoulder test locations, in approximate proportion to dust particle mass concentrations; nephelometers were used to obtain light scattering measurements in these plumes.

During the first and second intensive measurement periods two identical, collocated nephelometers were deployed on the unpaved shoulders, to determine their response to identical plume events for approximately one hour. They were then separated; one remained at all times in the untreated section, and the other was moved into one of the treated sections. B_{scat} signals: 1) responded to dust plumes associated with different vehicle types; and 2) when integrated over time, provided an estimated dust mass concentration for comparison to the filter measurements.

For the third intensive monitoring period, five newer, improved-technology nephelometers (Optec open-air Model NGN-2) were deployed on Bellevue Road. Five instruments allowed more nearly simultaneous assessment of emissions from each test section.

At the start of each period the five nephelometers were calibrated with span gas of known scattering coefficient ("SUVA", HFC-134A) and run with filtered air to assess the Raleigh scattering coefficient. They were then operated for one hour side by side on the untreated section to calibrate their collocated response to identical emission inputs. Following the collocated calibration, three of the instruments were moved into each of the test sections and one was moved five meters downwind of the nephelometer assigned to the untreated test section for "zone of influence" observations. At the end of the sampling period an additional set of zero air readings were taken to assess any change in the instruments performance.

5.2.3 Wind and Turbulence Measurements

During the second and third intensive measurement periods, ambient wind speed and direction was monitored at the road site using a single combination propeller anemometer and wind vane unit at 2.5 m above the surface.

During the third intensive measurement period, three-dimensional wind field measurements were obtained with a portable sonic anemometer placed on the test section road shoulders. The anemometer data: 1) measure the time-dependent wind field caused by the passage of a vehicle, i.e., the vehicle's "wake signature"; and 2) quantify the wind profile near the ground, thereby characterizing the aerodynamic forces available to suspend dust particles from the surface. This measurement provided both the magnitude of the

Table 5-2
Schedule of Suppressant Applications and Measurements on Bellevue Road

Suppressant Application or Measurement Event	Date
Application of "Enduraseal", "ChemShield", and "DSS-40" suppressants	July 12-13, 1995
First Intensive Study	July 15-20, 1995
Surface Characterization Measurements	July 20, 1995
Surface Characterization Measurements	September 21, 1995
Second Intensive Study	October 14-23, 1995
Surface Characterization Measurements	October 20, 1995
Surface Characterization Measurements	December 27, 1995
Surface Characterization Measurements	March 25, 1996
Third Intensive Study	June 6-11, 1996
Surface Characterization Measurements	June 14, 1996

three ambient wind speed vectors and the three-dimensional characteristics of the vehicle wakes.

5.2.4 Traffic Monitoring

Video images of passing vehicles and their associated turbulent wake-generated dust plumes were recorded at each test segment during intensive periods. Vehicle classifications and estimates of vehicle speeds are determined from the video tape records. Long term averages of the number of vehicles passing per day on Bellevue Road were obtained with the same type of traffic counter deployed on Fields Road (Section 4.2.7).

5.2.5 Measurement Schedule and Conditions

The unpaved shoulder measurement schedule is shown in Table 5-2. The three intensive studies coincided with the intensive periods at the unpaved road site: 1) following suppressant application and the end of the rainy season, July 15-20, 1995; 2) in the autumn, October 14-23, 1995; and 3) in the summer, June 6-11, 1996. The daily measurement protocol specified sampling periods for unpaved shoulders during the times of heaviest traffic volume, from 0800 to 1800 hours. The general weather conditions pertaining to both the unpaved road and shoulder site intensive studies are summarized in Section 4.3.

Placement of the emissions monitoring instrumentation was not static during the intensive monitoring periods. Because of the spatial inhomogeneity of the shoulder emissions, the instrumentation was generally moved to a different location within each test section on each intensive sampling day. The locations were chosen to reflect the variety of surface conditions found within each section and provide some indication of the range of emission rate associated with each test section. Within a test section there were regularly-disturbed portions of the shoulders, such as the areas around mail boxes and driveways, which are driven on each weekday (mail delivery) or on a weekly basis (garbage truck). The driveways of private residences are also regularly disturbed by the occupants of the residence. Disturbances on the road shoulder also occur as a function of random events that force vehicles of all types onto the shoulder. Therefore, virtually no portion of the road shoulders was free of vehicle tracks, even within a few days after application of the suppressants. The full range of surface conditions were targeted as locations in which the ambient monitoring instrumentation was placed.

5.3 Unpaved Shoulder Data Bases

The MRI nephelometer data were sampled at a rate of 1 Hz; the Optec data were sampled at 0.5 Hz. The raw data, in ASCII, comma-delimited format, were stored in files with the extension ".dat". The data records include nephelometer ID number, Julian date, time (hhmm), time (ss), nephelometer reading (mV), and an instrument status parameter. The data files are generally separated into collocated and non-collocated files. All these data have been manually scanned; obviously wrong or missing values have been corrected, flagged, or deleted.

Collocated nephelometer comparisons were conducted each intensive day. For a time period of about one hour where all nephelometers are operating simultaneously, averages and standard deviations were calculated for each instrument.

Due to the high sampling rate (10 Hz) for the sonic anemometer, 36,000 lines of data were stored per hour, resulting in single data files larger than one megabyte. Therefore data validation and processing had to be automated. Raw data are stored in ASCII files; each record includes time, three components of the velocity vector (m/s), and temperature (°C). Typically, an error in the data occurs every few thousand lines, resulting in additional, missing, or exchanged characters. An IDL program was written, to read the data and check the structure of every line for correct length, correct location of the constants (i.e., colons, periods, spaces, U, V, W, T), and correct ranges of variables. The program also checks for a positive time increment from line to line. The data from correct lines are written into the validated data file. Incorrect lines are written together with line numbers and error messages into an error file. No sonic data are available for June 9 and for collocated measurements.

The Dust Demonstration Study data file structure and definitions were introduced in Section 4.5.1. Detailed file structures are presented in Appendix A.

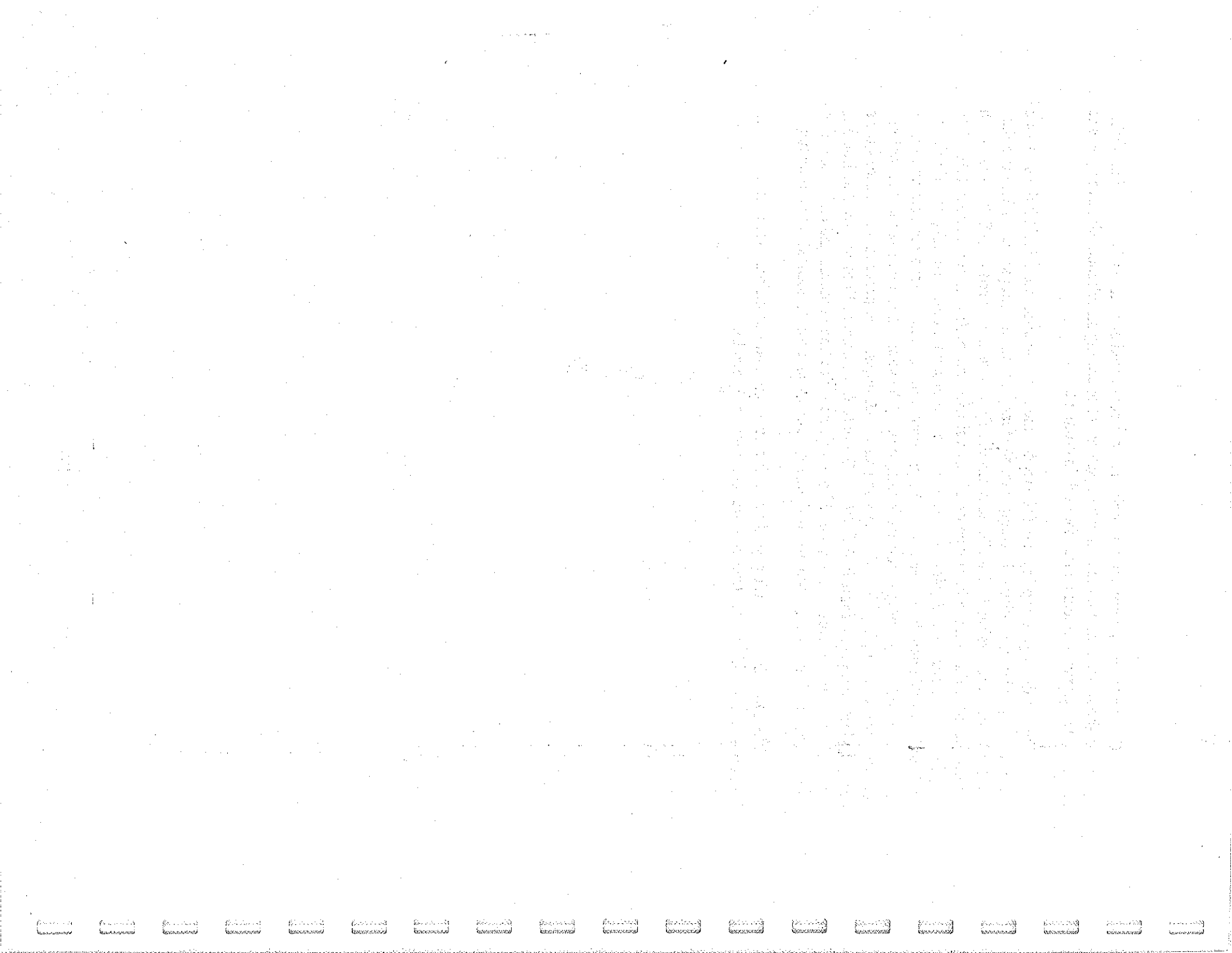

6.0 RESULTS FOR UNPAVED ROADS

6.1 Mass Concentration Measurements

Table 6-1 presents the average upwind, average downwind, and maximum and minimum mass concentrations measured at Fields Road during the three intensive measurement periods in July 1995, October 1995, and June 1996. These data are presented to provide an indication of the intensity of the emissions from the unpaved road with respect to the EPA 24-hour standard for PM_{10} of 150 $\mu g/m^3$. (The averaged data are not used to derive the emission rates. Emission rate calculations utilize the individual PM_{10} mass concentration values recorded by the downwind tower-mounted samplers.)

During the first intensive measurement period at Fields Road (July 22-27, 1995), average upwind PM_{10} mass concentrations ranged between 27.1 and 37.5 $\mu g/m^3$. The standard deviations of the background measurements for the test period were between 6.5 and 19.7 $\mu g/m^3$. The average uncertainty for individual upwind mass concentration measurements was ± 5.1 $\mu g/m^3$.

The average downwind concentrations presented in Table 6-1 are calculated from the measured concentrations for the samplers directly on the downwind tower plus the nearest overhead sampler. In July 1995 the average downwind concentrations ranged between 206.2 $\mu g/m^3$ for the untreated section and a low of 26.8 $\mu g/m^3$ for the petroleum emulsion/polymer mixture-treated section. The average uncertainty in the downwind mass concentrations was ± 6.7 $\mu g/m^3$. The average downwind concentrations show that only the untreated and biocatalyst-treated sections were producing emissions that were significantly higher than the background concentrations. (The suppressant products' brand and generic names are presented in Table 3-3.)

In the second intensive measurement period, October 17-22, 1995, much higher average upwind PM_{10} mass concentrations were measured (Table 6-1). The average values for each test section ranged from 48.3 to 94.5 $\mu g/m^3$. The day-to-day variation of the upwind PM_{10} mass concentrations in October 1995 was much higher than observed in July 1995. The standard deviations of the upwind measured concentrations was between ± 15.2 and ± 73.1 $\mu g/m^3$. This may reflect instances in which wind shifts played an important role in carrying particles toward the designated upwind samplers during the testing period. This is best illustrated for the days October 20 and 22, 1995. Elevated background concentrations were found on the untreated, petroleum emulsion/polymer mixture, and biocatalyst sections as compared with the value found on the polymer emulsion section on October 20. The polymer emulsion background mass concentration was approximately 10 times lower than the others. On October 22, 1995, the untreated and biocatalyst sections had background concentrations approximately twice those of the polymer emulsion and petroleum emulsion and polymer mixture sections. The average uncertainty in the individual mass concentration for the upwind measurements in October 1995 was ± 5.9 $\mu g/m^3$.

Table 6-1

Upwind, Average Downwind, Max and Min PM_{10} Mass Concentrations Measured for the Three Intensive Measurement Periods

Date	Untreated				Petroleum emulsion/polymer mixture				Biocatalyst				Polymer emulsion				Non-hazardous crude-oil-containing material			
	Upwind	Downwind Average	Max.	Min.	Upwind	Downwind Average	Max.	Min.	Upwind	Downwind Average	Max.	Min.	Upwind	Downwind Average	Max.	Min.	Upwind	Downwind Average	Max.	Min.
	$\mu g/m^3$	$\mu g/m^3$	$\mu g/m^3$	$\mu g/m^3$	$\mu g/m^3$	$\mu g/m^3$	$\mu g/m^3$	$\mu g/m^3$	$\mu g/m^3$	$\mu g/m^3$	$\mu g/m^3$	$\mu g/m^3$	$\mu g/m^3$	$\mu g/m^3$	$\mu g/m^3$	$\mu g/m^3$	$\mu g/m^3$	$\mu g/m^3$	$\mu g/m^3$	$\mu g/m^3$
7/22/95	24.2	71.0	193.7	21.4	30.1	27.0	31.6	15.5	22.6	67.3	133.9	21.3	45.3	32.6	41.1	27.2				
7/23/95	32.1	277.1	456.2	55.6	23.7	20.6	27.8	13.4	47.7	191.1	325.5	46.2	24.3	31.8	43.8	24.3				
7/24/95	27.8	150.9	264.0	38.0	16.2	20.2	35.7	17.5	20.5	126.7	223.9	30.4	17.2	36.1	54.1	23.7				
7/25/95	35.5	319.4	610.4	91.7	26.7	26.8	38.0	16.9	21.0	183.2	390.8	37.1	49.6	24.4	33.6	15.7				
7/26/95	25.4	285.7	615.0	66.8	26.1	26.0	49.0	15.5	44.1	236.7	446.5	72.3	18.7	40.0	94.1	18.4				
7/27/95	41.2	133.3	267.8	44.2	39.7	40.3	71.0	29.0	69.4	186.1	421.6	521.5	35.0	29.4	32.2	24.3				
Average	31.0	206.2			27.1	26.8			37.5	165.2			31.7	32.4						
Std. Dev.	6.5				7.7				19.7				13.8							
10/17/95	30.2	138.4	280.5	53.4	41.2	68.9	112.4	39.2	65.9	145.6	275.9	59.5	41.5	45.1	55.6	32.7				
10/18/95	86.7	373.5	675.0	24.4	41.7	148.4	264.1	53.3	57.9	453.4	882.1	101.3	56.2	56.9	71.3	45.7				
10/20/95	198.2	166.8	291.3	87.9	136.2	87.8	117.4	59.5	121.9	197.1	387.8	89.5	44.6	56.4	58.9	54.0				
10/21/95	24.5	229.4	539.2	34.6	26.1	97.8	151.7	47.9	25.6	259.6	482.5	47.9	29.5	27.1	32.6	20.4				
10/22/95	133.1	239.3	335.6	119.1	64.3	117.1	163.5	79.6	175.7	252.7	415.0	116.3	69.6	77.6	80.7	79.6				
Average	94.5	229.5			61.9	104.0			89.4	261.7			48.3	52.6						
Std. Dev.	73.1				43.7				59.4				15.2							
6/13/96	11.8	147.2	263.9	26.5	21.3	67.4	119.8	18.7	16.8	123.0	222.7	38.2	26.8	43.9	51.4	10.9	10.3	20.2	85.1	18.5
6/14/96	31.3	242.7	477.6	80.9	24.0	146.7	308.9	49.7	37.0	418.5	802.6	73.4	26.3	49.6	84.2	24.0	5.7	53.6	39.1	20.2
6/15/96	37.4	183.1	364.1	59.6	27.8	99.8	173.6	38.0	38.2	213.6	348.5	76.2	31.8	52.1	80.3	33.3	22.9	25.2	37.8	24.1
6/16/96	54.7	287.0	580.0	73.2	39.9	170.4	343.8	44.1	44.4	400.5	671.8	97.2	24.1	72.1	118.7	45.0	22.0	21.1	41.3	25.2
6/17/96	26.8	151.9	325.1	29.0	22.3	92.8	173.1	28.5	13.2	160.2	360.2	56.9	25.2	45.2	70.5	25.1	11.8	20.1	27.4	21.3
6/18/96	16.8	209.5	399.1	35.6	20.6	112.9	233.6	22.4	17.2	280.0	680.7	41.3	35.2	69.6	103.6	43.7	14.7	20.5	34.6	14.6
Average	29.8	203.6			26.0	115.0			27.8	266.0			28.2	55.4			14.6	26.8		
Std. Dev.	15.4				7.3				13.5				4.3				6.8			

Downwind average PM_{10} mass concentrations calculated for the October 1995 intensive measurement period were between 229.5 and 52.6 $\mu g/m^3$ for the untreated and polymer emulsion sections, respectively (Table 6-1). The average uncertainty in the downwind mass concentration measurements in October was ± 7.5 $\mu g/m^3$. The downwind concentrations calculated for the untreated, biocatalyst and petroleum emulsion and polymer mixture are between 1.7 and 2.9 times higher than the upwind concentrations. The polymer emulsion section shows only a slightly elevated downwind concentration as compared with the average upwind concentration for that section.

The last intensive measurement period was June 13-18, 1996, and upwind PM_{10} concentrations were similar to those found in July 1995. Upwind concentrations values ranged between 26.0 and 29.8 $\mu g/m^3$ during this time (Table 6-1). The average uncertainty in the upwind mass concentration values was ± 8.0 $\mu g/m^3$. The day to day variation in upwind concentrations was also much lower during the June 1996 intensive with site to site standard deviations between ± 4.3 and ± 15.4 $\mu g/m^3$ for the polymer emulsion and untreated section respectively.

Average downwind concentrations calculated for the June 1996 intensive ranged from a high of 266.0 $\mu g/m^3$ for the biocatalyst section to a low of 20.1 $\mu g/m^3$ for the "Non-Hazardous Crude-Oil-Containing Materials" (NHCOCM) section (Table 6-1). The average uncertainty in the downwind mass concentrations was about 10 $\mu g/m^3$. The average downwind concentrations were much higher than the upwind for this measurement period.

6.2 Emission Rates

6.2.1 Emission Rate Calculation

The emission rates (PM_{10} mass produced per vehicle-kilometer traveled, grams per VKT) for each of the test sections were calculated from the vertical mass concentration profile measurements and the record of the kilometers traveled by the test vehicle. To calculate the emissions the individual measurements that characterized the vertical PM_{10} mass concentration profile of the dust plume were utilized.

6.2.1.1 Unpaved Road Upwind PM_{10} Profile Analyses

For each test section, PM_{10} sampler #1 is located 30 meters upwind of the road at 2 meters above the surface. This concentration ($\mu g/m^3$) measured at this point is:

$$C = \frac{m}{Qt} \tag{6-1}$$

where: C = concentration ($\mu g/m^3$)
m = particulate sample mass (μg)
Q = sampler flow rate (m^3/s)
t = duration of sampling (s)

The concentration at any height is (Goosens, 1985):

$$C_1 = C_2\left(\frac{z_1}{z_2}\right)^{-\beta} \tag{6-2}$$

where: C_1 is the measured concentration ($\mu g/m^3$) at the height z_1 (m)
C_2 is the predicted concentration ($\mu g/m^3$) at the height z_2 (m)
β characterizes the decrease in concentration with height

The value of β is a function of the sedimentation velocity and the wind friction velocity. Equation 6-2 is derived as follows. At any height z:

$$F = C\, v_d \tag{6-3}$$

where: F = downward directed vertical flux of particles at height z
C = concentration of dust at height z
v_d = velocity of deposition

The upward vertical flux is:

$$F' = -K_A \frac{dC}{dz} \tag{6-4}$$

where: K_A = coefficient of exchange for aerosols.

At equilibrium, $F = F'$:

$$C v_d = -K_A \frac{dC}{dz} \tag{6-5}$$

For neutral atmospheric conditions:

$$K_m = \kappa\, u_*\, z \tag{6-6}$$

where: K_m is the eddy diffusivity
κ is von Karmans constant (≈ 0.4)
u_* is friction velocity

The inertia of small particles can be neglected compared with the velocity fluctuations of the air. For this case, $K_m = K_A$ and:

$$K_A = \kappa\, u_*\, z \tag{6-7}$$

can be assumed.

From this, Equation 6-5 becomes:

$$Cv_d = -\kappa u_* z \frac{dC}{dz} \tag{6-8}$$

The solution of this differential equation is:

$$C_1 = C_2 \left(\frac{z_1}{z_2} \right)^{-\frac{v_d}{\kappa u_*}} \tag{6-9}$$

The value of the exponent β in Equation 6-2 is:

$$\beta = \frac{v_d}{\kappa u_*} \tag{6-10}$$

According to Chamberlain (1967), the deposition velocity v_d (Equation 6-3) depends on the friction velocity u_*. However, at sufficiently low values of u_*, v_d approaches the terminal fall velocity u_∞ (Gregory, 1961). For neutral conditions:

$$\beta = \frac{v_\infty}{\kappa u_*} \tag{6-11}$$

Equations 6-10 and 6-11 show that the exponent β depends on atmospheric conditions and particle size. For non-neutral conditions the value of β can be determined using a stability correction term (Goosens, 1985).

The average friction velocity (u_*, m/s) is calculated from a least squares regression that fits the wind data to the Prandtl-von Karman equation (Bergeron and Abrahams, 1992). The regional u_* determines the range of particle sizes carried in suspension. If the ratio v_d / u_* is < 0.1, the particles will remain suspended in the air (Gillette, 1977). From the point concentration measured upwind of the road, the concentration profile with height was estimated from Equation 6-2. The friction velocity was determined from the wind velocity profile obtained from the on-site meteorological tower using standard boundary layer theory (e.g. Nickling and Gillies, 1993). The cut-point of the particle sizes collected by the sampler is 10 μm or less aerodynamic diameter (v_d = 0.003 m/s, Davies, 1966); therefore the measured concentration (C_1) and friction velocity were used to calculate the concentrations at any height above and below the sampling height using Equation 6-2. Subtraction of the upwind concentration profile from the measured concentrations at each of the samplers in the array then gave the PM_{10} concentrations attributable to road emissions. The background-subtracted downwind concentrations were subsequently used to estimate the PM_{10} emission rate. The theoretical change in background PM_{10} mass concentration as a

function of height, to 10 m, proved to be less than the uncertainties in the mass concentration measurements. Therefore the single value of upwind mass concentration was used to define the background concentration at any sampling height.

6.2.1.2 Unpaved Road Downwind PM_{10} Profile Analyses

The net flux measurement at the midpoint of the suppressant test section was multiplied by the length of the section, 541 meters, to derive the total flux. The downwind PM_{10} concentration profile was divided into four bins, each represented by an average PM_{10} concentration that was attributable to roadway contributions to the atmospheric loading.

Downwind, background subtracted PM_{10} concentrations were considered to be significantly greater than the background, and hence indicative of roadway emissions, if the following condition was met:

$$MSGDN > ((MSGUUP^2 + MSGUDN^2))^{0.5} \quad (6\text{-}12)$$

where: MSGDN = downwind, background subtracted PM_{10} mass concentration ($\mu g/m^3$)
MSGUUP = uncertainty in the upwind PM_{10} mass concentration
MSGUDN = uncertainty in the downwind PM_{10} mass concentration

The flux of particles produced by the vehicles during the sampling period was calculated as follows:

$$F = \sum C_i V_i h_i L \quad (6\text{-}13)$$

where F = the flux of PM_{10} ($\mu g/s$)
C_i = average bin concentration (i=1 to 4) ($\mu g/m^3$)
V_i = the average wind velocity perpendicular to the control section (m/s)
h_i = bin width (m)
L = 541 m

F, the total flux of PM_{10} particles, multiplied by the duration of the test, gave the net value of PM_{10} mass emitted from the road surface during the test period. This value was converted to a flux per unit vehicle kilometer traveled (VKT).

With low ambient wind speeds, the plume rose over the top of the downwind tower and impacted one or both of the two samplers suspended on the overhead cable. Without taking this mass contribution into account, the total flux of particles would be underestimated. The calculated regional friction velocity (u_*, m/s) approximated the vertical wind velocity component. The relationship between friction velocity and the vertical flux of dust particles has been demonstrated theoretically (Gillette and Passi, 1988) and also has been measured experimentally in the atmosphere (Gillette, 1977; Nickling and Gillies, 1993).

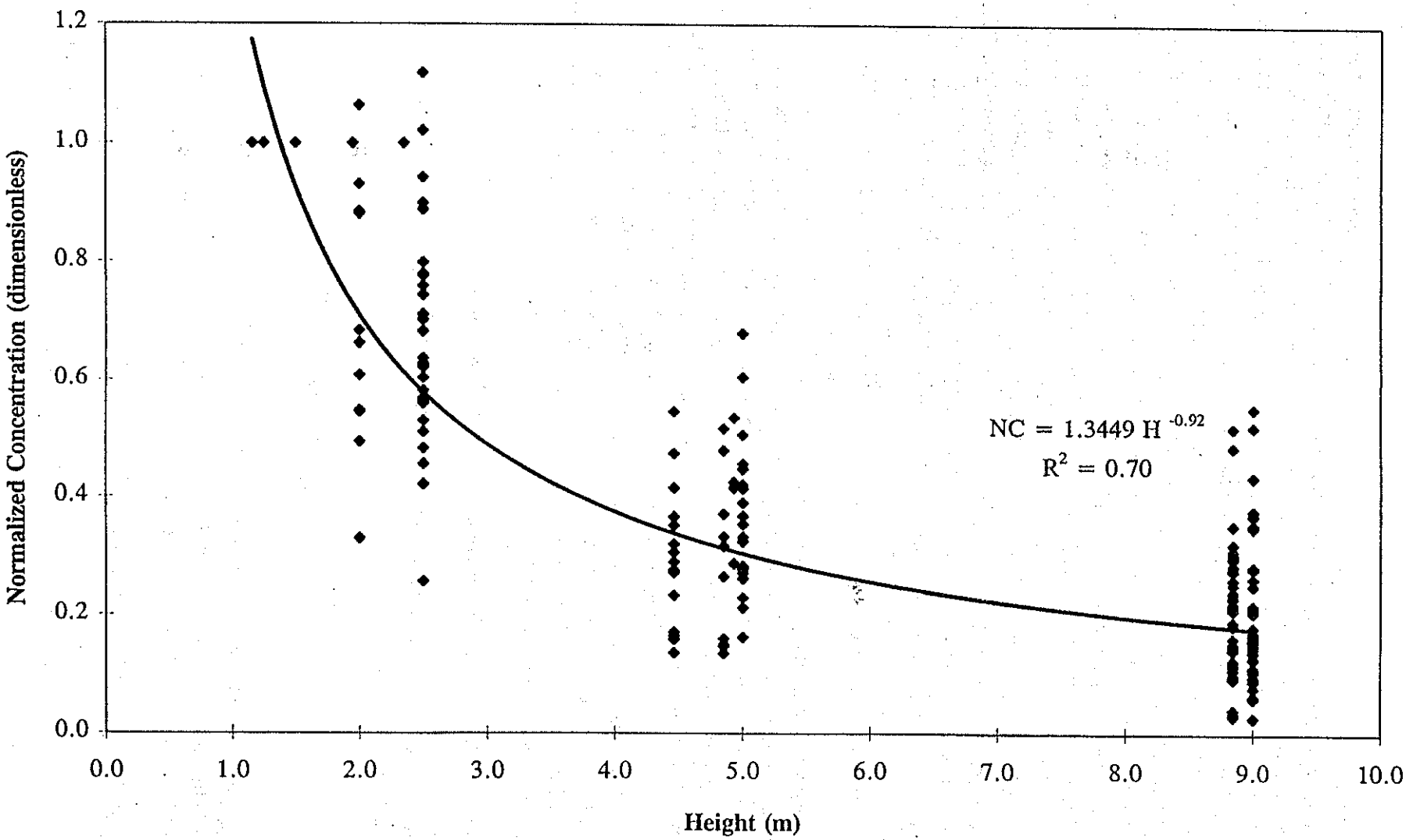

Figure 6-1 Normalized concentration of PM_{10} as a function of height above the road surface.

For test surfaces that were actively emitting, the downwind measured concentrations were significantly higher than the upwind background concentrations. Characteristic vertical mass concentration profiles were observed. Figure 6-1 shows the form of the vertical profiles measured on the downwind tower, with mass concentrations normalized to allow comparison among the different test surfaces. This figure shows that there is a rapid decrease of mass concentration with height a short distance (one to two meters) from the emitting surfaces. The flux estimates are therefore dominated by the mass concentration measurements obtained at the lower tower levels. Direct field observations by several investigators have shown that the concentrations of suspended sediment over eroding surfaces decreases as a power function of height with exponents ranging from -0.25 to -0.35 (Chepil and Woodruff, 1957; Shinn *et al.*, 1976; Gillette , 1977; Nickling, 1978). Goosens (1985) found a lower exponent value of -0.186 for a slowly-moving dust cloud raised by the passage of motor vehicles. However, Goosens (1985) collected samples that had passively deposited in sediment traps. The exponent found in this study, -0.92, is considerably greater than has been reported in other studies. This may result from the sampling methodology which does not depend on particle settling as Goosens (1985) used, but sampled the plume dust with a controlled flow and aerodynamic size cut. Previous studies did not sample a specific size fraction of the dust.

Elevated concentrations resulting from vehicle wakes were sometimes detected by the upwind tower samplers. If the ratio of v_d/u_* is less than or equal to 0.1, the particles will remain in suspension (Gillette, 1977). Given a v_d of 0.003 m/s for a 10 μm diameter particle, the regional friction velocity must be above 0.03 m/s for the particles to remain in suspension. The range of friction velocities calculated from the measured wind velocity profiles was 0.12 m/s to 0.34 m/s, corresponding to average wind velocities measured at 9 m of 2.4 m/s to 6.5 m/s. The range of the ratio of v_d/u_* is 0.01 to 0.03 indicating that during any test, 10 μm particles would be carried upward by the vertical component of the wind velocity. After the dissipation of the vehicle eddies, the suspended particles were transported back past both towers and were therefore sampled on the downwind side.

6.2.1.3 Unpaved Road Emission Rate Calculation: Summary

The upwind background PM_{10} flux was given by the flux per unit area integrated over the upwind side of the box:

$$Fu = \int_0^{10m} C_u(z) V_N L dz \qquad (6\text{-}14)$$

where: $C_u(z)$ = the upwind concentration profile (Equation 6-9)
V_N = the average windspeed perpendicular to the road
L = the test segment length (541 meters), and z is the vertical coordinate.

The integrated "exposure" due to upwind sources is then:

$$E_u = F_u T_s, \qquad (6\text{-}15)$$

where: T_s = the sampling time interval (6 hours)

E_u = the total PM_{10} mass which enters the calculation box from upwind sources in the sampling interval.

The PM_{10} flux emitted from the box is:

$$Fe = \sum_{1}^{6} C_i V_{Ni} h_i L \qquad (6\text{-}16)$$

The integrated PM_{10} mass which is generated within the box is E_{tot}:

$$E_{tot} = [F_e - F_u] T_s \qquad (6\text{-}17)$$

6.2.2 Emission Rate Estimates

The emission rates calculated for the first intensive measurement period, July 22-27, 1995, for each of the Fields Road test sections are shown in Table 6-2. The values range from a high of 962 (±68) g-PM_{10}/VKT for the untreated section, to zero detectable emissions from the petroleum emulsion and polymer mixture (+40 g-PM_{10}/VKT) and the polymer emulsion (+42 g-PM_{10}/VKT) treated sections for several of the tests. The untreated and biocatalyst test sections produced the greatest PM_{10} emissions; the lowest emissions were produced by the sections treated with the petroleum emulsion and polymer mixture and the polymer emulsion. Uncertainties in individual test run emission rate values were calculated by propagating the combined mass concentration uncertainty in the upwind and downwind measurements through Equations 6-14 through 6-17.

Emission rate estimates for the second intensive monitoring period, October 17-22, are shown in Table 6-3. The untreated and biocatalyst test sections continued to produce the greatest PM_{10} emissions. The petroleum emulsion and polymer mixture test section showed a marked increase in its average emission rate (134 (±63) g-PM_{10}/VKT) during this period, while the polymer emulsion test section showed a small decrease.

The emission rate estimates for the final intensive monitoring period, June 13-18, 1996, are shown in Table 6-4. The average emission rate for the untreated section decreased for this interval while the three original suppressant-treated sections show increases. The NHCOCM section had the lowest average emission rate of 24 (±22) g-PM_{10}/VKT. The trends in the changes in emission rates through time for the three test sections are shown in Figure 6-2.

6.2.3 Emission Rate Estimates: Analysis of Variance

Analysis of variance tests (ANOVA) can be used to discern if the emission rates among surfaces are significantly different. ANOVA compares the observed variances in the samples and determines the probability that the differences are due to chance variations or that the samples represent different populations. Table 6-5 shows ANOVA analysis for the emission rates calculated for each intensive measurement period as well as between

Table 6-2
PM_{10} Emissions Measured from Fields Road during Intensive 1 (July 1995)

Date	Velocity (km/hr)	Untreated (g PM_{10}/vkt)	Biocatalyst (g PM_{10}/vkt)	Petroleum emulsion/ polymer mixture (g PM_{10}/vkt)	Polymer emulsion (g PM_{10}/vkt)
7/22/95	40	470	200	0	0
7/24/95	40	430	340	0	70
7/26/95	40	800	500	11	60
7/23/95	55	950	480	0	60
7/25/95	55	960	510	7	0
7/27/95[a]	55	350	390	20	10
avg. 40		567	347	4	43
std. 40		203	150	6	38
avg. 55		753	460	9	23
std. 55		349	62	10	32
average		660	403	6	33
std. dev.		275	120	8	33

[a] wind from the south

Table 6-3
PM_{10} Emissions Measured from Fields Road during Intensive 2 (October 1995)

Date	Velocity (km/hr)	Untreated (g PM_{10}/vkt)	Biocatalyst (g PM_{10}/vkt)	Petroleum emulsion/ polymer mixture (g PM_{10}/vkt)	Polymer emulsion (g PM_{10}/vkt)
10/17/95[a]	40	475	461	128	16
10/20/95[a]	40	368	393	121	33
10/22/95[a]	40	307	448	118	17
10/18/95	55	243	268	65	1
10/21/95	55	1471	924	237	0
avg. 40		383	434	122	22
std. 40		85	36	5	10
avg. 55		857	596	151	1
std. 55		868	464	122	1
Average		573	499	134	13
standard dev.		509	250	63	14

[a] wind from the south

Table 6-4

PM_{10} Emissions Measured from Fields Road during Intensive 3 (June 1996)

Date	Velocity (km/hr)	Untreated (g PM_{10}/vkt	Biocatalyst (g PM_{10}/vkt	Petroleum emulsion polymer mixture (g PM_{10}/vkt)	Polymer Emulsion (g PM_{10}/vkt	NHCOCM (g PM_{10}/vkt)
6/13/96	40	189	155	67	19	32
6/15/96	40	190	250	86	24	4
6/17/96	40	122	147	71	17	14
6/14/96	55	751	1361	427	83	64
6/16/96	55	300	526	189	68	9
6/18/96	55	516	697	254	82	20
avg. 40		167	184	75	20	17
std. 40		39	57	10	4	14
avg. 55		522	861	290	78	31
std. 55		226	441	123	8	29
Average		523	474	106	33	24
std. dev.		357	301	116	30	22

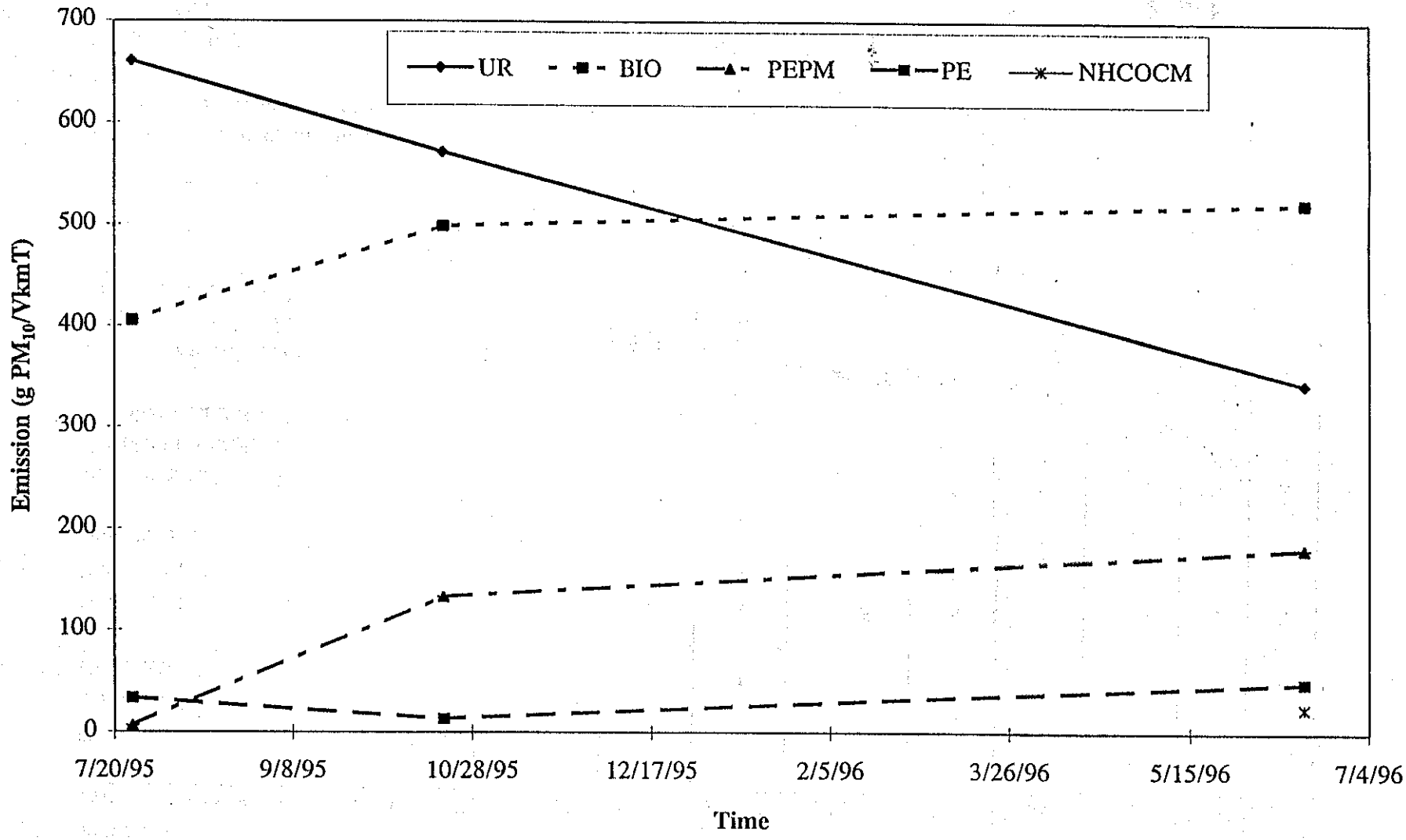

Figure 6-2 Changes in average PM_{10} emission rates as a function of time.

Table 6-5

Analysis of Variance (ANOVA) for Unpaved Road Emissions Between Suppressants and as a Function of Time

Suppressant Type and Intensive	Un I1	Un I2	Un I3	Bio. I1	Bio. I2	Bio. I3	PEP I1	PEP I2	PEP I3	PE I1	PE I2	PE I3
Untreated I1[a]	I	I		I			S			S		
Untreated I2[b]		I			I			S			S	
Untreated I3[c]						I			I			S
Biocatalyst I1					I	I	S	S	S	S	S	S
Biocatalyst I2						I		S	S		S	S
Biocatalyst I3									I			S
Petroleum Em/Mix I1								S	S	I	S	S
Petroleum Em/Mix I2									I		S	S
Petroleum Em/Mix I3												S
Polymer Emulsion I1											I	I
Polymer Emulsion I2												I
Polymer Emulsion I3												
NHCOCM			S			S			S			I

I = no statistical significance
S = significant statistical difference
[a] July, 1996
[b] October, 1995
[c] June, 1996

intensives to assess the changes in emission rates as a function of time (weathering and vehicular activity).

The data indicate that for the first intensive measurement period (July 22-27, 1995):

- No difference between emission rates for untreated and biocatalyst sections;
- No difference between emission rates for the petroleum emulsion and polymer mixture and polymer emulsion test sections;
- Statistically significant difference between the high emitters (untreated and biocatalyst sections) and the low emitters (petroleum emulsion and polymer mixture and polymer emulsion sections); the test sections treated with the petroleum emulsion and polymer mixture and polymer emulsion suppressants produced significantly less PM_{10} than the untreated and biocatalyst sections.

For the second intensive measurement period (October 17-22, 1995):

- No difference between emission rates for the untreated and biocatalyst sections, and no differences between the first and second intensives;
- Statistically significant differences when the untreated and biocatalyst sections are compared to both the petroleum emulsion and polymer mixture and the polymer emulsion-treated sections;
- Statistically significant difference between the petroleum emulsion and the polymer mixture/polymer emulsion sections;
- Statistically significant difference for the petroleum emulsion and polymer mixture section's emission rates, compared for the first and second intensives;
- No significant difference between emission rates for the polymer emulsion section between the first and second intensives.

For the second intensive measurement period, there was a noticeable change in emission rates only for the petroleum emulsion and polymer mixture test section, which produced on average 21 times as much PM_{10} per vehicle-kilometer approximately 2.5 months after application.

For the third intensive measurement period (June 13-18, 1996):

- No difference among emission rates for the untreated, biocatalyst, and petroleum emulsion and polymer mixture test sections, and no differences between intensives 2 and 3.

- Statistically significant difference, polymer emulsion compared to untreated, biocatalyst and petroleum emulsion and polymer mixture sections.

- No difference in emission rates for the polymer emulsion section between intensives 2 and 3.

- Statistically significant difference among the NHCOCM and the untreated, biocatalyst, petroleum emulsion/polymer mixture sections.

- No significant difference between the NHCOCM and the polymer emulsion section.

6.3 Comparisons of Emission Rate Estimates to Previous Studies

These estimated PM_{10} emissions rates are comparable to those presented in previous studies. Table 2-6 summarizes the results of several studies that examined PM_{10} emissions on unpaved roads as a function of vehicular traffic and suppressant application. For example, on an untreated section of gravel road in Arizona, Stevens (1991), reported a range of emission rates from 660 1,360 g-PM_{10}/VKT for unpaved roads with silt contents between 4.3% and 11%. Considering all cases from the Stevens (1991) study the average emission rate from the untreated, unpaved road with an average silt content of 7.5% was 950 g-PM_{10}/VKT. By comparison, the untreated section of Fields Road (average silt content of 6.4%) had an emission rate of 523 (±357) g-PM_{10}/VKT.

Flocchini *et al.* (1994) measured PM_{10} emission on unpaved farm roads in the San Joaquin Valley and reported a range of emissions for an untreated road of 420 to 3,620 g/VKT which is larger than the range of emissions observed on the untreated section of Fields Road. However, in the Flocchini *et al.* (1994) study the higher emission rates were for an unpaved test section with an average silt content of over 20%, approximately 3 times greater than the silt content of the untreated section of Fields Road In addition, the silt loading (g/m^2) of the Flocchini *et al.* (1994) test section was 1.6 times greater than on Fields Road.

For test sections that were treated with the suppressants, lignin sulfonate, magnesium chloride, and an oil-based product, Flocchini *et al.* (1994) reported an average range for PM_{10} emissions between 40 and 340 g-PM_{10}/VKT which is similar to the range found in this study, 24 (±22) to 474 (±301) g-PM_{10}/VKT for the suppressant-treated test sections.

6.4 Comparisons of Emission Rate Estimates to AP-42 Model

The AP-42 empirical dust emission model (U.S. EPA, 1995) was discussed in Section 2 of this report. Figure 6-3 shows the comparison between the emission rates derived for Fields Road test sections, with the standard emission model estimates for unpaved roads generated by the AP-42 model. The input parameters used to obtain the emissions estimates

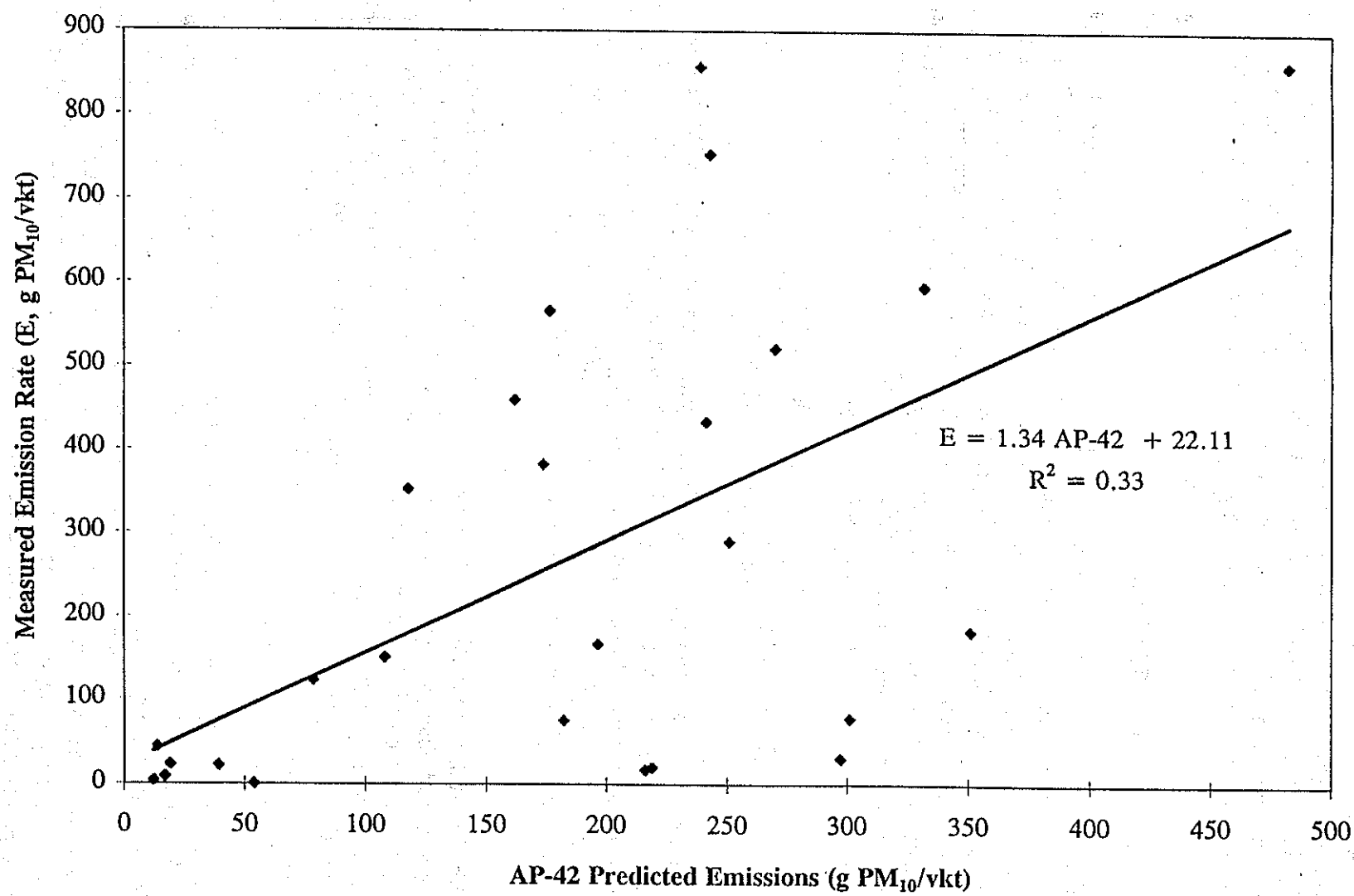

Figure 6-3 Average measured emission rates on Fields Road compared with AP-42 predicted emissions.

using the AP-42 model were the environmental conditions measured on Fields Road (e.g. silt content, vehicle weight). As can be seen in Figure 6-3 there is considerable scatter in the data, which Flocchini *et al.* (1994) also found in a similar comparison (Figure 6-4). Both studies show an underestimation of emissions using the AP-42 model; in the case of the Flocchini *et al.* (1994) study, the underestimation is highest when silt contents are greater than 20%.

6.5 Suppressant Control Efficiency

The PM_{10} control efficiency of the tested suppressants have been calculated by comparing test section emission rates: as discussed in Section 2-5, the PM_{10} emission rate from the test section treated with the suppressant is compared to the emission rate from a nearby untreated ("control") section. This procedure assumes that the environmental conditions at the two sections can be considered equivalent. This assumption is valid because measurements were taken simultaneously on each section for the same time periods on each day of testing. Suppressant efficiency is defined as the percent reduction in emissions between the treated and untreated sections:

$$\%\ efficiency = \left[1 - \left(\frac{treated\ emission\ rate}{untreated\ emission\ rate}\right)\right] \times 100 \qquad (6\text{-}18)$$

Table 6-6 shows the efficiencies of the three suppressants based on the PM_{10} emission rates measured during the first intensive. This study period began four days after the suppressant applications were finished, and continued for six days. The petroleum emulsion and polymer mixture and polymer emulsion average efficiencies were 99% (±2%) and 94% (±6%), respectively. The biocatalyst treatment's average efficiency, 33% (± 25%), is much lower.

With almost three months' weathering and vehicular traffic, the efficiencies of two of the suppressants had changed significantly from the first intensive, as shown in Table 6-7. By October 1995, the biocatalyst section produced PM_{10} at a greater rate, on average, than the untreated section as indicated by the negative efficiency value of -5% (±30%). The petroleum emulsion and polymer mixture treatment reduced emissions by 72% (±8%) while the polymer emulsion suppressant maintained the highest efficiency rating, with a 96% (±4%) reduction in PM_{10} emissions.

Eleven months after application, the suppressant efficiencies had declined, as shown in Table 6-8. The biocatalyst section continued to produce PM_{10} emissions at levels that were indistinguishable from the untreated section. The biocatalyst treatment's efficiency was -38% (±37%) for the third intensive measurement period. The efficiency of the petroleum emulsion and polymer mixture suppressant declined to 49% (±10%) and the polymer emulsion treatment's efficiency declined to 86% (±5%). After eight months' aging, the NHCOCM suppressant's efficiency was 92% ±6%.

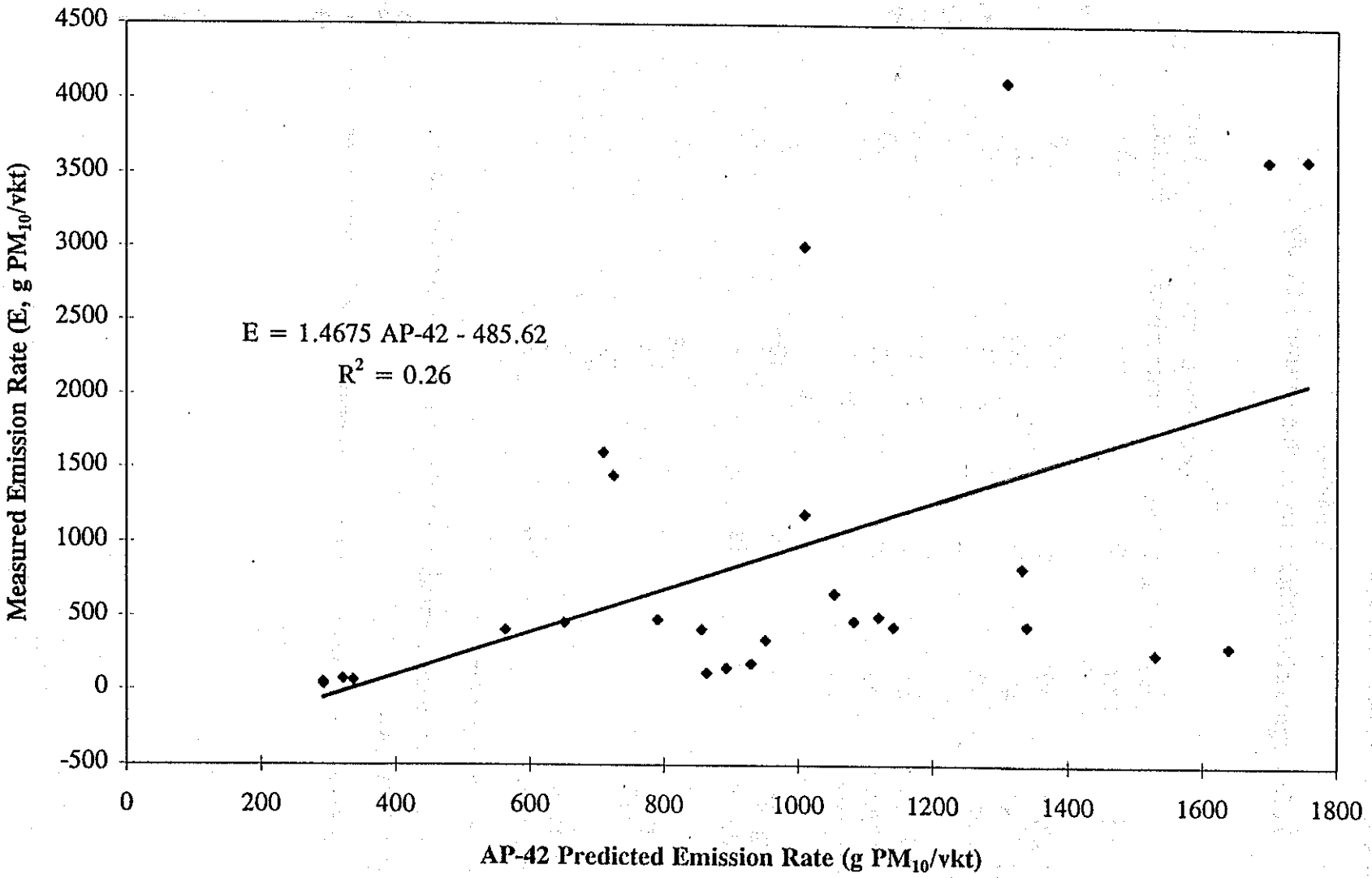

Figure 6-4 U.C. Davis measured PM_{10} emission rates compared with AP-42 estimated emissions.

Table 6-6
PM_{10} Suppression Efficiencies during Intensive 1 (July 1995)

Date	Velocity (km/hr)	Biocatalyst[a] (%)	Petroleum emulsion/ polymer mixture (%)	Polymer Emulsion (%)
7/22/95	40	56	100	100
7/24/95	40	20	100	83
7/26/95	40	37	99	93
7/23/95	55	50	100	94
7/25/95	55	47	99	100
7/27/95[b]	55	-13	94	97
avg. 40		38	100	92
std. 40		18	1	9
avg. 55		28	98	97
std. 55		36	3	3
Average		33	99	94
std. dev.		26	2	6

[a] negative values denote emissions greater than the untreated section
[b] wind from south

Table 6-7
PM_{10} Suppression Efficiencies during Intensive 2 (October 1995)

Date	Velocity (km/hr)	Biocatalyst[a] (%)	Petroleum emulsion polymer mixture (%)	Polymer emulsion (%)
10/17/95[b]	40	3	73	97
10/20/95[b]	40	-8	67	91
10/22/95[b]	40	-46	61	94
10/18/95	55	-10	73	100
10/21/95	55	37	84	100
avg. 40		-17	67	94
std. 40		26	6	3
avg. 55		14	79	100
std. 55		33	8	0
Average		-5	72	96
std. dev.		30	9	4

[a] negative values denote emissions greater than the untreated section
[b] wind from south

Table 6-8
PM_{10} Suppression Efficiencies during Intensive 3 (June 1996)

Date	Velocity (km/hr)	Biocatalyst[a] (%)	Petroleum emulsion/ polymer mixture (%)	Polymer emulsion (%)	NHCOCM (%)
6/13/96	40	18	65	90	83
6/14/96	40	-32	55	87	98
6/15/96	40	-20	42	86	89
6/16/96	55	-81	43	89	91
6/17/96	55	-75	37	77	97
6/18/96	55	-35	51	84	96
avg. 40		-11	54	88	90
std. 40		26	12	2	8
avg. 55		-64	43	83	95
std. 55		25	7	6	3
Average		-37	49	85	92
std. dev.		37	10	5	6

[a] negative number denotes emissions were higher than the untreated section

Figure 6-5 shows the average Fields Road suppressant control efficiencies derived for all three intensive data sets.

6.6 Suppressant Control Efficiency Estimates: Analysis of Variance

To determine if the PM_{10} suppressant efficiencies were significantly different among suppressant types and through time, a series of ANOVA tests were run on the data from each intensive measurement period. Table 6-9 shows the results of those tests. The results show that in the first intensive measurement period there was:

- No significant difference in the efficiencies of petroleum emulsion and polymer mixture and polymer emulsion treatments in reducing PM_{10} emissions;
- The petroleum emulsion and polymer mixture and polymer emulsion efficiencies were significantly greater than that of biocatalyst.

Analysis of the second intensive's data indicates:

- biocatalyst was ineffective in reducing PM_{10} emissions;
- The efficiency of petroleum emulsion and polymer mixture was significantly less than polymer emulsion, and also less than it was in the first intensive;
- The polymer emulsion's efficiency remained unchanged between the first and second intensives.

Analysis of the third intensive's data indicates:

- The biocatalyst suppressant was ineffective in reducing PM_{10} emissions;
- The petroleum emulsion and polymer mixture's efficiency declined further between the second and third intensives;
- The efficiency of the polymer emulsion suppressant had declined significantly since the second intensive.
- At this time, the efficiency of the "NHCOCM" treatment was greater than that of the other three suppressants.

6.7 Surface Characterization Measurements

Critical road surface characteristics thought to affect PM_{10} emissions were discussed in Section 2. The following surface measurements were performed based on samples taken according to the schedule shown in Table 4-3: analysis of the amount of loose surface material; aggregate size distribution; surface silt content by percent; mass loading (g/m^2) using two different collection techniques; surface strength; and the strength of aggregates.

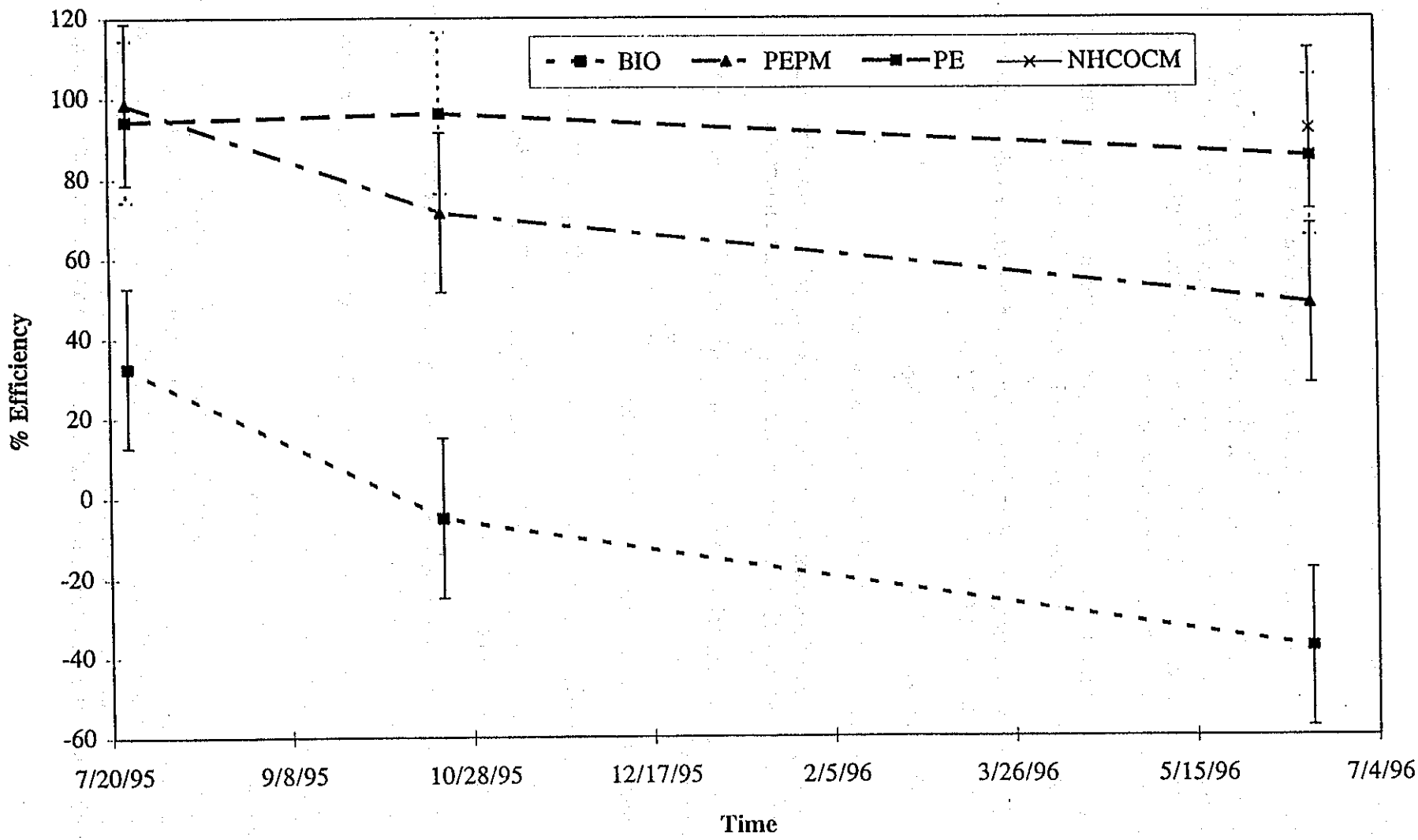

Figure 6-5 PM_{10} emissions control efficiency as a function of time.

Table 6-9
Analysis of Variance (ANOVA) for Suppression Efficiencies Between Suppressants and as a Function of Time

Suppressant Type and Intensive	Bio. I1	Bio. I2	Bio. I3	PEP I1	PEP I2	PEP I3	PE I1	PE I2	PE I3
Biocatalyst I1[a]		S	S	S	S	I	S	S	S
Biocatalyst I2[b]			I	S	S	S	S	S	S
Biocatalyst I3[c]						S	S	S	S
Petroleum Em/Mix I1					S	S	I	I	S
Petroleum Em/Mix I2						I	S	S	S
Petroleum Em/Mix I3							S	S	S
Polymer Emulsion I1								I	S
Polymer Emulsion I2									S
Polymer Emulsion I3									
NHCOCM	S	S	S	S	S	S	I	I	S

I = no statistical significance
S = significant statistical difference
[a] July, 1996
[b] October, 1995
[c] June, 1996

This section presents the trends observed in these measurements through the duration of this project and also examines their relationships with measured PM_{10} emissions.

The changes in Fields Road surface characteristics resulted from two processes: exposure to weather and the continued action of vehicle traffic. Weathering of the surface was caused primarily by rainfall events that probably caused aggregate breakdown or washout of the chemical binding agents associated with the suppressants. In addition solar radiation probably caused some weakening of the adhesive properties of the suppressants and aided in evaporating any volatile components. During the time period from August 1, 1995 to June 18, 1996, 344 mm of precipitation were recorded at the Merced County airport, approximately 30 miles from Fields Road. The monthly precipitation values for this period are shown in Table 6-10. Rain was first recorded in the area in December 1995, five months after the suppressants were applied. Above average rainfall amounts were observed in December 1995, and January, February, and May 1996.

Traffic on Fields Road was light. Table 6-11 summarizes the vehicle traffic for the times it was monitored through the study period. On average, 14 vehicles per day traveled through the section of Fields Road in which the test plots were situated during the July 1995-August 1996 period. In addition to the everyday vehicle traffic, approximately 1,800 total passes (96 per day) were made by the test vehicle during the three intensive measurement periods.

The appearance of the suppressed surfaces changed as indicated by video and still photographic records. General observations of the changes at the Fields Road sites, from July 1995 through August 1996, are as follows:

<u>July 1995</u>

- Initially the surfaces were very level as a result of the grading that preceded suppression application.
- The untreated section was composed of a relatively thick, loose surface layer.
- The surface treated with biocatalyst remained approximately the same color, and there was a noticeable amount of loose surface material.
- The polymer emulsion section was characterized by a white, pliable, film-like covering several millimeters thick.
- The road bed in the petroleum emulsion/polymer mixture section was much darker than prior to application and the suppressant was noticeably sticky. There was little evidence of loose material in the smaller size fractions on this section.

Table 6-10
Monthly Rainfall During the Dust Demonstration Field Study as Measured at Merced Airport

Month	Measured Precipitation (mm)	Long-Term Average Precipitation (mm)
Aug-95	0	0.76
Sep-95	0	4.83
Oct-95	0	15.24
Nov-95	0	38.62
Dec-95	82.55	45.45
Jan-96	80.01	60.2
Feb-96	87.12	52.32
Mar-96	46.74	50.8
Apr-96	21.34	27.94
May-96	26.16	10.02
Total	343.92	306.18

Table 6-11
Vehicle Traffic on Fields Road

Date	Vehicle Counts	Average No. vehicles per day
September-October, 1995	519	17
October-December, 1995	606	9
December, 1995-March, 1996	823	10
March-June, 1996	na	na
June-July, 1996	505	17
July-August, 1996	720	19
Average		14

September 1995

- The untreated section maintained its cover of loose surface particles over a hard base. It appeared that there was a sorting process occurring, with larger particles accumulating on the surface and some fining with depth.

- Petroleum emulsion/polymer mixture section: Still showed a distinct color difference and was much darker than the other sections. The center section of this test section was best preserved with more break-up towards the edges.

- Polymer emulsion section: Rips and holes were developing in the surface film and this was more evident towards the outer edges. Very little loose material except in the small areas where the surface film had been damaged.

- Biocatalyst section: No signs of crusting and was covered with loose sediment.

October 1995

- Untreated section: Some indication of preferential traffic movement by the development of tire track patterns.

- Petroleum emulsion/polymer mixture section: Color has faded somewhat. More loose surface material. Defined pattern of tire tracks forming.

- Polymer emulsion section: Increasing break-up of the surface film, but maintaining good overall integrity.

- Biocatalyst section: Some tire track development.

- NHCOCM section: this treatment applied at this time; appearance much like a paved road, except not as smooth as blacktop or cement.

December 1995

- Untreated section: Surface appears moist. Amount of loose surface material is reduced. It has been washed away by rain or re-incorporated into the road bed.

- Petroleum emulsion/polymer mixture section: Color continues to fade. Decline in loose surface material due to moisture effects.

- Polymer emulsion section: Increasing break-up of the surface film, but maintaining good overall integrity.

- Biocatalyst section: Decline in loose surface material due to moisture effects.

- NHCOCM section: Some pits in the surface, in which loose material collects; some crumbling in areas near road edges.

March 1996

- Untreated section: More loose surface material.
- Petroleum emulsion/polymer mixture section: Color continues to fade now almost completely indistinguishable from control section. Increase in loose surface material. Some coherent crust patches are still apparent.
- Polymer emulsion section: Increasing break-up of the surface film, estimate approximately 75 % of the film is still together.
- Biocatalyst section: Increase in loose surface material.
- NHCOCM section: More surface pits in which loose material collects; more crumbling at road edges; loose material more concentrated near edges.

June 1996

- Untreated section: No apparent change from March 1996.
- Petroleum emulsion/polymer mixture section: Color continues to fade now almost completely indistinguishable from control section. Increase in loose surface material. Some coherent crust patches are still apparent.
- Polymer emulsion section: Increasing break-up of the surface film, estimate approximately 65% of the film is still together.
- Biocatalyst section: No apparent change from March 1996.
- NHCOCM section: Continued pitting and crumbling at edges; concentration of loose material near edges.

July 1996 and August 1996

- Untreated section: No apparent change from March 1996.
- NHCOCM section: No apparent change from June 1996.

6.7.1 Bulk Loading of Loose Surface Material

The loose surface material on the Fields Road test sections was collected using two different methodologies. The first method was to sweep up the loose sediment with a fine bristled brush from a strip of unpaved road, running perpendicular to the direction of the

road, of known width and length. Weighing the sample and knowing the sampled area provided a measure of the amount of loose surface material per unit area. The second method removed the loose surface material from a strip of road with a vacuum device.

Figure 6-6 shows the changes observed in the bulk surface loading with the sweep method and Figure 6-7 the changes observed using the vacuum collection method. Both figures show similar trends in changes in the bulk surface loading through time, except for the high initial value for the biocatalyst suppressant using the sweep method (Figure 6-6). The general trends are:

- A rapid increase in loose surface material from July 1995 to September 1995 for the untreated, biocatalyst and petroleum emulsion and polymer mixture sections indicated by both collection methods.

- A decrease in December 1995 for the same three sections, followed by an increase through to June 1996 for all sections.

- The polymer emulsion section shows a gradual increase in the amount of loose surface material from July 1995 to June 1996.

- General increase in loose surface material on NHCOCM-treated section, October 1995 to June 1996. After June 1996, the vacuum collection data indicate roughly constant amounts of surface material in the untreated section and decreased amounts in the NHCOCM-treated section.

6.7.2 Percent Silt Content in Surface Material

The percentages of bulk surface material mass due to particles in the silt size fraction (particle diameters less than 75 μm) were determined for the bulk surface samples collected by the sweep and vacuum methods. The silt content of the surface material is an important input parameter into the AP-42 emissions model. The changes in surface silt content through time provides one indication of the potential emission capability of unpaved roads. The range of average percent silt contents found for the test sections using the sweep collection method was from a low of 0.4% (±0.2%) for the petroleum emulsion and polymer mixture section immediately after suppressant application to a high of 12.5% (±2.3%) for the biocatalyst section in June 1996. The silt content percentages determined for the vacuum samples covers a similar range, from a low of 1.1% (±1.8%) to a high of 13.0% (±5.9%), both for the biocatalyst section. Figures 6-8 and 6-9 show the changes in the percent silt content of the road surface as a function of time for the sweep and vacuum methods, respectively. The general trends in the data are:

- An increase in percent silt content for all sections after application in July 1995, to September and October 1995. This is shown from both collection methods except the vacuum method, which indicates a decrease in silt content for the untreated section during this time.

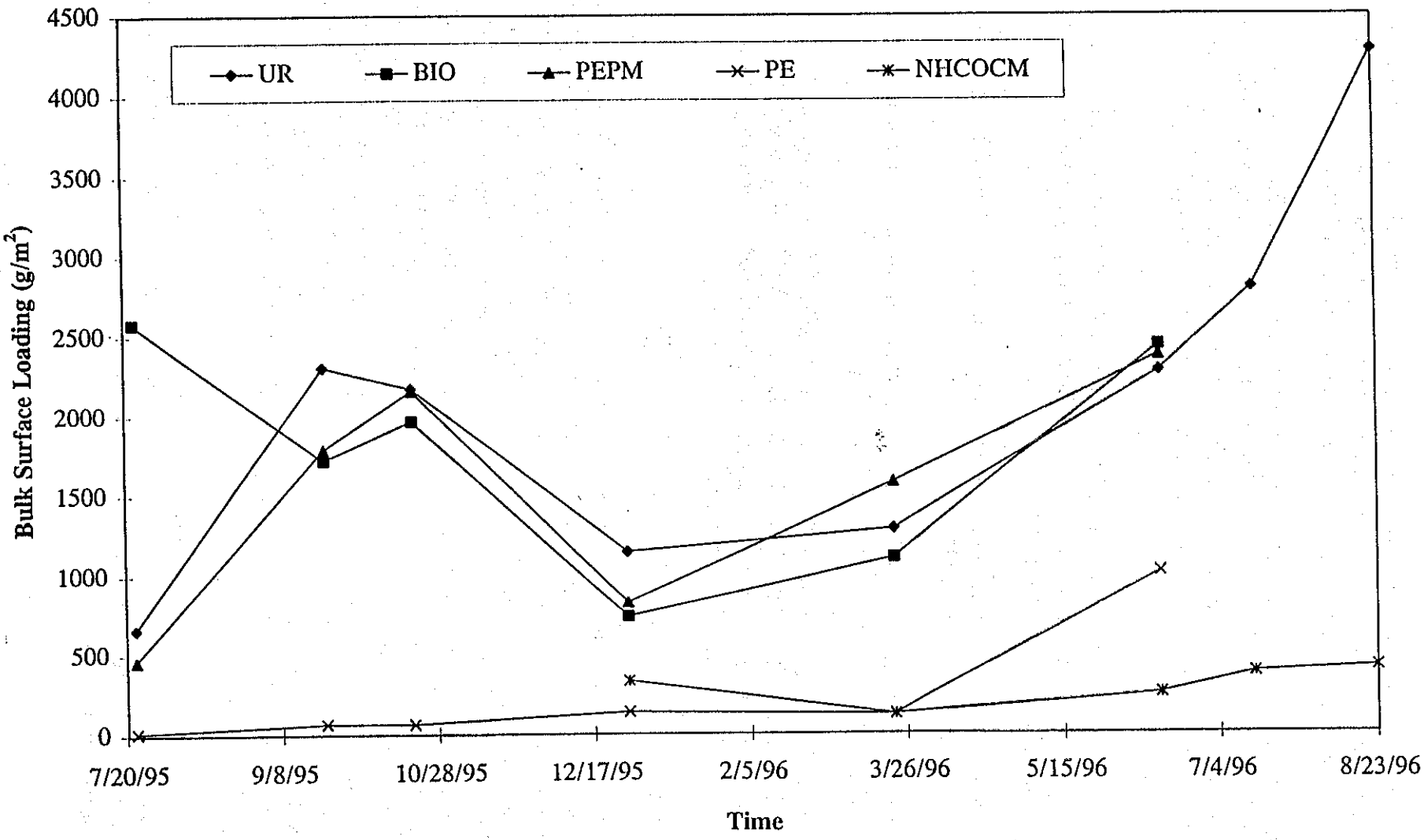

Figure 6-6 Changes in the bulk surface loading (g/m^2) as a function of time.

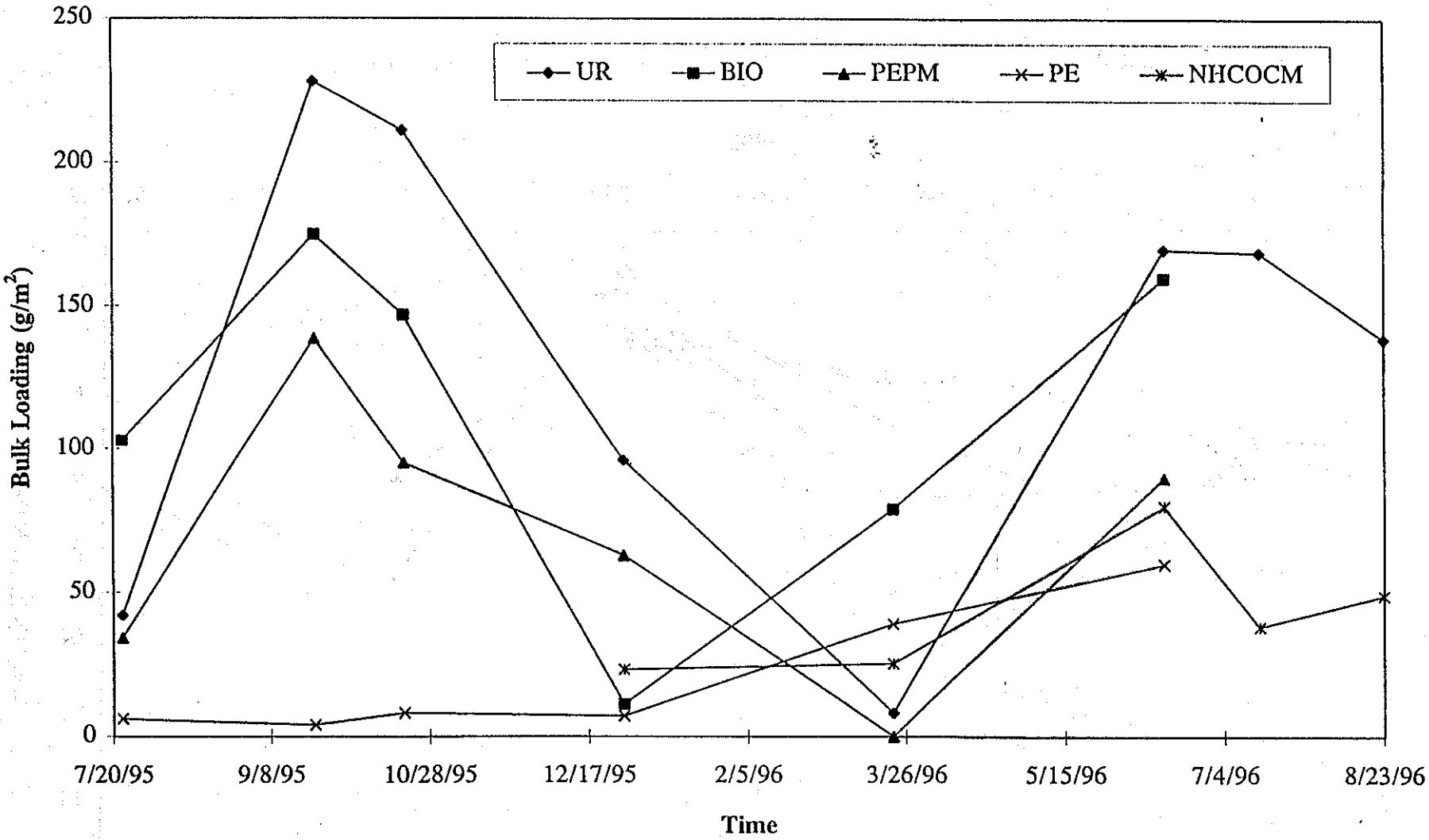

Figure 6-7 Changes in the bulk surface loading as a function of time as determined from vacuum collected samples.

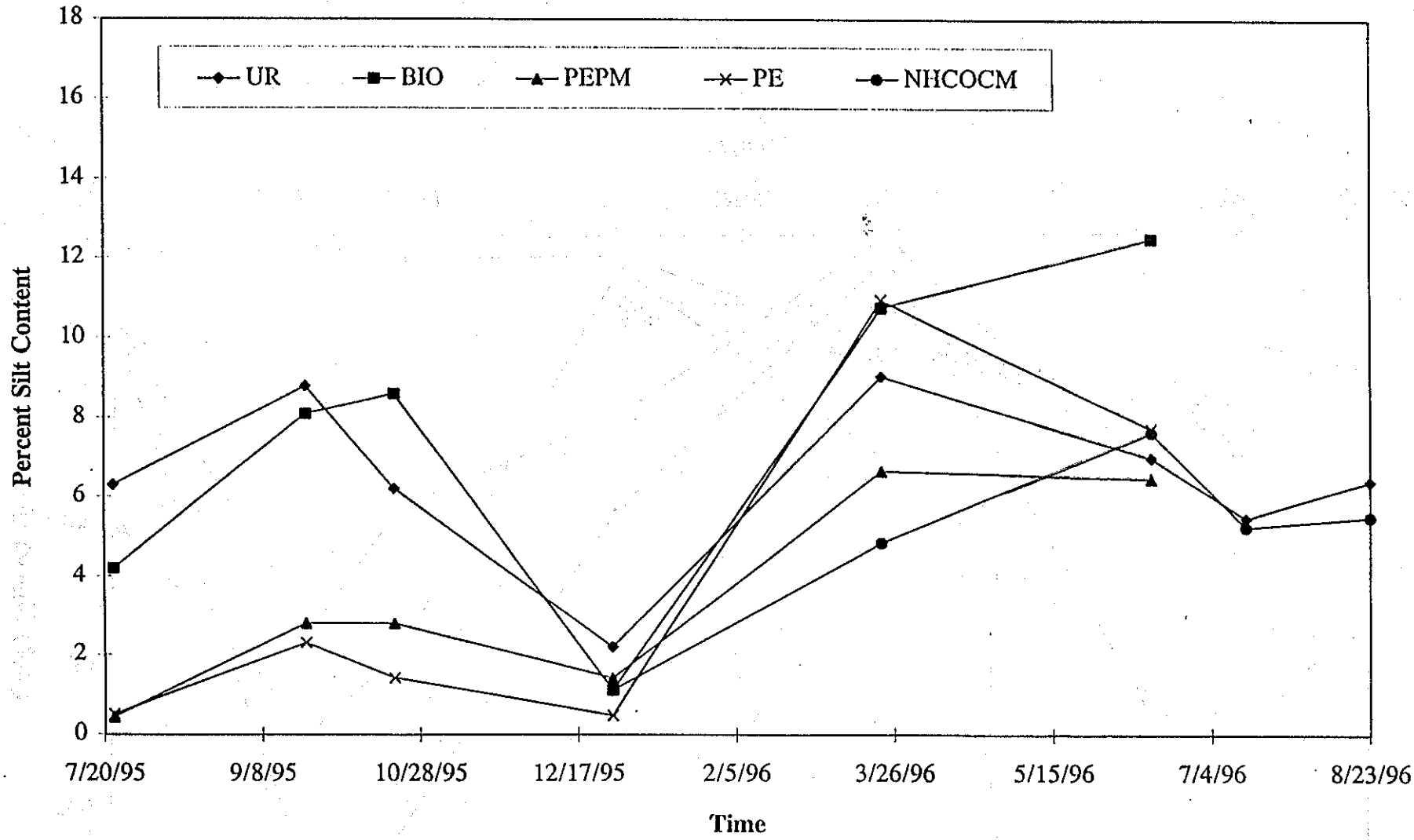

Figure 6-8 Changes in the percent silt content as a function of time as determined from the sweep collected surface samples.

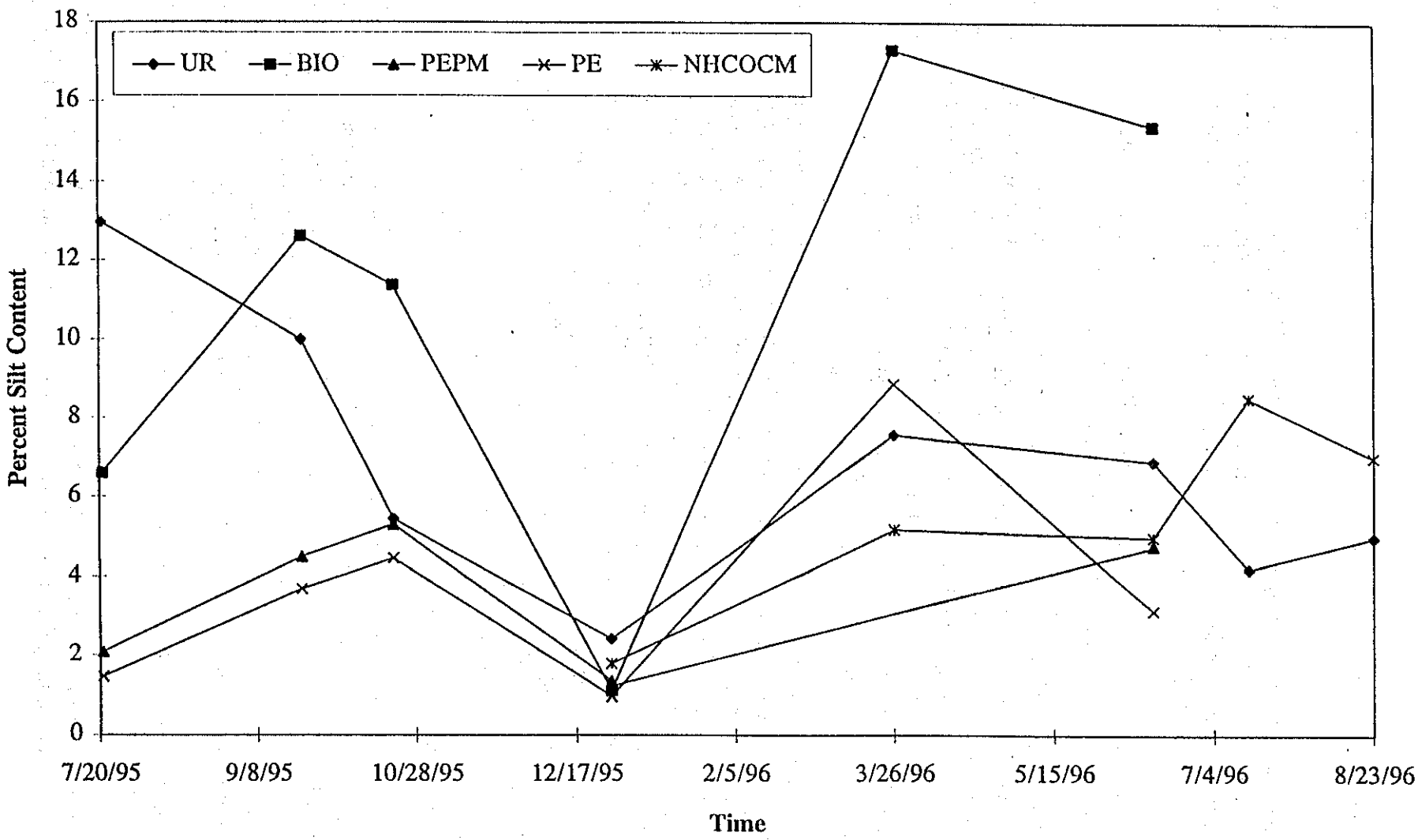

Figure 6-9 Changes in the percent silt content as a function of time as determined from the vacuum collected surface samples.

- A decrease in silt content from October 1995 through December 1995 for all test sections.

- An increase in silt content from December 1995 to March 1996, followed by decline from March 1996 to June 1996, except for biocatalyst in the sweep samples and petroleum emulsion and polymer mixture in the vacuum samples; these data continue to increase.

- After June 1996, the untreated and NHCOCM sections show decreasing silt contents except for the vacuum-collected NHCOCM sample.

For the last intensive measurement period supplemental measurements were made on the collected surface samples. Two additional sieves were introduced below the 75 μm sieve to further subdivide the samples into additional size categories. The sample mass was apportioned (by percentage) according to the mass of soil particles with diameters from 38 to 75 μm, from 25 to 38 μm, less than 25 μm. Table 6-12 shows the relative percentages of total silt, and the three size sub-divisions for the surface samples collected by sweep and vacuum methods in June, July, and August 1996.

The samples are dominated by the 38 to 75 μm size range with an average of 70.2% in the sweep samples and 75.9% on the vacuum samples. In the particle size range 25 to 38 μm, the average percent by mass in the sweep samples is 26.8% and for the vacuum samples it is 16.4%. The mass in particles less than 25 μm is 3.1% and 7.6% for the sweep and vacuum samples respectively. These data suggest that the silt content of the loose surface material is dominated by the coarser silt particles. The 25 μm sieve results suggest that the PM_{10} content of the road surface is low; however this methodology may under estimate actual PM_{10} content, as particles this small do not easily pass through sieves due to their cohesive properties. They also tend to adhere to larger particles, even under mechanical agitation, due to Van der Waals forces and (especially in this case) electrostatic attraction which will be augmented by the sieving procedure.

6.7.3 Bulk Silt Loading

The amount of silt in the surface sediments of the unpaved road can also be expressed in terms of its mass per unit area. The amount of silt expressed in g/m^2 was determined for each of the bulk samples of loose surface material. This measurement seems to provide a more realistic indicator of emission potential. The "Percent Silt Content" measurement presented in the previous section gives no direct indication of the amount of dust available for resuspension by vehicles. For example, a very small amount of surface material may consist mostly (to a high percentage) of silt, but this small reservoir would quickly be depleted. The bulk silt loading provides a better measure of the net amount of the source material available for resuspension and subsequent transport.

The bulk silt loadings cover a much broader range than the percent silt values. They range over four orders of magnitude for the sweep-collected samples and over three orders of

Table 6-12
Size Fractions in the Silt Range by Percent of the Total Mass of Surface Samples from Fields Road

Site	Date	Collection Method	Total % Silt <75 µm	% Silt by Size Fraction 75-38 µm	38–25 µm	>25 µm
Pet. Em. w/ Polymer Mix	6/16/96	sweep	6.9	4.4	2.4	0.1
Pet. Em. w/ Polymer Mix	6/16/96	sweep	6.1	3.8	2.2	0.1
Biocatalyst	6/16/96	sweep	15.7	6.8	8.7	0.2
Biocatalyst	6/16/96	sweep	9.3	5.5	3.4	0.4
Polymer Emulsion	6/16/96	sweep	7.3	4.8	2.2	0.4
Polymer Emulsion	6/16/96	sweep	8.2	5.4	2.1	0.6
Untreated	6/16/96	sweep	7.2	4.8	2.2	0.2
Untreated	6/16/96	sweep	4.9	3.7	1.0	0.2
Untreated	7/23/96	sweep	4.0	2.9	0.9	0.2
Untreated	7/23/96	sweep	6.9	5.3	1.1	0.6
NHCOCM	6/16/96	sweep	5.5	4.9	0.6	0.0
NHCOCM	6/16/96	sweep	9.8	8.4	1.5	0.0
NHCOCM	7/23/96	sweep	5.6	4.6	1.0	0.0
NHCOCM	7/23/96	sweep	4.9	3.7	1.0	0.2
Pet. Em. w/ Polymer Mix	6/16/96	vacuum	5.0	3.3	1.3	0.4
Pet. Em. w/ Polymer Mix	6/16/96	vacuum	4.5	3.4	0.7	0.4
Biocatalyst	6/16/96	vacuum	3.1	2.5	0.5	0.2
Biocatalyst	6/16/96	vacuum	12.5	6.7	3.2	2.7
Polymer Emulsion	6/16/96	vacuum	3.1	2.5	0.5	0.2
Untreated	6/16/96	vacuum	7.1	4.7	2.0	0.3
Untreated	6/16/96	vacuum	6.7	5.0	0.7	1.1
Untreated	7/23/96	vacuum	3.5	3.1	0.3	0.1
Untreated	7/23/96	vacuum	5.0	4.3	0.3	0.4
NHCOCM	6/16/96	vacuum	4.0	3.3	0.4	0.3
NHCOCM	6/16/96	vacuum	6.0	5.2	0.8	0.0
NHCOCM	7/23/96	vacuum	7.0	5.3	1.6	0.1
NHCOCM	7/23/96	vacuum	10.1	7.5	1.8	0.8

magnitude for the vacuum-collected samples. The lowest silt loading is 0.8 g/m^2 for the polymer emulsion section immediately after application, for both collection methods, to a high of 300 g/m^2 for biocatalyst in June 1996 for the sweep sample and 260 g/m^2 for biocatalyst at the same time for the vacuum sample. In general, the vacuum sample bulk silt contents are lower than those of the sweep samples by a factor of 0.08. Figures 6-10 and 6-11 show the bulk silt loadings determined by the sweep and vacuum methods, respectively, for the duration of the project. The general trends are:

- The polymer emulsion and the petroleum emulsion and polymer mixture have initial silt loadings several orders of magnitude lower than the untreated and biocatalyst sections.

- Bulk silt loading increases from July 1996 to September 1996 for the untreated biocatalyst and petroleum emulsion and polymer mixture test sections. This increase is not observed for the polymer emulsion section.

- In December, silt loadings in the sweep samples drop to below values measured immediately after application. The silt loadings in the vacuum samples follows a similar pattern, but not to the same degree of reduction.

- In every case, except for the vacuum samples of petroleum emulsion and polymer mixture and biocatalyst, silt loadings increase from December 1995 to March 1996. The petroleum emulsion and polymer mixture and biocatalyst sections show slight decreases in silt loading during this period.

- From March 1996 through to June 1996 silt loading increases in all cases except for the petroleum emulsion and polymer mixture section vacuum sample.

6.7.4 Surface Strength

An index of surface strength (kg/cm^2) was obtained for this study by measuring the resistance of the test surfaces to an vertical force applied with a Proctor Penetrometer®. Transects of the road width were made with measurements taken every 0.25 meters; two transects were done for every measurement period. The changes observed in the average surface strength for each test section as a function of time are shown in Figure 6-12 and the average strength measurements for each sampling period are shown in Table 6-13. The general trends observed were:

- The strength measurements of the surfaces in July 1995 were similar with a range between approximately 145 and 195 kg/cm^2.

- Surface strength declined for the untreated, polymer emulsion and petroleum emulsion and polymer mixture sections between July 1995 and December 1995, except for the biocatalyst section, which showed an increase.

- Surface strength increased in all cases from December 1995 to March 1996.

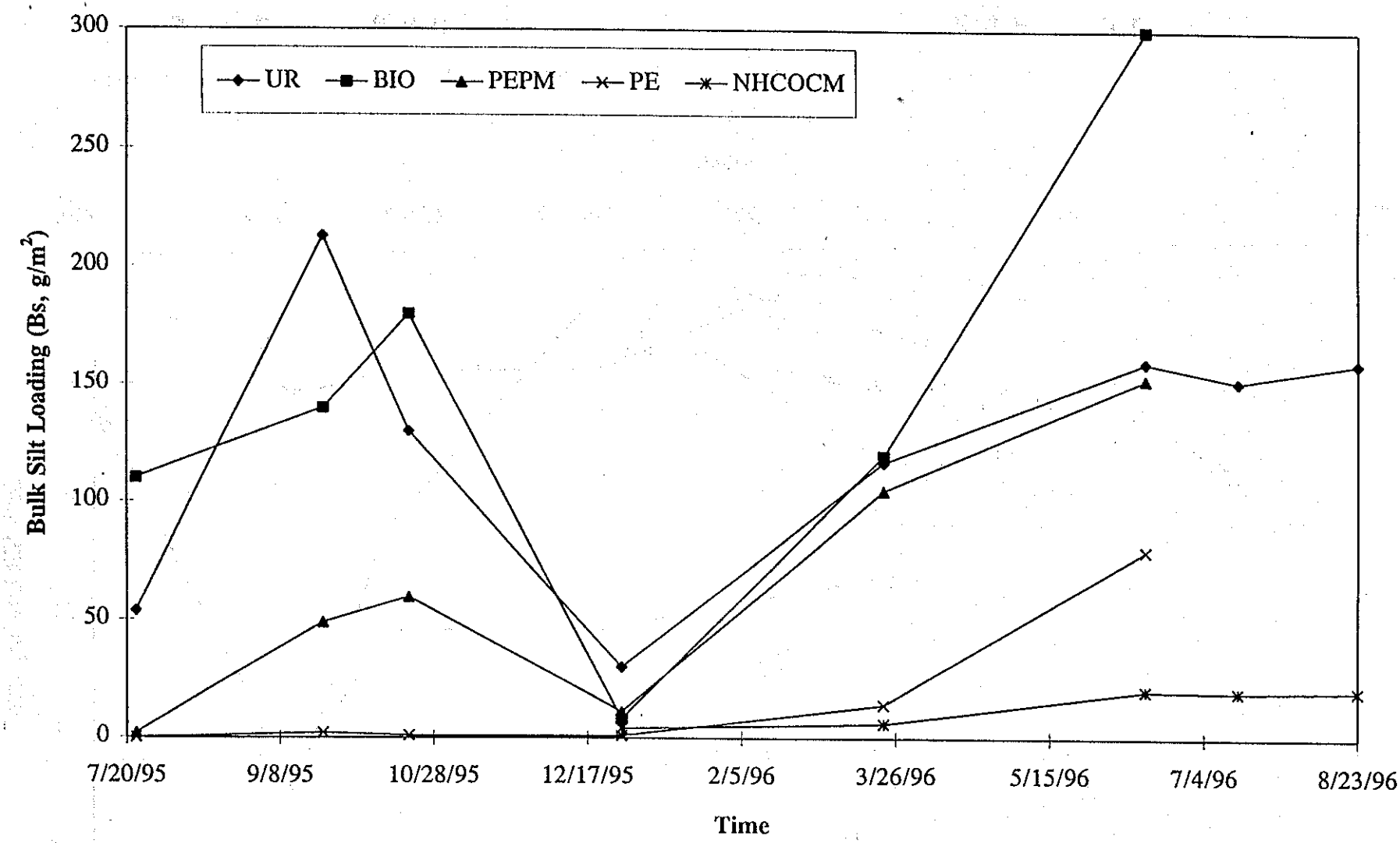

Figure 6-10 Changes in bulk silt loading as a function of time as determined from sweep collected samples.

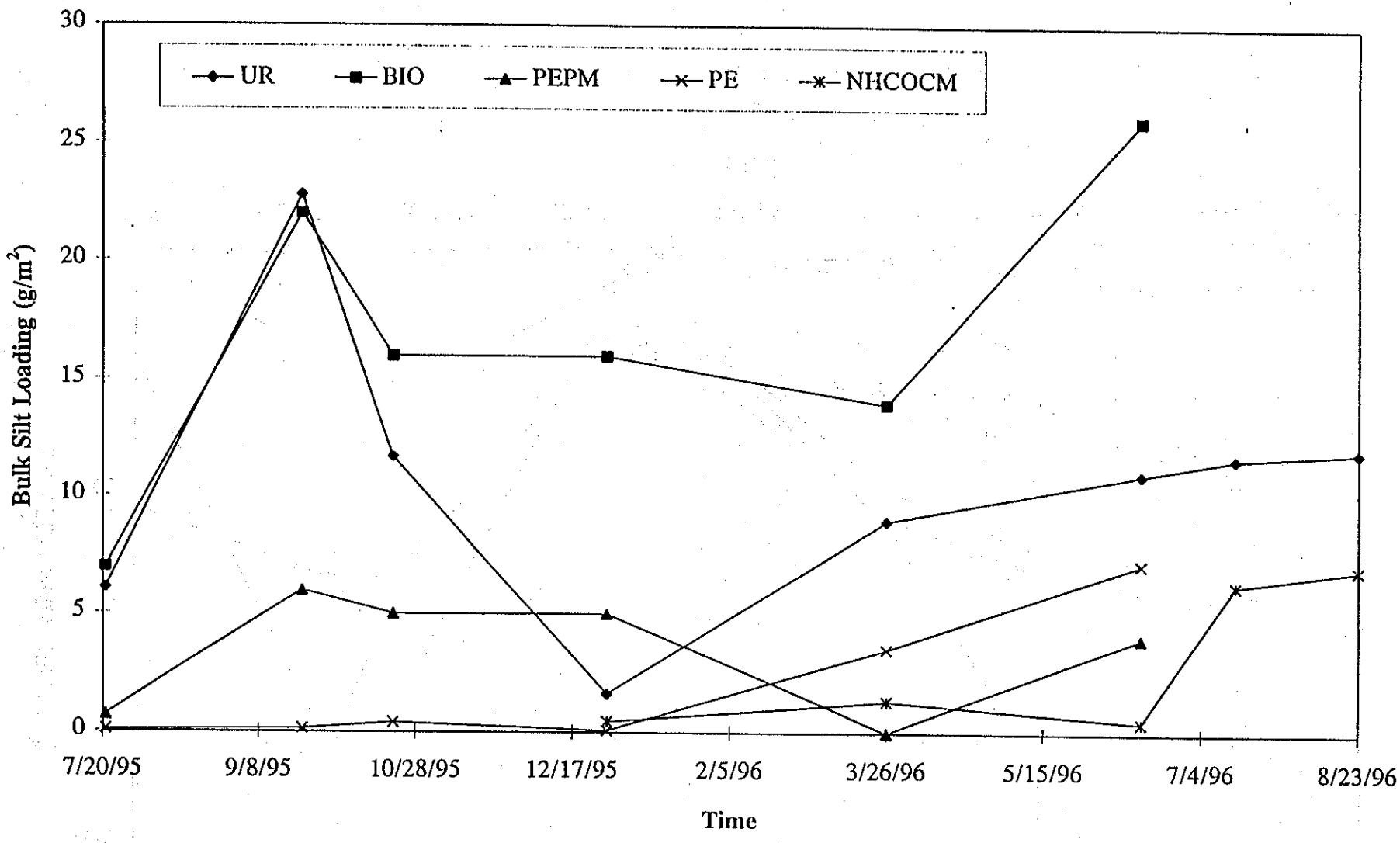

Figure 6-11 Changes in bulk surface silt loading as a function of time as determined from vacuum collected samples.

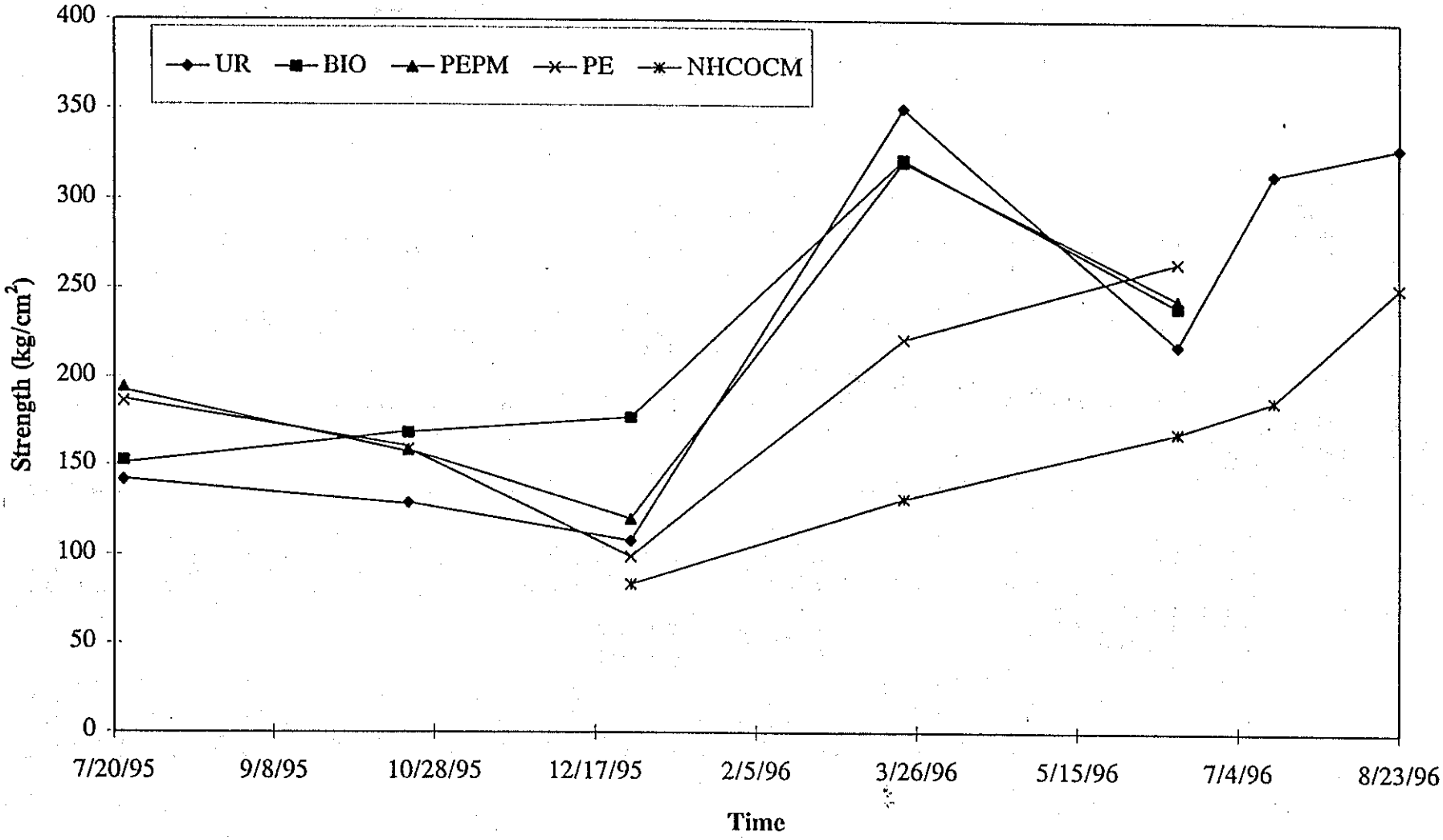

Figure 6-12 Changes in surface strength as a function of time.

Table 6-13
Average Strength Measurements of Test Sections on Fields Road

Site Id	Date	Average Strength (kg/cm^2)	St. Dev. (kg/cm^2)	Max. (kg/cm^2)	Min. (kg/cm^2)
Pet. emul./poly mix	07/21/95	218	126	366	23
Pet. emul./poly mix	07/22/95	169	26	183	93
Pet. emul./poly mix	10/22/95	166	31	183	70
Pet. emul./poly mix	10/22/95	151	40	183	49
Pet. emul./poly mix	12/28/95	120	82	254	0
Pet. emul./poly mix	03/21/96	324	94	366	70
Pet. emul./poly mix	03/21/96	318	91	366	65
Pet. emul./poly mix	06/16/96	230	68	275	63
Pet. emul./poly mix	06/16/96	259	39	275	108
Biocatalyst	07/21/95	138	54	183	42
Biocatalyst	07/22/95	168	26	183	75
Biocatalyst	10/22/95	169	26	183	106
Biocatalyst	12/28/95	148	76	256	14
Biocatalyst	12/28/95	208	86	366	56
Biocatalyst	03/21/96	318	66	366	163
Biocatalyst	03/21/96	328	61	366	155
Biocatalyst	06/16/96	226	57	275	91
Biocatalyst	06/16/96	252	45	275	142
Polymer emulsion	07/22/95	176	20	183	90
Polymer emulsion	07/22/95	196	97	366	20
Polymer emulsion	10/22/95	161	35	183	49
Polymer emulsion	10/22/95	157	32	183	96
Polymer emulsion	12/28/95	106	57	240	20
Polymer emulsion	12/28/95	92	51	197	14
Polymer emulsion	03/21/96	215	70	366	113
Polymer emulsion	03/21/96	229	83	366	144
Polymer emulsion	06/16/96	269	18	275	212
Polymer emulsion	06/16/96	261	31	275	184
Untreated	07/22/95	129	51	183	42
Untreated	07/22/95	154	77	275	11
Untreated	10/22/95	116	48	183	35
Untreated	10/22/95	141	52	183	14
Untreated	12/28/95	109	38	200	39
Untreated	12/28/95	107	43	175	14
Untreated	03/21/96	348	41	366	217
Untreated	03/21/96	354	39	366	225
Untreated	06/16/96	186	82	275	51
Untreated	06/16/96	247	52	275	68
Untreated	07/16/96	307	73	366	135
Untreated	07/16/96	323	57	366	197
Untreated	08/23/96	340	32	366	273
Untreated	08/23/96	320	54	366	194
NHCOCM	12/28/95	80	30	169	17
NHCOCM	12/28/95	88	29	131	19
NHCOCM	03/21/96	133	31	192	54
NHCOCM	03/21/96	130	34	211	42
NHCOCM	06/16/96	171	52	275	66
NHCOCM	06/16/96	167	51	275	49
NHCOCM	07/16/96	150	42	183	34
NHCOCM	07/16/96	225	62	338	65
NHCOCM	08/23/96	255	72	366	99
NHCOCM	08/23/96	248	87	366	42

- Surface strength declined between March 1996 and June 1996 for petroleum emulsion and polymer mixture, biocatalyst and the untreated sections. It continued to increase in the polymer emulsion and NHCOCM sections.

- Surface strength in the NHCOCM-treated section increased steadily from the date of application.

To determine if the measurements taken on the different test sections represented different populations or were indistinguishable in terms of their strength characteristics, a series of ANOVA tests were run. Table 6-14 shows the results of the ANOVA testing that examined the strength measurements among the suppressants and also for the same suppressants through time. The results of the ANOVA analysis can be summarized as:

- In July 1995 the untreated and biocatalyst-treated sections had the lowest strength, and were not statistically different. The petroleum emulsion/polymer mixture and polymer emulsion sections have higher average surface strength measurements from the untreated and biocatalyst-treated sections, but were not significantly different from each other.

- In October 1995 there was no change in the strength characteristics of the untreated and biocatalyst test sections from July 1995. The surface strength of the petroleum emulsion/polymer mixture and polymer emulsion sections decreased significantly, but were not different from the strength measured for the biocatalyst-treated section.

- In June 1996 the strength measurements for all surfaces were significantly greater than had been observed for the previous two intensives. The polymer emulsion and biocatalyst-treated sections' strength measurements were the highest followed by petroleum emulsion/polymer mixture and the untreated section. The NHCOCM section had the lowest average strength measurement.

- The NHCOCM had significantly lower strength than the four other test sections for each site visit, including non-intensive measurement periods. The surface strength of the NHCOCM section increased significantly between each measurement period except between the June 1996 and July 1996 sampling dates.

Two distinctly different responses to the applied vertical force of the penetrometer were observed on different test sections. For the polymer emulsion and NHCOCM sections, the penetrometer entered the surface with a slower, deforming-type penetration. The other mode of failure that was observed on the other three sections is better described as a brittle failure. In this case the surface usually responds to the applied pressure at some point by "shattering" of the surface creating small aggregates. The deformation-type penetration was observed on all sections in December 1995, when the moisture content of the sediment was greater than 4% by weight. The strength measurements do not differentiate the two failure types, and the strength measurements in some cases may show equivalence between sections;

Table 6-14
Analysis of Variance (ANOVA) for Surface Strength Measurements on the Unpaved Road as a Function of Suppressant Type and Time

Suppressant Type and Intensive	Un I1	Un I2	Un I3	Bio. I1	Bio. I2	Bio. I3	PEP I1	PEP I2	PEP I3	PE I1	PE I2	PE I3
Untreated I1[a]		I	S	I			S			S		
Untreated I2[b]			S		S			S			S	
Untreated I3[c]						I			I			S
Biocatalyst I1					I	S	S			S		
Biocatalyst I2						S		I			I	
Biocatalyst I3									I			I
Petroleum Em/Mix I1								S	S	I		
Petroleum Em/Mix I2									S		I	
Petroleum Em/Mix I3												S
Polymer Emulsion I1											S	S
Polymer Emulsion I2												S
Polymer Emulsion I3												
NHCOCM			S			S			S			S

I = no statistical significance
S = significant statistical difference
[a] July, 1996
[b] October, 1995
[c] June, 1996

however the mode of failure may have important implications for emissions reduction. In brittle failure, particles are created that can subsequently be ground up by tires. In plastic deformation, no particles are created upon failure and the road bed can deform under an applied vertical stress without rupturing. How often a surface, such as the polymer emulsion or NHCOCM section, can plastically deform before it is subject to brittle failure is not known.

6.7.5 Mean Aggregate Size

The aggregate size distribution, defined as the size fraction between 6.3 mm and 0.25 mm, was determined through a "soft sieve methodology" (Appendix B.4). The analysis was performed only on sweep-collected surface samples because vacuum collection could alter the size distribution due to the violent extraction process and travel down the lines into the vacuum bag.

Figure 6-13 illustrates the changes in the mean aggregate size determined by the method of moments (Folk, 1980) from the measured particle size distribution. Figure 6-13 illustrates the following trends:

- There is an initial gradation of mean aggregate size between the test sections established in July 1995. The untreated section has the smallest mean size, 1.4 mm (±1.2 mm), followed by biocatalyst with a mean of 3.4 mm (±1.9 mm), polymer emulsion with a mean size of 4.9 mm (±2.3 mm), and petroleum emulsion and polymer mixture with a mean size of 5.9 mm (±2.9 mm).

- The untreated surface mean aggregate size remains unchanged during the 11 months in which measurements were carried out.

- From July 1995 to June 1996 the mean aggregate size of petroleum emulsion and polymer mixture declined steadily. The mean size in June 1996 was 2.1 mm (±1.5 mm).

- The mean aggregate size of the biocatalyst surface decreased to 2.7 mm (±1.8 mm) by October 1996, and increased to 3.8 mm in December 1996. This most likely reflects a sampling bias due to the wetness of the surface from which the smaller particles could not be effectively removed by the sweep method. The mean size decreased to 2.8 mm (±1.9 mm) by June 1996.

- The polymer emulsion surface shows an initial increase in mean aggregate size to 8.1 mm (±2.5 mm) in September 1995. This indicates a sampling bias by the sweep methodology. The relatively sediment-free surface of the polymer emulsion section was covered with large aggregates and a very thin veneer of fines, which the sweep method has difficulty picking up. After October 1996 there is a steady decline in the mean size to a value of 2.7 mm (±1.8 mm) in June 1996. By this time the surface film is sufficiently degraded to allow the buildup

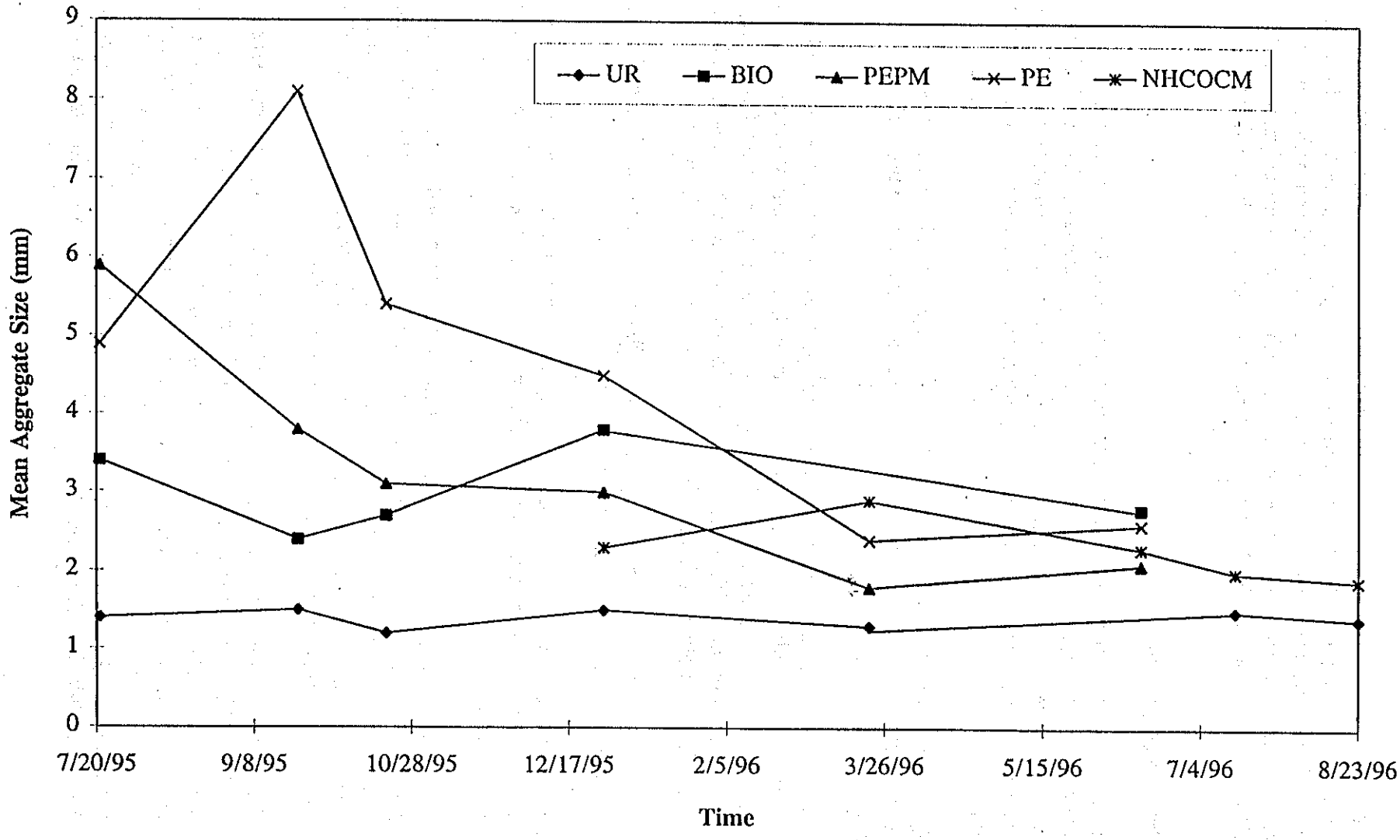

Figure 6-13 Changes in the mean aggregate size (mm) as a function of time.

of loose fines in the exposed areas; these fines are more effectively sampled by the sweep method.

- There is little change in the mean aggregate size measured for the NHCOCM section, for the duration of this study.

6.7.6 Moisture Content

Moisture influences emissions if it is available in sufficient quantities; when the moisture content is less than approximately 1%, it is not significantly effective in reducing fugitive emissions.

Figure 6-14 shows the changes in surface moisture content (of the top 5 millimeters) of the road bed during the duration of this study. Initially, the values are between 0.52% and 1.09%; the biocatalyst and petroleum emulsion and polymer mixture sections had approximately double the moisture content of the polymer emulsion and the untreated sections. This may reflect the application methodology for the biocatalyst, which involved scarification of the road surface and then repeated working of the moistened surface material with the grader and roller to finish the process. This procedure may have injected moisture to a greater depth than a simple topical application of water, and the moisture content would have been maintained longer in the road as a result. In the case of the petroleum emulsion and polymer mixture, some of the moisture content may be reflective of the volatilization of the heavier bituminous oils in the sediment/suppressant matrix and therefore not a true measure of moisture content. The polymer emulsion treatment received only a topical application of water during its application and the untreated section had not received any moisture input in the form of rain since June 1995.

The soil moisture conditions after the July 1995 intensive can be summarized as:

- Soil moisture content decreased in October to range between 0.34% and 0.83%.
- There was an increase in soil moisture due to the above-average rainfall in December. This resulted in lower surface strength measurements in December. Surface strength is inversely proportional to moisture content.
- Soil moisture content declined to a range of 0.44% to 0.77% for the three suppressants applied in July 1995.
- The indicated moisture content of the NHCOCM section exceeds that of the other sections; however, this may be due to the evaporation of volatile constituents of the NHCOCM material during the heating process involved in the moisture content determination.

The measured moisture contents, which were less than 1% on average during intensive measurement periods, indicate that this surface characteristic would not significantly affect emissions among the different test surfaces.

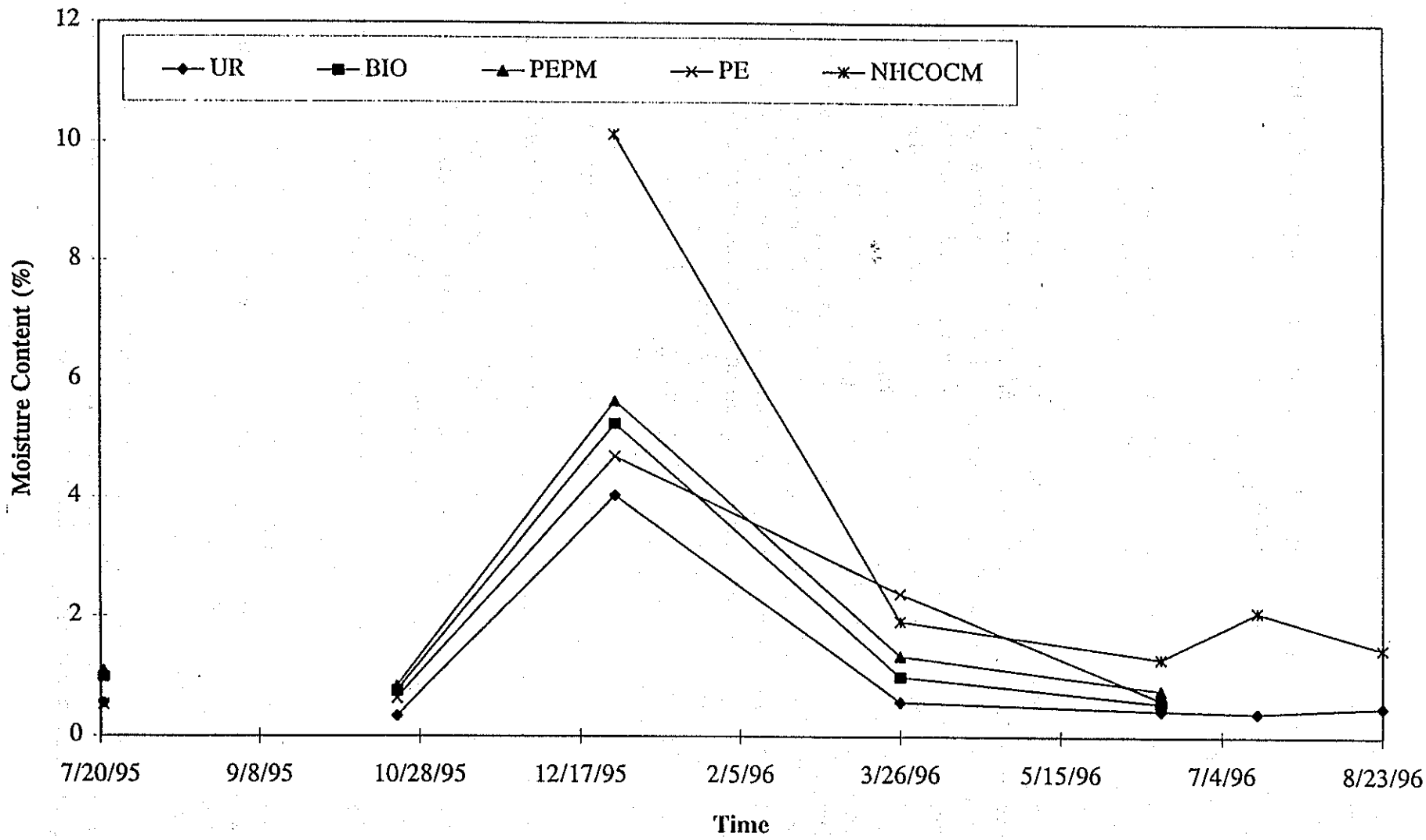

Figure 6-14 Changes in unpaved road moisture content (percent of sample mass) as a function of time.

6.8 Surface Characteristics and Emissions

The basis of the AP-42 emission equation (U.S. EPA, 1994) is empirical relationships that, in part, relate the characteristics of the surface to the emissions of PM_{10} as a function of vehicular traffic. During this study detailed measurements of the AP-42 input variables were taken as well as other surface characteristics that were hypothesized to have significant effects on the emission rates. The changes in the measured surface characteristics were discussed in Section 6.4. In this section the relationships observed between specific surface characteristics and PM_{10} emissions caused by vehicle traffic are presented and discussed.

6.8.1 Bulk Loading and Emissions

There was no significant relationship between measures of the bulk surface loading, collected by both the sweep and vacuum collection techniques, and the emissions of PM_{10} from the test surfaces.

6.8.2 Percent Silt and Emissions

The percent silt content of bulk surface samples is one of the inputs in the AP-42 model for estimating PM_{10} emissions from unpaved roads. In this study no significant relationship was found between the percent silt content of the surface sweep samples collected during each intensive measurement period and the emissions of PM_{10} caused by vehicle traffic if the data from all intensives is combined. The relationship does not improve if the data is further segregated by vehicle velocity. Although this relationship was not found to be significant for the combined data set for all three measurement periods significant relationships between percent silt content and PM_{10} emission rates were observed for individual intensive measurement periods. Figure 6-15 shows the relationship between emissions (g/VKT) and percent silt content for the July 1995 intensive.

Comparing the average percent silt content of the vacuum collected surface samples with the average emission rates for intensive measurement periods the relationship strengthens somewhat. Figure 6-16 shows the scatterplot of the emissions of PM_{10} as a function of percent silt content. The data can be partitioned on the basis of vehicle speed (Figures 6-17 and 6-18) which shows that emissions increase as a function of speed, as the silt content does not change between test days, but does change as a function of longer time intervals (Figure 6-8 and 6-9).

6.8.3 Bulk Silt Loading and Emissions

The actual amount of silt present in the surface sediments, which potentially contains the reservoir of PM_{10}, was measured for the surface sweep and vacuum collected samples. The relationship between the bulk surface loading of silt particles, expressed in g/m^2, and the measured emission rates was examined. The relationship between this measure of the silt loading for the surface sweep samples and emissions proved to be only marginally better than for the measure of silt expressed as a percent. The bulk silt loading measured in the

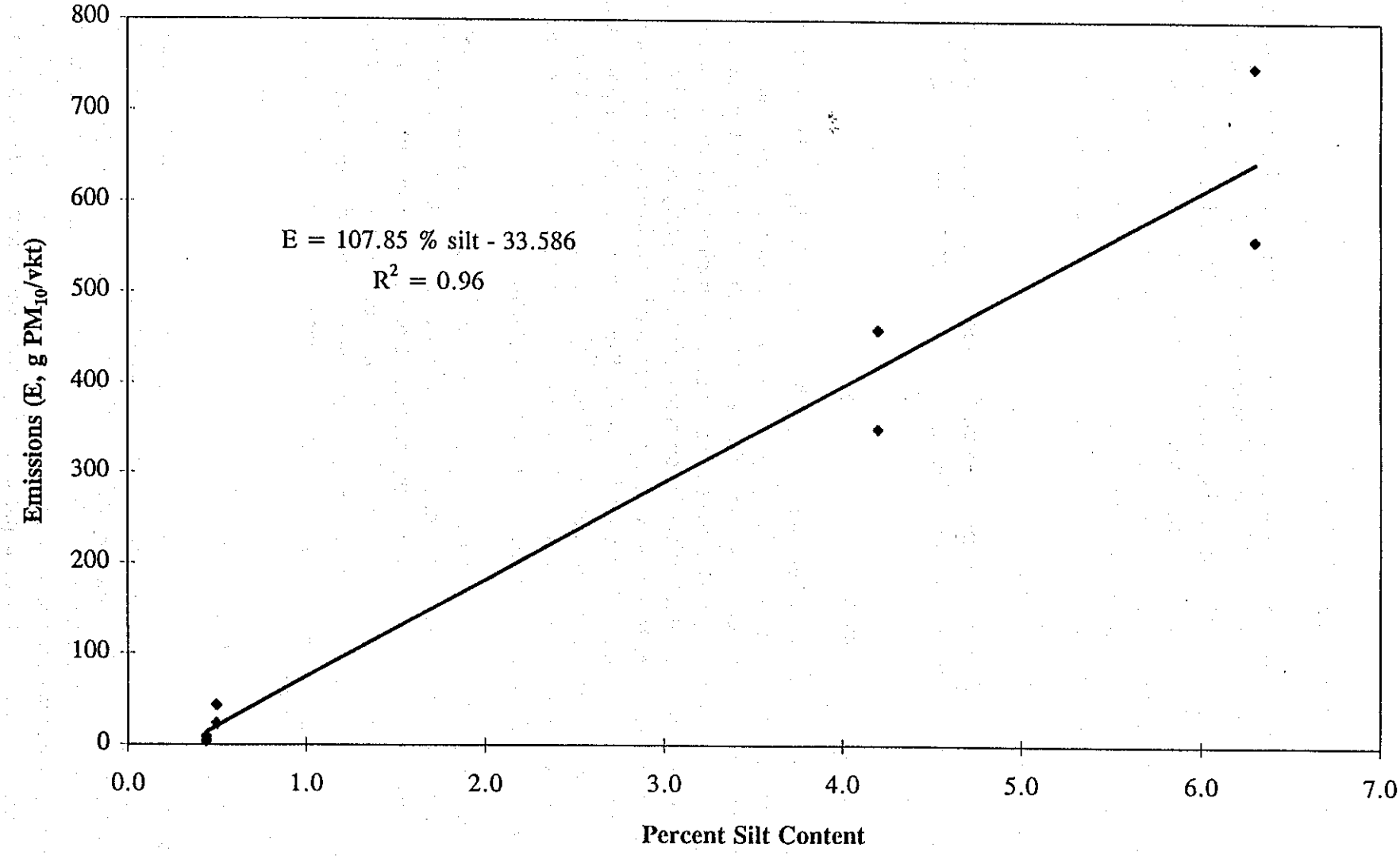

Figure 6-15 Emissions as a function of percent silt content from surface sweep samples for the July, 1995 intensive measurement period.

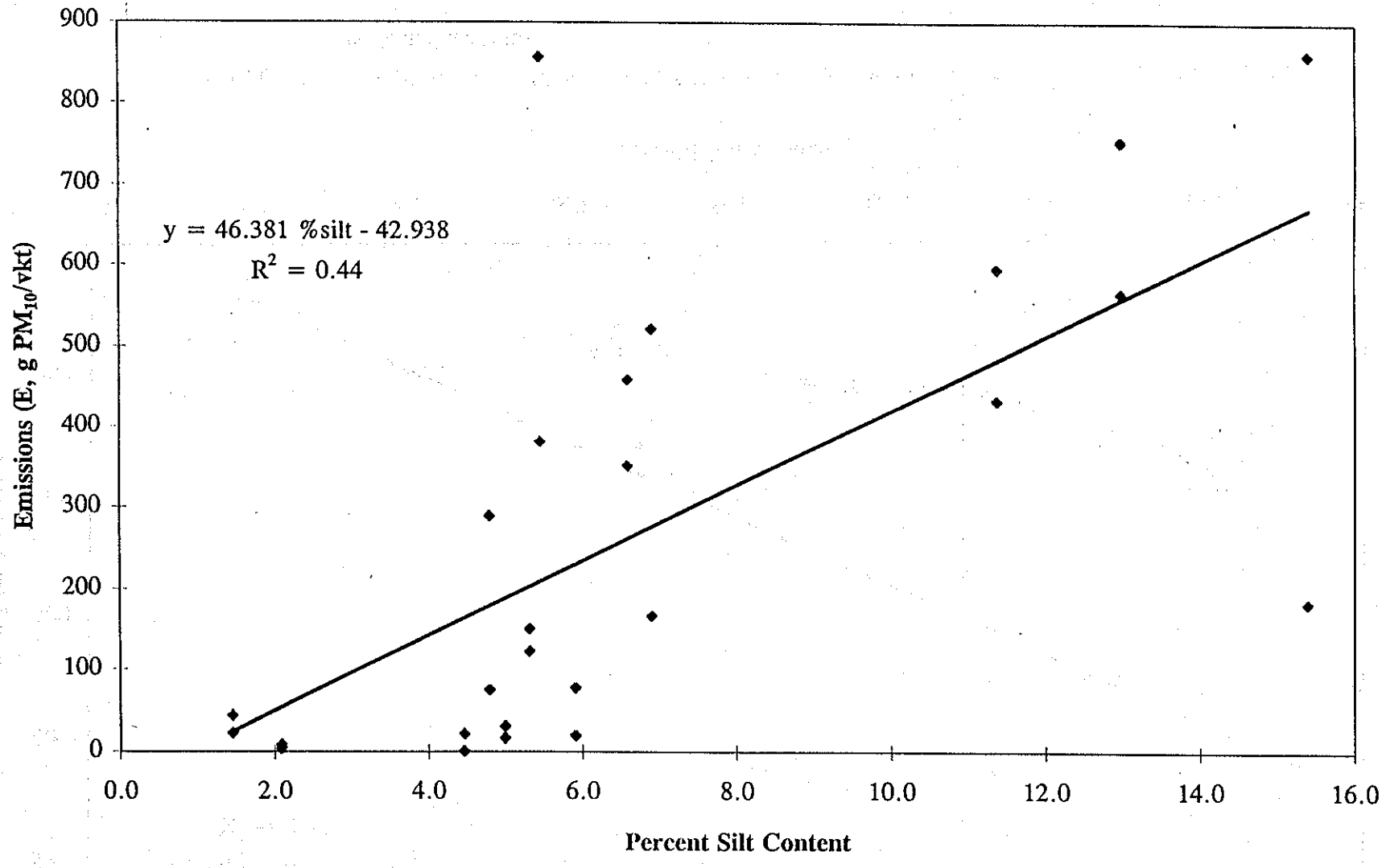

Figure 6-16 Emissions as a function of percent silt content as determined from surface vacuum collected samples for all intensive measurement periods combined.

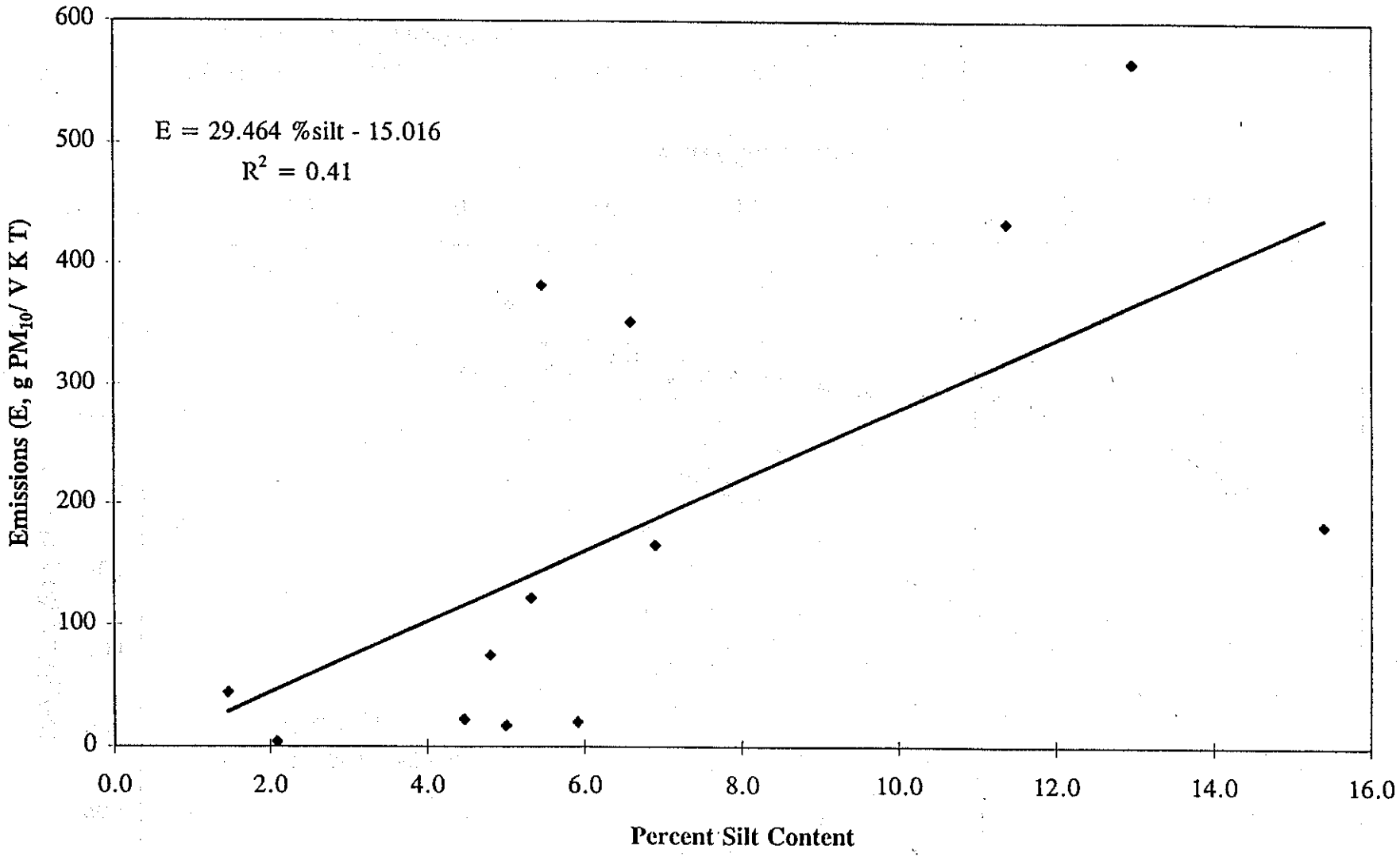

Figure 6-17 Emissions at a vehicle speed of 40 km/hr as a function of percent silt content for vacuum collected samples.

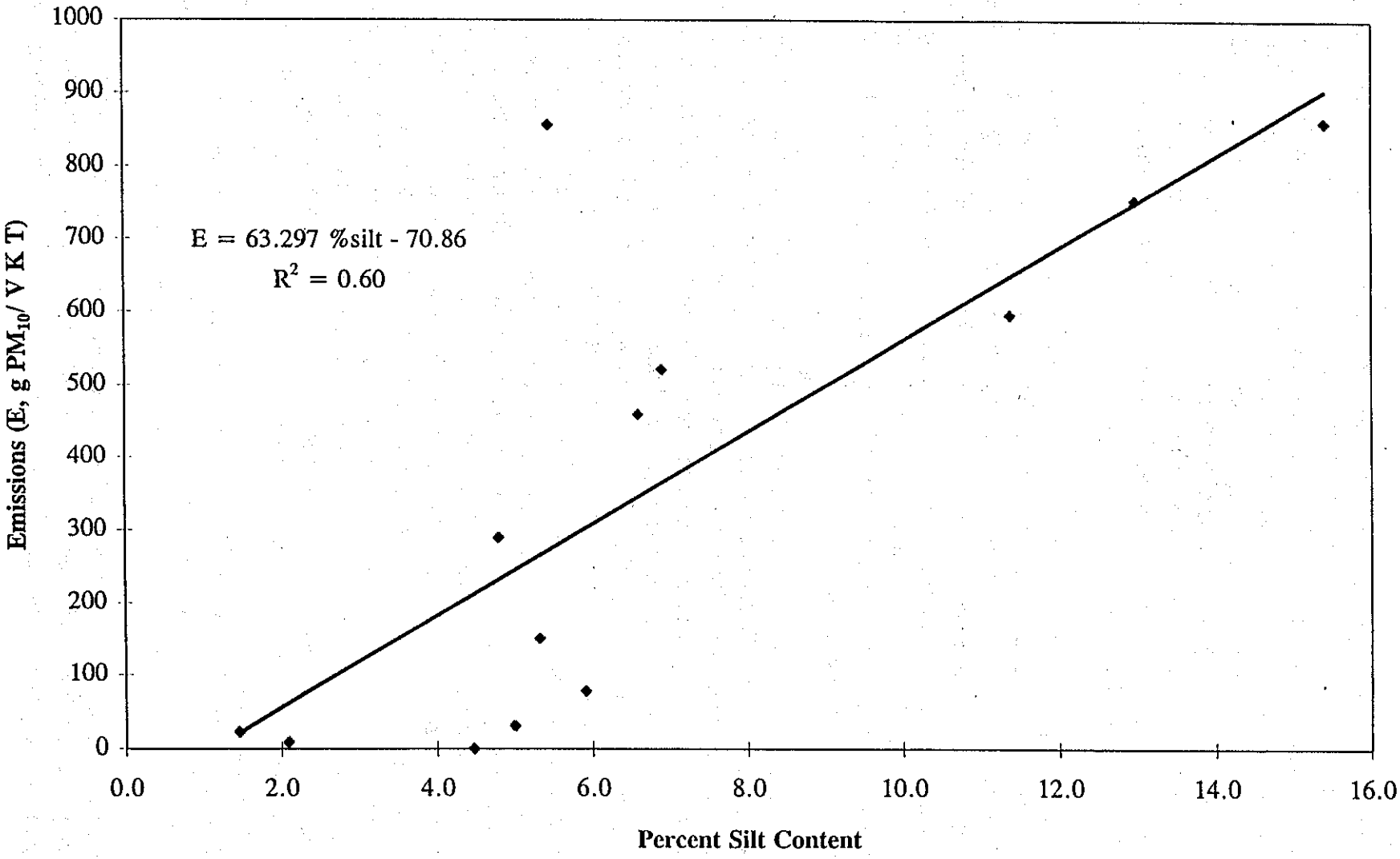

Figure 6-18 Emissions at a vehicle speed of 55 km/hr as a function of percent silt content for vacuum collected samples.

vacuum-collected samples again showed an increased correlation with the emissions, particularly for the tests in which the vehicle velocity was 55 km/hr (Figure 6-19). It would appear that the greater the vehicle speed the more effective the process by which the PM_{10} particles are ejected from the reservoir into the ambient air. One of the reasons for the relatively poor correlation between the silt content measured in the surface sediment and the measured emissions is that PM_{10} emissions are not only a function of simply the ejection of existing PM_{10} particles into the air stream by the vehicles. Additional particles may be produced by the action of the vehicle tires on the road surface and the efficiency of this process is linked with vehicle speed.

For the sweep and vacuum samples taken during the last intensive measurement period in June 1996 more detailed particle size analysis of the silt fraction was carried out. Figure 6-20 illustrates the observed relationship between the bulk silt content (g/m^2) and the calculated emission rates for all the test surfaces combined for June 1996. The dependence of emissions upon the total silt content (all particles <75 μm) in the sweep-collected samples is clearly demonstrated. This can also be shown for the vacuum-collected samples. However, upon further size fractionation of the silt material the strength of the relationship declines for each of the size classes.

The measure of the full silt content amount, in which the PM_{10} particles reside, in part, appears to be a better indicator of the strength of emissions than if the amounts of the smaller size fractions are known. However, this may more accurately reflect problems in the particle size analysis used to determine the amount of the smaller size fractions. In this research a vigorous sieving technique was used to evaluate the amount of silt in the surface samples following the methodology of Cowherd *et al.* (1990). This method has been used in other studies to determine the silt content of sediment samples (Flocchini *et al.*, 1994). For the surface samples obtained in June 1996 two additional sieves were placed in the nest, a 38 μm and a 25 μm screen size to further size segregate the silt component. Fine particles have very strong adhesive forces associated with them and they have an affinity to stick to each other as well as to other large particles. The adhesive forces are a combination of van der Walls forces and electrostatic attraction. During vigorous sieving the electrostatic forces will be reinforced by the shaking. Under these conditions it will be difficult to effectively drive the particles through the sieve screens and size segregation by this method becomes suspect. A concerted effort is underway, especially in the wind erosion research community, to develop a methodology to measure the PM content of sediment, which can then be related to emissions. Methodologies that have been used to estimate the PM_{10} component of sediments include sonic sieving (Hagen *et al.*, 1995), air fall columns (Fryrear *et al.*, 1995; Malcom and Raupach, 1991), resuspension chambers (Caravacho *et al.*, 1995) and hydrometer analysis (Haun, 1995). However, none of these techniques have successfully linked a measured particle size distribution of the sediment being examined to the emission rate of PM_{10}.

The usefulness of the bulk silt content (g/m^2) measurement can be further illustrated if its relationship with the PM_{10} reduction efficiency is examined. Figure 6-21 illustrates this relationship including data from all three intensive measurement periods. The data suggests

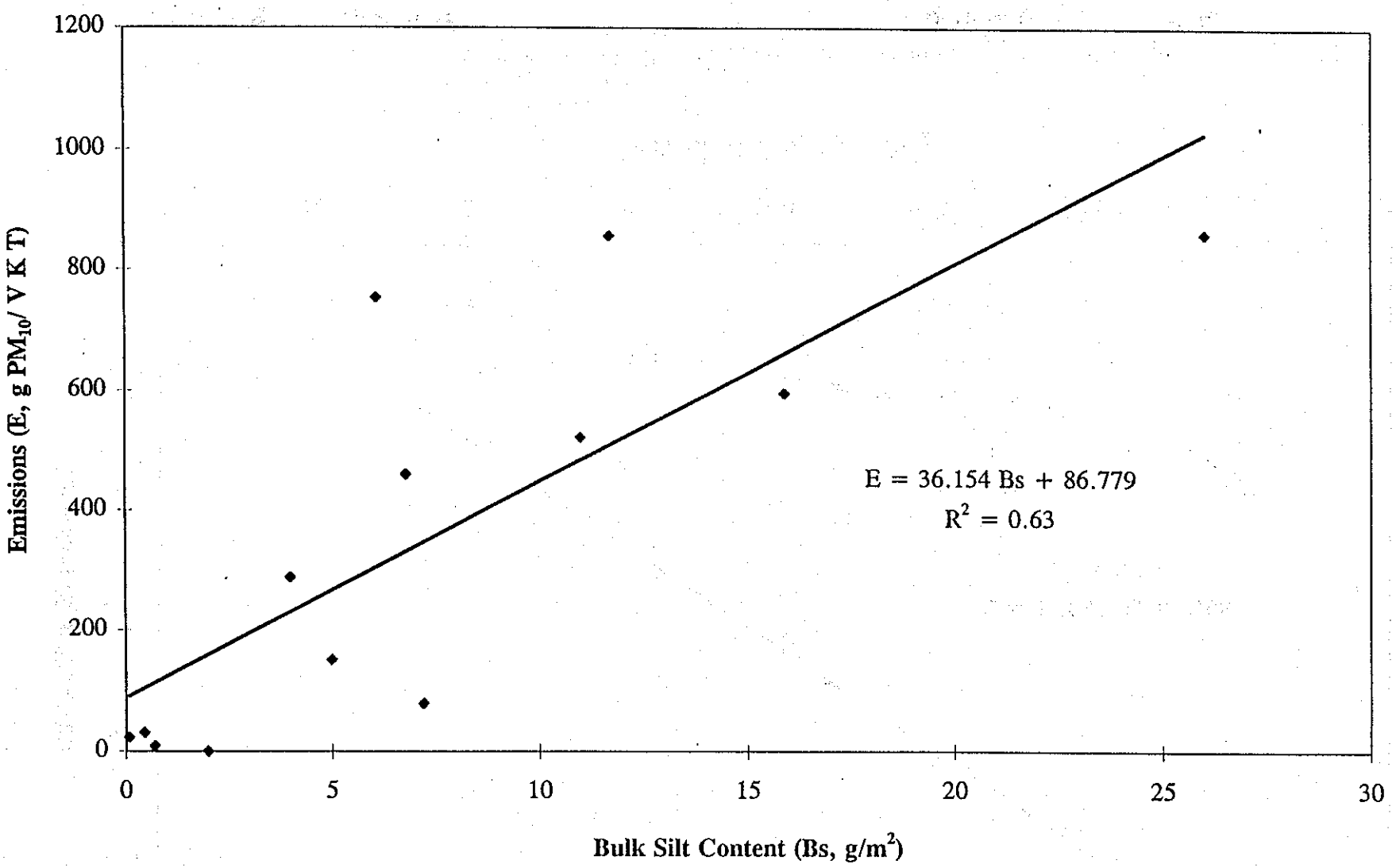

Figure 6-19 Emissions at a vehicle speed of 55 km/hr as a function of bulk silt content determined from surface vacuum-collected samples.

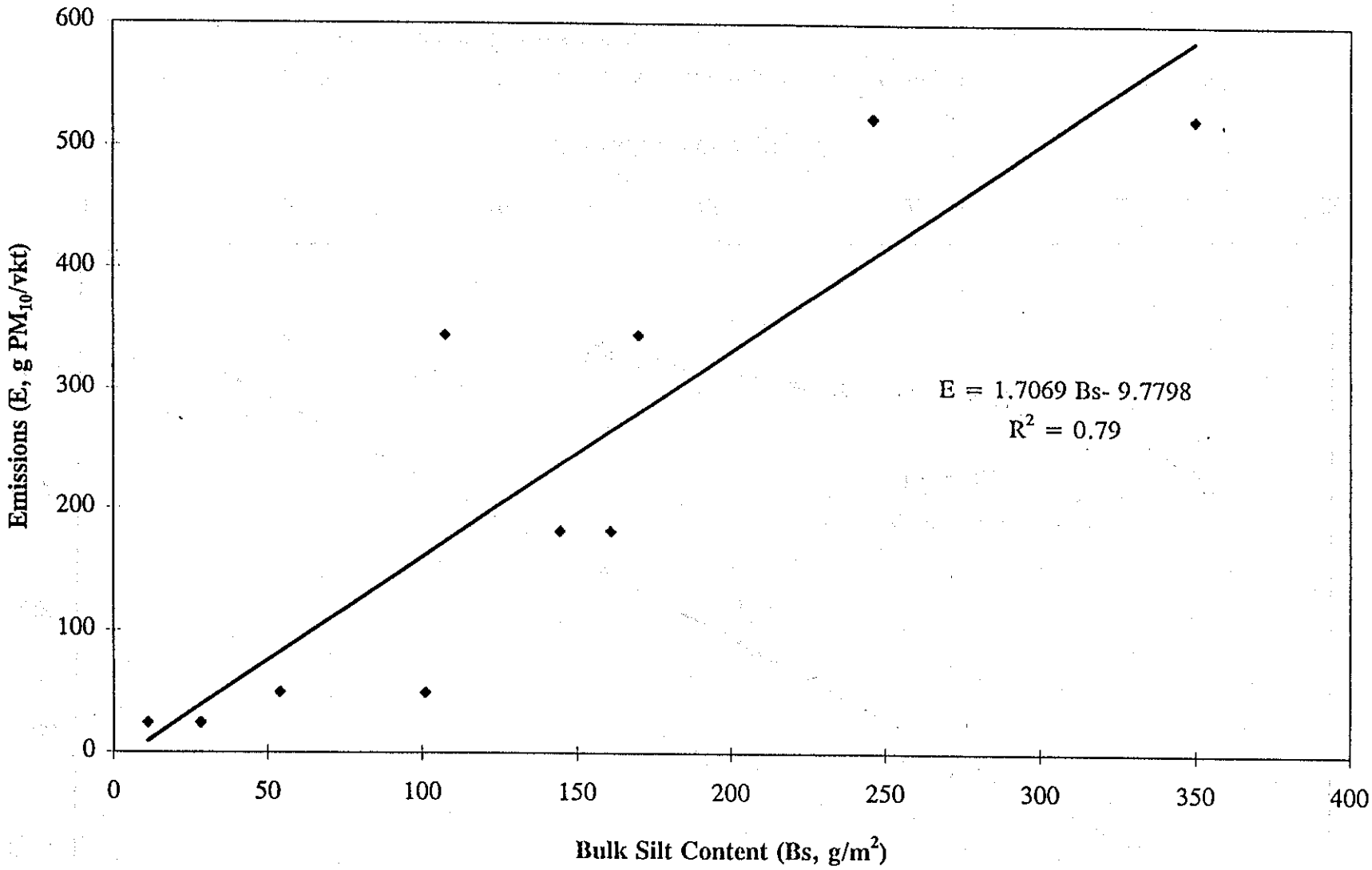

Figure 6-20 Emissions as a function of bulk silt content determined from sweep collected samples for June 1996.

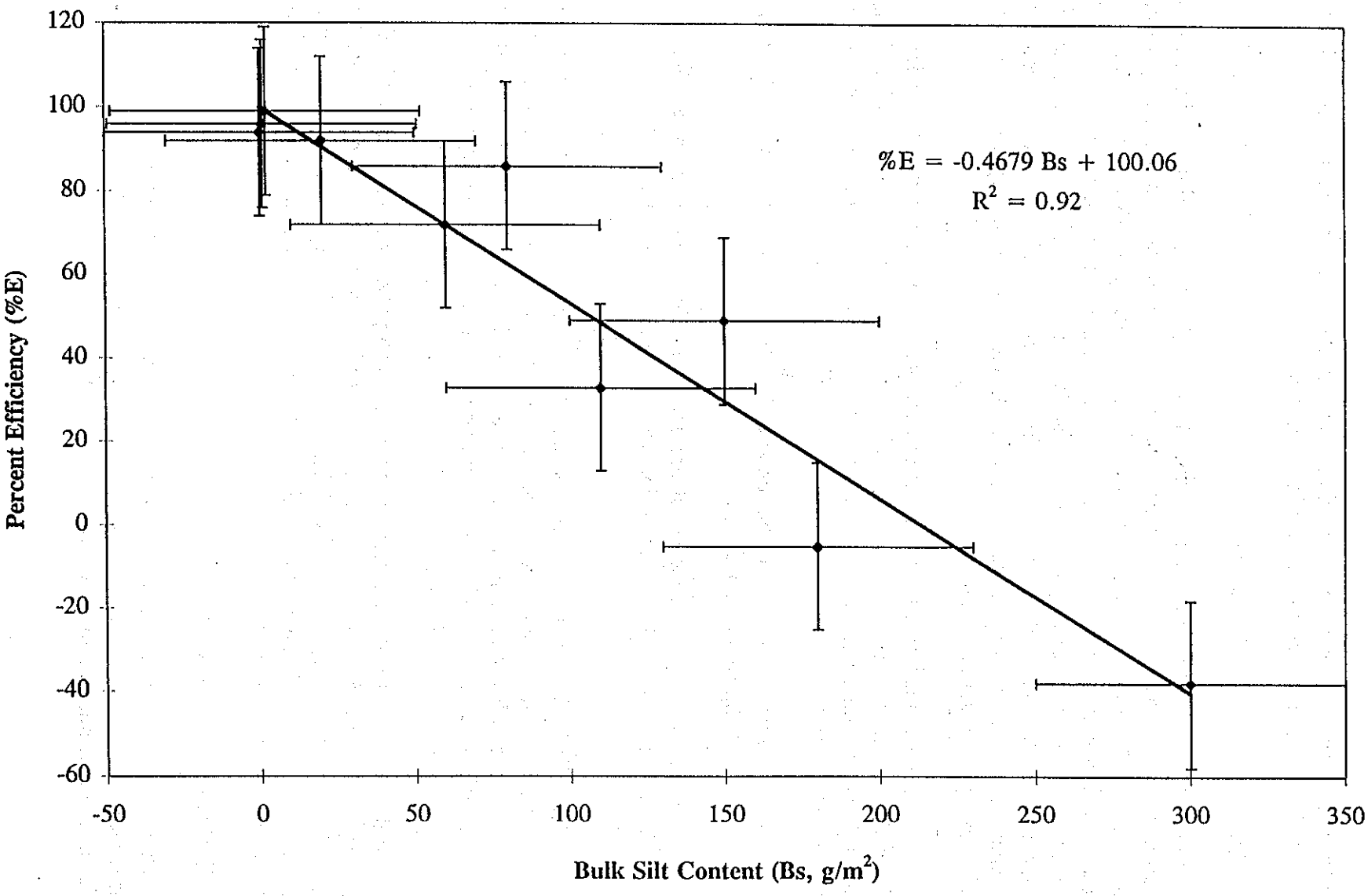

Figure 6-21 Efficiency in PM_{10} emission reductions as a function of bulk silt content.

that 50% efficiency is achieved by maintaining bulk surface silt contents at levels of 100 g/m^2 and 99% efficiency is achieved at a bulk silt content ≤ 6.0 g/m^2.

6.8.4 Surface Strength and Emissions

In section 6.4.4 the surface strength characteristics of the test section on Fields Road were discussed and observational information presented that identified two distinct types of failure of the road surface. The penetrometer tests revealed that three test surfaces, the untreated, the biocatalyst, and the petroleum emulsion with polymer mixture usually failed by fracturing. However, the polymer emulsion surface failed with a plastic deformation when the surface film was in place. The low emission rates and high efficiency of reducing PM_{10} emissions for the polymer emulsion, throughout the study period, appear to, in part, reflect its ability to resist brittle failure.

The role of surface strength, as measured by the penetrometer, was not clearly defined in this study except for the observation of failure type and its relationship with PM_{10} emissions. However, the strength measurements also indicate several other trends that can be summarized as follows:

- The untreated section, which has on average the lowest strength characteristics is a relatively high emitter of PM_{10}.
- For the biocatalyst and the petroleum emulsion with polymer mixture, emission rates increased as their strength increased significantly from July 1995 to June 1996.
- The NHCOCM section had consistently the lowest surface strength values, as well, the failure mode was of the plastic deformation type. In addition, this section had low emission rates as compared to the untreated, biocatalyst and the petroleum emulsion with polymer mixture which had higher strength values and tended to have the brittle type failure.

For the biocatalyst and the petroleum emulsion with polymer mixture it may be that the increased hardness is linked to increased PM_{10} emissions due to the more efficient creation of PM_{10} by the grinding or pulverizing action of vehicle tires on the harder road surface. Road bed material may be more easily broken down when it is ground between tires and an increasingly stronger surface.

6.8.5 Emissions and Moisture Content

During each of the intensive measurement periods, the percent moisture content by weight for samples taken from the road surface where less than 1%, which would not have a significant effect on emission rates between the test sections.

6.9 Quality Assurance Audit

Dr. Jitendra Shah, an experienced air quality researcher and field auditor (G2 Environmental Inc., Washington, DC), was retained by DRI to conduct an independent field audit for this study. Dr. Shah visited the Fields Road and Bellevue Road sites on June 12-13, 1996. Dr. Shah monitored all field measurement activities, emphasizing PM_{10} sampler and meteorological instrument accuracies. The wind speed and direction instruments were found to be operating within specifications. Flow audits were conducted on the two field transfer standard flowmeters, and on fifteen randomly-chosen PM_{10} samplers. With the samplers set at nominal 5 L/m flow rates, the audit flowmeter confirmed that all flows were within 10% of this setpoint, and only two flows were more than 5% different from the setpoint. However, Dr. Shah noted that the field flowmeters both exhibited consistent flow differences, in the 0.1 to 0.2 L/m range, compared to the audit instrument. These differences are close to the resolution of this type of flowmeter, 0.1 L/m.

7.0 RESULTS FOR UNPAVED SHOULDERS

7.1 Descriptive Data Analysis

7.1.1 Traffic on Bellevue Road

Bellevue Road is a relatively busy road that is utilized by a variety of vehicles. It is used by local residents to access their homes and as a route to G Street which provides access to the city of Merced. It is also used by the city and regions' waste-disposal trucks as an access road from Merced and the surrounding areas to the local landfill site on Highway J-59. Large trucks hauling aggregates to and from the several plants located on Highway J-59 are also a common vehicle type observed on Bellevue Road. Other vehicles seen on Bellevue include school buses, trucks of various sizes, farm vehicle (tractors with implements), garbage trucks (weekly collection) and the mail delivery vehicle (daily delivery).

The following records of traffic on Bellevue Road during the study period are available:

- A record from a pneumatic traffic counter for each of the intensive measurement periods (Table 7-1). This record contains the number of vehicles during the daily eight-hour PM_{10} sampling period and the total vehicle number for the whole day. On average, 1,019 vehicle counts (±149) were recorded in an eight-hour test period (0800 - 1600). The 24-hour average traffic count was 1,951 (±310). This includes several longer duration measurements of traffic counts from periods in which the traffic counter was left in place between the intensives.

- Records of vehicles taken during the intensive measurement periods by observers. These records contain information on vehicle type and time and direction of passage. Due to the fact that there was no dedicated observer, observations were only recorded during breaks from other activities. These records are therefore incomplete and have not been utilized in the final analysis

- Video recordings of the traffic exist for most of the intensive measurement periods. Some of these video tapes were analyzed for the calculation of emission rates from nephelometer measurements. Total traffic counts and traffic counts segregated into four different vehicle categories are listed in Table 7-2 for individual recording periods and in Table 7-3 summarized by day, and for weekdays and weekends. Note that the fraction of "dust entraining vehicles," (see Section 7.1.4) is on the average three times lower on weekends (i.e., 7%) than on weekdays (i.e., 21%). A much smaller fraction of the video tapes was analyzed in more detail listing vehicle type and time and direction of passage.

Table 7-1
Vehicle Traffic on Bellevue Road

Date	Number of vehicles per 8-hr. sampling period	Average number of vehicles per day (24-hrs.)
7/15/95	987	1752
7/16/95	1038	1955
7/17/95	941	1703
7/18/95	982	1759
7/19/95	977	1743
7/20/95	986	1849
10/14/95	920	1733
10/15/95	930	1655
10/16/95	947	malfunction in counter
10/19/95	973	malfunction in counter
10/23/95	982	ended monitoring 16:00 hrs. 10/23/95
October 95-Dec-95	no daily monitoring	2875
3/21/96 3/23/96	site visit, no daily monitoring	1786
6/6/96	995	1934
6/7/96	1128	2157
6/8/96	1127	2098
6/9/96	1224	2198
6/10/96	1125	2062
6/11/96	1502	ended monitoring 16:00 hrs. 6/11/96
Average	1016	1951
Standard Dev	145	310

Table 7-2
Traffic Counts for Bellevue Road, June 6, 1996 to June 11, 1996

Date	6/6/96	6/7/96		6/8/96		6/9/96		6/10/96		6/11/96	
Start Time	14:51	13:16	15:33	12:12	15:03	11:59	14:46	11:21	14:00	11:03	13:44
End Time	16:19	14:49	17:07	14:15	16:40	14:00	15:48	13:19	16:02	12:54	15:47
Time Span	1:27	1:33	1:34	2:03	1:37	2:02	1:03	1:59	2:02	1:51	2:03
Time/DEV(s)	150	185	235	296	341	261	375	115	188	115	99
DEV[a] Total	35	30	24	25	17	28	10	62	39	58	75
DEV 1[b]	20	13	14	16	12	20	6	11	12	13	7
DEV 2[c]	11	11	7	2	5	7	4	24	20	16	19
DEV 3[d]	4	6	3	7	0	1	0	27	7	29	49
Non DEV[e]	182	147	183	247	235	317	191	159	198	169	195
DEV/Vehicles	16%	17%	12%	9%	7%	8%	5%	28%	16%	26%	28%
Vehicles	217	177	207	272	252	345	201	221	237	227	270

a: DEV: Dust Entraining Vehicles
b: DEV 1: Small Vehicles (e.g., cars, pickups, vans) Pulling a Trailer
c: DEV 2: Large Vehicles (e.g., trucks, buses, large Rvs)
d: DEV 3: Very Large Vehicles (e.g., semis, large vehicles pulling a trailer)
e: Non DEV: Non Dust Entraining Vehicles, i.e. Small Vehicles (e.g., cars, pickups, vans)

Table 7-3
Daily Traffic Counts for Bellevue Road, June 6, 1996 to June 11, 1996

Day of Week	Thursday	Friday	Saturday	Sunday	Monday	Tuesday			
Date	6/6/96	6/7/96	6/8/96	6/9/96	6/10/96	6/11/96	Weekday	Weekend	Total
Time Span	1:27	3:07	3:40	3:04	4:01	3:54	12:29	6:44	19:13
Time/DEV(s)	150	207	314	291	143	106	139	303	172
DEV[a] Total	35	54	42	38	101	133	323	80	403
DEV 1[b]	20	27	28	26	23	20	90	54	144
DEV 2[c]	11	18	7	11	44	35	108	18	126
DEV 3[d]	4	9	7	1	34	78	125	8	133
Non DEV[e]	182	330	482	508	357	364	1233	990	2223
DEV/Vehicles	16%	14%	8%	7%	22%	27%	21%	7%	15%
Vehicles	217	384	524	546	458	497	1556	1070	2626

a: DEV: Dust Entraining Vehicles
b: DEV 1: Small Vehicles (e.g., cars, pickups, vans) Pulling a Trailer
c: DEV 2: Large Vehicles (e.g., trucks, buses, large Rvs)
d: DEV 3: Very Large Vehicles (e.g., semis, large vehicles pulling a trailer)
e: Non DEV: Non Dust Entraining Vehicles, i.e. Small Vehicles (e.g., cars, pickups, vans)

7.1.2 PM_{10} Mass Concentration Measurements with Portable Samplers

Tables 7-4, 7-5, and 7-6 present the upwind and downwind mass concentrations measured with portable PM_{10} survey samplers at Bellevue Road during the three intensive measurement periods in July and October 1995 and June 1996. The tables also show the daily average upwind and downwind PM_{10} mass concentrations and their associated uncertainties for the daily, 8-hour sampling periods.

During the first intensive measurement period, July 15-20, 1995, the daily upwind PM_{10} mass concentrations ranged between a low of 13.1 $\mu g/m^3$ and a high of 60.8 $\mu g/m^3$. The average mass uncertainty associated with an individual mass concentration measurement was ± 4.5 $\mu g/m^3$. The mean upwind concentration for this period was 31.6 $\mu g/m^3$ with a standard deviation of ± 13.9 $\mu g/m^3$.

The downwind mass concentrations in the same period were between 13.1 $\mu g/m^3$ and 40.7 $\mu g/m^3$. The average mass uncertainty associated with an individual downwind mass concentration measurement was ± 4.3 $\mu g/m^3$. The mean downwind concentration was 26.7 $\mu g/m^3$ with a standard deviation of ± 10.1 $\mu g/m^3$.

A greater range of upwind PM_{10} mass concentrations was measured during the October 14-23, 1995 intensive. Daily concentrations were between 23.1 $\mu g/m^3$ and 151.7 $\mu g/m^3$. The average mass uncertainty associated with an individual upwind mass concentration measurement was ± 4.5 $\mu g/m^3$. The mean upwind concentration was 65.5 $\mu g/m^3$ with a standard deviation of ± 29.6 $\mu g/m^3$. The average upwind concentration was twice the value of the average upwind mass concentration measured in the July 1995 intensive measurement period and also exhibited more variability.

The downwind PM_{10} mass concentrations in October 1995 were between 36.6 $\mu g/m^3$ and 172.5 $\mu g/m^3$ with an average mass uncertainty of ± 4.6 $\mu g/m^3$. The mean downwind concentration was 62.0 $\mu g/m^3$ with a standard deviation of ± 29.6 $\mu g/m^3$. The mean downwind and upwind mass concentrations were very similar during the October measurement period.

In the June 6-11, 1996, intensive measurement period, upwind mass concentrations were between 4.6 $\mu g/m^3$ and 68.8 $\mu g/m^3$. The lowest measured concentration, 4.6 $\mu g/m^3$ on the organic emulsion section, June 10, sits very much as an outlier to all the other measured mass concentration values and should be considered suspect. The average mass uncertainty for an individual mass concentration measurement for this intensive is ± 6.3 $\mu g/m^3$. The mean upwind concentration during the June 1996 intensive was 32.8 $\mu g/m^3$. The standard deviation associated with the mean upwind mass concentrations is ± 11.5 $\mu g/m^3$ indicating that the day-to-day variability had declined from the October 1995 measurement period. The mean upwind mass concentration for June 1996 is similar to the July 1995 mean upwind concentration value.

The quality assurance (field audit) procedures described in Section 6.9 also applied to the portable Minivol samplers used at the Bellevue Road sites.

Table 7-4
Upwind and Downwind PM_{10} Concentrations Measured at Bellevue Road, July , 1995

Site	7/15/95 Up ($\mu g/m^3$)	7/15/95 Down ($\mu g/m^3$)	7/16/95 Up ($\mu g/m^3$)	7/16/95 Down ($\mu g/m^3$)	7/17/95 Up ($\mu g/m^3$)	7/17/95 Down ($\mu g/m^3$)	7/18/95 Up ($\mu g/m^3$)	7/18/95 Down ($\mu g/m^3$)	7/19/95 Up ($\mu g/m^3$)	7/19/95 Down ($\mu g/m^3$)	7/20/95 Up ($\mu g/m^3$)	7/20/95 Down ($\mu g/m^3$)
Untreated	60.8	40.7	23.1		27.8	22.3	13.1	26.9	37.8	22.6		35.1
Organic emulsion	38.7	28.9	30.4	29.9	25.2	30.4	20.1	14.4	26.3	19.4	19.3	23.5
Acrylic co-polymer	56.2	47.2	32.2	18.9	23.5	13.1	29.5	23.6	35.3	25.7	20.9	26.8
Endosperm hydrate	47.9	37.6	42.0	25.8	29.3	31.4	20.5	24.8	59.6	43.5	33.1	27.3
Average	50.9	38.6	31.9	24.9	26.5	24.3	20.8	22.4	39.7	27.8	24.4	28.2
Standard Dev.	9.7	7.6	7.8	5.5	2.6	8.5	6.7	5.5	14.1	10.8	7.5	4.9

Table 7-5
Upwind and Downwind PM_{10} Concentrations Measured at Bellevue Road, October 1995

Site	10/14/95 Up ($\mu g/m^3$)	10/14/95 Down[a] ($\mu g/m^3$)	10/15/95 Up ($\mu g/m^3$)	10/15/95 Down ($\mu g/m^3$)	10/16/95 Up ($\mu g/m^3$)	10/16/95 Down ($\mu g/m^3$)	10/19/95 Up ($\mu g/m^3$)	10/19/95 Down ($\mu g/m^3$)	10/23/95 Up ($\mu g/m^3$)	10/23/95 Down ($\mu g/m^3$)
Untreated	55.9	66.2	48.4	43.4	29.4	43.0	65.4	61.7	78.5	85.5
		42.5		47.7		36.7		68.8		91.4
Organic emulsion	51.7	52.8	46.5	9.1	23.1	35.6	55.2	91.8		89.8
		56.1		46.5		32.5		65.6		85.6
Acrylic co-polymer	69.5	63.0	64.3	55.2	151.7	172.5	78.1	66.3	100.7	95.2
		72.8		59.6		54.5		62.5		101.7
Endosperm hydrate	68.4	65.7	58.5	53.5	43.4	36.6	64.2	67.1	98.6	97.6
		63.4				50.0				78.3
Average	61.4	60.3	54.4	45.0	61.9	57.7	65.7	69.1	92.6	90.7
Standard Dev.	8.9	10.1	8.4	16.8	60.5	50.7	9.4	10.3	12.2	6.1

[a] two downwind samplers in each section

Table 7-6
Upwind and Downwind PM_{10} Concentrations Measured at Bellevue Road, June, 1996

Site	6/6/96 Up ($\mu g/m^3$)	6/6/96 Down[a] ($\mu g/m^3$)	6/7/96 Up ($\mu g/m^3$)	6/7/96 Down ($\mu g/m^3$)	6/8/96 Up ($\mu g/m^3$)	6/8/96 Down ($\mu g/m^3$)	6/9/96 Up ($\mu g/m^3$)	6/9/96 Down ($\mu g/m^3$)	6/10/96 Up ($\mu g/m^3$)	6/10/96 Down ($\mu g/m^3$)	6/11/96 Up ($\mu g/m^3$)	6/11/96 Down ($\mu g/m^3$)
Far Up/Down	31.5	45.5	42.7	45.9	38.4	36.1	34.2	26.3	26.9	17.0	36.7	37.5
Untreated	33.4	43.9	29.5	40.6	28.9	30.0	25.5	20.5	41.0	34.3	36.9	35.3
		44.9				33.9		13.0		33.6		
Organic emulsion	32.0	39.7	36.1	36.8	32.6	35.1	15.5	22.6	20.5	21.8	4.6	53.9
		33.9		33.3		35.6		27.2		16.5		37.2
Acrylic co-polymer	44.4	38.3	37.4	46.4	47.7	35.0	31.2	28.0	19.3	31.4	38.9	44.3
		39.7		46.5		40.1		22.6		42.7		31.4
Endosperm hydrate	27.9	27.0	32.4	37.3	29.5	30.4	22.2	12.8	41.4	31.4	68.8	37.0
		34.0		33.1				51.1		34.7		45.6
Average	33.8	39.1	35.6	41.0	35.4	34.5	25.7	21.6	29.8	28.6	37.2	39.5
Standard Dev.	6.2	6.2	5.0	5.4	7.8	3.3	7.4	6.0	10.8	9.2	22.7	7.4

[a] two downwind samplers in each section except far-upwind and far-downwind

7.1.3 Shoulder Contributions to Measured PM_{10} Mass Concentrations

In general, the upwind and downwind PM_{10} mass concentrations are very similar for most days of testing. In many cases the sampler that was designated as being upwind, on the north side of Bellevue Road, has a higher value than the downwind or south sample. If it is assumed that the sampler that has a larger mass concentration in an upwind-downwind pair represents a possible addition of PM_{10} mass, it is necessary to determine if the additional mass is greater than the combined uncertainty of both mass measurements. The difference in the upwind-downwind masses was considered to be significant if it met the following criterion:

$$\text{Delta} > ((\text{MSGUUP}^2 + \text{MSGUDN}^2))^{0.5} \qquad (7\text{-}1)$$

where: Delta = difference in the upwind and downwind PM_{10} mass concentrations ($\mu g/m^3$)

MSGUUP = uncertainty in the upwind PM_{10} mass concentration

MSGUDN = uncertainty in the downwind PM_{10} mass concentration

In the July 1995 intensive measurement period sixteen out of the twenty-four paired upwind and downwind samples had greater mass in the upwind designated samples and only four had designated downwind samples greater than the upwind. In the other four samples, there was no discernible difference in the two measurements. Table 7-7 shows PM_{10} mass concentrations between the paired upwind and downwind samples for the July 15-20, 1995. If the difference in PM_{10} mass concentration measurements between the paired upwind/downwind samples is assumed to represent a contribution from the road shoulders, the data suggests that in July 1995 the untreated section contributes, on average, 20.4 $\mu g/m^3$ to the total measured PM_{10} concentration. The sections with suppressant contribute between 5.9 and 8.3 $\mu g/m^3$. Taking into account the uncertainty in the mass concentration measurements there is no discernible difference between the PM_{10} mass concentration contributions of the three suppressant-treated sections. However, the data suggests that the sections with suppressant did have reduced PM_{10} emissions as compared to the untreated section.

During the October 14-23, 1995, measurement period, of the twenty paired upwind and downwind samples taken on the four test sections, there were only ten in which a significant difference between the upwind and downwind PM_{10} mass concentrations was observed. One significant sample was found for the endosperm hydrate (6.6 $\mu g/m^3$) and acrylic co-polymer (20.8 $\mu g/m^3$) section, five were observed on the organic emulsion section and three for the untreated section. The average PM_{10} mass concentration contribution for the organic emulsion was 20.8 ($\pm$10.5) $\mu g/m^3$ and 10.4 ($\pm$3.1) $\mu g/m^3$ for the untreated section. Due to the overlap in the standard deviation values between the two measurements it is not possible to determine if they are significantly different. The PM_{10} mass concentration measurements taken in October 1995 do not indicate that there were detectable emissions

Table 7-7
Average PM_{10} Mass Concentration Differences Between Paired Upwind and Downwind Samples, July 1995

	Untreated ($\mu g/m^3$)	Endosperm hydrate ($\mu g/m^3$)	Acrylic co-polymer ($\mu g/m^3$)	Organic emulsion ($\mu g/m^3$)
up > down average	19.4	12.1	10.6	6.9
up > down std. dev	4.0	5.0	1.9	2.9
down > up average	21.4	3.2	5.9	4.8
down > up std. dev.	10.8	1.6		0.7

from the unpaved shoulders nor were there any detectable differences between the test sections.

Twenty four paired upwind and downwind PM_{10} samples were taken during the June 6-11, 1996, intensive measurement period on Bellevue Road. In addition, six paired far upwind-downwind samples were also taken. These samples were taken at a distance greater than 100 m from the road.

Table 7-6 shows the far upwind and downwind PM_{10} mass concentrations measured during June 1996. The test for significant difference in measured mass (Equation 7-1) was applied to each days' paired measurement which resulted in only one significant difference between far-upwind and far-downwind measurement, on June 6. On this date the downwind mass concentration was higher than the upwind by 14.0 $\mu g/m^3$. However, the standard deviation of the entire far upwind and downwind samples was ± 8.5 $\mu g/m^3$ which puts the mass concentration difference close to the uncertainty.

For the twenty-four paired upwind-downwind samples taken in the unpaved shoulder region of Bellevue Road, only thirteen proved to have a detectable change in the downwind PM_{10} mass concentrations compared to the upwind values. One sample occurred on the endosperm hydrate, three on the untreated, four on the acrylic co-polymer and five on the organic emulsion. However, when compared with the far-upwind values for the same days these counts decrease. For this comparison, there are two cases for the endosperm hydrate, two for the untreated, one for the acrylic co-polymer, and one for the organic emulsion section. This decrease in the number of significant differences in upwind-downwind masses is a result of the far-upwind values of PM_{10} mass concentrations being higher than the upwind samples taken closer to the road. When the higher far-upwind mass concentration value is subtracted from the downwind values, the difference between the two samples becomes negligible. This occurs for the organic emulsion section on 6/9/96 and 6/11/96 and for the acrylic co-polymer section on 6/10/96. For the cases where a significant downwind mass concentration was found with the far-upwind subtracted, the average gains were 12.9 $\mu g/m^3$ (± 5.7) for endosperm hydrate, 12.9 (± 0.7) $\mu g/m^3$ for the untreated, 15.7 $\mu g/m^3$ for the acrylic co-polymer and 17.2 $\mu g/m^3$ for the organic emulsion section. There was only one significant measurement for both the acrylic co-polymer and organic emulsion sections.

Of the 106 paired upwind-downwind filter measurements of PM_{10} mass concentrations taken on the unpaved shoulders of Bellevue Road there were 33 cases in which there was a significant difference in the PM_{10} mass concentrations. The detectable contributions of PM_{10} mass concentration ranged between approximately 6 and 20 $\mu g/m^3$ in an eight-hour test period, and no test section contributed at levels greater than any other. The exception is the July 1995 measurements where the untreated section average PM_{10} mass concentrations contribution that could be attributable to unpaved shoulder emissions was twice that of the sections with suppressant. The range of PM_{10} mass concentrations attributable to unpaved shoulder emissions (6 to 20 $\mu g/^3$) measured with the portable survey samplers is comparable to the range of PM_{10} mass concentrations that was estimated using a second measurement technique, the fast-response nephelometer (section 7.2.1). However,

there is relatively poor agreement for June 11, 1996, when the nephelometer measured much higher traffic related PM_{10} concentrations which were not evident in the filter-based measurements.

It was recognized from observations that visible emissions of dust from road shoulders are inhomogeneous in space and occur intermittently through time. They were also observed to be relatively small-scale, short-lived events when they were seen. One possible explanation that only 31% of the paired upwind-downwind samples showed mass concentration differences is that the portable survey samplers may under-collect PM_{10} particles carried in the fast-moving turbulent jets created by the passing vehicles. In recognizing the nature of the dust emissions observed on unpaved shoulders, fast response nephelometers and a sonic-anemometer were used to characterize the dust plumes associated with vehicle traffic and to provide a comparison with the filter-based measurements of PM_{10} mass concentrations.

7.1.4 Sonic Anemometer and Nephelometer Measurements

Dust entrainment from unpaved shoulders along paved roads is thought to be mainly due to brief bursts of increased wind velocity generated by passing vehicles. In this study a sonic anemometer, located directly adjacent to the road in the untreated shoulder section, was used to quantitatively measure the three Cartesian components of the flow velocity at 10 Hz sampling rate. This makes it possible to quantify the burst-induced shear stresses on the road surface which cause dust entrainment. These Reynolds shear stresses on the shoulder surface are proportional to the turbulent kinetic energy density (TKED, (N/m^2)) of the burst (Clifford and French, 1993) with:

$$TKED = 0.5\,\rho(u'^2 + v'^2 + w'^2) \qquad (7\text{-}2)$$

where ρ (kg/m^3) is the density of air and u', v', w' are the three Cartesian components of the fluctuating turbulent flow velocity, which have been statistically separated from the mean flow velocity (Reynolds, 1895). In this study, an average of over 50 sonic anemometer samples, equivalent to five seconds, has been used to define the mean flow velocities. A typical graph of the TKED while a large tandem trailer passes by is shown in Figure 7-1.

Vehicle induced spikes in the TKED are very short, typically lasting only a fraction of a second. This fact highlights the importance of the high frequency (10 Hz) measurement of wind velocities with the sonic anemometer. The peak value of these spikes depends strongly on the type of vehicle. For example Figure 7-2 shows the TKED of a high speed van plotted on the same scale as used in Figure 7-1.

From Figures 7-1 and 7-2, it is obvious that the vehicle induced TKED can vary by more than an order of magnitude depending on the type of vehicle. Vehicles have been grouped into four classes according to the peak values of the TKED measured on the side of the road where the vehicle travels:

DEV 1: TKED > 10 N/m^2small vehicles (e.g., cars, pickups, vans) with trailer

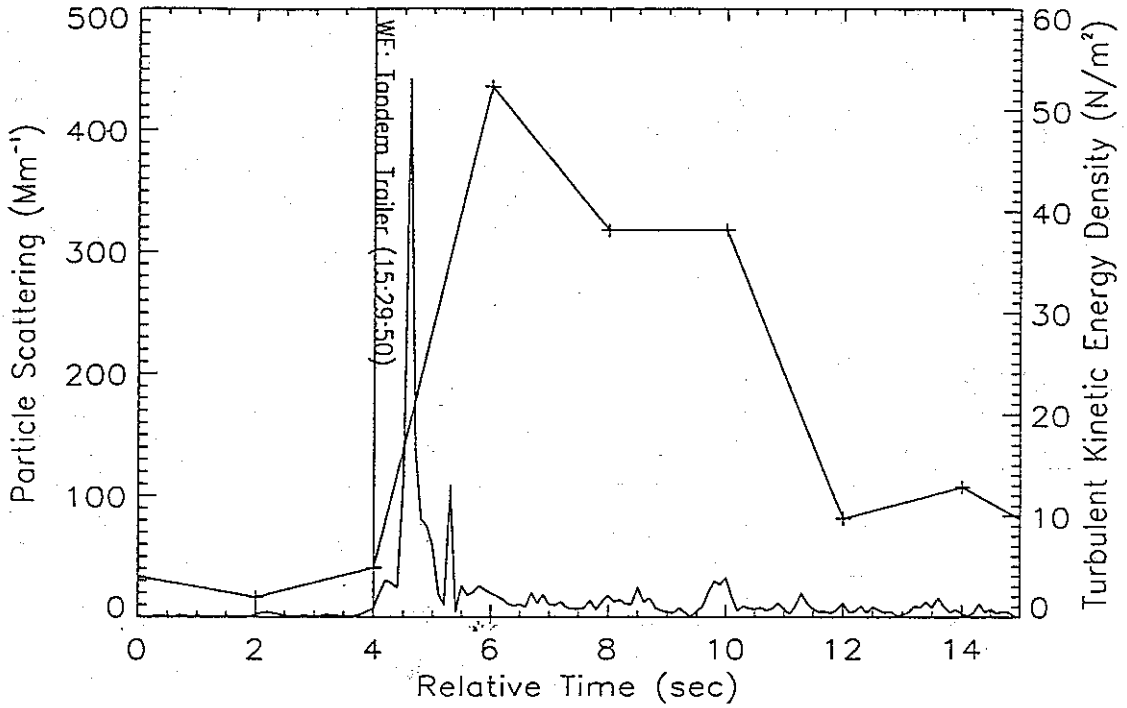

Figure 7-1: Turbulent kinetic energy density (smooth line) measured with a sonic anemometer and particle scattering (data points marked by crosses) measured with nephelometer 1 induced by a tandem trailer (time indicated by vertical line) traveling at high speed (≈ 60 mph) on June 11, 1996.

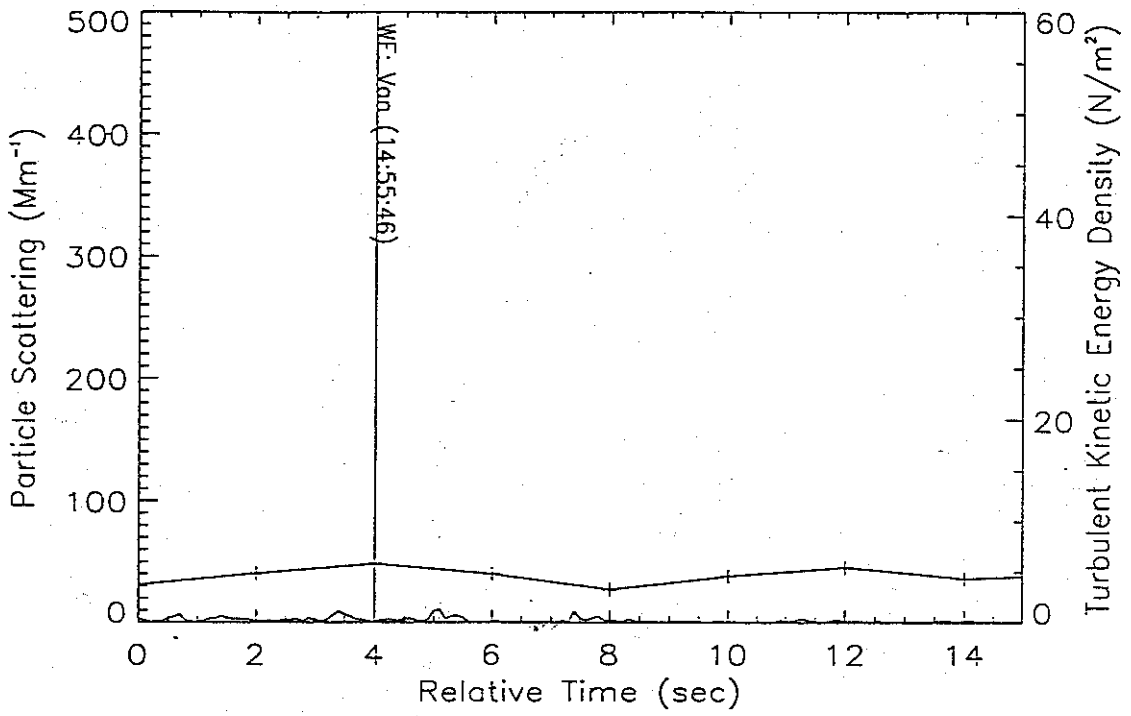

Figure 7-2: Turbulent kinetic energy density (smooth line) measured with a sonic anemometer and particle scattering (data points marked by crosses) measured with nephelometer 1 induced by a van (time indicated by vertical line) traveling at high speed (≈ 60 mph) on June 11, 1996.

DEV 2: TKED > 10 N/m^2 large vehicles (e.g., trucks, buses, large RVs)

DEV 3: TKED > 20 N/m^2 very large vehicles (e.g., semis, large vehicles with trailer)

Non DEV: TKED < 10 N/m^2 small vehicles (e.g., cars, pickups, vans)

where: DEV stands for "Dust Entraining Vehicle" as discussed in the following

All TKED values were measured with vehicles traveling at high speed , i.e., 50 to 60 mph. This study has not been able to investigate the dust entrainment process as a function of vehicle speed as vehicles on Bellevue Road have a narrow, mono-modal speed distribution with nearly all vehicles traveling between 50 and 60 mph. The classification into four vehicle groups is not necessarily dependent on vehicle size only, but probably more on their aerodynamic properties. For example, cars towing a trailer (DEV 1) may have a similar size as a van or sport utility vehicle (Non DEV) but their poor aerodynamics induces large bursts in wind velocity and therefore in TKED.

Four nephelometers (Optec NGN-2) were used to measure vehicle entrained dust directly along the road side, while a fifth nephelometer (Optec NGN-2) is located 6 m farther away from the road with

- nephelometer 1 located in the untreated section,
- nephelometer 2 located 6 m farther away from the road than nephelometer 1 in the untreated section,
- nephelometer 3 located in the section treated with organic emulsion,
- nephelometer 4 located in the section treated with acrylic co-polymer, and
- nephelometer 5 or 6 located in the section treated with endosperm hydrate.

An example of particle light scattering due to dust entrained by a passing vehicle is shown in Figure 7-1. Note that the sampling rate of the nephelometer is only 0.5 Hz, much lower than that of the sonic anemometer. In addition, the nephelometer measures only for about 0.25 s during each sample. This does not pose much of a problem for the relatively long dust event shown in Figure 7-1. However, some dust events are significantly shorter due to a higher wind speed perpendicular to the road. In this case, dust events are registered sometimes only in one nephelometer sample or not at all. This does not influence averages over many vehicles, but makes quantitative analysis of single events highly questionable. In addition vehicle distance from the shoulder can vary from section to section, further invalidating the quantitative analysis of dust events resulting from a single vehicle.

Dust entrainment, as measured by the nephelometers, is usually induced by a peak of the TKED larger than 10 N/m^2. These large peaks are consistently generated by vehicles of

large size (e.g., semis, trucks, buses, large RVs) or by vehicles with very poor aerodynamics (e.g., about any vehicle pulling a trailer) traveling at high speed (50 - 60 mph). This relatively small subset of the total traffic is being referred to as "dust entraining vehicles" or abbreviated DEV. Other vehicles do not entrain substantial amounts of PM_{10} during normal driving (e.g., see Figure 7-2) and their peak TKED is commonly around 1-2 N/m^2. Exceptions can be due to driving on the unpaved shoulder, for example.

The quantitative analysis of nephelometer measurements is presented in Section 7-2 with the application of emission rate calculations.

7.2 Emission Rates

7.2.1 Methodology of Emission Rate Calculation

The nephelometers measure the light scattering extinction B_{scat} (Mm^{-1}) which has a quasi-constant component $B_{Rscat.}$ = 11.6 Mm^{-1} (at 15°C and 1013 mB) due to Rayleigh scattering (scattering from gas molecules) and a widely varying component $B_{Pscat.}$ due to particle scattering. The particle scattering extinction can directly be calculated from the nephelometer measurements as

$$B_{Pscat} = B_{Scat} - B_{Rscat} . \tag{7-3}$$

If there is no road traffic or other events inducing bursts of particles, the particle scattering extinction fluctuates symmetrically around some background value. In this case its average value equals its median value. Road traffic introduces brief, but relatively infrequent peaks in the particle scattering extinction measured directly at the road side due to entrained dust. These peaks can be substantially higher than the background value. The median value is virtually unchanged due to the small fraction of time during which these peaks are present. However, the average value changes, reflecting the large increase of the particle scattering extinction during these events. Therefore, the difference between average and median value of $B_{pscat.}$ is a good measure of the average traffic induced particle extinction component $BT_{Pscat.}$ with

$$BT_{Pscat.} = Average(B_{Pscat.}) - Median(B_{Pscat.}). \tag{7-4}$$

As light scattering measurements are dominated by small particles, i.e., PM_{10}, measured scattering extinction can be related to an average PM_{10} concentration CT_{AV} ($\mu g/m^3$) by

$$CT_{AV} = \sigma_C \, BT_{Pscat.}, \tag{7-5}$$

where

$$\sigma_C = 0.4 \frac{m^2}{g} \tag{7-6}$$

is the scattering efficiency assumed for crustal particles as entrained by traffic.

Equation 7-5 can also be used to obtain a scattering efficiency for background PM_{10} from far-upwind/far-downwind PM_{10} sampler results and the daily medians of $B_{pscat.}$ from the nephelometer measurements. The resulting background aerosol scattering efficiency, σ_b = 1 m^2/g, is substantially larger than that assumed for vehicle entrained crustal PM_{10} in the immediate vicinity of the road σ_C = 0.4 m^2/g (Equation 7-6). This difference is reasonable, as background PM_{10} commonly contains more fine particles which have a higher scattering efficiency than the coarser crustal particles entrained by traffic. This difference also emphasizes that, while nephelometer measurements can be used as high sampling rate surrogates for PM_{10} samplers, they do not measure PM_{10} concentrations but weigh particle concentrations with the particle scattering efficiency, which is particle size-dependent. The scattering efficiency peaks approximately at the wavelength of the scattered light (e.g., 0.5 μm) and falls off towards larger sizes, about inversely proportional to the particle diameter. Scattering efficiencies of spherical particles of known refractive index and size can be calculated exactly using Mie theory (Mie, 1908). The analysis of nephelometer data could be improved by calculating scattering efficiencies for vehicle entrained particles from a measurement of their particle size distribution.

The average traffic entrained PM_{10} concentration CT_{AV} yields an average PM_{10} flux density FD_{AV} (μg/(m^2s)) perpendicular to the road, due to the average perpendicular wind velocity component V_i with

$$FD_{AV} = V_i \, CT \tag{7-7}$$

where V_i maybe obtained from the measurement of wind speed and direction on a nearby meteorological tower, which is available every 15 min. An alternative source are the sonic anemometer data which have a much higher recording frequency (10 Hz) and are taken at a more representative location, directly at the road side. However, sonic anemometer velocities are available only part of the time and have therefore only been used for comparison purposes.

For a nephelometer placed adjacent to the road, at a distance of about 2 - 3 m from passing vehicles, the exposure time to the dust plume can be approximated by the time it takes the vehicle to pass by the instrument, i.e., as the ratio of vehicle length L_{veh} and vehicle velocity V_{Veh}:

$$t_{Exp} = \frac{L_{Veh}}{V_{Veh}} . \tag{7-8}$$

The flux density, FD, in this plume is enhanced over the average flux density, FD_{AV}, by the ratio of the average time, t_{Veh}, during which one dust-entraining vehicle passes by, to the average exposure time, t_{Exp}, and FD may be written as

$$FD = \frac{t_{Veh}}{t_{Exp}} FD_{AV} . \tag{7-9}$$

The total PM_{10} flux, F (g/s), in the plume of an entraining vehicle can be obtained by multiplying the flux density, FD, with the plume area (the normal vector of the plume area is horizontal and perpendicular to the road), i.e.,

$$F = FD\,A = FD(W\,H) = FD(L_{Veh}\,H), \tag{7-10}$$

where the plume area, A, is the product of plume width, W, and plume height, H. Plume width and height are estimated to equal the length, L_{Veh}, of the passing vehicle and 3 m, respectively. The PM_{10} flux per vehicle-km-traveled, F_{VKM} (g/VKT), is well suited to obtain emission estimates for geographical areas. It can be obtained from the flux, F, as:

$$F_{VKM} = \frac{F}{V_{Veh}}. \tag{7-11}$$

Using the above equations, the PM_{10} flux per vehicle km, F_{VKM}, can be expressed in a rather simple form as:

$$F_{VKM} = H\,t_{Veh}\,V_i\,CT_{AV}, \tag{7-12}$$

where several quantities used in the derivation have canceled. This equation may be used to calculate PM_{10} fluxes from either nephelometer measurements using Equation 7-3 or from PM_{10} samplers if the traffic component of the average PM_{10} concentration, CT_{AV}, can be obtained, for example, from up-and downwind measurements.

7.2.2 Emission Rate Calculations for Bellevue Road

Using these concepts and equations, simultaneous measurements with all non-collocated nephelometers have been analyzed for about 26 hours of data taken during the period from June 6, 1996, to June 11, 1996.

Traffic records from video recordings (Table 7-3) were used to calculate the average time, t_{Veh}, during which one dust entraining vehicle passes by. Video recordings were available for about 75% of the analyzed time periods with an availability of more than 65% for this period on any given day. Traffic frequency and composition during gaps was assumed to be identical to the rest of the measurement period.

Results for the average and median particle scattering, B_{pscat}, the average traffic-induced particle scattering, Bt_{pscat}, the average traffic-induced PM_{10} concentration and the resulting PM_{10} emission rates per vehicle-km-traveled are shown in Tables 7-8 to 7-13, for the individual days. PM_{10} emission rates are calculated both using perpendicular wind velocities, V_i, obtained both from the meteorological tower and from the sonic anemometer. However, rates calculated with sonic anemometer wind velocities should be used only for comparison purposes as sections of these data were not available. Table 7-14 contains the weighted average of PM_{10} emission rates over all six days. The number of "dust entraining vehicles" was used as weighting function. The emission rates (averaged over six days, calculated with meteorological tower wind velocities) range from 7.61 g/VKT to 9.71 g/VKT for road side nephelometers and agree with each other within their standard deviations. This

Table 7-8
Emission Rate Calculation for June 6, 1996 from 14:13:34 to 16:18:40

Number of dust entraining vehicles = 50
Average time per dust entraining vehicle t_{Veh} = 150 s
Average wind velocity perpendicular to road from meteorological tower V_i = 0.92 m/s
Average wind velocity perpendicular to road from sonic anemometer V_i = 1.57 m/s

	Neph. 1	Neph. 2	Neph. 3	Neph. 4	Neph. 5
Average (B_{Pscat} (Mm^{-1}))	51.55	36.30	86.76	81.05	NA
Median B_{pscat} (Mm^{-1})	45.25	33.30	83.30	73.09	NA
BT_{Pscat} (Mm^{-1})	6.30	2.99	3.46	7.96	NA
CT_{AV} ($\mu g/m^3$)	15.74	7.48	8.64	19.90	NA
$F_{v\text{-}km}$ [a] (g/VKT)	**6.51**	**3.10**	**3.58**	**8.23**	**NA**
$F_{v\text{-}km}$ [b] (g/VKT)	11.11	5.28	6.10	14.04	NA

a: Calculated with wind velocities from the meteorological tower
b: Calculated with wind velocities from the sonic anemometer

Table 7-9
Emission Rate Calculation for June 7, 1996 from 12:25:56 to 17:06:56

Number of dust entraining vehicles= 81
Average time per dust entraining vehicle t_{Veh} = 207 s
Average wind velocity perpendicular to road from meteorological tower V_i = 1.17 m/s
Average wind velocity perpendicular to road from sonic anemometer V_i = 1.26 m/s

	Neph. 1	Neph. 2	Neph. 3	Neph. 4	Neph. 5
Average (B_{Pscat} (Mm^{-1}))	57.00	37.12	36.43	61.87	NA
Median B_{pscat} (Mm^{-1})	53.90	34.84	35.02	55.33	NA
BT_{Pscat} (Mm^{-1})	3.10	2.27	1.40	6.54	NA
CT_{AV} ($\mu g/m^3$)	7.75	5.69	3.51	16.35	NA
$F_{v\text{-}km}$[a] (g/VKT)	**5.62**	**4.13**	**2.55**	**11.86**	**NA**
$F_{v\text{-}km}$[b] (g/VKT)	6.07	4.45	2.75	12.81	NA

a: Calculated with wind velocities from the meteorological tower
b: Calculated with wind velocities from the sonic anemometer

Table 7-10
Emission Rate Calculation for June 8, 1996 from 11:55:06 to 16:39:52

Number of dust entraining vehicles= 54
Average time per dust entraining vehicle t_{Veh} = 314 s
Average wind velocity perpendicular to road from meteorological tower V_i = 0.77 m/s
Average wind velocity perpendicular to road from sonic anemometer V_i = 1.13 m/s

	Neph. 1	Neph. 2	Neph. 3	Neph. 4	Neph. 5
Average (B_{Pscat} (Mm^{-1}))	35.65	29.89	25.77	57.92	NA
Median B_{pscat} (Mm^{-1})	31.62	26.52	17.73	49.12	NA
BT_{Pscat} (Mm^{-1})	4.03	3.37	8.05	8.80	NA
CT_{AV} ($\mu g/m^3$)	10.07	8.41	20.12	22.00	NA
$F_{v\text{-}km}$[a] (g/VKT)	**7.30**	**6.10**	**14.59**	**15.96**	**NA**
$F_{v\text{-}km}$[b] (g/VKT)	10.71	8.95	21.40	23.41	NA

a: Calculated with wind velocities from the meteorological tower
b: Calculated with wind velocities from the sonic anemometer

Table 7-11
Emission Rate Calculation for June 9, 1996 from 11:47:08 to 15:48:26

Number of dust entraining vehicles= 50
Average time per dust entraining vehicle t_{Veh} = 291 s
Average wind velocity perpendicular to road from meteorological tower V_i = 1.77 m/s
Average wind velocity perpendicular to road from sonic anemometer V_i = NA

	Neph. 1	Neph. 2	Neph. 3	Neph. 4	Neph. 6
Average (B_{Pscat} (Mm^{-1}))	41.92	29.20	21.62	NA	35.17
Median B_{pscat} (Mm^{-1})	39.99	27.67	11.49	NA	29.85
BT_{Pscat} (Mm^{-1})	1.93	1.53	10.13	NA	5.32
CT_{AV} ($\mu g/m^3$)	4.83	3.82	25.33	NA	13.30
$F_{v\text{-}km}$[a] (g/VKT)	**7.44**	**5.89**	**39.03**	**NA**	**20.50**
$F_{v\text{-}km}$[b] (g/VKT)	NA	NA	NA	NA	NA

a: Calculated with wind velocities from the meteorological tower
b: Calculated with wind velocities from the sonic anemometer

Table 7-12
Emission Rate Calculation for June 10, 1996 from 11:20:34 to 16:17:08

Number of dust entraining vehicles= 124
Average time per dust entraining vehicle t_{Veh} = 143 s
Average wind velocity perpendicular to road from meteorological tower V_i = 0.68 m/s
Average wind velocity perpendicular to road from sonic anemometer V_i = 1.02 m/s

	Neph. 1	Neph. 2	Neph. 3	Neph. 4	Neph. 6
Average (B_{Pscat} (Mm^{-1}))	42.63	28.31	25.76	NA	21.77
Median B_{pscat} (Mm^{-1})	32.80	19.53	17.22	NA	19.33
BT_{Pscat} (Mm^{-1})	9.83	8.78	8.53	NA	2.44
CT_{AV} ($\mu g/m^3$)	24.57	21.96	21.33	NA	6.09
$F_{v\text{-}km}$[a] (g/VKT)	**7.12**	**6.36**	**6.18**	**NA**	**1.77**
$F_{v\text{-}km}$[b] (g/VKT)	10.70	9.56	9.29	NA	2.65

a: Calculated with wind velocities from the meteorological tower
b: Calculated with wind velocities from the sonic anemometer

Table 7-13
Emission Rate Calculation for June 11, 1996 from 10:57:26 to 16:09:06

Number of dust entraining vehicles= 177
Average time per dust entraining vehicle t_{Veh} = 106 s
Average wind velocity perpendicular to road from meteorological tower V_i = 0.24 m/s
Average wind velocity perpendicular to road from sonic anemometer V_i = 0.29 m/s

	Neph. 1	Neph. 2	Neph. 3	Neph. 4	Neph. 6
Average (B_{Pscat} (Mm^{-1}))	87.91	73.96	67.69	69.80	79.65
Median B_{pscat} (Mm^{-1})	39.97	32.15	29.17	37.57	34.67
BT_{Pscat} (Mm^{-1})	47.94	41.81	38.51	32.23	44.98
CT_{AV} ($\mu g/m^3$)	119.86	104.52	96.28	80.57	112.46
$F_{v\text{-}km}$[a] (g/VKT)	**9.31**	**8.12**	**7.48**	**6.26**	**8.74**
$F_{v\text{-}km}$[b] (g/VKT)	10.85	9.46	8.71	7.29	10.18

a: Calculated with wind velocities from the meteorological tower
b: Calculated with wind velocities from the sonic anemometer

Table 7-14
Weighted Average of Emission Rates for the Period June 6 though June 11, 1996

Number of dust entraining vehicles= 537
Average time per dust entraining vehicle t_{Veh} = 172 s

	Neph. 1	Neph. 2	Neph. 3	Neph. 4	Neph. 6
$F_{v\text{-}km}$[a] (g/VKT)	**7.61**	**6.23**	**9.71**	**9.24**	**7.94**
St. Dev. Mean (g/VKT)	**0.59**	**0.75**	**4.43**	**2.06**	**4.26**
$F_{v\text{-}km}$[b] (g/VKT)	10.02	8.16	9.01	11.88	7.07
St. Dev. Mean (g/VKT)	0.89	1.04	2.48	3.22	3.71

a: Calculated with wind velocities from the meteorological tower
b: Calculated with wind velocities from the sonic anemometer

fact leads to the conclusion that within the precision of these measurements emission rates for the untreated section and the three treated sections are identical. The weighted average emission rate derived from all these nephelometers on all six days is 7.75 g/VKT with a standard deviation of 1.8 g/VKT. However, it should be kept in mind that the standard deviation is only an indication of the precision of the emission rate. Its accuracy is also influenced by errors in other values used in the calculation, such as plume height and particle scattering efficiency, and by unusual dust entrainment events, for example due to vehicles swerving onto the shoulder. Therefore, the emission rate is estimated to be 8 ± 4 g/VKT.

Nephelometer 2 was set back from the road side and located behind nephelometer 1 along the untreated section. measurements. Its average emission rate is about 20% lower than that of Nephelometer 1, a result that is barely significant according to the standard deviations of the two values. However, it should be kept in mind that the emission rate for nephelometer 1 is at least 10% higher than that of nephelometer 2 for each single day of measurement, the only consistent ranking between the nephelometer derived emission rates. The 20% drop off in traffic induced PM_{10} concentrations over 6 m is consistent with the results from Fields Road (see Section 8.3).

One remaining question is why the upwind and downwind PM_{10} samplers were not able to conclusively detect traffic induced PM_{10} concentrations. According to the nephelometer measurements, the average traffic induced PM_{10} concentrations CT_{AV} vary from around 5 $\mu g/m^3$ on some days to around 100 $\mu g/m^3$ on June 11, 1996 (Tables 7-8 through 7-13). While the portable PM_{10} samplers might not be able to detect 5 $\mu g/m^3$, they should be easily able to measure 100 $\mu g/m^3$. Possible explanations for them failing to do so, range from PM_{10} sampling problems in short traffic induced wind bursts (see also Section 7.1.3) to the fact that nephelometers do not measure PM_{10} mass directly but use light scattering as a surrogate (see also Section 7.2.1).

In summary, the nephelometer measurements indicate an emission rate of 8 ± 4 g/VKT for a "dust entraining vehicle" (i.e., a vehicle with large size or poor aerodynamics) traveling at high speed. No significant differences between emission rates of the untreated and the three treated sections were measured.

7.3 Changes in Surface Characteristics

This section presents the trends observed in the surface characterization measurements on the Bellevue Road test sections through the duration of this project and also examines their relationships within the context of PM_{10} emissions.

The changes in Bellevue Road shoulder surface characteristics resulted from two processes: exposure to weather and the action of vehicle traffic that purposefully traveled on the road shoulders or was a result of random movements from the road to the shoulder. Vehicle traffic that was observed to regularly use the shoulders included: school buses, postal delivery vehicles, and garbage trucks. Farm vehicles also used the shoulders, especially when traffic approached from behind, but also in the event of oncoming traffic.

Weathering of the surface was caused primarily by rainfall events that probably caused aggregate breakdown or washout of the water soluble chemical binding agents associated with the suppressants. In addition, solar radiation may have caused some weakening of the adhesive properties of the suppressants. This may include weakening of the polymer chains used in some of the suppressants by exposure to ultra-violet light, for example in the acrylic co-polymer. Exposure to sunlight can also cause evaporation of any volatile components or resins that help to bind sediment. This type of evaporation may have occurred in the organic emulsion suppressant which has pine tree resins as a base for creating particle adhesion.

The monthly precipitation values for the field portion of this research project are shown in Table 6-10. Rain was first recorded in the area in December 1995, five months after the suppressants were applied. Above average rainfall amounts were observed in December 1995, and January, February, and May 1996.

The traffic counts, average daily traffic volume and characteristics on Bellevue Road were identified in Section 7.1.1. Unfortunately, the traffic counting system did not allow for the determination of the amount of traffic that was exclusively on the shoulder areas. However, visual observation of the state of the shoulder areas revealed that within the first week after application of the suppressants, significant proportions of the surface were observed to be impacted upon by vehicle traffic.

During the July 1995 intensive measurement period it became clear that the unpaved shoulders of Bellevue road were highly dynamic environments. The sections with suppressants were not only subject to the aging process associated with weathering, but also to the actions of vehicle traffic similar to travel on an unpaved road such as Fields Road. This is likely the most important mechanism for causing the deterioration of the suppressant treated surfaces and creating potentially entrainable particles on the unpaved road shoulders.

The appearance of the suppressed surfaces changed as indicated by video and still photographic records. General observations of the changes at the Bellevue Road sites, from July 1995 through June 1996, are as follows:

July 1995

- Untreated: Surface is covered with loose sediment intermixed with large areas of heavily consolidated sediment. The shoulders are more friable and easily broken up near the outside edges.

- Endosperm hydrate: There are considerable amounts of loose material that are not bonded together. There is no real evidence either of crusting or bonded sediments attributable to the suppressant application.

- Acrylic co-polymer: After application there was a milky-white, skin like covering over the shoulder material. The surface was "sticky". The film was damaged with bare patches appearing within days of application.

- Organic emulsion: The surface is visibly darker after treatment. It is pliable and there is not much loose surface material. It tends to break-up towards the outside edges.

September 1995

- Untreated: Relatively little change was observed. Surface is dominated by loose material with some evidence that there is more material towards the outside edges.

- Endosperm hydrate: Surface is completely broken up where shoulder traffic is expected, around mailboxes and driveways. Not much evidence that any suppressant remains.

- Acrylic co-polymer: Surface film observed in July is completely broken at areas around driveways and mailboxes. Surface integrity of suppressant film is estimated at <50%. Film is more severely broken up at distances ≥1 m from the pavement edge.

- Organic emulsion: The crust is broken through where there has been traffic on the shoulder, at field entrances and within 1 m of the pavement edge. Loose material is increasing on the surface. Overall integrity of crust is estimated at 70%.

October 1995

- Untreated: A coarse to finer gradation of particle size appears to be developing from the pavement towards the outside edges of the shoulders.

- Endosperm hydrate: No major, observable changes from September 1995. The surface is dominated by loose material and the sorting phenomenon was also noted on this section.

- Acrylic co-polymer: No evidence of the suppressant film remained. Surface is now dominated by loose material.

- Organic emulsion: The crust continues to degrade, the amount of loose surface material appears to be increasing. Crust integrity is estimated at ≤50%.

December 1995

- Untreated: Appears that fine material has been washed from the shoulder region by December rain. Vehicle tracks are more obvious in the moist soil.

- Endosperm hydrate: Deep vehicle tracks are evident in the visibly moist sediment.

- Acrylic co-polymer: Lots of vehicle tracks can be seen in the shoulder region.

- Organic emulsion: The original color difference noted in this section is very much reduced. The crust continues to breakdown.

March 1996

- Untreated: There is a notable gradation from coarse to finer particles from the pavement towards the outer edges of the shoulders. This is also true for the acrylic co-polymer and Endosperm hydrate sections.

- Endosperm hydrate: The surface is dominated by loose material in most areas with some bare, crusted areas.

- Acrylic co-polymer: The surface is dominated by loose material.

- Organic emulsion: The surface crust was very broken up. Integrity was estimated at ≤20%. Loose material was found even on the patches that maintained crust integrity.

June 1996

- Untreated: The surface was dominated by loose material with some bare crusted patches.

- Endosperm hydrate: The surface was dominated by loose material with some bare crusted patches. There was no evidence of any suppressant.

- Acrylic co-polymer: The surface was dominated by loose material with some bare crusted patches. There was no evidence of any suppressant.

- Organic emulsion: The surface is dominated by loose surface material. Some larger crust patches remain.

7.3.1 Bulk Loading of Loose Surface Material

The loose surface material on the Bellevue Road shoulder test sections was collected using two different methodologies. The first method was to sweep up the loose sediment with a fine bristled brush from a strip of known width and length running perpendicular to the direction of the road, for both the north and south side unpaved shoulders. Weighing the sample and knowing the sampled area provides a measure of the amount of loose surface material per unit area. The second method removed the loose surface material from a strip of shoulder with a vacuum device.

Figure 7-3 shows the observed changes in the bulk surface loading of loose material (particles ≤6.3 mm) collected by the sweep technique on the untreated and three treated sections of Bellevue Road shoulders. Figure 7-4 shows the trend in the same surface characteristic for the vacuum collected samples. The general trends in the data can be summarized as:

- The highest initial loading (July 1995) of loose surface material was on the untreated section of the shoulders (1,600 g/m^2) as determined from the sweep collected samples. The endosperm hydrate and acrylic co-polymer had similar amounts of loose bulk material (sweep collected) with 960 g/m^2 and 1,250 g/m^2, respectively. The organic emulsion section had notably less loose surface material at 160 g/m^2.

- The vacuum collected bulk surface samples covered a smaller range of values between 60 and 100 g/m^2 for the July 1995 samples.

- The amount of loose surface material increased on all surfaces by September 1995 for both measurement techniques. The greatest increase was observed on the organic emulsion section which increased by almost a factor of 10 for the sweep technique sampling method to 1,560 g/m^2. In the same time the amount of loose surface material increased by a factor of 1.8 for the untreated, 1.7 for endosperm hydrate and by a factor of three for acrylic co-polymer which now had the greatest amount of loose material at 3,940 g/m^2. For the vacuum collected samples the loose material increased by a factor of 2.2 for organic emulsion, and factor of three for both the endosperm hydrate and acrylic co-polymer.

- By October 1996 the amount of loose surface material collected with the sweep technique showed a continued increase only on the organic emulsion section. Increases were observed on the organic emulsion and acrylic co-polymer sections from the vacuum collected samples. Decreases in the bulk surface loading was observed for all other cases.

- A decrease in bulk surface loading was noted for all cases, for both collection methods in December 1995.

- An increase in bulk surface loading, as determined from sweep samples, was observed for all sections after December 1995 through June 1996. The range of values in June 1996 was between 4,440 and 5,590 (±500) g/m^2. The amount of bulk surface material on the test sections had increased by approximately five times since July 1995. A similar trend was observed for the vacuum collected samples. The amount of bulk surface material increased approximately 1.6 times from the July 1996 values.

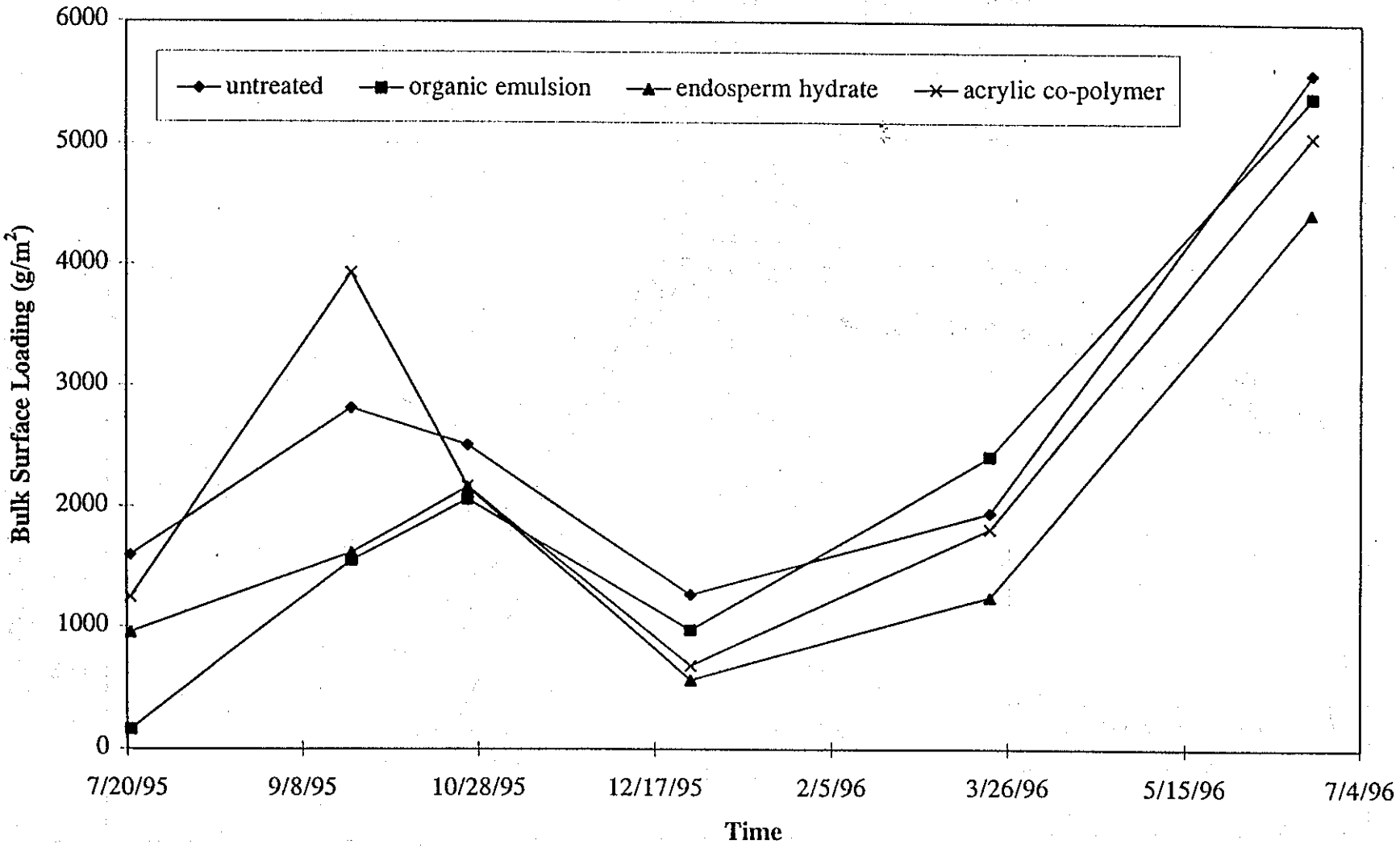

Figure 7-3 Changes in bulk surface loading on Bellevue Road as a function of time as determined from sweep collected samples.

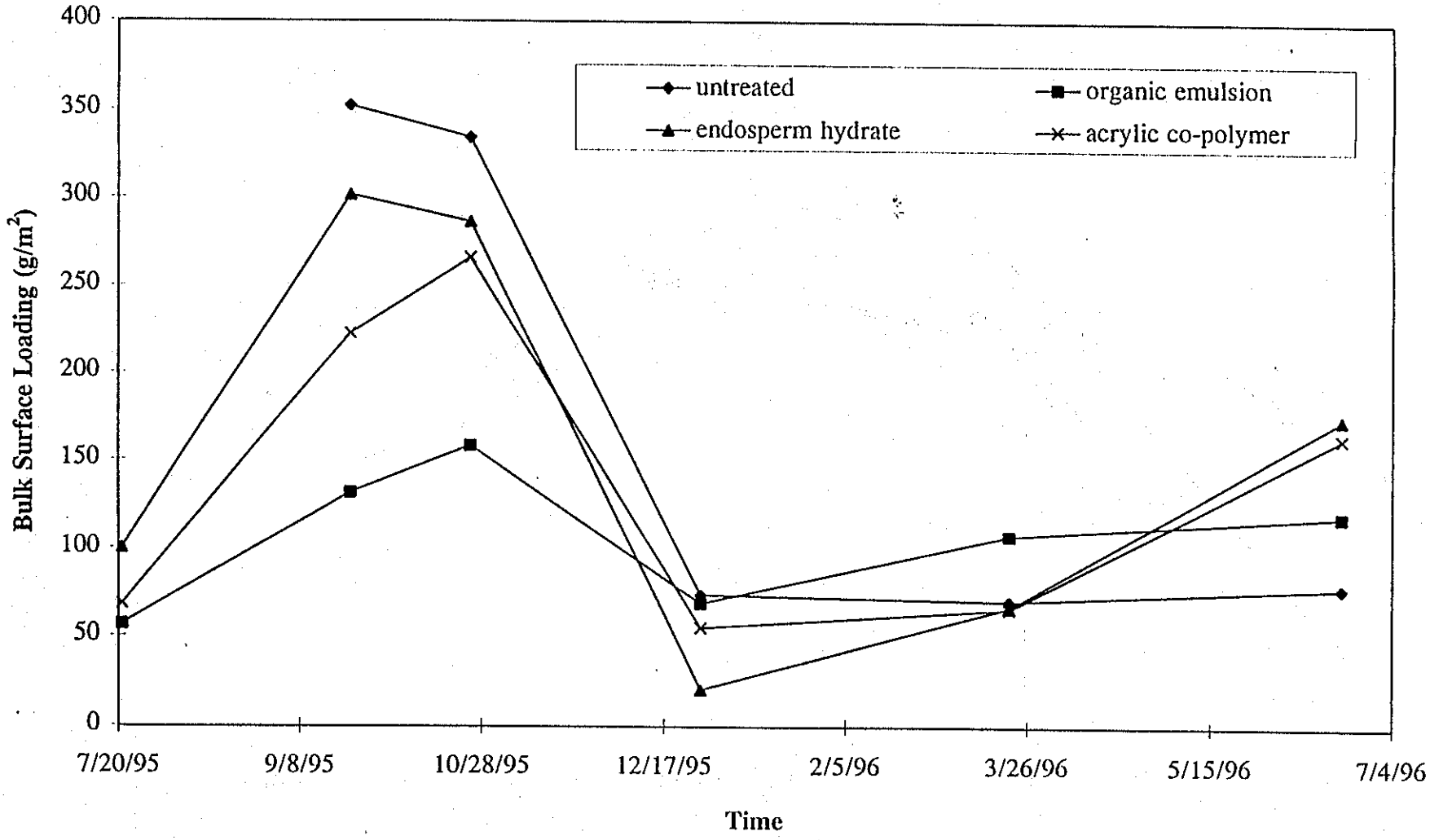

Figure 7-4 Changes in the bulk surface loading as a function of time as determined from surface samples collected with the vacuum technique.

7.3.2 Percent Silt Content in Surface Material

The surface samples of loose material removed from the test sections by the two collection techniques were analyzed for their percent silt content (particles <75 μm) using the same methodology as was used on the Fields Road samples (Appendix B.2). Figure 7-5 shows the changes in the percent silt content of the sweep collected samples as a function of time. Figure 7-6 shows the changes in the percent silt content of the vacuum collected samples. The general trends in the data can be summarized as follows:

- In July 1995 the organic emulsion section had the lowest percent silt content of the test sections with a value of 0.5% (±0.5%). The silt content of the endosperm hydrate and acrylic co-polymer was 2.6% (±1.5%) and 1.5 (±0.2%) respectively. The silt content of the vacuum collected samples was higher than in the sweep samples. The range of silt content was between 3.5% and 8.9%. The organic emulsion again had the lowest silt content of 3.5% (±4.0%).

- The percent silt content increased in September 1995 in the sweep collected samples. In this period it ranged between 1.3% (± 0.2%) and 3.4% (± 0.3%). The percent silt content in the vacuum samples did not show the same pattern. There was an increase in percent silt content in the endosperm hydrate to 6.4% (±0.6%), but a decline in both the acrylic co-polymer and organic emulsion sections.

- In October 1995 there were slight increases in percent silt content of the surface sweep samples from the endosperm hydrate, organic emulsion and untreated sections over the September values, and a decrease in the acrylic co-polymer value to 1.3 % (±0.2%). The percent silt content of the vacuum samples showed relatively large increases for the acrylic co-polymer and untreated sections with a small increase in the organic emulsion section. The percent silt content of the vacuum samples from the endosperm hydrate section declined in this period.

- The silt content of all the test sections declined in December 1995 due to a combination of increased moisture content and possibly the washing of the fine particles from the surface as a result of precipitation derived run-off. This was evident in both the sweep and vacuum collected samples.

- The sweep collected samples taken in March 1996 show the silt content increased on all test sections. This pattern is mirrored in the vacuum collected samples, however, the acrylic co-polymer section has only a small increase compared to the other sections.

- The largest single increase in percent silt content of the sweep samples was observed between March 1996 and June 1996. By June 1996 the percent silt content had increased by, on average, a factor of three and in each case was greater than that measured in July 1995. The same trend was observed in the vacuum collected samples except for the acrylic co-polymer which showed a

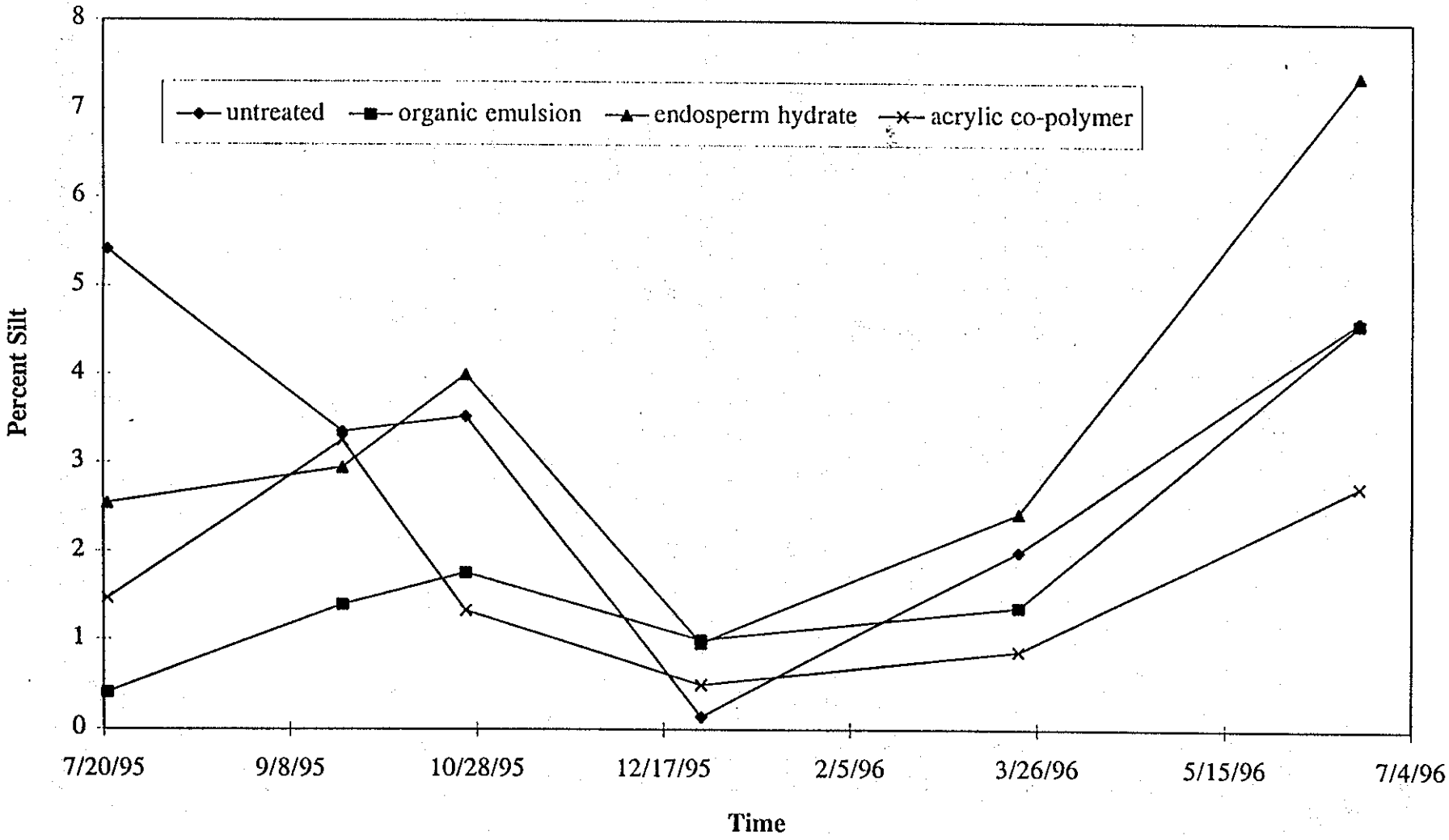

Figure 7-5 Changes in the percent silt content as a function of time as determined from sweep collected surface samples .

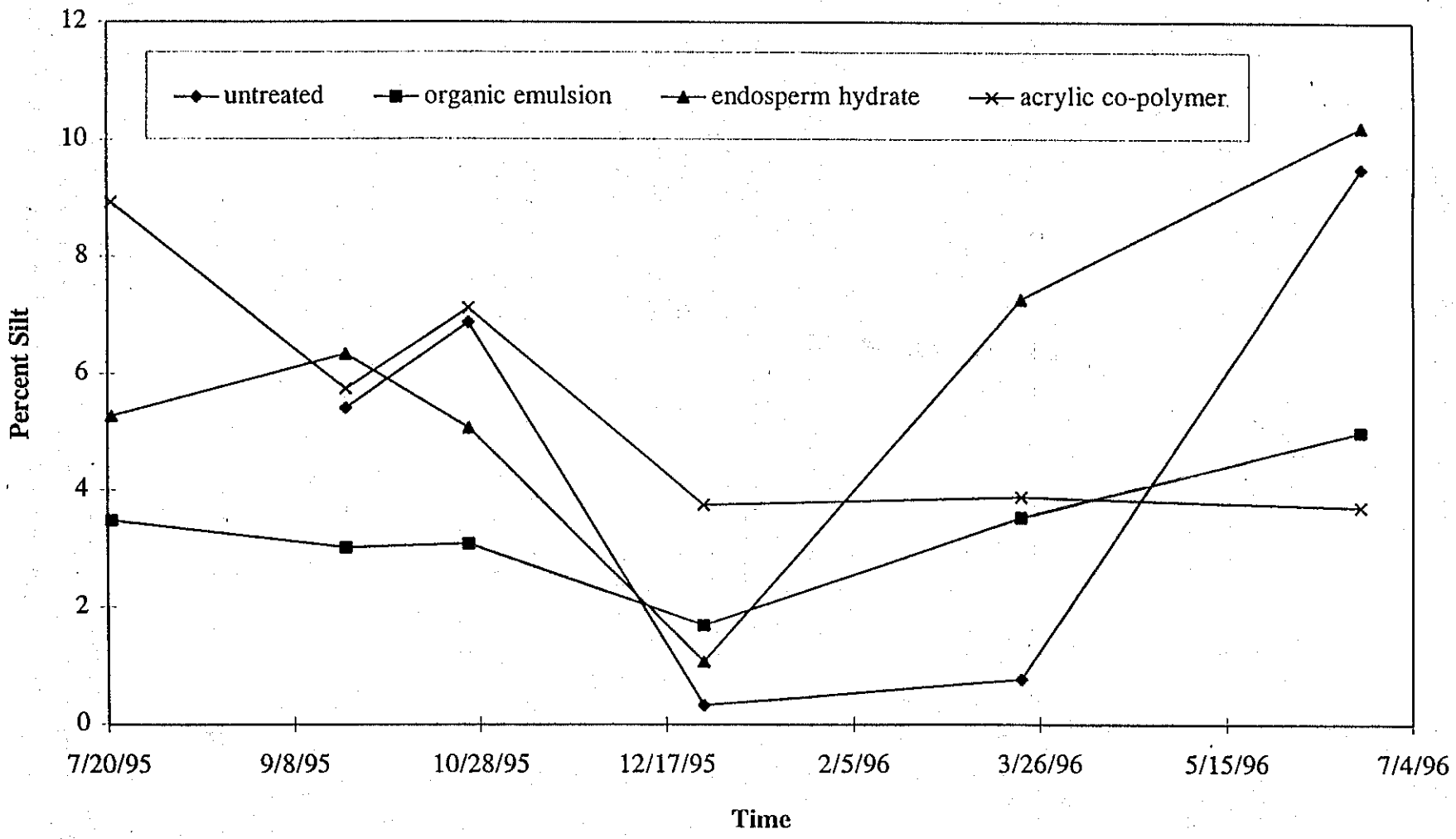

Figure 7-6 Changes in surface silt content as a function of time as determined from vacuum collected samples .

slight decline. However, in the case of the acrylic co-polymer this difference is not significant taking the uncertainties in the measurements into consideration.

7.3.3 Bulk Silt Loading

The amount of silt in the surface sediments of the unpaved shoulders can also be expressed in terms of its mass per unit area. The amount of silt expressed in g/m^2 was determined for each of the bulk samples of loose surface material. The changes through time in bulk silt loading of the sweep collected samples is shown in Figure 7-7 and in the vacuum collected samples in Figure 7-8. The general trends in the data can be summarized as follows:

- In July 1995 the range of silt content was between 0.4 ($\pm$0.1) g/m^2 for the organic emulsion and approximately 20.0 ($\pm$0.1) g/m^2 for the acrylic co-polymer and endosperm hydrate sections. The vacuum-collected samples showed the same pattern, a low organic emulsion value of 2.0 ($\pm$0.1) g/m^2, and higher values for the acrylic co-polymer and endosperm hydrate surfaces with values of 5.0 ($\pm$0.1) g/m^2 and 7.0 ($\pm$0.1) g/m^2, respectively.

- The bulk silt content of the sweep and vacuum collected surface samples increased in the three treated sections in September 1995. The greatest absolute increases were observed in the acrylic co-polymer and endosperm hydrate sections, but the greatest relative increase was in the organic emulsion section where silt content increased by a factor of 52 to 2.100 ($\pm$0.070) g/m^2. However, the organic emulsion section still had six times less silt than acrylic co-polymer, four times less than the untreated, and two times less than the endosperm hydrate section. A similar pattern of increased silt content was also found in the vacuum collected samples.

- The silt content continued to increase for the organic emulsion and Endosperm hydrate section through to October 1995. A slight decrease was observed for the untreated section, but a much larger decrease was observed in the acrylic co-polymer.

- The silt content of all the test sections declined in December 1995 due to a combination of increased moisture content and possibly the washing of the fine particles from the surface as a result of precipitation derived run-off. This is evident in both the sweep and vacuum collected samples.

- The sweep collected samples taken in March 1996 show the silt content increased on all test sections.

- The largest single increase in bulk silt content of the sweep samples was observed between March 1996 and June 1996. By June 1996 the silt content had increased by, on average, a factor of seven times from the March 1996 values, and in each case was greater than that measured in July 1995. The same trend was observed in

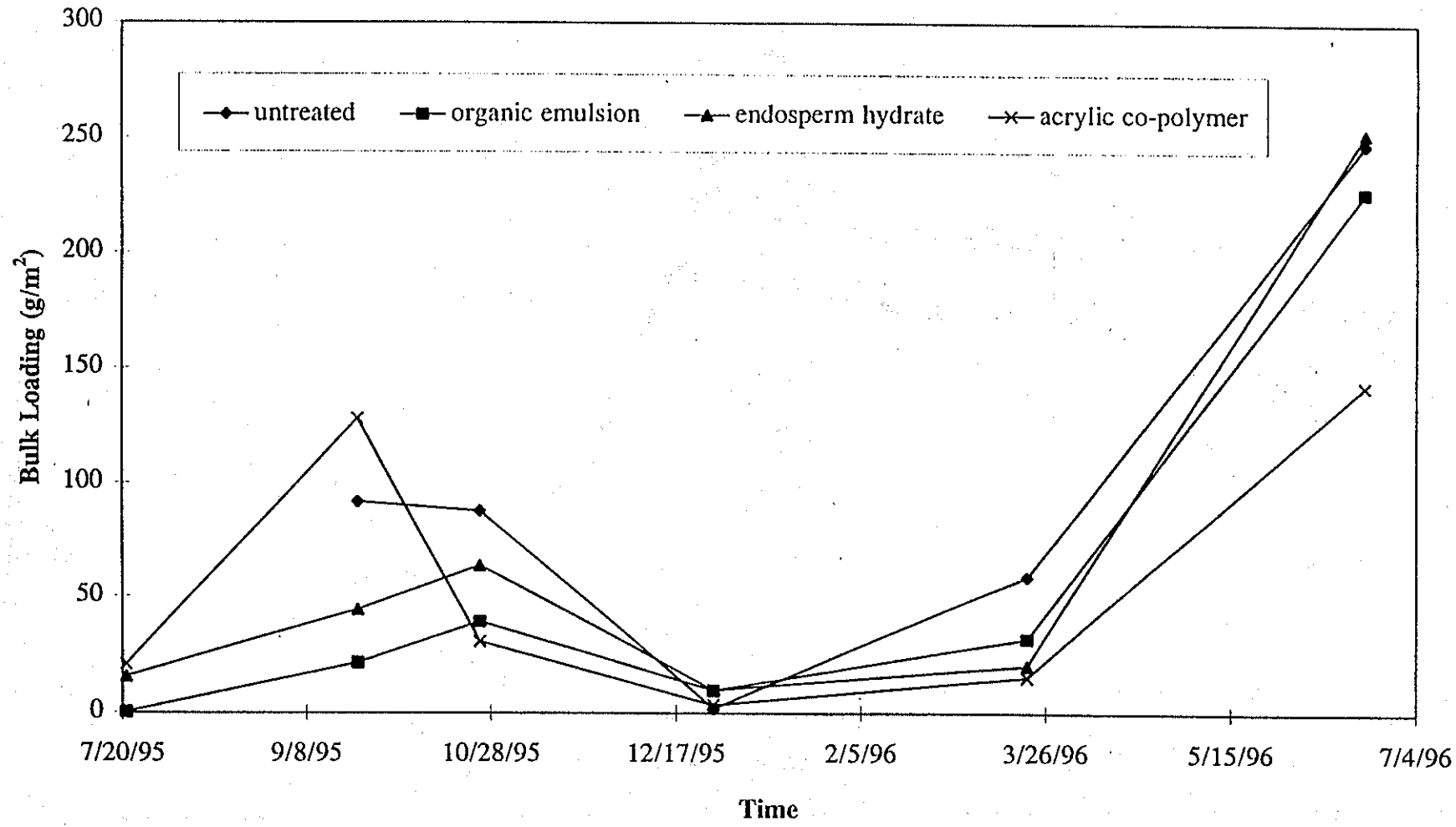

Figure 7-7 Changes in bulk silt loading as a function of time as determined from sweep collected samples.

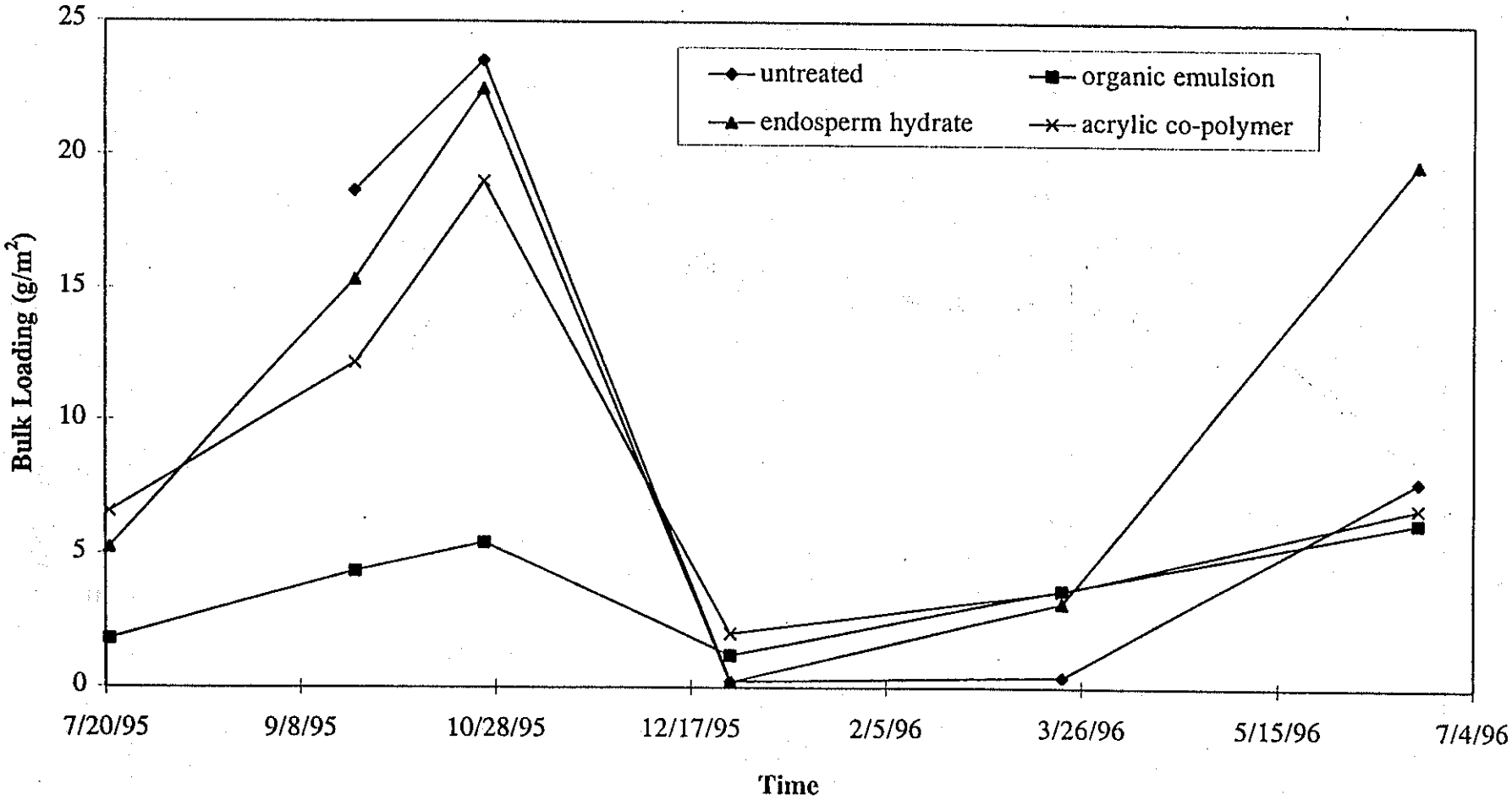

Figure 7-8 Changes in bulk silt loading as a function of time as determined from vacuum collected samples.

the vacuum collected samples. The greatest single increase in these samples was observed in the endosperm hydrate were the increase in silt content was by a factor of approximately 6.5 times to 20.0 (±0.1) g/m^2.

7.3.4 Surface Strength

An index of surface strength (kg/cm^2) was obtained for this study by measuring the resistance of the test surfaces to a vertical force applied with a Proctor Penetrometer®. Transects of the shoulder width were made with measurements taken every 0.25 meters; four transects, two on each of the north and south shoulders, were done for every measurement period. The changes observed in the average surface strength for each test section as a function of time are shown in Figure 7-9. The general trends observed were:

- In July 1995 the organic emulsion had the lowest average surface strength value of 26 (±16) kg/cm^2. The endosperm hydrate strength value was 105 (±53) kg/cm^2 and the acrylic co-polymer was 110 (±64) kg/cm^2. Breakage of the probe resulted in no untreated section measurements.

- By September 1995 the range of average strength measurements for the test surfaces was 81 (±78) kg/cm^2 for the untreated section to 141 (±47) kg/cm^2 for the acrylic co-polymer section. The organic emulsion section average surface strength increased to 103 (±70) kg/cm^2.

- The surface strength on the four shoulder test sections decreased in December due to higher soil moisture contents from precipitation inputs.

- The average surface strength increased on each surface in March 1996 as the surfaces dried. The range of values in this period was between 60 (± 50) and 113 (±66) kg/cm^2.

- In June 1996 the largest increase in surface strength was observed for each of the test sections. The range of values for surface strength was 229 (±106) kg/cm^2 for endosperm hydrate to 268 (±103) kg/cm^2 for the untreated section. By June 1996 the surface strengths associated with each test section were indistinguishable from each other.

7.3.5 Mean Aggregate Size

Figure 7-10 illustrates the changes in the mean aggregate size determined by the method of moments (Folk, 1980) from the measured particle size distributions. Figure 7-10 illustrates the following trends:

- There is a general trend of a decrease in mean aggregate size after suppressant application through to September 1995.

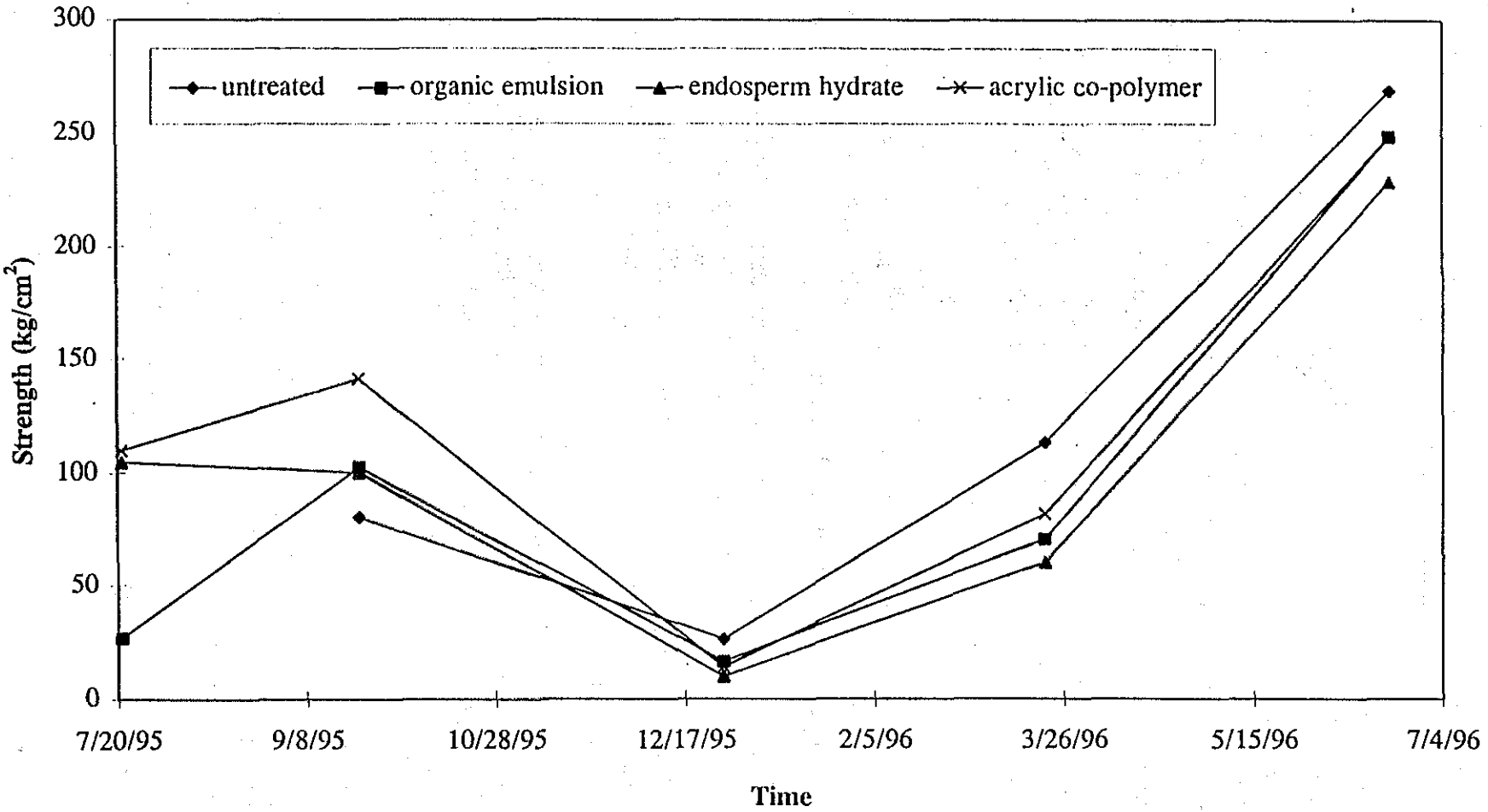

Figure 7-9 Changes in surface strength as a function of time.

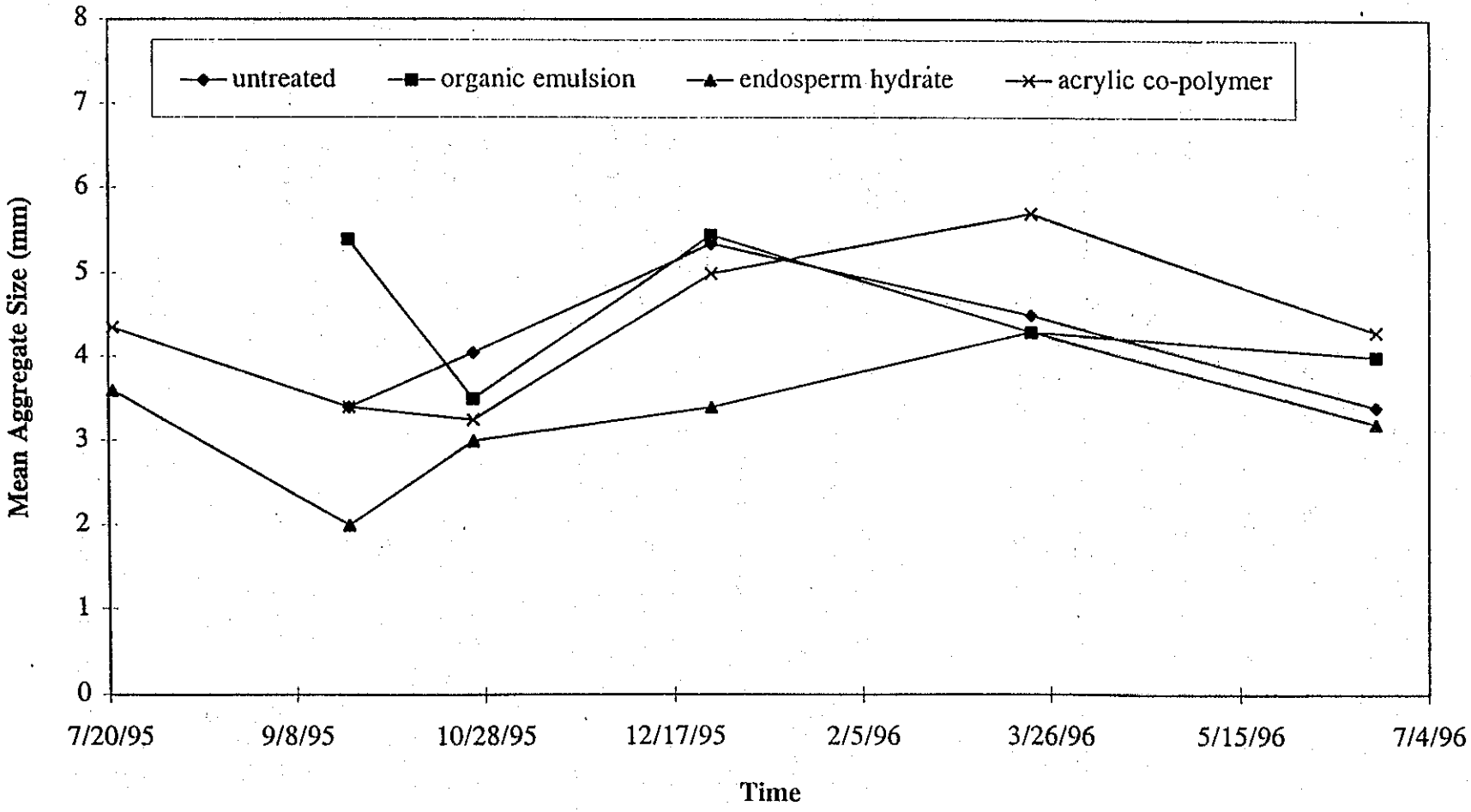

Figure 7-10 Changes in mean aggregate size as a function of time.

- Mean aggregate size increased through to December 1995. This most likely reflects the loss of fine particles in the winter months due to transport off the shoulders by run-off or a re-integration of fines into the sediment matrix under the loose surface material.

- In March 1996 the mean aggregate size of the acrylic co-polymer and organic emulsion sections continued to increase while the untreated section and endosperm hydrate sections decreased.

- The mean aggregate size of each test section decreased by June 1996. However, the decrease in the organic emulsion section was only marginal.

- The high standard deviations associated with the mean aggregate size calculations precludes any definitive statements being made on the changes in this property between test sections and through time.

7.3.6 Moisture Content

The moisture content of surface samples of the road shoulders during each site visit were below 1% by sample weight except for the December 1995 samples which averaged 7.8% (±3.0%). Moisture contents less than 1% have little effect on particle entrainment by wind on susceptible surfaces.

7.3.7 Surface Characteristics and PM_{10} Emissions

It is difficult to connect the surface characterization measurements with PM_{10} emissions from the shoulders. This is due to the similarity in emission rates for all surfaces estimated from the nephelometer data. However, some general observations can be made with within the context of the Fields Road results. These can be summarized as follows:

- The organic emulsion section has low levels of bulk silt content in July 1995. The bulk silt content lies between the values calculated for the petroleum emulsion and polymer mixture and the polymer emulsion mixture in July 1995. The PM_{10} control efficiency for organic emulsion at this time, based on the relationship shown in Figure 6-21, would be 100%. For the acrylic co-polymer and endosperm hydrate section the PM_{10} control efficiency would be approximately 92%. The bulk silt content values suggest that in July 1995 there is only a limited reservoir of potential PM_{10} particles available for ejection. However, the Fields Road model is based on PM_{10} emissions as a function of direct entrainment by vehicle tires and aerodynamic wake effects.

- Each of the Bellevue Road sections treated with suppressants experienced a rapid increase in bulk surface silt loading within the first few months of application as the surfaces broke down from repeated vehicle traffic and weathering. This

indicates there are also associated increases in the amount of potentially available PM_{10} particles.

- By June 1996 the bulk silt loadings were at levels that are comparable to those found on the high PM_{10} emitting sections on Fields Road.

- The organic emulsion section initially had low surface strength values and failure of the surface was by plastic deformation and surface loading of loose material and silt were very low. Within a few months the strength had increased, but it was obvious from observations of the surface that brittle failure was becoming dominant and there was an increase in loose surface material accompanying the increase in strength. The loss of pliability seems to explain the rapid decomposition of the organic emulsion crust.

- The surface characterization measurements showed that the shoulder suppressants quickly lost their effectiveness to bind the surface and did not prevent the build-up of silt sized particles that are the reservoir of PM_{10} sized particles.

8.0 IMPLICATIONS FOR PM MONITORING AND ATTAINMENT

8.1 Emissions Inventory

PM_{10} emission rate estimates derived in previous measurements are summarized in Table 2-6 and Section 6.2.4. Because few studies report size-segregated data yielding PM_{10} estimates, comparison data are quite limited. As stated in Section 6.2.4, emissions estimates that were derived for silt loadings similar to those found in this Demonstration Study agree with the new findings reported here, to within a factor of about two.

Table 8-1 also compares the Fields Road untreated section PM_{10} emission rate estimates to those calculated by the U.S. EPA's AP-42 empirical equation (Section 6.2.5). As suggested by the previous discussion, Table 8-1 shows that the average measured emissions rates usually exceed those calculated by AP-42. The ratio of the measured to the calculated rates varies from about 1 to about 3.5, with an average value of about 2.5. The third intensive results provide the closest comparisons, corresponding to the decreased emissions noted in Section 6 (Figure 6-2). (There is no clear explanation for this decrease, based on the surface measurements on the untreated section, hence the decreased emission rate may indicate natural variation rather than an unexplained data trend.)

Table 8-1 also shows that both the calculated and the measured emission rates increase with vehicle speed, as AP-42 indicates. However, the average measured data do not show the dependence on "Percent Silt" that is predicted by AP-42.

8.2 Zone of Influence and Sampler Siting

The "Zone of Influence" of an emissions source is a useful concept for: 1) estimating the impact of a given source on near and distant receptors; 2) estimating the magnitude of the emissions required to raise PM_{10} concentrations by a given amount at a given receptor; and 3) choosing representative (non-biased) locations for samplers. The first application is operationally defined as estimating the distance from the source at which concentrations have fallen off to 10% of their near-source value. The second application is defined as the distance at which a receptor sampler measures 1 $\mu g/m^3$ resulting from the emissions. These definitions are source- and receptor-oriented, respectively. The 1 $\mu g/m^3$ level is close to the measurement uncertainty involved in this type of study; it is about the minimum concentration which can be detected in a superposition of PM_{10} contributions to ambient levels (Chow *et al.*, 1996).

Figure 8-1 presents a summary of downwind PM_{10} concentration data measured during the third intensive study on Fields Road. In order to better measure the downwind extent of the untreated test section's emissions, samplers were deployed at two meters above the surface, 15, 30, and 45 meters downwind (south) from the south edge of the road. The graph shows the "normalized" downwind values; it is their ratios to the near sampler (downwind tower) values which are plotted. The available data satisfactorily agree with an exponential fit, with a correlation coefficient of 0.9.

Table 8-1
Average Emission Rates versus AP-42 Estimated Emissions for the Untreated Section of Fields Road

Measurement Period	Percent Silt	Vehicle Speed (km/hr)	Vehicle weight (Mg)	Vehicle # wheels	Calculated AP-42 Rate (g/vkt)	Measured Emission Rate (g/vkt)	Ratio: Measured/Calculated Rates
First Intensive[a]	6.3	40	1.5	4	180	560	3.1
Second Intensive [b]	6.2	40	1.5	4	170	360	2.1
Third Intensive[c]	7	40	1.5	4	200	170	0.9
First Intensive[a]	6.3	55	1.5	4	240	750	3.1
Second Intensive [b]	6.2	55	1.5	4	240	840	3.5
Third Intensive[c]	7	55	1.5	4	270	520	1.9

[a] July 22-27, 1995
[b] October 17-22, 1995
[c] June 13-18, 1996

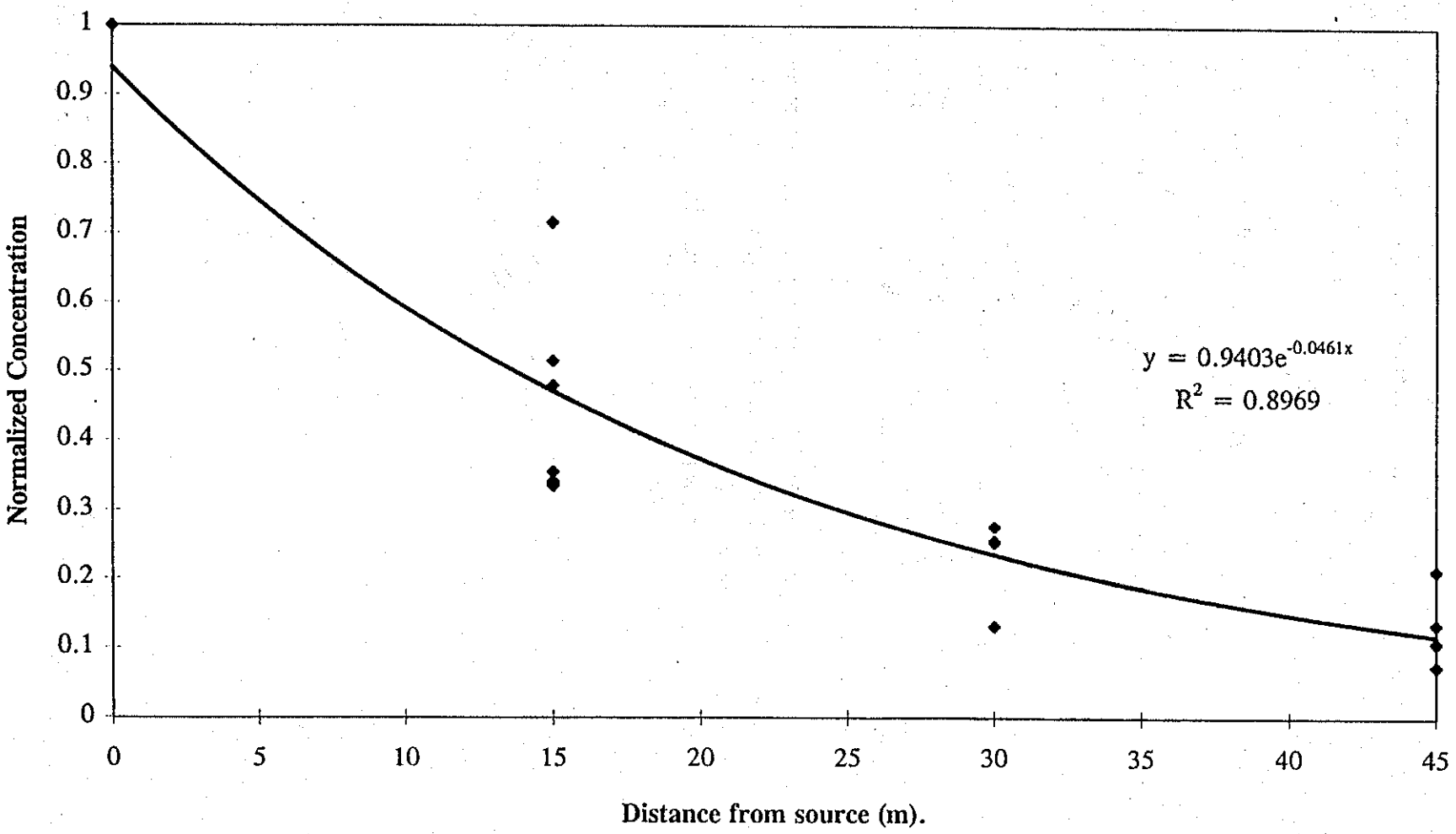

Figure 8-1 Downwind changes in normalized PM_{10} concentration at 2 m height.

Two physical reasons account for depletion in particle concentrations during dry-weather transport: 1) dispersion and dilution; 2) deposition. Mineral particles ten micrometers in diameter (PM_{10}) fall with a terminal velocity of less than one centimeter per second, in still air. Turbulent air flow complicates the situation, because deposition of particles very close to the ground surface or to vegetation may be enhanced, but at the same time upward vertical mixing is also enhanced. Generally, available plume models predict little or negligible deposition losses of PM_{10} particles over downwind distances of hundreds of meters, with wind speeds as low as were common during these measurements (less than 7 m/s). The remaining explanation for the results summarized in Figure 8-1 is that plume dilution is the predominant mechanism: concentrations fall off downwind as the emissions are mixed with cleaner air. This inference would also apply to other important constituents, like particulate nitrate, sulfate, and organics. These particulates are smaller than ten micrometers diameter, which makes deposition even less effective.

Figure 8-1 shows that the Fields Road untreated section emissions had fallen off to about 10% of their near-source value at about 45 meters, the farthest downwind sampler position in the third intensive study. Therefore, the "source-oriented" Zone of Influence is about 45 meters. Accounting for some variability and uncertainty, a reasonable operational statement is that the source-oriented 10% zone is about 50 meters, plus or minus 10 meters, downwind from the unpaved road.

The "receptor-oriented" Zone of Influence is easily derived by computing the distance at which the average near-source concentration has fallen off to 1 $\mu g/m^3$ at two meters height (roughly comparable to human inhalation height). The average, two-meter height concentration measured on the downwind tower during the third intensive was 410 $\mu g/m^3$, which determines that this PM_{10} source would, on average, contribute 1 $\mu g/m^3$ at a distance of about 130 meters (less than one-tenth of a mile).

The implications for unbiased sampler placement are: 1) for low wind speeds, the PM_{10} contributions of this type of source are less than uncertainties at distances exceeding about 150 meters (one-tenth of a mile); and 2) the contributions of this type of source, even with low winds, are underestimated by a factor of ten at a distance of about 50 meters (approximately 165 feet).

These findings are presented in the context of the third intensive study, and may not immediately apply to all other situations. For example, the downwind Zone of Influence is probably extended by greater wind speeds and by greater vertical mixing. PM_{10} concentrations observed in the San Joaquin Valley result from the merged contributions of many sources located at varying distances from receptors. Such "superposition" is assured by the relatively ineffective rate of PM_{10} deposition in dry conditions.

8.3 Control Measures

This Demonstration Study tested seven dust suppressant products over a period of one year, including an unusually wet winter. The three suppressants applied to the unpaved

shoulders of Bellevue Road did not significantly reduce the PM_{10} emissions measured in this Study. For a range of reasons and causes, those products were not efficient in this application. One suppressant applied to an unpaved section of Fields Road was not effective in reducing PM_{10} emissions, compared to an untreated section. Two suppressants did significantly reduce emissions, but the performance of one of these products had deteriorated extensively by the end of the Study. The remaining products were efficient at better than the 80% level at the end of the Study, proving that PM_{10} suppression in this application is an achievable goal.

The surface measure that best indicated suppressant performance was the bulk silt loading determined by the sweep method. While there is no direct, quantitative relationship that allows estimation of PM_{10} emission rates based on silt loadings, it is clear that this surface measure is a very important gauge of suppressant efficiency. Based on the data acquired in this Study, it appears that silt loadings in excess of 200 g/m^2 indicate that the suppressant is inefficient. Silt loadings less than 20 g/m^2 indicate suppressant efficiencies that probably exceed 90%. Good suppressant performance also appears to result from the mechanical behavior of the treated surface, as indicated by the surface strength measurements. Suppressants which form a strong but flexible surface layer are more efficient than those which form a brittle layer. A brittle layer quickly fractures and fragments, while a flexible layer can survive repeated vehicle usage.

Based on these measurements and observations, the following specifications are recommended, as a minimum, for the selection of efficient PM_{10} suppressant products for the San Joaquin Valley:

- the product should reduce silt loadings to 20 g/m^2 or less, and preserve this specification during the full range of weather conditions encountered;
- the product should establish and maintain a flexible surface layer not subject to brittle failure;
- the product should be impervious to leaching or washout by rain or snow.

9.0 SUMMARY, CONCLUSIONS AND RECOMMENDATIONS

This section summarizes the methodology and results of the dust suppression demonstration studies conducted during 1995 and 1996 in California's San Joaquin Valley.

9.1 Summary

A one-year study of unpaved road and unpaved shoulder PM_{10} emissions and suppressants was conducted on public roads located in Merced County in California's San Joaquin Valley. Commercially available dust suppressant products were applied to four unpaved road and three unpaved shoulder test sections on Fields Road and Bellevue Road, respectively. Each test location also included untreated sections for comparison. Suppressants applied to 500-meter test sections of Fields Road were: 1) a biocatalyst product; 2) a polymer emulsion mixture; 3) a petroleum emulsion and polymer mixture; and 4) non-hazardous crude-oil-containing material. Suppressants applied to 700-meter test sections of unpaved shoulders along Bellevue Road were: 1) an organic emulsion; 2) endosperm hydrate; and 3) an acrylic co-polymer.

For the unpaved road tests, PM_{10} was measured upwind and downwind of each test section. PM_{10} emission rates were estimated by a profile method including two overhead samplers to allow a more full characterization of dust plumes. Net PM_{10} emissions from suppressant test sections were obtained by subtracting the upwind-source profile from the downwind-source profile, and by combining the resulting PM_{10} mass concentrations with meteorological data. The net flux from a test section is the product of the profile concentrations, the lengths of test sections, and the perpendicular wind speeds. This flux multiplied by the length of the sampling period and divided by the vehicle-miles-traveled (VMT) during the test gives the PM_{10} emission rate. Tests were conducted right after suppressant application, three months later, and eleven months later to determine how dust suppression properties changed with time and use.

Soil surface measurements taken at six-week intervals determined how the mechanical properties of the treated surfaces changed after suppressant application. These measurements included: bulk loose surface material areal densities, silt (i.e., material in the less-than-75-micrometer size fraction), surface densities, percent silt content in surface material, aggregate size distributions and stability determinations, moisture content, and surface strengths.

The PM_{10} emissions were combined with detailed records of vehicle traffic in order to provide: 1) the emission rates as PM_{10} mass produced per vehicle-kilometer traveled for each of the suppressant test sections, and 2) the efficiencies of the different suppressants in reducing PM_{10} emissions.

For the unpaved shoulder study, a different approach was required because the dust plumes were much more localized and short-lived. In addition to upwind and downwind PM_{10} sampling, fast-response observations from light scattering and turbulence sensors were

used to characterize the dust suspension. The light scattering data combined with an estimated scattering coefficient indicate PM_{10} concentrations in the shoulder plumes. Surface measurements characterized changes in the mechanical properties of the shoulders. This approach gave: 1) two measures of PM_{10} emissions, one which summed all emissions over several hours, and one which responded to and measured each dust plume created by each passing vehicle; 2) a three-dimensional measurement of the turbulence caused by each passing vehicle, because this air motion initiates the dust plumes; and 3) quantification of the mechanical behavior of the suppressants.

9.2 Conclusions

Conclusions were drawn with respect to emissions rates from unpaved roads and shoulders, dust suppression effectiveness, surface properties as indicators of effectiveness, the zone of influence of road dust emissions, and costs to apply and maintain dust suppression.

9.2.1 Emission Rates

- Emission rates from the untreated and suppressant-treated unpaved road sections ranged from zero to 2.8 pounds of PM_{10} per mile (zero to 800 grams per kilometer) for a vehicle speed of 25 mph (40 km/h) and from zero to 5.0 pounds of PM_{10} per mile (1.4 kilograms per kilometer) for a vehicle speed of 35 mph (55 km/h). These are comparable to, and as variable as, emission rates measured in other studies.

- Emission rates from the untreated road sections were as much as 3.5 times those estimated by the EPA's AP-42 emission factor using the road characteristics measured in this study. The AP-42 gives reasonable estimates for PM_{10} emissions rates when silt contents are less than 10% and vehicle speeds exceed 55 km/hr.

- PM_{10} emission rates from unpaved shoulders are estimated to be 0.03 ± 0.015 pounds per mile (8 ± 4 grams per kilometer) for large vehicles (trucks, semis, vehicles with trailers) traveling from 50 to 60 miles per hour. The estimation of unpaved shoulder emission rates involved new and unique measurement methods.

9.2.2 Suppressant Effectiveness

- The polymer emulsion product established a durable and flexible surface coating on the unpaved road. It was an effective suppressant, even after vehicular use including about 100 vehicle passes per day during the intensive study periods, and the effects of an unusually wet winter. The effectiveness of the polymer emulsion exceeded 80%, on average, during the final measurement period, 11 months after application.

- The non-hazardous crude-oil-containing material was 93% effective after eight months' aging. This material did not undergo the full 11-month test period, but it endured the harshest weather between October 1995 and June 1996.

- The effectiveness of the petroleum emulsion/polymer mixture was 71% after three months, and 53% after 11 months. This product was very effective right after suppressant application. It survived winter weather but deteriorated significantly after 11 months.

- The biocatalyst product was only marginally efficient (33%) right after application, and it deteriorated rapidly even before winter weather occurred.

- None of the suppressants applied to the unpaved shoulders were effective for any appreciable period. These suppressants broke down quickly under the effects of ordinary vehicle traffic (such as daily mail deliveries to residences) and random shoulder traffic (such as temporary passenger car pullovers). It appeared that these activities caused major deterioration in suppressant efficiencies even without winter weather.

- Road shoulders are dynamic environments with respect to vehicle traffic. Suppressants must be robust to withstand the continual action of vehicle tires. Suppressants that are effective on unpaved roads would probably also be efficient on unpaved shoulders. Suppressants that perform well on surfaces without major activity may not withstand the wear and tear on unpaved shoulders.

9.2.3 Surface Properties

- The major surface properties that define low-emitting, well-suppressed surfaces are: 1) surface silt loading; and 2) the strength and flexibility of suppressant material as a surface layer or cover.

- Silt loading is the best indicator of suppressant efficiency. Silt loadings of less than 20 grams of loose silt per square meter of surface area (kg/m^2) are associated with efficiencies that exceed 90%. Silt loadings that exceed 200 g/m^2 are no different from untreated sections in terms of efficiency.

- Suppressants that create surface conditions that allow plastic deformation or resist brittle failure have an increased likelihood for long-term reduction efficiency for PM_{10} emissions on unpaved roads.

9.2.4 Zone of Influence

- The "Zone of Influence" is operationally defined from source- and receptor-oriented perspectives. From the source perspective, it is the distance from the emissions source at which concentrations have fallen off to 10% of their

near-source value; and from the receptor perspective, it is the distance at which a receptor sampler measures 1 $\mu g/m^3$ resulting from the emissions.

- Downwind data from the Fields Road untreated section show that emissions had fallen off to about 10% of their near-source value at 45 m, near the farthest downwind sampler position in the third intensive study. Therefore, the "source-oriented" Zone of Influence is ~50 m downwind from the unpaved road. The "receptor-oriented" Zone of Influence estimated from the June 1996 test data is 130 m, the distance at which this PM_{10} source would, on average, contribute 1 $\mu g/m^3$ to an ambient measurement. Plume dilution is the predominant mechanism for these "Zones of Influence" – concentrations fall off downwind as the emissions are mixed with cleaner air.

9.2.5 Costs of Suppressants

- Suppressant costs in 1995 ranged from $0.09 to $1.22 per square yard. For each ten feet of lane width, the material cost in one mile would be ~$600 for a suppressant costing $0.10 per square yard, and ~$6,000 for a suppressant costing $1.00 per square yard.

- Costs for the polymer emulsion mixture, the most effective suppressant for the entire measurement period, were $0.36 to $0.58 per square yard for a simple topical application, and $0.93 per square yard for a scarified application.

- Surface preparation and application costs vary widely from one product to another. Application and road preparation costs often exceed the cost of suppressant materials.

9.3 Recommendations

Several of the lessons learned in this study can be applied to future studies.

- Upwind/downwind sampling is costly and is impractical to apply for every suppressant. Surface silt content (kg/m^2 of particles <75 μm) might be an inexpensive surrogate for testing effectiveness, as it was shown to be related to emissions. Further research is necessary to develop methods to measure the actual PM_{10} component of sediment. This could lead to better estimates of PM_{10} emission rates and more cost-effective methods to evaluate suppressants.

- The products tested in this study do not represent all products on the market, especially newly-developed compounds. Additional testing of suppressant products is needed to evaluate the efficiencies and durabilities of a broader range of compounds.

- The measurements conducted during this study do not directly address the issue of aggregate gravel as a control measure.. Aggregates applied to unpaved surfaces

may increase dust and PM_{10} emissions rather than suppress them. This speculation should be addressed with further experiments. The expense of aggregate gravel is significant; application should be stopped if it increases PM_{10} emissions when used on certain unpaved surface types.

- Direct, continuous measurements of PM mass are preferable to the light scattering measurements used in this study to measure instantaneous dust emissions from unpaved shoulders. These measurement methods should have a response time of ~10 seconds. Fast-flow devices have been designed for unique, experimental applications, but are not generally available for PM_{10} sampling applications.

10.0 REFERENCES

Ahuja, M.S., Paskind, J., Houck, J.E. and Chow, J.C. (1989). Design of a Study for the Chemical and Size Characterization of Particulate Matter Emissions from Selected Sources in California. In *Transactions: Receptor Models in Air Resources Management*, J.G. Watson, Ed. Air & Waste Management Association, Pittsburgh, PA., pp 145-158.

Allen, J.R.L. (1985). Principles of Physical Sedimentology. London: Allen and Unwin, 272 p.

Anderson, R.S, M. Sorensen, and B.B. Willetts (1990). A Review of Recent Progress in Our Understanding of Aeolian Sediment Transport. Research Report No. 213, Dept. of Theoretical Statistics, Institute of Mathematics, University of Aarhus, Denmark.

Anspaugh, L.R., J.H. Shinn, P.L. Phelps, and N.C. Kennedy (1975). Resuspension and Redistribution of Plutonium in Soils. *Hlth. Phys.* **29**:571-582.

ASTM (1990a). Standard Test Method for Amount of Material in Soils Finer than No. 200. In *Annual Book of ASTM Standards*. Document D1140. American Society for Testing and Materials, Philadelphia, PA, pp. 193-194.

ASTM (1990b). Standard Test Method for Particle-Size Analysis of Soils. In *Annual Book of ASTM Standards*. Document D422. American Society for Testing and Materials, Philadelphia, PA, pp. 94-100.

Bagnold, R.A. (1937). The Transport of Sand by Wind . *Geog. J.*, **89**:409-438.

Bagnold, R.A. (1941). The Physics of Blown Sand and Desert Dunes. London: Methuen, pp. 1-241.

Barone, J.B., L.L. Ashbaugh, B.H. Kusko, and T.A. Cahill (1981). The Effect of Owens Dry Lake on Air Quality in the Owens Valley with Implications for the Mono Lake Area. ACS Symposium Series, No. 167, Atmospheric Aerosol: Source/Air Quality Relationships, **18**:327.

Beggs, T.W. (1985). User's Guide: Fugitive Dust Control Demonstration Studies. Prepared for U.S. Environmental Protection Agency, Cincinnati, OH, by JACA Corp., Fort Washington, PA.

Belly, P.Y. (1964). Sand Movement by Wind. U.S. Army Coastal Eng. Res. Center Tech. Mem. 1:1-38.

Bergeron, N.E., and A.D. Abrahams (1992). Estimating Shear Velocity and Roughness Length from Velocity Profiles. *Water Resources Research* **28**(8):2155-2158.

Best, J.L. (1993). On the Interactions between Turbulent Flow Structures, Sediment Transport, and Bedform Development: Some Considerations from Recent Experimental Research. In *Turbulence: Perspectives on Flow and Sediment Transport*, N.J. Clifford, J.R. French, and J. Hardisty, eds. Chichester: John Wiley & Sons, pp. 61-92.

Bisal, F., and J. Hsieh (1966). Influence of Moisture on Erodibility of Soil by Wind. *Soil Sci. Soc. Am. J.* **102**:143-146.

Braaten, D.A., R.H. Shaw, and K.T. Paw U (1993). Boundary-Layer Flow Structures Associated with Particle Reentrainment. *Boundary-Layer Meteorology* **65**:255-272.

Bradford, J.M., and R.B. Grosman (1982). In-situ Measurement of Near-Surface Soil Strength by the Fall-Cone Device. *Soil Sci. Soc. Am. J.* **46**:685-688.

Cahill, T.A. (1979). Ambient Aerosol Sampling with Stacked Filter Units. Federal Highway Admisistration, Office of Research and Development, Washington D.C., FHWA-RD-78-178.

California Air Resources Board (1991). Emission Inventory 1989. California Air Resources Board, Technical Support Division, Emission Inventory Branch, Sacramento, CA.

Caravacho, O.F., L.L. Ashbaugh, R.T. Matsumura, R.J. Southard, and R.G. Flocchini (1995). Measurement of PM_{10} Potential from Agricultural Soils Using a Dust Resuspension Chamber. In *Proceedings, International Conference on Air Pollution from Agricultural Operations*, Feb. 7-9, Kansas City, Missouri, pp. 87-92.

Chamberlin, A.C. (1967). Transport of Lycopodium Spores and Other Small Particles to Rough Surfaces. In *Proc. of the Royal Society of London, Ser. A*, pp. 45-70.

Chepil, W.S. (1942). Measurement of Wind Erosiveness by Dry Sieving Procedure. *Sci. Agr.* **23**:154-160.

Chepil, W.S. (1952). Improved Rotary Sieve for Measuring State and Stability of Dry Soil Structure. *Soil Sci. Amer. Proc.* **16**:113-117.

Chepil, W.S. (1956). Influence of Moisture on Erodibility of Soil by Wind. *Soil Sci. Soc. Proc.*, **20**:288-292.

Chepil, W.S., and N.P. Woodruff (1957). Sedimentary Characteristics of Dust Storms: Visibility and Dust Concentrations. *Amer. J. Sci.* **255**:104-114.

Chepil, W.S., and N.P. Woodruff (1963). The Physics of Wind Erosion and Its Control. *Advances in Agronomy* **15**:211-299.

Chow, J.C., J.G. Watson, R.T. Egami, C.A. Frazier, Z. Lu, A. Goodrich, and A. Bird (1990). Evaluation of Regenerative-Air Vacuum Street Sweeping on Geological Contributions to PM_{10}. *J. Air Waste Manage. Assoc.* **40**:1134-1142.

Chow, J.C., and J.G. Watson (1992). Fugitive Emissions Add to Air Pollution. *Environ. Protection* **3**(5):26-31.

Chow, J.C., J.G. Watson, D. Lowenthal, P. Solomon, K. Magliano, S. Ziman, and L.W. Richards (1992). PM_{10} Source Apportionment in California's San Joaquin Valley. *Atmos. Environ.* **26**(18):3335-3354.

Chow, J.C., J.G. Watson, D.H. Lowenthal, P.A. Solomon, K. Magliano, S.D. Ziman and L.W. Richards (1993). PM_{10} and $PM_{2.5}$ Compositions in California's San Joaquin Valley. *Aerosol Sci. Technol.*, **18**, 105-128.

Chow, J.C., E.M. Fujita, J.G. Watson, Z. Lu, D.R. Lawson and L.L. Ashbaugh (1994a). Evaluation of Filter-Based Aerosol Measurements during the 1987 Southern California Air Quality Study. *Environ. Mon. Assess.*, **30**:49-80.

Chow, J.C., J.G. Watson, E.M. Fujita, Z. Lu, and D.R. Lawson (1994b). Temporal and Spatial Variations of $PM_{2.5}$ and PM_{10} Aerosol in the Southern California Air Quality Study. *Atmos. Environ*, **28**, 2061-2080.

Chow, J.C., J.G. Watson, J.E. Houck, L.C. Pritchett, C.F. Rogers, C.A. Frazier, R.T. Egami, and B.M. Ball (1994c). A Laboratory Resuspension Chamber to Measure Fugitive Dust Size Distributions and Chemical Compositions. *Atmos. Environ.*, **28**(21)3463-3381.

Chow, J.C., J.G. Watson, D.H. Lowenthal, and R.J. Countess (1996a). Sources and Chemistry of PM_{10} Aerosol in Santa Barbara County, CA. *Atmos. Environ.* **30**(9):1489-1499.

Chow, J.C., J.G. Watson, Z. Lu, D.H. Lowenthal, C.A. Frazier, P.A. Solomon, R.H. Thuillier, and K. Magliano (1996b). Descriptive Analysis of $PM_{2.5}$ and PM_{10} at Regionally Representative Locations during SJVAQS/AUSPEX. *Atmos. Environ.* **30**(12):2079-2112.

Chow, J.C., and J.G. Watson (1997). Imperial Valley/Mexicali Cross Border PM_{10} Transport Study. Final Report. DRI Document No. 8623.2F. Prepared for U.S. Environmental Protection Agency, Region IX, San Francisco, CA, by Desert Research Institute, Reno, NV.

Chow, J.C., J.G. Watson, M.C. Green, R.T. Egami, D.H. Lowenthal, J.A. Gillies, C.F. Rogers, D. DuBois, C.L. Frazier, J. Derby, D.L. Freeman, Y. Mi, and T. Minor, (1997). Fugitive Dust and Other Source Contributions to PM_{10} in Nevada's Las Vegas Valley. DRI Document No. 4039.1F, prepared for Clark County Department of Comprehensive Planning, Las Vegas, NV, by Desert Research Institute, Reno, NV.

Clark County Health District APCD (1981). 1980 Annual Report on Status of Air Pollution Control in the Las Vegas Valley. Clark County Health District, Air Pollution Control Division, Las Vegas, NV.

Clifford, N.J., and J.R. French (1993). Monitoring and Modeling Turbulent Flow: Historical and Contemporary Perspectives. In *Turbulence: Perspectives on Flow and Sediment Transport*, N.J. Clifford, J.R. French, and J. Hardisty, eds. Chichester: John Wiley & Sons, pp. 93-120.

Corn, M., and F. Stein (1965). Re-entrainment of Particles from a Plane Surface. *Am. Ind. Hyg. Ass. J.* **26**:325-336.

Cowherd, C., G.E. Muleski, and J.S. Kinsey (1988). Control of Open Fugitive Dust Sources, Final Report. Prepared for the U.S. Environmental Protection Agency, Research Triangle Park, NC, by Midwest Research Institute, Kansas City, MO.

Cowherd, C., P. Englehart, G.E. Muleski, J.S. Kinsey, and K.D. Rosbury (1990). Control of Fugitive and Hazardous Dusts. Noyes Data Corp., Park Ridge, NJ, 471 p.

Cuscino, T., Jr., G.E. Muleski, and C. Cowherd (1983a). Determination of the Decay in Control Efficiency of Chemical Dust Suppressants. In *Proceedings-Symposium on Iron and Steel Pollution Abatement Technology for 1982*. U.S. Environmental Protection Agency, Research Triangle Park, NC.

Cuscino, T., Jr., G.E. Muleski, and C. Cowherd (1983b). *Iron and Steel Plant Open Source Fugitive Emission Control Evaluation*. EPA-600/2-83-110, U.S. Environmental Protection Agency, Research Triangle Park, NC, October 1983.

Davies, C.N. (1966). *Aerosol Science*. London: Academic Press, p. 468.

Eldred, R.A. (1988). IMPROVE Sampler Manual Version 2, Air Quality Group, Crocker Nuclear Lab, University of California, Davis, CA.

Eldred, R.A., T.A. Cahill, M. Pitchford, and W.C. Malm (1988). IMPROVE – A New Remote Area Particulate Monitoring System or Visibility Studies. Paper No. 88-54.3, presented at the Air Pollution Control Association 81st Annual Meeting, Dallas, TX, 1988.

ETC (1981). A Demonstration of Fugitive Dust Control Effectiveness on Selected Open Dust Sources in South Buffalo, NY. Report prepared for Erie County Department of Environment and Planning by Energy Technology Consultants, Inc.

Federal Register (1987a). Revisions to the National Ambient Air Quality Standards for Particulate Matter: 40 CFR Parts 51 and 52. *Federal Register*, **52**, 24634, 1 July 1987.

Federal Register (1987b). Regulations for Implementing Revised Particulate Matter Standards: 40 CFR Parts 51 and 52. *Federal Register*, **52**, 24672, 1 July 1987.

Federal Register (1987c). Air Programs: Particulate Matter (PM_{10}) Fugitive Dust Policy: 40 CFR Parts 50 and 52. *Federal Register*, **52**, 24716, 1 July 1987.

Federal Register (1987d). Ambient Air Monitoring Reference and Equivalent Methods: 40 CFR Part 53. *Federal Register*, **52**, 24724, 1 July 1987.

Federal Register (1987e). Ambient Air Quality Surveillance for Particulate Matter: 40 CFR Part 58. *Federal Register*, **52**, 24736, 1 July 1987.

Federal Register (1987f). Reference Method for the Determination of Particle Matter as PM_{10} in the Atmosphere. *Federal Register*, **52**, 24664, 1 July 1987.

Federal Register (1991). Designations and Classifications for Initial PM_{10} Nonattainment Areas: 40 CFR Part 81. *Federal Register*, **56**, 11101.

Federal Register (1993). Reclassification of Moderate PM_{10} Nonattainment Areas to Serious Areas: 40 CFR Part 81. *Federal Register*, **58**, 3334, 8 January 1993.

Federal Register (1994). Designations of Areas for Air Quality Planning Purposes: 40 CFR Part 81. *Federal Register*, **58**, 67334, 20 January 1994.

Federal Register (1996). Proposed Requirements for Designation of Reference and Equivalent Methods for $PM_{2.5}$ and Ambient Air Quality Surveillance for Particulate Matter – Proposed Revisions to 40 CFR Parts 53 and 58. U.S. Environmental Protection Agency, Research Triangle Park, NC.

Feeney, P.J., T.A. Cahill, R.G. Flocchini, R.A. Eldred, D.J. Shadoan, and T. Dunn (1975). Effect of Roadbed Configuration on Traffic Derived Aerosols. *JAPCA* **25**:1145.

Flocchini, R.G., T.A. Cahill, R.T. Matsamura, O. Carcacho, and Z.-Q. Lu (1994). Evaluation of the Emissions of PM_{10} Particulates from Unpaved Roads in the San Joaquin Valley. Final report prepared for the San Joaquin Valley Unified Air Pollution Control District, U. S. EPA, and California Air Resources Board, April, 1994, 61 p.

Flocchini, R.G., T.A. Cahill, M.L. Pitchford, R.A. Eldred, P.J. Feeney, and L.L. Ashbaugh (1981). Characterization of Particles in the Arid West. *Atmos. Environ.* **15**:2017.

Folk, R.L. (1980). Petrology of Sedimentary Rocks. Austin, TX: Hemphill Publishing Co., p. 184.

Frankel R. (1993). A Review of Methods for Measuring Fugitive PM_{10} Emission Rates. EPA/454-R-93-037. U.S. Environmental Protection Agency, Office of Air Quality Planning and Standards, Research Triangle Park, NC, November, 1993.

Fryrear, D.W., J.B. Xiao, and W. Chen (1995). Wind Erosion and Dust. In *Proceedings, International Conference on Air Pollution from Agricultural Operations*, Feb. 7-9, Kansas City, MO, pp. 57-64.

Garland, J.A. (1979). Resuspension of Particulate Material from Grass and Soil. AERE-R9452, HSMO, London.

Gillette, D.A. (1977). Fine Particulate Emissions Due to Wind Erosion. *Trans. Am. Soc. Agric. Eng.* **20**:980-987.

Gillette, D.A., and R. Passi (1988). Modeling Dust Emission Caused by Wind Erosion. *J. Geophys. Res.* **93**(D11):14233-14242.

Gillette, D.A., and P.H. Stockton (1989). The Effect of Non-Erodible Particles on Wind Erosion of Erodible Surfaces. *J. Geophys. Res.* **94**(D10):12885-12893.

Gillette, D.A., J. Adams, A. Endo, D. Smith, and R. Kihl (1980). Threshold Velocities for Input of Soil Particles into the Air by Desert Soils. *J. Geophys. Res.* **85**(C10):5621-5630.

Gillette, D.A., J. Adams, D. Muhs, and R. Kihl (1982). Threshold Friction Velocities and Rupture Moduli for Crusted Desert Soils for the Input of Soil Particles into the Air. *J. Geophys. Res.* **87**(C11):9003-9015.

Gillies, J.A. (1994). A Wind Tunnel Study of the Relationships Between Complex Surface Roughness Form, Flow Geometry and Shearing Stress. Ph.D. Thesis, University of Guelph, 231 p.

Gomes, L., G. Bergametti, G. Coude-Gaussen, and P. Rognon (1990). Submicron Desert Dusts: A Sandblasting Process. *J. Geophys. Res.* **95**:13927-13935.

Goosens, D. (1985). The Granulometric Characteristics of a Slowly-Moving Dust Cloud. *Earth Surface Processes and Landforms* **10**,353-362.

Grau, R.H. (1993). Evaluation of Methods for Controlling Dust. Technical Report GL-93-25. U.S. Army Corps of Engineers. September, 1993.

Greeley, R., and J.D. Iversen (1985). Wind as a Geological Process. Cambridge: Cambridge University Press, p. 333.

Gregory, P.H (1961). The Microbiology of the Atmosphere. London: Leonard Hill.

Hagen, L.J., N. Mirzamostafa, and A. Hawkins (1995). PM_{10} Generation by Wind Erosion. In *Proceedings, International Conference on Air Pollution from Agricultural Operations*, Feb. 7-9, Kansas City, Missouri, pp. 79-85.

Haun, J.A. (1995). Estimation of PM_{10} from Vacant Lands in the Las Vegas Valley. Unpublished M.S. Eng. thesis, University of Nevada, Las Vegas.

Hewitt, T.R. (1981). The Effectiveness of Street Sweeping for Reducing Particulate Matter Background Concentration. Sirrine Environmental Consultants, Research Triangle Park, NC.

Hinds, W.C. (1986). Aerosol Technology. New York: Wiley Interscience.

Houck, J.E., Chow, J.C. and Ahuja, M.S. (1989). The Chemical and Size Characterization of Particulate Material Originating from Geological Sources in California. In *Transactions, Receptor Models in Air Resources Management*, J.G. Watson, Ed.. Air & Waste Management Association, Pittsburgh, PA, pp 322-333.

Houck, J.E., Goulet, J.M., Chow, J.C., Watson, J.G. and Pritchett, L.C. (1990). Chemical Characterization of Emission Sources Contributing to Light Extinction. In *Transactions, Visibility and Fine Particles*, C.V. Mathai, Ed. Air & Waste Management Association, Pittsburgh, PA, pp 437-446.

John, W., D.N. Fritter, and W. Winklmayer (1991). Resuspension Induced by Impacting Particles. *J. Aerosol Sci.* 22(6):723-736.

Kinsey, J.S., and A.J. Jirik (1982). Study of Construction Related Dust Control. Report prepared for Minnesota Pollution Control Agency, Roseville, MN, December, 1982.

Kinsey, J.S., and C. Cowherd, Jr. (1992). Fugitive Emissions. In *Air Pollution Engineering Manual*, A.J. Buonicore and W.T. Davis, eds. New York: Van Nostrand Reinhold, pp. 133-146.

Lancaster, N.J., and W.G. Nickling (1993). Aeolian Sediment Transport. In *Geomorphology of Desert Environments*, A. Abrahams and A. J. Parsons, eds., Chapman and Hall.

Lehrsch, G.A, and P.M. Jolley (1992). Temporal Changes in Wet Aggregate Stability. In *Transactions, ASAE*, 35(2):493.

Ley, T.W. (1994). An In-Depth Look at Soil Water Monitoring and Measurement Tools. *Irrigation Journal* 44:8-20.

Linsley, G.S. (1978). Resuspension of the Transuranium Elements - A Review of Existing Data. NRPB-R75, HSMO, London.

Logie, M. (1982). Influence of Roughness Elements and Soil Moisture of Sand to Wind Erosion. *Catena Supp.* 1:161-173.

Malcom, L.P., and M.R. Raupach (1991). Measurements in an Air Settling Tube of the Terminal Velocity Distribution of Soil Material. *J. Geophys. Res.* 96(D8):15275-15286.

Marshall, J.K. (1971). Drag Measurements in Roughness Arrays of Varying Density and Distribution. *Agr. Meteorol.* 8:269-292.

Mathai, C.V., J.G. Watson, F. Rogers, J.C. Chow, I. Tombach, J.O. Zwicker, T. Cahill, P. Feeney, R. Eldred, M. Pitchford, and P.K. Mueller (1990). Intercomparison of Ambient Aerosol Samplers Used in Western Visibility and Air Quality Studies. *Environ. Sci. Technol.* **24**:1090-1099.

Mie, G. (1908). Beitrage zur optik truber medien, speziell kolloidaler metallosungen. *Ann. Physik* **25**:377-445.

Mitra, A., C. Claiborn, B. L. Lamb and H. Westberg (1993). Measurement and Source Apportionment of PM_{10} Roadway Emissions. For Washington State Transportation Commission and U.S. Department of Transportation, Federal Highway Administration, February, 1993.

Mollinger, A.M., F.T.M. Nieuwstadt, and B. Scarlett (1993). Model Experiments of the Resuspension Caused by Road Traffic. *Aerosol Sci. Technol.* **19**(3):330-338.

Mueller, P.K, and J.G. Watson (1981). The SURE Measurements. Presented at 74th Annual Meeting Air Pollution Control Association, Pittsburgh, PA.

Muleski, G.E., and C. Cowherd (1987). Evaluation of the Effectiveness of Chemical Dust Suppressants on Unpaved Roads. Document # EPA-600/2-87-102. Air and Energy Engineering Research Laboratory, U.S. Environmental Protection Agency, Research Triangle Park, NC.

Muleski, G., and K. Stevens (1992). PM_{10} Emissions from Public Unpaved Roads in Rural Arizona. In *Transactions, PM_{10} Standards and Nontraditional Particulate Source Controls.*, J.C. Chow and D.M. Ono, eds. Air and Waste Management Association, Pittsburgh, PA, pp. 324-334.

Nicholson, K.W. (1993). Wind Tunnel Experiments on the Resuspension of Particulate Material. *Atmos. Environ.* 27A(2):181-188.

Nicholson, K.W., J.R. Branson, P. Geiss, and R.J Cannell (1989). The Effects of Vehicle Activity on Particle Resuspension. *J. Aerosol. Sci.* **20**:1425-1428.

Nicholson, K.W. and J.R. Branson (1990). Factors Affecting Resuspension. In *Highway Pollution: Proceedings of the Third International Symposium*, Munich, West Germany, R.S. Hamilton, D.M. Revitt, and R.M. Harrison, eds. *Road Traffic*, **93**:349-358.

Nickling, W.G. (1978). Aeolian Sediment Transport during Dust Storms: Slims River Valley, Yukon Territory, Canada. *Can. J. Earth Sci.* **15**:1069-1084.

Nickling, W.G., and J.A. Gillies (1993). Dust Emission and Transport in Mali, West Africa. *Sedimentology* **40**:859-868.

Patterson, E.M., and D.A. Gillette (1977). Measurements of Visibility vs Mass-Concentration for Airborne Soil Particles. *Atmos. Environ.* **11**:193-196.

Pilat, M.J., D.S. Ensor, and J.C. Bosch (1970). Source Test Cascade Impactor. *Atmos. Environ.* **4**:671.

Pinnick, R.G., G. Fernandez, B.D. Hinds, C.W. Bruce, R.W. Schaefer, and J.D. Pendelton (1985). Dust Generated by Vehicular Traffic on Unpaved Roadways: Sizes and Infrared Extinction Characteristics. *Aerosol Sci. Technol.* **4**:99-121.

Raabe, O.G., D.A. Braaten, R.L. Axelbaum, S.V. Teague, and T.A. Cahill (1988). Calibration Studies of the DRUM Impactor. *J. Aerosol Sci.*, **19**(2):183.

Rau, K.N., R. Narashima, and M.A.B. Naryanan (1971). Bursting in a Turbulent Boundary Layer. *J. of Fluid Mechanics* **80**:401-430.

Raupach, M.R. (1992). Drag and Drag Partition on Rough Surfaces. *Boundary-Layer Meteorology* **60**:375-395.

Raupach, M.R., R.A. Antonia, and S. Rajagopalan (1991). Rough-Wall Turbulent Boundary Layers. *Boundary-Layer Meteorology* **60**:375-395.

Record, F.A., and R.M. Bradway (1978). Philadelphia Particulate Study. EPA 68-02-2345. U.S. Environmental Protection Agency, Air Programs Branch, Philadelphia, PA, June 1978.

Reeks, M. W., J. Reed, and D. Hall (1985). The Long Term Suspension of Small Particles by a Turbulent Flow – Part III: Resuspension for Rough Surfaces. TPRD/B/0640/N85. CEGB Berkeley Nuclear Labs, Gloucestershire, U.K.

Reynolds, O. (1895). On the Dynamical Theory of Incompressible Viscous Fluids and the Determination of the Criterion. *Phil. Trans. R. Soc.* **186A**:123-164.

Roberts, J.W., H.A. Watters, C.A. Mangold, and A.T. Rossano (1975). Cost and Benefits of Road Dust Control in Seattle's Industrial Valley. *J. Air Poll. Cont. Assoc.* **25**(9):948-952.

Rosbury, K.D., and R.A. Zimmer (1983). Cost-Effectiveness of Dust Controls Used on Unpaved Haul Roads, Volume 1: Results, Analysis, and Conclusions. Report prepared under USBM Contract # J0218021 for the Bureau of Mines, United States Department of the Interior, by PEDCo Environmental, Inc.

Rosinski, J., G. Langer, C.T. Nagamoto, and J.S. Bogard (1976). Generation of Secondary Particles from Single Large Soil Particles upon Impact. In *Proc. of the Atmosphere-Surface Exchange of Particulate and Gaseous Pollutants*, Richland, WA, 4-6 Sept. 1974. Energy Res. and Dev. Admin. Symp. Ser. CONF740921. Nat. Tech. Inf. Serv., Springfield, VA, pp. 638-647.

Seton, Johnson, and Odell Inc. (1983). Portland Road Dust Demonstration Project. Final report prepared for Department of Public Works, City of Portland, OR.

Shinn, J.H., J.C. Kennedy, J.S. Koval, B.R. Clegg, and W.M. Porch (1976) Observations of Dust Flux in the Surface Boundary Layer for Steady and Nonsteady Cases. In *Proceedings, Atmosphere-Surface Exchange of Particulates and Gaseous Pollutants,* Richland, WA, 4-6 Sept. 1974. Energy Res. and Dev. Admin. Symp. Ser. CONF740921. Nat. Tech. Inf. Serv., Springfield, VA, pp. 625-637.

Stevens, K. (1991). Unpaved Road Emissions Impact. Final report prepared for Arizona Department of Environmental Quality by Midwest Research Institute, MRI Project No. 9525-L.

Svasek, T.N., and J.H. Terwindt (1974). Measurement of Sand Transport by Wind on a Natural Beach. *Sedimentology* **21**:311-322.

Thornthwaite, C.W. (1931). The Climates of North America According to a New Classification. *Geographical Review.* **21**:633-655.

Toogood, J.A. (1978). Relation of Aggregate Stability to Property of Alberta Soils. In *Modification of Soil Structure*, W.W. Emerson *et al.*, eds. New York: John Wiley & Sons.

U.S. Department of Agriculture (1960). Soil Classification, A Comprehensive System, 7th Approximation. USDA, Soil Survey Staff, Soil Conservation Service, 265 p.

U.S. Department of Agriculture (1962). Soil Survey, Merced Area California. USDA, Soil Conservation Service.

U.S. Department of Agriculture (1980). Soil Survey of Washoe County, Nevada, South Part. USDA, Soil Conservation Service.

U.S. Department of Commerce (1968). Climatic Atlas of the United States. U.S. Department of Commerce, Washington D.C.

U.S. Environmental Protection Agency (1981). Workbook: Demonstration Studies for Control of Nontraditional Particulate Sources. Contract No. 68-02-2535, Work Assignment No. 15. U.S. Environmental Protection Agency, Office of Air Quality Planning and Standards, Control Programs Operations Branch, March, 1981.

U.S. Environmental Protection Agency (1987). PM_{10} SIP Development Guidelines. EPA Document No. 450/2-86-001. U.S. Environmental Protection Agency, Research Triangle Park, NC.

U.S. Environmental Protection Agency (1988). Compilation of Air Pollutant Emission Factors. Volume I: Stationary Point and Area Sources. U.S. Environmental Protection Agency, Office of Air and Radiation, Office of Air Quality Planning and Standards, Research Triangle Park, NC.

U.S. Government Printing Office (1991). Clean Air Act Amendments of 1990. Conference Report to Accompany S. 1630, House of Representatives, Superintendent of Documents. U.S. Government Printing Office, Washington, D.C.

Watson, J.G., and J.C. Chow (1993). Ambient Air Sampling. Chapter 28 in *Aerosol Measurement: Principles, Techniques and Applications*, K. Willeke, ed. New York: Van Nostrand Reinhold, pp. 622-639.

Watson, J.G., J.C. Chow, J.J. Shah, and T. Pace (1983). The Effect of Sampling Inlets on the PM_{10} and PM_{15} to TSP Concentration Ratios. *JAPCA* **33**:114-119.

Watson, J.G., J.C. Chow, and C.V. Mathai (1989a). Receptor Models in Air Resources Management: A Summary of the APCA International Specialty Conference. *JAPCA* **39**:419-426.

Watson, J.G., P.J. Lioy, and P.K. Mueller (1989b). The Measurement Process: Precision, Accuracy and Validity. In *Air Sampling Instruments for Evaluation of Atmospheric Contaminants, 7th Ed.*, S.V. Hering, ed. American Conference of Governmental Industrial Hygeniests, Cincinnati, OH, pp. 51-57.

Weems, T. (1991). Survey of Moisture Measurement Instruments. *Irrigation Journal* **41**:12-16.

Wieringa, J. (1993). Representative Roughness Parameters for Homogeneous Terrain. *Boundary-Layer Meteorol.* **63**(4):323-364.

Williams, J.J. (1986) *Aeolian Entrainment Thresholds in a Developing Boundary Layer.* Unpubl. Ph.D. Thesis, Queen Mary and Westfield College, University of London, London, 524 p.

Zimmer, R, W. Reeser, and P. Cummins (1992). Evaluation of PM_{10} Emission Factors for Paved Streets. In *Transactions: PM_{10} Standards and Nontraditional Particulate Source Controls*, J.C. Chow and D. Ono, eds. Air & Waste Management Assoc., Pittsburgh, PA, pp. 311-323.

APPENDIX A

Data Base Structures
for the SJV Dust Demonstration Study

Table A-1
Data Base Structure for the SJV Dust Demonstration Study
Site Information File for Fields Road
(File: FRSITE.DBF)

Number of data records: 50
Date of last update: 10/01/96

Field	Field Name	Type	Width	Dec	Description
1	SITE	Character	11		Site identifier
2	SUPID	Character	10		Supplementary Identifier UR = Untreated Road COHEREX = CoherexPM Section SOILSEMENT = Soil Sement Section EMC = EMC^2 Section
3	SPN	Numeric	2		Sampler Position Number
4	LATD	Numeric	2		Degrees of North Latitude
5	LATM	Numeric	6	3	Minutes of North Latitutde
6	LOND	Numeric	3		Degrees of West Longitude
7	LONM	Numeric	6	3	Minutes of West Longitude
8	ELEV	Numeric	5	2	Elevation
9	DIST	Numeric	2		Duration

Table A-2
Data Base Structure for the SJV Dust Demonstration Study
Site Information File for Bellevue Road
(File: BRSITE.DBF)

Number of data records: 4
Date of last update: 10/01/96

Field	Field Name	Type	Width	Dec	Description
1	SITE	Character	11		Site identifier
2	SUPID	Character	10		Supplementary Identifier EN = Enduraseal US = Untreated Road HD = HydroShield DS = DSS-40
4	SLATD	Numeric	2		Start Degrees of North Latitude
5	SLATM	Numeric	6	3	Start Minutes of North Latitutde
6	SLOND	Numeric	3		Start Degrees of West Longitude
7	SLONM	Numeric	6	3	Start Minutes of West Longitude
8	ELATD	Numeric	2		End Degrees of North Latitude
9	ELATM	Numeric	6	3	End Minutes of North Latitutde
10	ELOND	Numeric	3		End Degrees of West Longitude
11	ELONM	Numeric	6	3	End Minutes of West Longitude

Table A-3
Data Base Structure for the SJV Dust Demonstration Study
Field Name Structure
(File: DDFLDNAM.DBF)

Number of data records: 55
Date of last update: 10/07/96

Field	Field Name	Type	Width	Dec	Description
1	FIELD_NAME	Character	10		Field Name
2	FIELD_TYPE	Character	1		Field Type
3	FIELD_LEN	Numeric	3		Field Length
4	FIELD_DEC	Numeric	3		Decimal Places in Field
5	EXPL	Character	60		Explanation of field
6	UNITS	Character	25		Units of measure
7	MEMO	Memo	10		Memo

Table A-4
Data Base Structure for the SJV Dust Demonstration Study
For Mass Concentration Samples During July 1995 Intensive
(File: AMB_POR1.DBF)

Number of data records: 348
Date of last update: 01/30/96

Field	Field Name	Type	Width	Dec	Description
1	SITE	Character	10		Site identifier
2	DATE	Date	8		Sampling date
3	SIZE	Character	3		Particle fraction: 2.5=$PM_{2.5}$ (0-2.5 μm) 10=PM_{10} (0-10 μm)
4	STRTHHMM	Character	4		Sample start time
5	STOPHHMM	Character	4		Sample stop time
6	TDURATION	Numeric	5	1	Sample duration (hours for portable sampling system)
7	TID	Character	10		Teflon filter ID
8	TFFLG	Character	5		Teflon filter flag
9	MSGF	Character	5		Gravimetry chemical analysis flags
10	TVOC	Numeric	10	4	Teflon filter volume, (m^3)
11	TVOU	Numeric	10	4	Teflon filter volume uncertainty, (m^3)
12	MSGC	Numeric	10	4	Mass by gravimetry, ($\mu g/m^3$)
13	MSGU	Numeric	10	4	Mass uncertainty, ($\mu g/m^3$)
14	SPSUMC	Numeric	10	4	Sum of measured species concentrations, ($\mu g/m^3$)
15	SPSUMU	Numeric	10	4	Sum of measured species uncertainty, ($\mu g/m^3$)
16	COMMENT	Memo	10		Comments

Table A-5
Data Base Structure for the SJV Dust Demonstration Study
For Mass Concentration Samples During October 1995 Intensive
(File: AMB_POR2.DBF)

Number of data records: 308
Date of last update: 02/16/96

Field	Field Name	Type	Width	Dec	Description
1	SITE	Character	10		Site identifier
2	DATE	Date	8		Sampling date
3	SIZE	Character	3		Particle fraction: 2.5=$PM_{2.5}$ (0-2.5 μm) 10=PM_{10} (0-10 μm)
4	STRTHHMM	Character	4		Sample start time
5	STOPHHMM	Character	4		Sample stop time
6	TDURATION	Numeric	5	1	Sample duration (hours for sampling system)
7	TID	Character	10		Teflon filter ID
8	TFFLG	Character	5		Teflon filter flag
9	MSGF	Character	5		Gravimetry chemical analysis flags
10	TVOC	Numeric	10	4	Teflon filter volume, (m^3)
11	TVOU	Numeric	10	4	Teflon filter volume uncertainty, (m^3)
12	MSGC	Numeric	10	4	Mass by gravimetry, ($\mu g/m^3$)
13	MSGU	Numeric	10	4	Mass uncertainty, ($\mu g/m^3$)
14	SPSUMC	Numeric	10	4	Sum of measured species concentrations, ($\mu g/m^3$)
15	SPSUMU	Numeric	10	4	Sum of measured species uncertainty, ($\mu g/m^3$)
16	COMMENT	Memo	10		Comments

Table A-6
Data Base Structure for the SJV Dust Demonstration Study
For Mass Concentration Samples During June 1996 Intensive
(File: AMB_POR3.DBF)

Number of data records: 586
Date of last update: 08/16/96

Field	Field Name	Type	Width	Dec	Description
1	SITE	Character	10		Site identifier
2	DATE	Date	8		Sampling date
3	SIZE	Character	3		Particle fraction: 2.5=$PM_{2.5}$ (0-2.5 μm) 10=PM_{10} (0-10 μm)
4	STRTHHMM	Character	4		Sample start time
5	STOPHHMM	Character	4		Sample stop time
6	TDURATION	Numeric	5	1	Teflon sample duration (hours for sampling system)
7	TID	Character	10		Teflon filter ID
8	TFFLG	Character	5		Teflon filter flag
9	MSGF	Character	5		Gravimetry chemical analysis flags
10	TVOC	Numeric	10	4	Teflon filter volume, (m^3)
11	TVOU	Numeric	10	4	Teflon filter volume uncertainty, (m^3)
12	MSGC	Numeric	10	4	Mass by gravimetry, ($\mu g/m^3$)
13	MSGU	Numeric	10	4	Mass uncertainty, ($\mu g/m^3$)
14	SPSUMC	Numeric	10	4	Sum of measured species concentrations, ($\mu g/m^3$)
15	SPSUMU	Numeric	10	4	Sum of measured species uncertainty, ($\mu g/m^3$)
16	COMMENT	Memo	10		Comments

Table A-7
Data Base Structure for the SJV Dust Demonstration Study
Meteorological Data Collected at the Bellevue Road Site During the Third Intensive
(File: FRMET.DBF)

Number of data records: 2738
Date of last update: 10/01/96

Field	Field Name	Type	Width	Dec	Description
1	SITE	Character	11		Site Identifier
2	YEAR	Numeric	4		Year
3	MONTH	Numeric	2		Month
4	DAY	Numeric	2		Day
5	JDAY	Numeric	3		Julian Day
6	HOUR	Numeric	4		Hour (hhmm)
7	WS10	Numeric	6	3	Wind Speed (m/s) at 10m
8	WD10	Numeric	7	3	Wind Direction (deg.) at 10m
9	WS125	Numeric	6	3	Wind Speed (m/s) at 1.25m
10	WD125	Numeric	7	3	Wind Direction (deg.) at 1.25m
11	WS5	Numeric	6	3	Wind Speed (m/s) at 5m
12	WS25	Numeric	7	3	Wind Speed (m/s) at 2.5m
13	TEMP	Numeric	6	3	Temperature (C)
14	RH	Numeric	6	3	Relative Humidity (%)

Table A-8
Data Base Structure for the SJV Dust Demonstration Study for Meteorological Data Collected at the Bellevue Road Site During the Third Intensive (File: BRMET3.DBF)

Number of data records: 181
Date of last update: 10/01/96

Field	Field Name	Type	Width	Dec	Description
1	DATE	Date	8		Date
2	TIME	Numeric	6		Time (hhmmss)
3	WSPD	Numeric	5	2	Wind Speed (m/s)
4	WDIR	Numeric	3		Wind Direction (Degrees)

Table A-9
Data Base Structure for the SJV Dust Demonstration Study for Co-located Nephelometer Data Collected at the Bellevue Road Site During the Third Intensive (File: BRCOLL3.DBF)

Number of data records: 20,047
Date of last update: 10/01/96

Field	Field Name	Type	Width	Dec	Description
1	DATE	Date	8		Date
2	TIME	Numeric	6		Time (hhmmss)
3	NEPH1	Numeric	7	3	Nephelometer 1 $((Mm)^{-1})$
4	NEPH2	Numeric	7	3	Nephelometer 2 $((Mm)^{-1})$
5	NEPH3	Numeric	7	3	Nephelometer 3 $((Mm)^{-1})$
6	NEPH4	Numeric	7	3	Nephelometer 4 $((Mm)^{-1})$
7	NEPH5	Numeric	7	3	Nephelometer 5 $((Mm)^{-1})$

Table A-10

Data Base Structure for the SJV Dust Demonstration Study for Non-Co-located Nephelometer and 2-Second-Average Sonic Anemometer Data Collected at the Bellevue Road Site During the Third Intensive

(File: BRNESON3.DBF)

Number of data records: 74,706

Date of last update: 10/01/96

Field	Field Name	Type	Width	Dec	Description
1	DATE	Date	8		Date
2	TIME	Numeric	6		Time (hhmmss)
3	NEPH1	Numeric	7	3	Nephelometer 1 ($(Mm)^{-1}$)
4	NEPH2	Numeric	7	3	Nephelometer 2 ($(Mm)^{-1}$)
5	NEPH3	Numeric	7	3	Nephelometer 3 ($(Mm)^{-1}$)
6	NEPH4	Numeric	7	3	Nephelometer 4 ($(Mm)^{-1}$)
7	NEPH5	Numeric	7	3	Nephelometer 5 ($(Mm)^{-1}$)
8	UWIND	Numeric	7	3	U-component of Vector Wind (m/s)
9	VWIND	Numeric	7	3	V-component of Vector Wind (m/s)
10	WWIND	Numeric	7	3	W-component of Vector Wind (m/s)
11	TEMP	Numeric	7	3	Temperature (C)

Table A-11
Data Base Structure for the SJV Dust Demonstration Study for
Consecutive Sonic Anemometer Data Collected at the Bellevue Road Site During the Third Intensive
(File: BRSONIC3.DBF)

Number of data records: 456,746
Date of last update: 10/01/96

Field	Field Name	Type	Width	Dec	Description
1	TIME	Numeric	6		Time (hhmmss)
2	UWIND	Numeric	7	3	U-component of Vector Wind (m/s)
3	VWIND	Numeric	7	3	V-component of Vector Wind (m/s)
4	WWIND	Numeric	7	3	W-component of Vector Wind (m/s)
5	TEMP	Numeric	7	3	Temperature (C)

Table A-12
Data Base Structure for the SJV Dust Demonstration Study for
Surface Strength Measurements
(File: DDSTRNG.DBF)

Number of data records: 114
Date of last update: 10/09/96

Field	Field Name	Type	Width	Dec	Description
1	SITEID	Character	11		Site Identifier
1	SUPID	Character	11		Supplementary Site Identifier
2	DATE	Date	8		Date
3	LOCATION	Character	3		Identifier for Transect Location S : Transect along South Side N : Transect along North Side S-1 : First Transect along South Side S-2 : Second Transect along South Side N-1 : First Transect along North Side N-2 : Second Transect along North Side
4	D000	Numeric	6	2	Surface strength (kg/cm^2) at distance of 0m along transect
5	D025	Numeric	6	2	Surface strength (kg/cm^2) at distance of 0.25m along transect
6	D050	Numeric	6	2	Surface strength (kg/cm^2) at distance of 0.50m along transect
7	D075	Numeric	6	2	Surface strength (kg/cm^2) at distance of 0.75m along transect
8	D100	Numeric	6	2	Surface strength (kg/cm^2) at distance of 1.00m along transect
9	D125	Numeric	6	2	Surface strength (kg/cm^2) at distance of 1.25m along transect
10	D150	Numeric	6	2	Surface strength (kg/cm^2) at distance of 1.50m along transect
11	D175	Numeric	6	2	Surface strength (kg/cm^2) at distance of 1.75m along transect
12	D200	Numeric	6	2	Surface strength (kg/cm^2) at distance of 2.00m along transect
13	D225	Numeric	6	2	Surface strength (kg/cm^2) at distance of 2.25m along transect
14	D250	Numeric	6	2	Surface strength (kg/cm^2) at distance of 2.50m along transect
15	D275	Numeric	6	2	Surface strength (kg/cm^2) at distance of 2.75m along transect
16	D300	Numeric	6	2	Surface strength (kg/cm^2) at distance of 3.00m along transect
17	D325	Numeric	6	2	Surface strength (kg/cm^2) at distance of 3.25m along transect
18	D350	Numeric	6	2	Surface strength (kg/cm^2) at distance of 3.50m along transect
19	D375	Numeric	6	2	Surface strength (kg/cm^2) at distance of 3.75m along transect
20	D400	Numeric	6	2	Surface strength (kg/cm^2) at distance of 4.00m along transect
21	D425	Numeric	6	2	Surface strength (kg/cm^2) at distance of 4.25m along transect
22	D450	Numeric	6	2	Surface strength (kg/cm^2) at distance of 4.50m along transect
23	D475	Numeric	6	2	Surface strength (kg/cm^2) at distance of 4.75m along transect
24	D500	Numeric	6	2	Surface strength (kg/cm^2) at distance of 5.00m along transect
25	D525	Numeric	6	2	Surface strength (kg/cm^2) at distance of 5.25m along transect
26	D550	Numeric	6	2	Surface strength (kg/cm^2) at distance of 5.50m along transect
27	D575	Numeric	6	2	Surface strength (kg/cm^2) at distance of 5.75m along transect
28	D600	Numeric	6	2	Surface strength (kg/cm^2) at distance of 6.00m along transect
29	D625	Numeric	6	2	Surface strength (kg/cm^2) at distance of 6.25m along transect

Table A-12 (continued)
Data Base Structure for the SJV Dust Demonstration Study for
Surface Strength Measurements
(File: DDSTRNG.DBF)

Number of data records: 114
Date of last update: 10/09/96

Field	Field Name	Type	Width	Dec	Description
30	D650	Numeric	6	2	Surface strength (kg/cm^2) at distance of 6.50m along transect
31	D675	Numeric	6	2	Surface strength (kg/cm^2) at distance of 6.75m along transect
32	D700	Numeric	6	2	Surface strength (kg/cm^2) at distance of 7.00m along transect
33	D725	Numeric	6	2	Surface strength (kg/cm^2) at distance of 7.25m along transect
34	D750	Numeric	6	2	Surface strength (kg/cm^2) at distance of 7.50m along transect
35	D775	Numeric	6	2	Surface strength (kg/cm^2) at distance of 7.75m along transect
36	D800	Numeric	6	2	Surface strength (kg/cm^2) at distance of 8.00m along transect
37	D825	Numeric	6	2	Surface strength (kg/cm^2) at distance of 8.25m along transect
38	D850	Numeric	6	2	Surface strength (kg/cm^2) at distance of 8.50m along transect
39	D875	Numeric	6	2	Surface strength (kg/cm^2) at distance of 8.75m along transect
40	D900	Numeric	6	2	Surface strength (kg/cm^2) at distance of 9.00m along transect
41	AVG	Numeric	6	2	Average surface strength (kg/cm^2)
42	STD	Numeric	6	2	Standard deviation of surface strength (kg/cm^2)
43	MIN	Numeric	6	2	Minimum surface strength (kg/cm^2)
44	MAX	Numeric	6	2	Maximum surface strength (kg/cm^2)

Table A-13
Data Base Structure for the SJV Dust Demonstration Study for
Surface Characterization Data
(File: DDSURF.DBF)

Number of data records: 57
Date of last update: 10/09/96

Field	Field Name	Type	Width	Dec	Description
1	SITEID	Character	11		Site Identifier
2	SUPID	Character	11		Supplementary Site Identifier
3	SID	Character	4		Sample Identifier
4	SAMPNO	Numeric	2		Sample Number
5	DATE	Date	8		Date
6	MCPCT	Numeric	7	3	Moisture Content (%)
7	BULK	Numeric	7	3	Bulk (kg/m^2)
8	SILTPCT	Numeric	5	1	Silt (%)
9	SILT	Numeric	8	4	Silt (kg/m^2)
10	AVGAG	Numeric	5	1	Average Aggregate Particle Size (mm)
11	STD	Numeric	5	1	Standard Deviation of Particle Size (mm)
12	STRAG	Numeric	5	1	Aggregate Strength (%)

Table A-14
Data Base Structure for the SJV Dust Demonstration Study for Surface Samples Collected Using Vacuum Method
(File: DDVAC.DBF)

Number of data records: 89
Date of last update: 10/09/96

Field	Field Name	Type	Width	Dec	Description
1	SITEID	Character	11		Site Identifier
2	SUPID	Character	11		Supplementary Site Identifier
3	SID	Character	4		Sample Identifier
4	SAMPNO	Numeric	2		Sample Number
5	DATE	Date	8		Date
6	BULK	Numeric	7	3	Bulk (kg/m^2)
7	SILTPCT	Numeric	5	1	Silt (%)
8	SILT	Numeric	8	4	Silt (kg/m^2)

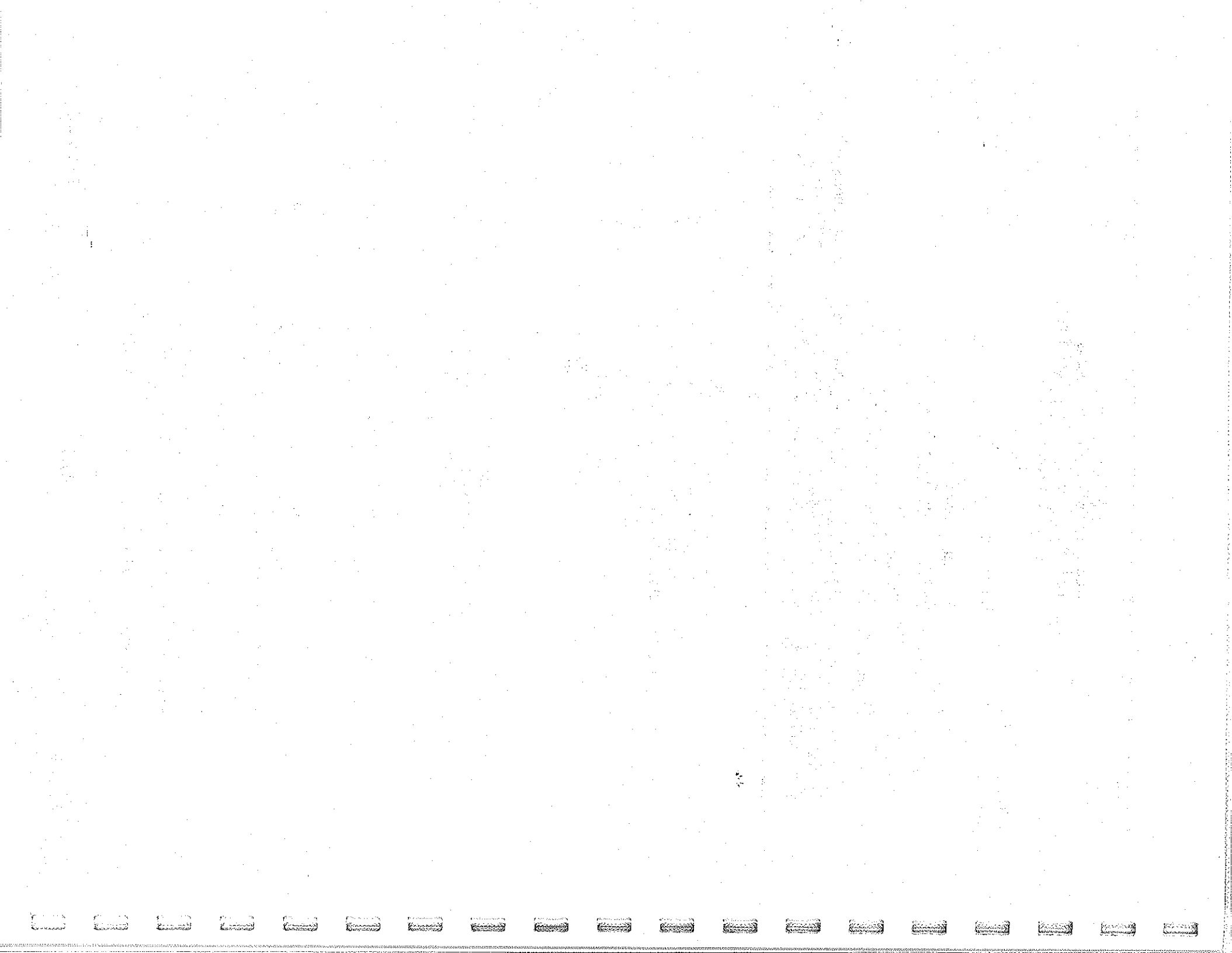

APPENDIX B

DRI Surface Characterization
Standard Operating Procedures

APPENDIX B

Surface Characterization Procedures

B.1 Aggregate Size Analysis

1) The sieves to be used in this procedure are 6.3 mm, 4 mm, 2 mm, 1 mm, 0.5 mm, 0.25 mm, and a pan.

2) Clean the sieves with compressed air and/or a soft brush.

3) Weigh each sieve and pan and record values.

4) Nest the sieves and pan in decreasing order with the pan on the bottom.

5) Weigh the sample to be analyzed (to 0.1g).

6) Dump the sample into the top sieve. Cover with the lid.

7) Rotate the covered sieve/pan unit by hand using broad sweeping arm motions in the horizontal plane. Complete 20 rotations at a speed just necessary to achieve some relative horizontal motion between the sieve and the particles.

8) Weigh each sieve and its contents and record the weight. Check the zero before every weighing.

9) After recording each weight the sediment in each sieve can be placed back into the same bag.

B.2 Silt Analysis Procedures

1) The sieves to be used in this procedure are 6.3 mm, 4.25 mm, 1.0 mm, 0.3 mm, 0.149 mm, 0.074 mm and a pan.

2) Clean the sieves with compressed air and/or a soft brush.

3) Weigh each sieve and pan and record values.

4) Nest the sieves and pan in decreasing order with the pan on the bottom.

5) Weigh the sample to be analyzed (to 0.1g)

6) Dump the sample into the top sieve. Cover with the lid and clamp the sieve nest into the shaker.

7) Turn on the shaker and run for 20 minutes. Remove sieve nest and then remove the pan and weigh the contents (leave in the pan), record the weight.

8) Replace pan and sieve for an additional 10 minutes. Remove sieve nest and then remove the pan and weigh the contents (leave in the pan). When the differences between two successive pan samples weighings (where the tare weight of the pan has been subtracted) is less than 3.0%, the sieving is complete.

9) Weigh each sieve and its contents and record the weight. Check the zero before every weighing.

10) After recording each weight the sediment in each sieve can be placed back into the same bag.

B.3 Moisture Content Analysis

1) Preheat the oven to approximately 110 °C. Record oven temperature.

2) Tare the aluminum foil weighing dishes. Record the tare weights.

3) Record the make , capacity, smallest division, and accuracy of the balance.

4) Place the sample for moisture content determination into a tare weighing dish. Zero the balance. Weigh the sample plus container. Record the mass.

5) Place the sample in the oven. and dry overnight.

6) Remove the sample container and weigh immediately.

7) Calculate the moisture content as the initial weight of the sample and container minus the oven dried weight of the sample and container divided by the initial weight of the initial sample.

B.4 Aggregate Stability

1) Measure out approximately 5 grams of sample of 1 mm size particles obtained from the samples that have been "soft-sieved" (see aggregate analysis SOP) into a tared weighing dish.

2) Record the weight to the nearest 0.001 grams

3) Place the sediment in the 1 mm sieve, place the pan below the 1 mm sieve, place the lid on the 1 mm sieve.

4) Shake the nested sieve/pan for one (1) minute.

5) Remove the sediment (gently sweep the remaining grains into a weighing dish) from the 1 mm sieve, weigh the sediment to the nearest 0.001 g. Record the weight.

6) After weighing, replace the grains into the 1 mm sieve.

7) Re-assemble the sieve, pan and lid.

8) Shake the nested sieve/pan for four (4) more minutes.

9) Remove the sediment (gently sweep the remaining grains into a weighing dish) from the 1 mm sieve, weigh the sediment to the nearest 0.001 g. Record the weight.

10) Aggregate stability is expressed as the percent change between the mass of 1 mm aggregates remaining after 1 minute and that left after the additional 4 minutes of shaking.

B.5 Bulk Surface Loading Determination, Sweep Method

1) Lay a tape measure across the width of the road or shoulder.

2) Using a standard dust pan and fine bristled brush sweep up the loose surface sediment along the transect defined by the tape measure. Note the length and width (the width of the dust pan)of the sampling area. Empty the contents of the dust pan into a zip-lock bag as is necessary, use more than one bag if sample volume is large. Label the samples bags with date, site ID and area sampled.

3) Try to avoid handling the sample too much to minimize aggregate breakdown

4) Return the sample to the lab.

5) Weigh the sample, subtract the weight of the bag.

6) Express the surface loading of loose material in terms of mass per unit area.

B.6 Bulk Surface Loading Determination, Vacuum Method

1) Lay a tape measure across the width of the road or shoulder.

2) Install the pre-weighed (stored in a zip-loc bag) into the vacuum.